UNIVERSITAT DE BARCELONA

Ultra-high resolution environmental and climatic reconstruction using oxygen and carbon isotopes of diatom frustules

Armand Hernández Hernández

ULTRA-HIGH RESOLUTION ENVIRONMENTAL AND CLIMATIC RECONSTRUCTION USING OXYGEN AND CARBON ISOTOPES OF DIATOM FRUSTULES

The Late Glacial and Early Holocene laminated sediments from Lago Chungará (Andean Altiplano, northern Chile)

Armand Hernández

PhD thesis

Universitat de Barcelona

June 2010

UNIVERSITAT DE BARCELONA

CSIC
Consejo Superior de Investigaciones Científicas

UNIVERSIDADE DA CORUÑA

ULTRA-HIGH RESOLUTION ENVIRONMENTAL AND CLIMATIC RECONSTRUCTION USING OXYGEN AND CARBON ISOTOPES OF DIATOM FRUSTULES

The Late Glacial and Early Holocene laminated sediments from Lago Chungará (Andean Altiplano, northern Chile)

Memòria presentada per l'Armand Hernández Hernández
per optar al grau de Doctor en Geologia.
Aquesta memòria ha estat realitzada dins del Programa de Doctorat
«Exploració, Anàlisi i Modelització de Conques i Sistemes Orogènics (Bienni 2004-2006)»
sota la direcció del Dr. Santiago Giralt Romeu i del Dr. Roberto Bao Casal,
i la tutoria del Dr. Alberto Sáez Ruiz.

Armand Hernández Hernández

Barcelona, Juny del 2010

Dr. Santiago Giralt Romeu

Dr. Roberto Bao Casal

Al meu pare

Agraïments

Ara mateix no estaries llegint aquesta tesi si no fos per totes les persones que m'envolten. Aquest és el moment d'agrair-los a tots la seva ajuda, el seu recolzament, la seva comprensió, la seva paciència (sobretot paciència), els seus ànims, la seva amistat, les seves rialles, i l'immens afecte que m'han donat. Si una cosa tinc molt clara és que sense tots ells mai hauria arribat fins aquí. Per això, i encara que sigui d'una forma molt discreta, m'agradaria donar-los les gràcies.

En primer lloc agrair l'esforç fet pels meus directors de tesi, ells saben millor que ningú com ha costat arribar fins aquí. Però ells també saben que durant tot aquest temps ha sorgit alguna cosa més que una relació director-doctorand. En Santi i el Roberto han estat amics, col·legues, pares, i alguna vegada «jefes» (sí, alguna vegada sí). Així només puc dir-vos: gràcies, gràcies i gràcies per tot. Aínda que tamén podería dicirvos: grazas, grazas e grazas por todo.

I wish to express my sincere thanks to Melanie J Leng and Philip A Barker, my English advisors, who have made a major contribution to this thesis. They went to a lot of trouble to make me feel comfortable in my new surroundings in England. Despite the language difficulties, they showed kindness and forbearance and made me very welcome. They believed in me, and if I may be considered a researcher, it is thanks to their support and encouragement. They were a source of inspiration and their advice proved invaluable in helping me to get to grips with isotope and diatom research. It was through Melanie and Phil that I became a member of the IBiS group.

I am especially grateful to Hillary J Sloane, who played a very important part in this study. Without her isotope analysis, this thesis would not have been written. In addition to being very supportive, she willingly took the time to teach me about the secrets of the fluorination line during my stay at NIGL (UK). I am also indebted to Christopher P Kendrick for undertaking the carbon isotope analysis.

També vull agrair l'ajuda, l'amistat i la dedicació del «compañero y gurú» Alberto Saéz, i el recolzament, les rialles, els savis consells i el suport econòmic d'en Juan José Pueyo. Tots nosaltres formem part d'un grup de recerca compacte on el que està per sobre de tot és el bon ambient i les ganes de fer les coses ben fetes. Aquí em venen al cap reunions de projecte, campanyes de camp, sopars... Per això, vull donar les gràcies a tot el grup de recerca: a Blas L Valero-Garcés padre de todo esto y gran maestro del Altiplano, a Ana Moreno por su actitud incansable y por estar siempre dispuesta a ayudar,

al Christian Herrera, por su ayuda desde Chile. També als que han anat arribant: en Jordi Catalán, en Sergi Pla, l'Olga Margalef, la Núria Cañellas i en Valentí Rull. Per últim, cal recordar als que ja no formen part del grup: la Conxita Taberner va ser qui em va donar l'oportunitat de començar aquest camí, Bogumila Klosowska, who not only helped me with the sampling but also with my English, i en Roger O Gibert i la Penélope González-Sampériz que van fer una part important del treball inicial al Lago Chungará.

És la meva obligació agrair el suport econòmic que he rebut mitjançant una beca FPI del Ministerio de Ciencia e Innovación (BES-2005-6971) i un contracte d'ajudant de recerca amb la Fundació Bosch i Gimpera (CENITE: VISION CO_2). Els projectes del Ministerio de Ciencia e Innovación ANDESTER (BTE2001-3225, BTE2001-5257-E), LAVOLTER (CGL2004-00683/BTE), GEOBILA (CGL2007-60932/BTE) i CONSOLIDER-Ingenio 2010 GRACCIE (CSD2007-00067) han permès el suport econòmic d'aquesta tesi durant aquests anys.

Per dur a bon port aquesta tesi s'han hagut de fer viatges, mostreigs, preparació de mostres i anàlisis. Per això no em puc oblidar de mostrar tot el meu agraïment a tothom que ho ha fet possible. Grateful acknowledgment is made to D. Schnurremberger, M. Shapley and A. Myrbo from the Limnological Research Center staff (USA) for their invaluable assistance in the field. Muchas gracias a toda la gente de la CONAF por ofrecerme su ayuda y apoyo. No olvido que estoy en deuda con Jimena Saavedra (CONAF), quien ayudó a que mi estancia en el Altiplano fuera una de las mejores experiencias que uno puede vivir. También agradecer a la familia Riroroko su hospitalidad durante la campaña de campo en la Isla de Pascua ya que, aunque el material obtenido allí no forme parte de esta tesis, sí forma parte del proyecto al que me debo. Durante los muestreos, la gente del IPE (Mayte, Mario, JuanPi,...) siempre ha estado dispuesta a ayudar, y en el laboratorio del ICTJA siempre he tenido la colaboración de Graciela Monzón. La actitud y predisposición para ayudar en todo lo posible por parte de Chelo Palacios, de la administración del ICTJA, ha sido de gran valor. Por tanto, gracias a todos ellos. I am also indebted to Michael Köhler (GFZ-Potsdam) for preparing the thin sections and to Andy Quin for helping me in the lab at LEC (UK). Special thanks are due to Elizabeth Hurrell for making my stay at LEC such a nice experience and for compiling a vocabulary of useful words in English and Spanish. Her «Catalan almond cookies» were unforgettable.

Thanks are due to Alice Chang for the many interesting and stimulating discussions about rhythmites and the self-sedimentation process. This thesis benefited substantially from the critical reviews of Antje Schwalb, Sarah Metcalfe and two anonymous persons. I wish to thank George von Knorring for improving the English of the final version of this thesis. No vull oblidar els meus inicis, i per això també li estic agraït a l'Emilio Ramos i al Mariano Marzo per donar-me l'oportunitat de fer recerca. Amb ells vaig poder començar a conèixer aquest món i fer els no sempre engrescadors cursos de doctorat.

També vull tenir un record especial per a tota aquella gent amb qui he compartit despatx durant aquest temps. Sóc perfectament conscient que no és fàcil compartir un espai així amb mi, i ells en lloc de posar males cares sempre s'han mostrat disposats a ajudar-me. Així doncs, moltes gràcies a l'Alfonso Muñoz, la Gemma Labraña, l'Almudena Lorenzo i la Marta Rejas, que han compartit amb mi el «zulo» del ICTJA; e a Manel Leira, Tânia Ferreira e Laia Rovira, que compartiron comigo «o laboratorio» no anexo da Facultade de Ciencias da UDC. Tamén agradecer a amizade, boa vontade e ganas de axudar da xente da UDC. Quizá eles tamén teñan parte de culpa de que decida acabar a tese en Galicia. Eles axudaron, pero tamén as marabillosas praias que alberga esta terra, a súa natureza, a súa rica gastronomía, a súa calidade de vida, a súa tranquilidade, os seus paxaros, a súa xente, o seu tempo (dacordo, o seu tempo non), e o seu "Mesón del Hockey" (o noso santuario), un claro exemplo de biodiversidade cunha tortilla marabillosa. Alí, xurdiron moitas ideas desta tese.

Una agraïment molt especial per la Patricia Cabello, ella va ser qui em va fer creure que jo podia fer una tesi, i qui em va ensenyar a no rendir-me mai i lluitar pel que realment vull. Sempre ha estat molt exigent, però alhora pacient, amb tot el que li he ensenyat perquè em donés la seva opinió. Per tant, ella també té gran part de culpa del resultat d'aquesta tesi.

Vull agrair a la Clara Prats tots els consells que m'ha donat des de la seva «experiència doctoril», hi ha una llista interminable de recomanacions, idees i discussions que m'han ajudat a arribar fins aquí. També vull donar les gràcies a la Núria Carrera per haver-me recolzat i escoltat en molts moments, per haver-me fet ser més crític amb mi mateix i per haver-me ajudat amb els seus coneixements de la geologia dels Andes.

Estic molt content, orgullós, i fins i tot sorprès, de la quantitat d'amics i companys que tinc. Aquí, estan inclosos tots els «Tragapans», la majoria dels quals han estat estudiants de geologia. Alguns no en van tenir prou amb la llicenciatura i han fet una tesi, un màster o simplement han allargat la carrera. Això ens ha permès compartir dinars, cafès i birres, fent més agradables les llargues jornades de feina a la Facultat. També vull donar les gràcies a tots els amics de Sant Feliu, que potser no han intervingut directament en la realització d'aquesta tesi però que són una part molt important de la meva vida. Ells són la gent de la «penya espardenya» o «Qtales», amb qui a vegades m'he sentit com un «bitxo raro» explicant les meves històries de diatomees, i la «gent de l'escola», «del MotoGP» i «de les calçotades», que m'han fet adonar que sóc un privilegiat cada cop que els he explicat les meves aventures de tesi (només els hi explicava les coses bones). També vull donar les gràcies als «amics de la piscina» que encara em queden i als «geòlegs» que ja no estan a la facultat. Amb tots ells comparteixo una part important de la meva vida i una gran amistat.

When I embarked upon my thesis, my supervisors told me that I would have to do a training period in the UK. I was apprehensive at first as I did not know anybody in England and as I spoke very

little English. But now I am very glad that I went. I met many kind and interesting people, I improved my English and I decided to return the following year. I should like to take this opportunity to thank all my friends and colleagues in England for their help and encouragement.

Per últim, gràcies a tota la meva família. Al meu pare per haver-me fet veure que aquest camí no seria fàcil, però que lluitant algun dia arribaria al final. Malauradament ell no ha pogut arribar a veure aquest final, però tal com parlava i em mirava sé que va marxar convençut de que ho aconseguiria. Papa, aquesta tesi és per tu. A la meva mare, per haver-me recolzat sempre i per haver tirat amb tota la seva força i energia d'aquest carro que anomenem família. Gracias mama. Al meu germà per ser el millor que m'ha passat a la vida, sempre he pensat així i tot aquest temps de tesi només ha fet que refermar aquesta idea. Gràcies Ferran per ser com ets, per fer-me sentir admirat, per dir-me sempre que té molt de mèrit el que faig, per fer-me riure, i pel teu suport lingüístic. A les meves iaies per haver aconseguit que estigui convençut i segur de fer el que faig i de ser com sóc. Ambdues, des de la seva experiència, sempre m'han dit el mateix: «El millor que pots fer és veure món i omplir-te d'experiències». I això és el que he fet i vull seguir fent. I als meus cosins, tiets i cosinets, per ser família i amics al mateix temps, ells sempre han admirat la meva feina, el meu valor i la meva determinació, i això m'ha fet avançar amb força durant tot aquest temps de tesi.

Gemma, no et pensis que m'oblido de tu! Junts estem compartint els millors anys de la nostra vida, i junts hem aconseguit acabar aquesta tesi. Gràcies per la teva paciència, gràcies pel teu amor, gràcies pel teu afecte, gràcies per la teva comprensió, gràcies per fer-me veure que no sempre tinc raó, gràcies per acompanyar-me en les meves bogeries, gràcies per fer-me feliç, gràcies per fer-me sentir estimat, gràcies pel teu somriure, gràcies als teus pares, gràcies per la teva lasagna d'espinacs i, evidentment, gràcies per la teva feina a l'Altiplano.

Gràcies a tots, gracias a todos, grazas a todos, thanks to everybody.

Resum

Introducció

Els isòtops estables de la sílice de les diatomees sovint s'han utilitzat amb èxit per dur a terme reconstruccions paleoambientals, especialment paleoclimàtiques. Els isòtops més emprats són els d'oxigen ($\delta^{18}O_{diatom}$) tot i que, darrerament, l'ús d'isòtops de carboni ($\delta^{13}C_{diatom}$), silici ($\delta^{30}Si_{diatom}$) i fins i tot nitrogen ($\delta^{15}N_{diatom}$) ha experimentat un increment important. Tot i això, molts camps romanen oberts i estan pendents de ser explorats amb aquests isòtops. Els isòtops estables de la sílice de les diatomees són especialment útils per poder obtenir informació en aquells registres sedimentaris on la presència de carbonats és escassa o nul·la, i en alguns casos ($\delta^{13}C_{diatom}$ i $\delta^{15}N_{diatom}$) per evitar efectes diagnètics en la senyal isotòpica obtinguda. L'anàlisi de $\delta^{18}O_{diatom}$ s'ha aplicat tant en sediments marins com en sediments lacustres. Per contra, la resta d'isòtops pràcticament no han estat utilitzats en sediments lacustres degut a la gran quantitat de factors que intervenen en la seva incorporació a les diatomees.

Per altra banda, els registres lacustres tropicals són molt importants per a dur a terme reconstruccions climàtiques, ja que es troben situats en una posició geogràfica clau per entendre els canvis climàtics del passat i, així, poder-nos donar informació fonamental per entendre els canvis climàtics del futur. Els llacs són uns excel·lents sensors dels canvis ambientals i, per tant, el seu rebliment sedimentari conté molta informació que ens pot ajudar a entendre millor els canvis ambientals que van succeir en el passat. Així doncs, l'estudi dels isòtops estables de les diatomees de sediments lacustres situats en llocs estratègics pot ser una font d'informació molt important per entendre els canvis ambientals del passat i, així, obtenir una visió privilegiada del context actual de canvi global.

Un d'aquests llocs estratègics és l'Altiplà Andí i, per tant, els llacs situats en aquesta regió són uns bons candidats per dur a terme aquest tipus de reconstruccions. Fins a l'actualitat, però, en els seus registres sedimentaris només s'han portat a terme anàlisis d'isòtops en carbonats i en matèria orgànica total. Tot i que les restes de diatomees acostumen a estar ben preservades en aquests registres, encara no s'han aplicat anàlisis de $\delta^{18}O_{diatom}$ i $\delta^{13}C_{diatom}$ en aquesta regió.

Objectius

Els objectius d'aquesta Tesi Doctoral són: 1) explorar les diferents possibilitats que pot oferir l'estudi de $\delta^{18}O_{diatom}$ i $\delta^{13}C_{diatom}$ de sediments lacustres en reconstruccions paleoambientals, i 2) dur a terme reconstruccions ambientals i climàtiques, tant a alta com a molt alta resolució temporal, de la regió del Lago Chungará (Altiplà Andí) durant el Tardiglacial i l'Holocè inicial, fent ús dels isòtops estables abans esmentats.

Característiques del Lago Chungará

El Lago Chungará (18º15'S, 69º10'W, 4520 m s.n.m.) es troba situat a l'Altiplà Andí (Andes Centrals, Xile), en un context tectònic i volcànic molt actiu. El llac es va formar com a conseqüència d'una esllavissada, durant un col·lapse parcial del volcà Parinacota, la qual va tallar el curs del riu Chungará donant lloc quasi d'immediat a la formació del llac. La data de formació del llac encara aixeca controvèrsia, però sembla clar que es va formar entre els 13000 i els 20000 anys BP.

El Lago Chungará presenta una morfologia irregular amb una longitud màxima de 8,75 km, una profunditat màxima de 40 m, una superfície total de 21,5 km^2 i un volum aproximat de 400 hm^3. Els marges nord i oest del llac són abruptes i estan formats per les vessants dels Volcans Parinacota i Ajoya, respectivament. Els marges sud i est, per contra, són de pendent suau, formats per les parts distals de diversos cons al·luvials i la vall del riu Chungará. Actualment, la principal entrada d'aigües al llac ve donada pel riu Chungará i la principal sortida d'aigua és per evaporació. El llac es pot considerar polimíctic i de oligomesoeutròfic cap a mesoeutròfic, amb un contingut d'1,2 g l^{-1} de sòlids dissolts. La conductivitat varia entre 1500 i 3000 µS cm^{-1}, és un llac alcalí i el seu quimisme és del tipus Na^+-Mg^{2+}-$HCO3^-$-$SO4^{2-}$. L'aigua del llac està enriquida isotòpicament respecte l'aigua de precipitació per mitjà de l'evaporació i els seus valors mitjans de $\delta^{18}O$ i δD són –1,1‰ SMOW i –39,2‰ SMOW, respectivament.

La regió del Lago Chungará està dominada per un clima majoritàriament àrid, amb una època humida anomenada «Invierno Boliviano». Aquesta època es concentra en els mesos de l'estiu austral i ve determinada per la migració cap al sud del cinturó de convergència intertropical, encarregat de portar les masses d'aire humides des de l'Oceà Atlàntic cap a l'Altiplà. En aquesta regió, un altre component important de la variabilitat climàtica entre anys diferents és el fenomen d'El Niño-Oscil·lació del Sud (ENSO). Per això, els anys considerats «Niño» presenten valors de precipitació més baixos i, en canvi, durant els anys considerats «Niña» els valors de precipitació són més elevats.

Treballs previs realitzats al Lago Chungará

Aquesta Tesi ha estat realitzada dins d'un grup de recerca multidisciplinar i, per tant, la seva idea i naixement sorgeixen dins d'aquest àmbit. Així, la feina realitzada per aquest grup és imprescindible per entendre el context en que s'emmarca aquesta tesi.

Al mes de novembre del 2002 es va portar a terme la campanya de sondeig del Lago Chungará, on es van recuperar quinze testimonis de sondatge. Tots aquests testimonis, de fins a 8 metres de longitud, van ser tallats en seccions de 1,5 metres de llargada i transportats al laboratori. Allà, i mitjançant un GEOTEK™ Multi-Sensor Core Logger (MSCL), es van mesurar a cada centímetre certes propietats físiques com la densitat, la velocitat de les ones p i la susceptibilitat magnètica. Amb posterioritat, els testimonis van ser tallats en dues meitats i es van descriure les seves textures, colors i estructures sedimentàries. Tot seguit es van preparar frotis segons les diverses facies descrites per estudiar la composició dels sediments. Totes aquestes dades, amb l'ajut de dades sísmiques obtingudes amb anterioritat, van permetre elaborar una reconstrucció 3D del rebliment sedimentari del Lago Chungará.

Els sondatges 10 i 11, situats a la zona central del llac, van ser seleccionats per dur a terme la reconstrucció paleoambiental de la zona. Amb aquests dos testimonis de sondatges es va construir un sondatge compost que representa deu metres del rebliment sedimentari. De base a sostre, el sondatge està format per dues unitats sedimentàries (unitats 1 i 2), que van ser dividides en dues subunitats (subunitats 1a, 1b, 2a, 2b). La subunitat basal 1a està formada per una alternança de làmines fines de color blanc i verd, molt riques en diatomees. La subunitat 1b està composta per intercalacions d'intervals laminats i massius de color marró i rics en diatomees. Alguns intervals centimètrics també són rics en carbonats. La subunitat 2a està formada per sediments massius marrons rics en diatomees i amb intercalacions de cendres volcàniques i carbonats. Per últim, la subunitat 2b està composta per sediments massius de color gris i negre rics en diatomees amb abundants intercalacions centimètriques de cendres volcàniques.

Els testimonis de sondatge també van ser analitzats per fluorescència de raigs-X, difracció de raigs-X, carboni total i carboni orgànic total, pol·len, associacions de diatomees i sílice biogènica total.

El model cronològic de la seqüència sedimentària del Lago Chungará està basat en 17 datacions radiocarbòniques realitzades en matèria orgànica total i macrofòssils de plantes aquàtiques, i en una datació feta mitjançant les sèries de desintegració de l'urani ($^{238}U/^{230}Th$) d'un nivell de carbonats. L'efecte reservori actual es va calcular a partir de datar el carboni orgànic dissolt a l'aigua del llac i corregir aquesta datació pels efectes dels tests termonuclears realitzats en superfície durant els anys 50 i 60. Totes les datacions es van calibrar mitjançant el software CALIB 5.02 per poder construir el model cronològic final.

Mètodes

Les metodologies emprades han estat basades en l'estudi de les aigües actuals del Lago Chungará, l'estudi petrogràfic dels sediments i l'estudi dels $\delta^{18}O_{diatom}$ i $\delta^{13}C_{diatom}$. Les dades obtingudes han estat tractades estadísticament per tal d'objectivar els resultats.

Al desembre del 2009 es van recollir mostres d'aigua del Lago Chungará i cossos d'aigua propers per tal de completar els mostratges realitzats amb anterioritat (2002 i 2004) pel propi grup de recerca. Les mostres d'aigua del Lago Chungará es van recollir cada 2 metres, en 2 perfils verticals de fins a 8 i 20 metres de fondària. In situ es van mesurar la conductivitat, la concentració d'oxigen, el pH, la temperatura i la salinitat. Per a l'anàlisi d'isòtops d'hidrogen i oxigen es van recollir 24 mostres que van ser analitzades per espectrometria de masses (ICP-IRMS) als Serveis Científico-Tècnics de la Universitat de Barcelona. Als mateixos laboratoris també es va dur a terme l'anàlisi per cromatografia de les concentracions iòniques dels elements principals.

Els sediments del Lago Chungará van ser mostrejats seguint tres estratègies:

1) Es van seleccionar tres intervals de sediments amb alternança mil·limètrica de làmines clares i fosques riques en diatomees, per a caracteritzar els canvis ambientals i climàtics que van tenir lloc durant la transició del Tardiglacial a l'Holocè inicial (12000-9400 anys cal BP). Aquests intervals van ser mostrejats làmina a làmina amb l'objectiu d'obtenir el màxim d'informació possible dels processos ambientals que van tenir lloc. Una primera selecció de mostres de làmines fosquesprocedents dels tres intervals, les quals indicarien les condicions ambientals de fons, van ser analitzades per a determinar els $\delta^{18}O_{diatom}$ amb la intenció de fer una reconstrucció de la evolució hidrològica del Lago Chungará durant aquest període. Un segon estudi isotòpic amb totes les mostres fosques d'un dels intervals va permetre reconstruir a molt alta resolució temporal (entre 4 i 24 anys) la influència de l'ENSO i de l'activitat solar durant el període de temps que inclou aquest interval.

2) Es van analitzar totes les mostres (clares i fosques) de l'anterior interval per a la determinació de $\delta^{18}O_{diatom}$, i una selecció d'11 mostres per a la determinació de $\delta^{13}C_{diatom}$ i $\%C_{diatom}$, per tal de caracteritzar a molt alta freqüència els canvis biogeoquímics que van tenir lloc durant la transició del Tardiglacial a l'Holocè inicial.

3) Es van determinar els valors de $\delta^{18}O_{diatom}$ i $\delta^{13}C_{diatom}$ de 51 mostres de diatomees per caracteritzar els canvis ambientals a alta freqüència registrats des del Tardiglacial fins al final de l'Holocè inicial (unitat 1).

Els intervals seleccionats també van ésser mostrejats per a fer observacions i descripcions petrològiques mitjançant microscopi òptic a partir de l'estudi de làmines primes. Alhora, un nombre representatiu de mostres també van ésser estudiades mitjançant el microscopi electrònic de rastreig (SEM).

L'anàlisi d'isòtops del frústuls de les diatomees requereix que les mostres estiguin formades quasi exclusivament per diatomees, ja que altres components com poden ser argiles, carbonats o cendres volcàniques, poden alliberar isòtops que distorsionin la senyal isotòpica real. Per tant, totes les mostres van ser tractades mitjançant agents químics, per a eliminar les substàncies amb composició química diferent de les diatomees, i mitjançant processos mecànics per a separar les substàncies no diatomítiques però amb igual composició que aquestes. Un cop les mostres estaven formades per més d'un 90% de diatomees, entre 5 i 10 mg de mostra van ser processats per alliberar els isòtops d'oxigen amb el mètode de fluorinització clàssica amb passos esglaonats i, així, poder eliminar amb garanties la capa superficial hidratada que presenta l'òpal de les diatomees. Un cop l'oxigen estructural de la sílice va ser alliberat, aquest va ésser convertit en CO_2 i analitzat mitjançant un espectròmetre de masses Finnigan MAT 253 dual inlet. Per altra banda, els isòtops de carboni van ser analitzats mitjançant la combustió de mostres d'entre 1 i 2 mg en un analitzador elemental Costech ECS4010 en fase amb un espectròmetre de masses VG dual inlet. Totes les anàlisis isotòpiques realitzades sobre els sediments es van dur a terme al NERC Isotope Geosciences Laboratory (Regne Unit), a càrrec de la Prof. Melanie J Leng.

La corba de grisos va ser utilitzada per obtenir, de manera objectiva, les diferències d'intensitat de colors de les làmines dels intervals estudiats. Per a la construcció de la corba de grisos es va utilitzar el paquet de software ImageJ.

Finalment, per obtenir els components periòdics que podien presentar els resultats dels $\delta^{18}O_{diatom}$ es van realitzar anàlisis freqüencials amb els mètodes Multi-Taper (MTM) i de Temps-Freqüència. Tots aquests tractaments estadístics de les dades es van dur a terme mitjançant el paquet de software R.

Evolució paleohidrològica del Lago Chungará (Altiplà Andí, nord de Xile) durant el Tardiglacial i l'Holocè inicial a partir dels isòtops d'oxigen de les diatomees

En aquest capítol es presenten els resultats obtinguts a partir de la determinació de $\delta^{18}O_{diatom}$ i la caracterització petrogràfica dels sediments. Per això, s'han seleccionat tres intervals de sediments laminats del registre sedimentari del Lago Chungará. L'objectiu ha estat establir l'evolució paleohidrològica del llac durant el Tardiglacial i l'Holocè inicial (ca 12000-9400 anys cal BP), i alhora mostrar com aquesta evolució pot tenir un paper clau en la interpretació dels isòtops d'oxigen.

L'estudi petrogràfic mitjançant làmines primes ha mostrat que els sediments laminats del Lago Chungará estan formats per ritmites compostes de làmines mil·limètriques clares i fosques. Les làmines clares estan formades quasi exclusivament per la diatomea planctònica *Cylostephanos andinus,* mentre que les làmines fosques són riques en matèria orgànica i contenen una mescla de diverses associacions

de diatomees. La formació de les làmines clares està relacionada amb «blooms» de diatomees de curta durada (dies o setmanes). Per contra, les làmines fosques representen les condicions limnològiques de base al llarg de diversos anys de deposició.

L'anàlisi de $\delta^{18}O_{diatom}$ ha estat realitzada únicament a les làmines fosques, que mostren una tendència general d'enriquiment isotòpic al llarg del període estudiat. La comparació dels valors de $\delta^{18}O_{diatom}$ amb la reconstrucció de l'evolució del nivell del llac duta a terme en treballs previs suggereix que, a més de canvis en la relació precipitació/evaporació (P/E), l'evolució d'altres factors hidrològics locals podrien haver dominat les variacions del registre de $\delta^{18}O_{diatom}$. Aquests canvis podrien ésser tant variacions de la pèrdua d'aigua subterrània com variacions de la relació superfície/volum de l'aigua del llac.

La reconstrucció hidrològica del llac mostra que durant la pujada més important del nivell del llac, la qual va succeir cap els 10400 anys cal BP, es van inundar marges molt més soms, donant com a resultat canvis en la morfologia del llac. Aquests canvis van provocar un increment de la relació superfície/volum del llac i, per tant, va augmentar l'evaporació, causant un enriquiment isotòpic de l'aigua del llac. D'altra banda, el llac, en trobar-se en els estadis inicials de la seva formació, segurament va patir modificacions en la seva hidrologia, com per exemple que la deposició de sediments va anar segellant el fons del llac, dificultant així la sortida d'aigua subterrània i disminuint el seu flux. Així, el temps de residència de l'aigua va augmentar i, alhora, va augmentar l'evaporació potencial. Per tant, ambdós factors són possibles causes de l'enriquiment isotòpic, més enllà dels factors climàtics.

Els treballs previs sobre $\delta^{18}O_{diatom}$ han fet especial èmfasi en qüestions com la contaminació, la diagènesi i les interaccions de l'aigua intersticial amb l'òpal de les diatomees com a factors determinants en les variacions de $\delta^{18}O_{diatom}$ més enllà de factors climàtics i, en canvi, els factors hidrològics locals, en gran mesura, han estat negligits. Els resultats d'aquest capítol demostren la complexa interacció que existeix entre els diversos factors que intervenen en els registres de $\delta^{18}O_{diatom}$ dels llacs hidrològicament tancats i com la seva interpretació necessita ser adaptada als diferents estadis d'evolució del llac.

Les senyals de l'ENSO i de l'activitat solar a partir dels isòtops d'oxigen de la sílice de les diatomees durant la transició Tardiglacial-Holocè inicial als Andes Centrals (18ºS)

Aquest capítol mostra, per primer cop, la reconstrucció del balanç hídric a l'Altiplà Andí a escala de desenes i centenes d'anys basada en $\delta^{18}O_{diatom}$ durant la transició Tardiglacial-Holocè inicial (11900-11450 anys cal BP). Les característiques texturals de les làmines estan explicades als capítols 4 i 6. Per a realitzar aquest estudi es van analitzar 40 mostres de làmines fosques consecutives de l'interval estudiat.

Els resultats obtinguts mostren una sèrie d'esdeveniments secs i humits a escala de desenes i centenars d'anys. Els episodis àrids corresponen a valors d'isotopia alts, mentre que els episodis humits estan indicats per valors isotòpics més baixos, degut a que el senyal isotòpic esta directament relacionat amb les variacions de la P/E a l'Altiplà. Les dades d'isotopia s'han comparat amb reconstruccions prèvies realitzades en el mateix sondatge amb la intenció de confirmar aquesta interpretació. Aquestes reconstruccions prèvies reflecteixen l'entrada d'elements terrígens i el balanç hídric al Lago Chungará. El resultat de la comparació ha estat satisfactori, mostrant una bona correlació entre les diferents reconstruccions. Tot i això, existeix un desfasament temporal sistemàtic entre elles. Aquest desfasament ha estat interpretat com que és degut al temps necessari perquè s'observin canvis significatius en els valors d'isòtops d'oxigen de l'aigua del llac i la seva posterior incorporació als frústuls de les diatomees, el qual és diferent al temps de resposta de les altres dues reconstruccions. Aquest fet permet destacar la resposta no lineal que sovint mostren els ecosistemes lacustres respecte als forçaments ambientals.

A l'interval estudiat s'han pogut identificar dues caigudes principals dels valors d'isotopia (11800 i 11550 anys cal BP) que estarien indicant unes majors condicions humides a escala de centenars d'anys. Al mateix temps, també s'ha pogut identificar un enriquiment isotòpic principal, per sobre dels nivells de base, que es localitza entre els 11990 i els 11550 anys cal BP i que indicarien una fase d'aridesa breu durant el Tardiglacial. El trànsit Tardiglacial-Holocè inicial també conté diverses caigudes de menor magnitud dels valors d'isotopia i que estarien associades a esdeveniments de major humitat a una escala temporal inferior (desenes d'anys).

Per altra banda, també s'han realitzat anàlisis espectrals dels valors obtinguts de $\delta^{18}O_{diatom}$, els quals mostren que, durant els esdeveniments amb més humitat, els canvis en les condicions atmosfèriques a l'Altiplà Andí estarien relacionats tant amb l'ENSO com amb l'activitat solar. Amb l'ajuda de les anàlisis espectrals s'han identificat freqüències de 7-9 anys i 15-17 anys, les quals es corresponen amb freqüències significatives del fenomen ENSO. Al mateix temps, també han estat identificades periodicitats de 11, 13 i 35 anys corresponents als cicles d'activitat solar Schwabe, Hale i Brückner, respectivament. El treball realitzat ha permès establir una relació entre l'activitat solar i l'ENSO a escala de desenes d'anys i superiors, i per tant és molt probable que el forçament, a causa de l'activitat solar al registre del Lago Chungará, sigui transmès mitjançant la modulació ENSO dels monsons d'Amèrica del Sud. Per altra banda, l'anàlisi de Temps-Freqüència duta a terme mostra que, encara que els forçaments per l'activitat solar i per l'ENSO van estar presents durant l'inici de l'Holocè, van ésser més intensos durant el Tardiglacial. Com s'observa a les anàlisis espectrals, probablement l'Holocè inicial va estar dominat per condicions de La Niña, que corresponen amb esdeveniments humits sobre l'Altiplà Andí. Molts estudis han demostrat forçaments ENSO durant la transició Glacial-Interglacial, però els resultats presentats

aquí mostren que aquest registre és una de les poques seqüències terrestres que preserva freqüències clau de l'ENSO i, per tant, està demostrant que aquests processos climàtics estan dominant la transició cap a l'Holocè.

Processos biogeoquímics que controlen els isòtops d'oxigen i carboni de la sílice de les diatomees presents en ritmites lacustres

L'objectiu d'aquest capítol ha estat la reconstrucció dels processos biològics, químics i sedimentaris que van donar lloc a la formació de les làmines del registre sedimentari del Lago Chungará. Al mateix temps, amb aquesta reconstrucció s'ha pogut demostrar com els cicles biogeoquímics i els registres sedimentaris dels llacs estan directa o indirectament relacionats amb el control climàtic de la hidrologia i amb els processos que tenen lloc a la conca de captació d'un llac.

Per aconseguir aquest objectiu s'han utilitzat: 1) els valors de $\delta^{18}O_{diatom}$ a cadascuna de les làmines de l'interval seleccionat (11990-11530 anys cal BP) i 2) els valors de $\delta^{13}C_{diatom}$ en 11 mostres, escollides segons la seva representativitat. D'altra banda, també s'ha dut a terme un estudi petrogràfic més detallat que al capítol 4.

Com es comenta al capítol 4, el registre laminat del Lago Chungará està format principalment per ritmites mil·limètriques clares i fosques de caràcter multianual. No obstant, l'estudi petrogràfic més detallat ha permès identificar una làmina intermèdia de color verd clar localitzada sempre entre una làmina clara i una fosca. Les làmines clares es van formar durant «blooms» extraordinaris de curta durada i estan bàsicament formades per *Cyclostephanos andinus* de mida gran (>50 μm). Aquests «blooms» extraordinaris de diatomees es van produir durant esdeveniments de gran mescla de la columna d'aigua i/o per episodis d'erosió excepcional de la conca de drenatge. En el primer cas l'ascens de les aigües riques en nutrients procedents de l'hipolimnion van permetre més disponibilitat de nutrients, mentre que en el segon cas, la font de nutrients seria al·lòctona. Les làmines de color fosc es van acumular al llarg de diversos anys sota diferents condicions de la columna d'aigua. Aquestes làmines estan formades per una barreja de diatomees, principalment teques més petites de *Cyclostephanos andinus* i per *Discostella stelligera*, i matèria orgànica. Aquestes làmines fosques reflecteixen el pas progressiu des de les condicions favorables per a que tinguin lloc els «blooms» extraordinaris de diatomees cap a les condicions de base del llac. Per últim, les làmines de color verd clar estan formades per components de les làmines clares que van canviant progressivament cap a la part superior a components de les làmines fosques. Aquestes làmines de color verd clar sempre es troben immediatament després d'una làmina clara, i podrien ser conseqüència d'un fenomen anomenat «auto-sedimentació» que indicaria la fi dels «blooms» excepcionals. Per tant, s'ha establert un nou model deposicional que, en aquest cas, estaria

format per triplets compostos d'una làmina clara a la part inferior, una làmina verda clara en posició intermèdia i una làmina fosca a la part superior.

Els valors de $\delta^{18}O_{diatom}$ i $\delta^{13}C_{diatom}$ a les ritmites s'han utilitzat per detectar oscil·lacions paleoclimàtiques i paleoambientals, ja que els valors d'isotopia han estat interpretats com variacions en la relació P/E i en la concentració de carboni dissolt a l'aigua del llac, respectivament. Els valors de $\delta^{18}O_{diatom}$ mostren que, majoritàriament, la formació de làmines clares va ser induïda per caigudes del nivell del llac, mentre que la formació de làmines fosques es va veure afavorida per pujades del nivell del llac. Aquestes dades d'isotopia, junt amb les dades cronoestratigràfiques, suggereixen que la deposició de les làmines clares va ésser provocada per esdeveniments ambientals extrems. L'ENSO i l'activitat solar són els principals forçaments climàtics que podrien estar desencadenant aquests esdeveniments, ja que afavoreixen els canvis hidrològics a escala interanual i de desenes d'anys a l'Altiplà Andí.

Les pertorbacions ambientals d'alta freqüència, induïdes per esdeveniments climàtics d'escala interanual o de desenes d'anys, difícilment queden registrades als sediments lacustres de l'Altiplà Andí. Tanmateix, els sediments laminats del Lago Chungará s'han mostrat com un bon registre per reflectir la intensitat de diversos fenòmens climàtics d'alta freqüència i els seus efectes en el cicle del carboni dels llacs.

Els registres isòtopics de $\delta^{18}O_{diatom}$ i $\delta^{13}C_{diatom}$ de la unitat laminada del Lago Chungará (dels 12400 als 8400 anys cal BP)

En aquest capítol es presenten els registres isotòpics de $\delta^{18}O_{diatom}$ i $\delta^{13}C_{diatom}$ de la unitat sedimentària laminada i rica en diatomees del Lago Chungará, la qual abasta dels 12400 als 8400 anys cal BP. Les dades de l'anàlisi provenen de 51 mostres. L'objectiu ha estat caracteritzar els canvis ambientals i climàtics que van succeir als Andes Centrals durant el període de temps estudiat.

El registre de $\delta^{18}O_{diatom}$ s'ha interpretat com indicador de la hidrologia del llac i del balanç d'humitat regional a escala de centenars i milers d'anys, mentre que les variacions de $\delta^{13}C_{diatom}$ és molt probable que estiguessin condicionades per canvis en la productivitat del fitoplàncton i en la concentració i origen del diòxid de carboni dissolt a l'aigua ($CO_{2(aq)}$).

Han estat identificades tres fases climàtiques principals durant el Tardiglacial i l'Holocè inicial: 1) una fase humida durant la transició Tardiglacial-Holocè inicial (12400-10100 anys cal BP), 2) una fase seca a l'Holocè inicial (10100-9100 anys cal BP), i 3) una fase progressivament més humida durant l'última part de l'Holocè inicial (9100-8400 anys cal BP).

Encara que la fase humida de la transició Tardiglacial-Holocè inicial coincideix amb una tendència cap a un mínim en la insolació, l'establiment de condicions climàtiques semblants a les de La Niña a la zona tropical de l'Oceà Pacífic s'imposarien al forçament per precessió. Per altra banda, durant aquest

període no es va registrar al Lago Chungará cap esdeveniment equivalent al Younger Dryas de l'hemisferi nord. El mínim d'insolació als ca. 10000 anys cal BP va tenir un paper clau durant l'Holocè inicial (10100-9100 anys cal BP), provocant la migració cap al Nord de la zona de convergència intertropical (ITCZ). Aquesta, junt amb la debilitació de les condicions ENSO, va sotmetre els Andes tropicals a un període de sequera extrema. El retorn cap a condicions més humides va tenir lloc al voltant dels 9000 anys cal BP seguint un increment en la insolació estival austral. Aquest darrer període va haver de ser breu, ja que molts registres climàtics de l'Altiplà Andí mostren l'inici d'un important període sec al voltant dels 8000 anys cal BP com a conseqüència d'un afebliment de les condicions de l'ENSO. Tot i això, es requereixen més anàlisis en tota la unitat no laminada (unitat 2) del registre del Lago Chungará per poder confirmar aquesta hipòtesi.

L'anàlisi isotòpica de la matèria orgànica inclosa dins de les parets dels frústuls de les diatomees en sediments lacustres ha demostrat que diversos factors, com la productivitat fitoplanctònica o l'origen del carboni i llur concentració, interaccionen donant com a resultat oscil·lacions en els valors de $\delta^{13}C_{diatom}$. Aquestes oscil·lacions també revelen interaccions entre la reserva de carboni de l'aigua del llac i la conca de drenatge. Durant els períodes humits els valors de $\delta^{13}C_{diatom}$ mostren que la contribució de materials externs, a més de la productivitat fitoplanctònica del llac, van incrementar significativament la reserva de carboni de l'aigua del llac, mentre que els períodes secs van afavorir l'acumulació de carboni format al mateix llac i el posterior enriquiment dels valors de $\delta^{13}C_{diatom}$. L' alliberament del CO_2 de l'hipolímnion durant els períodes de mescla també va poder causar una baixada dels valors de $\delta^{13}C_{diatom}$. Així doncs, les mesures de $\delta^{18}O_{diatom}$ i $\delta^{13}C_{diatom}$ s'han mostrat com a eines molt útils per entendre els patrons climàtics regionals i els processos d'interacció entre el llac i la seva conca de drenatge. Aquest capítol posa èmfasi en que l'anàlisi conjunta de $\delta^{18}O_{diatom}$ i $\delta^{13}C_{diatom}$ poden ajudar a entendre millor el paper dels llacs en el cicle del carboni a escala global, sobretot dins del context del canvi global actual.

Conclusions

En aquesta tesi s'han obtingut conclusions de caire metodològic, limnològic i climàtic:

- Diversos factors ambientals, més enllà dels forçaments climàtics, poden influir en els valors de $\delta^{18}O_{diatom}$. Els registres de $\delta^{18}O_{diatom}$ en sistemes lacustres tancats no poden ser simplement interpretats en termes de sec o humit, sinó que és imperatiu entendre la hidrologia de cada sistema. Per la seva part, l'anàlisi de $\delta^{13}C_{diatom}$ ha demostrat que aquesta tècnica és una eina vàlida per a fer reconstruccions del cicle del carboni als llacs, així com per donar un millor punt de vista del cicle del carboni a nivell global.

- La unitat sedimentària laminada del Lago Chungará està formada per ritmites multianuals compostes per triplets de làmines de color clar, verd clar i fosc. Aquestes làmines són riques en diatomees

i són el resultat de processos lacustres diferents. Les làmines de color clar es van formar com a conseqüència de «blooms» extraordinaris de molt curta durada (dies o setmanes) que van tenir lloc durant episodis de turbulència extrema i/o episodis d'erosió excepcional de la conca de recepció. Les làmines de color verd clar es van formar com a resultat del final dels «blooms» extraordinaris, i per últim, les làmines de color fosc es van dipositar al llarg de diversos anys sota diferents condicions de la columna d'aigua i, per tant, representen les condicions de base del llac.

- Els valors de $\delta^{18}O_{diatom}$ ens mostren que tant les làmines clares com les làmines fosques es poden formar en períodes secs i en períodes humits. Tot i així, aquest valors també mostren que els «blooms» extraordinaris van ésser més intensos amb condicions de baix nivell del llac. En la majoria de casos la formació de làmines clares es va veure afavorida per baixades del nivell del llac, mentre que la formació de làmines fosques es va veure especialment induïda per pujades del nivell del llac. Al mateix temps, els valors de $\delta^{13}C_{diatom}$ indiquen que la disponibilitat de carboni va ser superior durant el «blooms» extraordinaris de diatomees. La combinació d'ambdós registres ha destacat les complexes relacions entre els processos limnològics, els processos de la conca de drenatge, la hidrologia i els forçaments climàtics. Durant els períodes amb més precipitació indicats pels valors baixos de $\delta^{18}O_{diatom}$, la contribució relativa del carboni extern, a més de la productivitat fitoplanctònica, van incrementar les reserves de carboni total al llac, tal i com indiquen els valors de $\delta^{13}C_{diatom}$. Per contra, els períodes secs (valors elevats de $\delta^{18}O_{diatom}$) van afavorir els processos d'acumulació de carboni format al propi llac, com demostren els valors elevats de $\delta^{13}C_{diatom}$.

- El registre d'isotopia de la unitat laminada del Lago Chungará exposa clarament que, segons l'escala temporal, un tipus de forçament pot dominar sobre els altres en la interpretació del valors de $\delta^{18}O_{diatom}$ i $\delta^{13}C_{diatom}$.

- A escales temporals de centenars i milers d'anys, factors hidrològics com són canvis en la relació de la pèrdua d'aigua pel flux subterrani o per evaporació i/o en l'extensió del llac poden jugar un paper molt important. Tot i això, l'evolució temporal a més baixa freqüència de $\delta^{18}O_{diatom}$ a la unitat laminada del Lago Chungará posa de manifest els principals canvis en el balanç hídric regional, els quals estarien relacionats amb forçaments orbitals i amb condicions similars a les que es donen durant els fenòmens ENSO.

- Per altra banda, a escales de temps de desenes d'anys, els valors de $\delta^{18}O_{diatom}$ estarien induïts per fenòmens climàtics d'altra freqüència. Les oscil·lacions en els valors de $\delta^{18}O_{diatom}$, que indiquen canvis en el balanç de precipitació/evaporació a la regió del Lago Chungará, serien el resultat de canvis en les condicions atmosfèriques sobre l'Altiplà Andí, provocats tant per l'ENSO com per l'activitat solar. Per tant, la transició Glacial-Interglacial, va estar dominada per canvis abruptes en les condicions climàtiques i no pas per un canvi progressiu d'aquestes condicions.

Contents

Chapter 1

Introduction

Stable isotopes from marine and lacustrine sedimentary records have been used to improve our understanding of the evolution of the Earth since the end of World War II (e.g. McCrea, 1950; Urey et al. 1951, Emilliani, 1955). Oxygen and carbon isotopes in microfossil carbonates have been widely used to carry out palaeoenvironmental reconstructions (see reviews in Ito, 2001; Richardson, 2001; Schwalb, 2003; Leng and Marshall, 2004; Grottoli and Eakin, 2007; Ravelo and Hillarie-Marcel, 2007). However, calcareous microfossils (mainly foraminifera, molluscs and ostracods) are not always present in marine or lacustrine sediments owing to unfavourable ecological or post-depositional conditions. These non-carbonated sediments sometimes contain abundant biogenic silica (mainly diatoms), rendering them suitable for studies of stable isotopes (e.g. Shemesh et al. 1992, 1995, 2001; Rietti-Shati et al. 1998; Rosqvist et al. 1999, 2004, Barker et al. 2001, 2007; Rioual et al. 2001; Leng et al. 2001, 2005a; Hu and Shemesh, 2003; Jones et al. 2004; Lamb et al. 2005; Polissar et al. 2006; Tyler et al. 2008; Mackay, 2007; Mackay et al. 2008; Swann et al. 2008, 2010; Jonsson et al. 2010). For this reason, considerable progress has been made in the study of biogenic silica using isotopes in recent years (see Leng and Barker, 2006; Crosta and Koç, 2007, and Swann and Leng, 2009 for reviews).

In lacustrine sedimentary materials changes in isotope oxygen values (from both carbonates and biogenic silica) are usually related to changes in temperature or isotope composition of the lake water ($\delta^{18}O_{lakewater}$) (Leng and Marshall, 2004; Leng and Barker, 2006). On the other hand, carbon isotopes in bulk organic matter ($\delta^{13}C_{bulk}$) are commonly used to demonstrate changes in carbon cycle and productivity which are often climatically induced (Meyers and Teranes, 2001; Leng et al. 2005b). Using oxygen and carbon isotope ratios in palaeoenvironmental reconstruction is, however, not easy, given that the sedimentary record can be influenced by a wide range of interlinked environmental processes ranging from local hydrology to regional climate change.

Diatom oxygen isotopes ($\delta^{18}O_{diatom}$) are increasingly being used for palaeoenvironmental reconstructions in lacustrine sedimentary records (see Leng and Barker, 2006 for a detailed review). Although they have been applied in long-scale palaeoclimatic reconstructions (e.g. Rietti-Shati et al. 1998;

Rosqvist et al. 1999; Rioual et al. 2001; Barker et al. 2007; Mackay, 2007; Swann et al. 2010), they can also be used in many other fields. On the other hand, considerable progress has been made in the use of organic inclusions within the diatom frustule from marine sedimentary records in recent years (Singer and Shemesh, 1995; Crosta and Shemesh, 2002; Des Combes et al. 2008). However, very little systematic work has been undertaken on the analysis of the diatom carbon isotope composition ($\delta^{13}C_{diatom}$) in lacustrine sediments (Hurrell et al. submitted).

Tropical proxy records offer valuable insights into past climate and environmental changes of the Earth and into possible future climate change scenarios (Thompson et al. 1998; Barker et al. 2001). The tropics are implicated in forcing global climate shifts at interannual to orbital time scales (Gasse, 2000; Timmermann et al. 2007; Wanner et al. 2008; Chiang, 2009). The global impact of the El Niño–Southern Oscillation (ENSO) variability is one example of how climate phenomena can propagate rapid changes worldwide (Placzek et al. 2006, Merkel et al. 2010). Furthermore, high-frequency climate variability often exerts a considerable influence on human activities (i.e. monsoons, El Niño) in low latitudes. Thus, it is essential to investigate the past tropical climate variability in order to better understand the regional and global climate changes (Thompson et al. 2005). Research into tropical regions has therefore become a key issue among palaeoclimatologists.

The tropics of South America host the world's largest river, and have higher total terrestrial primary productivity and biological diversity than any other continental region of comparable size (Rigsby et al. 2005). Influenced by the tropical circulation in the north, and by the mid-latitude westerlies in the south, the Central Andes are an ideal site to study past variations of atmospheric circulation systems. Thus, the Andean Altiplano has become a key region for the study of late Quaternary climate change in South America. Although this region is very arid today, it has shown significant moisture changes during the Late Glacial and Holocene. Lake sediments, ice cores, pollen profiles, tree rings, glacial deposits together with modeling studies are important sources of information about past environmental conditions in this high-altitude mountain region (e.g. Thompson et al. 1998; Baker et al. 2001a; Garreaud et al. 2003; Goslin et al. 2008; Kull et al. 2008; Solíz et al. 2009; Villalba et al., 2009).

Sedimentary records of high-altitude Andean Altiplano lakes are good candidates for carrying out oxygen isotope studies to reconstruct the late Quaternary climatology of the region (Valero-Garcés et al. 2000). They usually preserve an excellent centennial- to millennial-scale record of effective moisture fluctuations and source changes during the Late Glacial and Holocene despite the fact that the interpretation is not always straightforward (e.g. Baker et al. 2001a; Grosjean et al. 2001; Fritz et al. 2004). Oxygen and carbon isotope analyses in carbonates ($\delta^{18}O_{carbonate}$ and $\delta^{13}C_{carbonate}$) and $\delta^{13}C_{bulk}$ have been successfully used to reconstruct the hydrological responses to climate change in different Andean lacustrine systems to date (e.g. Schwalb et al. 1999; Valero-Garcés et al. 1999; Seltzer et al. 2000; Wolfe

et al. 2001; Abbott et al. 2003; Rowe et al. 2003). No attempt, however, has been made to use $\delta^{18}O_{diatom}$ and $\delta^{13}C_{diatom}$despite the fact that they are usually the best preserved fossils in the sedimentary record of the Andean Altiplano lakes.

1.1 Lakes

Although lakes constitute at present about 1% of the Earth's continental surface, containing less than 0.02% of the water in the hydrosphere, their importance is far greater than these meagre figures suggest (Talbot and Allen, 1996; Wetzel, 2001). Lakes and lake deposits have been the subject of many studies owing to their economic importance (e.g. Robins, 1983; Tiercelin, 1991). Many modern lakes are a vital source of food and water, and the sediments of some of them constitute a source of valuable minerals (i.e. borax) (Swihart et al. 1996). Thus, the question 'What is a lake?' may be posed. According to the Encyclopedia Brittanica (1962), a lake is a mass of still water situated in a depression of the ground without direct communication with the sea. Natural lakes are located in depressions such as ponds and include those that have not resulted from the construction of dams such as impoundments and reservoirs (Meybeck, 1995).

1.1.1 Lake types

Lakes can be classified according to their origin (Wetzel, 2001), chemistry (Eugster and Hardie, 1995), mixing periods (Lewis, 1983), temperature (Hutchinson and Löffler, 1956) and trophic state (Hutchinson, 1969). A satisfactory classification would be based on their origin (Margalef, 1983). Although lakes may be due to a variety of natural processes such as landslides, rivers, dissolutions, or even meteoritic impacts, the most usual origins are volcanic, tectonic and glacial (Wetzel, 2001). Lakes of volcanic origin may be formed by lava flows that obstruct a river valley, forming a new lacustrine basin (e.g. Lake Yojoa, Honduras) (Devevey et al. 1993) or by crater explosion and collapse forming a depression that fills up with rainwater (e.g. Holzmaar, Germany) (Zolitschka, 1992). Large lakes primarily tectonic in origin can be grouped into: a) lakes that are formed in extensional rift valleys (e.g Lake Baikal, Russia) (Colman et al. 1995), b) associated with pull-apart basins (e.g. Lake Issyk-Kul, Rep Kyrgyzstan) (De Batist et al. 2001), or c) formed on slowly subsiding sags in cratonic areas (e.g Lake Chad, Rep Chad) (Durand, 1982). Finally, lakes in glaciated regions are generally small and may be proglacial (e.g Lake Malaspina, USA) (Gustavson, 1975) caused by ice-damming, by barriers composed of moraine (e.g. Imja Lake, Nepal) (Chikita et al. 2000), or by ice scour, freeze-thaw and by valley glaciation (e.g. Pitt Lake, Canada) (Ashley and Moritz, 1979) (Fig. 1.1).

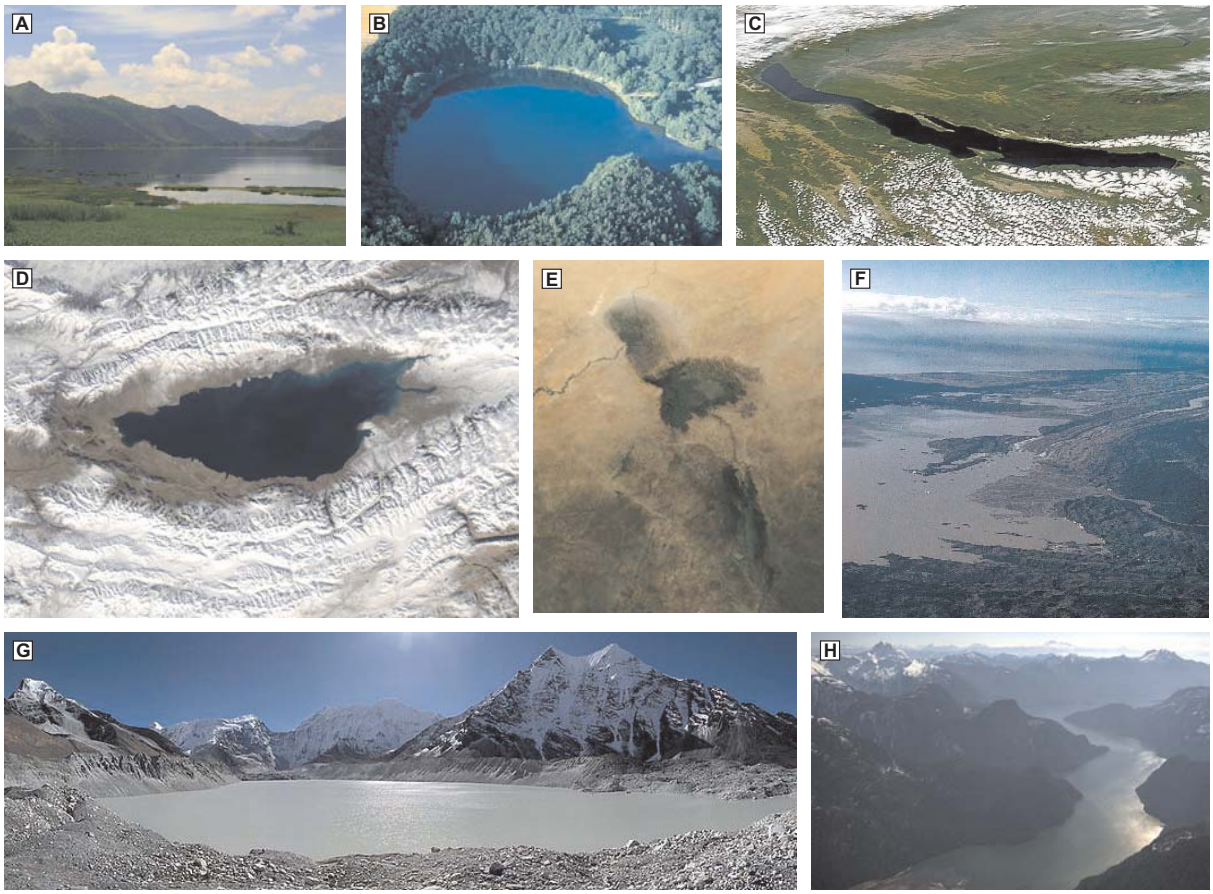

Figure 1.1. Images of different types of lakes according to their origin. A) Lake Yojoa (Honduras) is an example of a lake formed by a lava flow that obstructed a river valley; B) Lake Holzmaar (Germany) resulted from volcanic activity. After a crater explosion and collapse, the lake filled up with rainwater; C) Lake Baikal (Russia), lake of tectonic origin formed in an ancient rift valley. It is the world's deepest lake; D) Lake Issyk-Kul (Rep Kyrgyzstan) is an example of a lake of tectonic origin associated with a pull-apart basin; E) other lakes of tectonic origin are those formed on slowly subsiding sags in cratonic areas, such as Lake Chad (Rep Chad); F) Lake Malaspina (USA) is an example of a lake of proglacial origin; G) glacial lakes can also be formed by ice-damming, i.e. barriers composed of a moraine (e.g. Imja Lake, Nepal); and H) Pitt Lake (Canada) is placed in a valley of glacial origin.

1.1.2 Physical, Chemical and biological characteristics of lakes

Physical features

Physical processes in lakes are important because they are linked to external environmental forcing events such as climate (Cohen, 2003). For instance, lake level oscillations are mainly attributed to water outputs and inputs that are commonly controlled by climate. In addition, light and heat penetration regulate the distribution of organisms and the mixing of the water column leaving their signal in the sediment characteristics (Imboden and Wüest, 1995).

Inputs and outputs of lake waters in combination with the morphometry of the lake basin determine the lake level. Water inputs to the lake include rainfall, surface runoff and groundwater inflow whereas outflows include surface outflow, evaporation and groundwater loss (Talbot and Allen, 1996; Cohen,

2003; Darling et al. 2005; Leng and Barker, 2006). If water inputs and outputs of the lake are equal over a short time span the lake water level remains constant and can then be considered as an open lake. By contrast if significant variations in the lake level occur as the ratio of inputs and outputs changes, the lake is closed (Street-Perrott and Harrison, 1985).

The depth of light penetration into the lake water and the manner in which it is absorbed determine the distribution of the organisms and heat in the lake (Dehaan, 2003). It has recently been suggested that productivity in a large proportion of the world's unproductive lakes is limited by light and not by nutrients as is commonly believed (Karlsson et al. 2009). Lakes can be divided into two zones: those that are penetrated by sufficient light to allow photosynthesis (photic zone), and those that lie below these (aphotic zone). Between these two zones is a zone where photosynthesis equals respiration, which is known as the compensation depth (Brönmark and Hanson, 2005). Light penetration varies because of differences in suspended sediment (turbidity), plankton and dissolved solid content (Cohen, 2003).

On the other hand, heat enters lakes as solar radiation and from geothermal sources. Solar radiation penetrates the lake and heats the water, but the penetration is exponentially reduced with depth (Ragotzkie, 1978). Heat is irregularly distributed in the water column, and is redistributed by mixing. Mixing can be induced by wind, density inestabilities and/or turbulent water inflows when the external forcings are strong enough to counteract the density differences (Imboden and Wüest, 1995). When turbulent mixing or density instabilities are not strong enough to mix the water column vertically, this can become stratified. Stratification in a lake is also influenced by morphometry, depth, solute concentrations, the temperature of the atmosphere, solar irradiation and wind speed (Lewis, 1983). Stratification results from the high temperature differences between surface and bottom waters. This stratification separates the water masses by a thermocline. The surface water mass is termed the epilimnion and the bottom water mass is known as the hypolimnion (Fig. 1.2). Vertical mixing and stratification in the water column of the lake regulate the distribution of dissolved gases and nutrients in various temporal cycles (Cohen, 2003). Lake mixing can be seasonal or occur at longer temporal scales throughout changes in the thermal structure. Lakes can be classified according to their mixing regimes as amictic (never mix), monomictic cold and warm (mix once per year), dimictic (mix twice per year) or polymictic cold and warm (mix repeatedly throughout year) (Hutchinson and Löffler, 1956; Lewis, 1983). Lakes that are only partially mixed are termed meromictic.

Chemical features

Chemical processes in lakes are closely related to external climate and watershed factors. Solute concentrations regulate the distribution of organisms, and the precipitation or dissolution of mineral

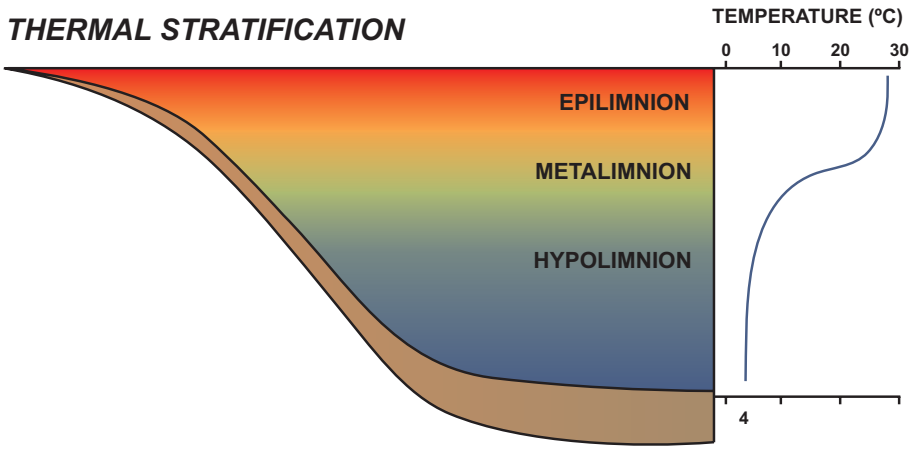

Figure 1.2. Thermal stratification in lakes. Deep lakes generally become physically stratified into three identifiable layers, known as the epilimnion, metalimnion, and hypolimnion. The epilimnion is the upper, warm layer, and is typically well mixed. Below the epilimnion is the metalimnion or thermocline region, a layer of water in which the temperature declines rapidly with depth. The hypolimnion is the bottom layer of colder water that is separated from the epilimnion by the metalimnion. The change of density in the metalimnion acts as a physical barrier that prevents mixing of the upper and lower layers for several months in summer (modified from Horne and Goldman, 1994)

phases (Chalie and Gasse, 2002). Non-marine waters are dominated by four cations, calcium, magnesium, sodium and potassium, and three anions, bicarbonate, sulphate and chloride. Silica can also be a significant dissolved component in alkaline lakes. The relative proportions of these and other ions are largely determined by the geology of the catchment (Eugster and Hardie, 1995).

Dissolved oxygen is a very important component of the water chemistry since it is a product of the photosynthesis and is responsible for oxidation processes. Oxygen concentrations in the water column are a function of productivity, respiration, temperature and mixing, which are all linked to climate and morphometry (Martin et al. 1998). Reduction and oxidation reactions depend on the capacity of the water to oxidise or reduce, and oxygen is one of the most prominent oxidising agents present in lakes. On the other hand, for reduction to occur the absence of oxygen is as necessary as the availabilty of a reducing agent (Davison, 1993; Hamilton-Taylor and Davison, 1995; Hamilton-Taylor et al. 2007). Both oxygen content and redox conditions affect the distribution of organisms, bioturbation and the precipitation or dissolution of minerals (Cohen, 2003).

Nutrients are chemical elements or simple compounds that are essential for organisms. C, which is an important nutrient in lake waters, occurs in various organic and inorganic forms. The lacustrine carbon cycle is related to the fixation of these carbon forms in the water column according to productivity or pH conditions (Cole et al. 2007). C can enter the lake as atmospheric carbon dioxide (CO_2), which is fixed by photosynthesisers (authocthonous carbon), or as a result of the degradation of terrestrial organic matter (allochthonous carbon). It can also enter as HCO_3^- through ground and surface waters from the

catchment (Brönmark and Hanson, 2005). CO_2, which plays a key role in photosynthesis and in other areas of the lacustrine carbon cycle, is one of the most important drivers of climate change (Cole et al. 1994; Dean and Gorham, 1998).

Other nutrients such as P, N and Si are present in small concentrations in lake waters and may therefore limit the growth of lacustrine organisms (Horne and Goldman, 1994; Wetzel, 2001; Cohen, 2003). The atomic relationship C:N:P is considered to be 106:6:1 in plankton, conforming to the so-called Redfield ratio (Reynolds, 2006). Departure from this ratio imposes nutrient limitations on plankton growth. If the N:P in the water is higher than the Redfield ratio, phytoplankton will be phosphorous limited. The opposite is true if N:P is lower. C, N and P as well as the Si needed for diatom growth are thus considered the major nutrient elements for primary productivity in lakes (Margalef, 1983).

P has traditionally been considered the main growth-limiting nutrient for algae in most lakes, and therefore the main determinant of their productivity levels (e.g. Wetzel, 2001). Given that the «phosphorous limitation paradigm» is controversial, lake productivity co-limitation by multiple nutrients is today considered to be more the rule than the exception (Sterken, 2008). P enters the lake as a result of weathering of the catchment via sediment release or by atmospheric deposition (Brönmak and Hansson, 2005). Sediments are in general richer in P than lake water. Depending on pH, redox conditions, and Fe concentrations, P can be released to the epilimnion, prompting primary productivity (Cohen, 2003).

N enters the lake by precipitation, by input from surface and groundwater drainage, but also by fixation of atmospheric hydrogen (Brönmak and Hansson, 2005). NO_3^- is an abundant source of N for phytoplankton, whereas NH_4^+ and NO_2^- are present in much lower quantities. When P is not a limiting factor, such as in eutrophic lakes, the lake can be limited by N. Under these circumstances, organisms capable of N fixation, such as cyanobacteria, become dominant in the plankton.

Si, which is required by diatoms for wall silicification, is mainly taking up by diatoms as dissolved $Si(OH)_4$ to form silica (Willén, 1991). Although a large amount of silica in lakes is supplemented with the inflowing waters, the rate of uptake by diatoms is so high that it can fall to unmeasurable values during the period of summer stratification (Harris, 1986).

The availability of these nutrients is linked to watershed characteristics and internal mixing processes, which in turn regulates the primary productivity of lakes. The trophic status is detemined by lake productivity (Hutchinson, 1969). Infertile soils release relatively little N and P leading to less productive lakes, which are classified as oligotrophic or mesotrophic. Watersheds with rich organic soils or agricultural regions that are usually enriched with fertilizers yield much higher nutrient loads, resulting in more productive, eutrophic (even hyper-eutrophic) lakes (Horne and Goldman, 1994).

Fractionation processes of stable isotopes are related to regional climate parameters, organic matter sources and/or photosynthesis. These processes are discussed below in section 1.4.

Biological features

Biotic systems are the most complex components of lake systems, involving numerous species and the interaction between them and/or the external environment (Margalef, 1983). The different communities of organisms (planktonic, nektonic and benthic) are distributed as a function of their habitats, which are influenced by light, turbulence and proximity to the lake floor. Planktonic organisms are drifting organisms that inhabit the pelagic zone of the water column. Nektonic organisms also inhabit the pelagic zone but are able to swim against the water flow and so control their position. Benthic organisms inhabit the lowest level of a body of water, including the sediment surface and some sub-surface layers (Emiliani, 1991). Planktonic organisms are grouped into phytoplankton (e.g. cyanobacteria, dinoflagellates, diatoms) and zooplankton (e.g. rotifers, arthropods, copepods, insects). Nektonic organisms include fish, large crustaceans and tetrapods. Benthic organisms can be various algae, vascular plants, sponges, bryozoans, annelids, crustaceans, insects and molluscs. All these organisms are conditioned by abiotic factors such as light (Hill, 1996), dissolved oxygen (Dinsmore et al. 1999), pH (Battarbee, 1984), salinity (Bos et al. 1999), nutrient availability (Leland and Berkas, 1998), water turbulence (Johnson and Wiederholm, 1989), and substrate (Burkholder, 1996). Additionally, biotic effects, such as grazing, predation, competition and symbiotic interactions are also key processes in the distribution of freshwater organisms (Kitchell and Carpenter, 1993).

1.1.3 Lacustrine sediments

Lake sediments constitute accurate sources of information about the lake history (Cohen, 2003, Smol, 2008, Cabrera et al. 2009). On the other hand, ancient lacustrine basins contain extensive evaporitic and oil shale deposits which have provided sites for the economic exploitation of resources such as uranium and hydrocarbons (Robbins, 1983).

The material deposition at the bottom of a lake involves both horizontal and vertical transport processes. The former process is mainly due to clastic deposition from rivers and streams at the bottom of the lake. Depending on the geographical location of a particular lake, wind-blown, ice-rafted and volcanic material may also be locally important. The nature and size of the surrounding drainage basins exert a major influence on the input of terrigenous sediment. The sedimentation rates of this clastic material are usually irregular over time and are mainly associated with river discharge and catchment runoff, attaining occasionally very high values (up to several cm per year) (Dussart, 1961).

Shorelines in lacustrine environments may be marked not by beaches but by stands of macrophytes (Livingstone and Melack, 1984). Siliciclastic sediments along lake margins are generally concentrated

around river mouths given that the absence of tides means that wave attack may be limited to a narrow zone along the shores of hydrologically open lakes. In closed lakes, seasonal or longer-term variations in lake level may distribute the effects of littoral processes over a large area. Abandoned beach ridges, which are preserved as staircase-like features around the margin of modern closed basins, provide some of the most striking evidence for former high lake levels (Talbot and Allen, 1996). The offshore deposition is mainly regulated by dispersion and sedimentation of fine-grained suspended matter determined by lake circulation patterns. When lakes are stratified, the distribution of suspended sediment may be greatly influenced by density contrasts within the water column. Bottom-hugging density underflows are also effective in distributing fine-grained sediments over large areas of deep lake basins (Cohen, 1990). Ultimately, when an adequate clastic supply exists, turbidity currents can be a major source of sediment to the offshore areas of large lakes (Lambert and Giovanoli, 1988; Scholz et al. 1993).

On the other hand, vertical deposition mainly consists of suspended materials of chemical and biological origin formed within the lake. In diluted lakes, these are typically carbonate, siliceous or iron mineral accumulations whereas saline waterbodies can produce a wide range of carbonate, evaporate and silicate minerals.

According to Kelts and Hsü (1978) calcareous sediments are formed by one or more of the four following processes: a) inorganic precipitation generally associated with the photosynthetic activities of plants or, less commonly, induced by evaporation, changes in temperature, or mixing of water masses; b) production of calcareous shells, surface encrustations or skeletal elements of living organisms; c) clastic input of allochthonous carbonate particles derived from the drainage basin; and by d) postdepositional or early diagenetic precipitation.

Large amounts of biogenic silica accumulate in some modern lakes (Talbot and Allen, 1996). Diatoms are the principal source of this silica, although sponges may locally make a contribution. Where silica supplies are not limiting, diatoms can outcompete other autotrophic species to become extremely abundant and major sediment contributors. Lakes or areas of the lake floor starved of clastic sediment may accumulate considerable thickness of diatomaceous ooze. Moreover, seasonal plankton blooms can produce diatom-rich laminae interbedded in sediments (Owen and Crossley, 1992; Ishihara et al. 2003; Chu et al. 2005; Simola, 2007; Jacques et al. 2009; Lindqvist and Lee, 2009). Although not widespread, sediments rich in iron minerals occur in some lakes. The Fe is believed to be derived from regolith and transported in colloidal or adsorbed form as part of the suspended load of incoming rivers. In lacustrine environments, this chemical element coprecipitates with silica (Lemoalle and Dupont, 1976).

Saline minerals form after Ca-Mg carbonates precipitate from the water body (Talbot and Allen, 1996). They are usually produced by evaporative concentration, but temperature changes can also cause their precipitation. Saline minerals are found in three principal environments (Eugster and Hardie,

1978): a) in perennial brine bodies or saline lakes, b) as efflorescent crusts on and around ephemeral salt pans, and c) as cements within sediment deposited in and around these water bodies. Gypsum is commonly the first mineral to form after Ca-Mg carbonates, but it precipitates only if the alkaline earth elements have not previously been depleted by carbonate production. Thereafter, the saline minerals that precipitate depend upon the initial composition of the inflow, which is in turn a function of the geology of the catchment (Eugster and Hardie, 1978; Talbot and Allen, 1996).

Lakes can also be important sites for the accumulation of organic matter. Lacustrine deposits often have contents of organic matter that are significantly above the average of sediments and sedimentary rocks. The organic matter in lakes has three principal sources: terrestrial vegetation, marginal macrophyte swamps, and phytoplankton. The remains of phytoplankton are most abundant in open-water, offshore sediments of large lakes, waterbodies receiving little clastic supply, in the middle of large crustal sag basins, and in areas where low slope gradients do not favour the widespread distribution of clastic material by density currents (Talbot, 1988). In contrast, where the lake margin is steep, density flows can transport terrestrial and marginal plant debris far offshore (Le Fournier et al. 1990). The preservation of large amounts of organic matter in lakes is dependent upon rates of organic productivity, anoxic bottom conditions, or a combination of both (Talbot, 1988).

This sedimentation in lakes is therefore highly variable and is affected by six major factors (Fig. 1.3): watershed geology, watershed climate, ontogeny of the lake, inflow and outflow hydrology, internal water circulation, and organic productivity (Cohen, 2003). Hence, many lake sequences should be studied, at least, centimetre by centimetre in order to document the full range of sedimentary environments (Tallbot and Allen, 1996).

Rhythmites

Rhythmites are defined as «sequences of finely laminated, regular alternations of two or more contrasting sediment types» (Talbot and Allen, 1996). These repetitive clusters are called couplets when formed by two facies, but the pattern of repetition may be more complex, involving three (triplets) or even more repetitive sediment types (Cohen, 2003). They are particularly useful for reconstructing high resolution records of terrestrial climate because their individual laminae can provide valuable information about the variable processes responsible for generating each component defining the rhythmite (Simola, 2007; Shunk et al. 2009). The component sediments of a rhythmite may be a combination of clastic, chemical and/or organic deposits rich in organic matter (Fig. 1.4). When diatoms are preserved in laminated sediments, they often provide environmental records of high quality. The rhythmically laminated sediments, mainly made up of diatom frustules, may reflect the regular yearly succession and the seasonal blooms of planktonic diatoms (Simola, 1992). In other cases, the absence of such seasonality may indicate a non-annual rhythmite.

Watershed geology	Fabric/mineralogy of source sediments Sediment, solute & groundwater supply Erodibility of source materials **Mode of lake formation**
Watershed climate	Weathering intensity & transport rates Sediment, solute & groundwater supply Brine evolution/authigenic mineralisation Mixing frequency/redox state of sediments **Lake origin & evolution** **Inflow/outflow hydrology** & lake level fluctuations Solute/temperature effects on diagenesis
Mode of lake formation/evolution	Fabric/mineralogy of sediments Particle/solute supply **Watershed geology** Basin morphometry & sediment delivery **Internal circulation** Sediment accomodation and facies geometry Hydrotermal and groundwater effects on diagenesis
Inflow/outflow hydrology	Lake level fluctuation and facies migration Authigenic mineralisation Sediment focussing/redistribution **Internal circulation (water depth)** Redox-related mineralisation Subsurface brine evolution
Internal circulation	Suspended sediment settling patterns **Organic productivity** Redox state & bioturbation (extent of organic-rich deposits) Redox-related mineralisation and diagenesis Sediment focussing
Organic productivity	Biogenic particle production Community and evolutionary change/effects on sediments Organic particle flux Redox-related mineralisation and diagenesis Extent of organic-rich deposits

Figure 1.3. Major factors affecting the broad-scale differences observed in lake sedimentation patterns, facies development, and facies geometry. Note that even these «major» factors are not independent of one another but instead affect each other (shown in bold) through a complex web of interactions (modified from Cohen, 2003)

The accumulation and preservation of thick rhythmite sequences requires a special combination of environmental conditions. There must be a periodic variation in the nature of the sediment reaching a lake floor and are favourable environment for rhythmite preservation (Kelts and Hsü, 1978; Zolitschka et al. 2000; Francus et al. 2008; Besonen et al. 2008). Kelts and Hsü (1978) proposed the following scenarios where a) bioturbation is minimised to preserve laminae, b) sedimentation rates are high even in oxic conditions, c) bottom current activity is minimised to preclude resuspension, d) the floor below the wave base is relatively extensive and flat to prevent incoherent sediment from creeping or sliding down-

slope, e) gas bubble generation is minimised so as not to disrupt lamination, f) there is a a seasonally variable flux of mineral and organic matter from epilimnion that settles through the water column, and where g) particle settling occurs fast enough for environmental variations to be transmitted to the lake floor.

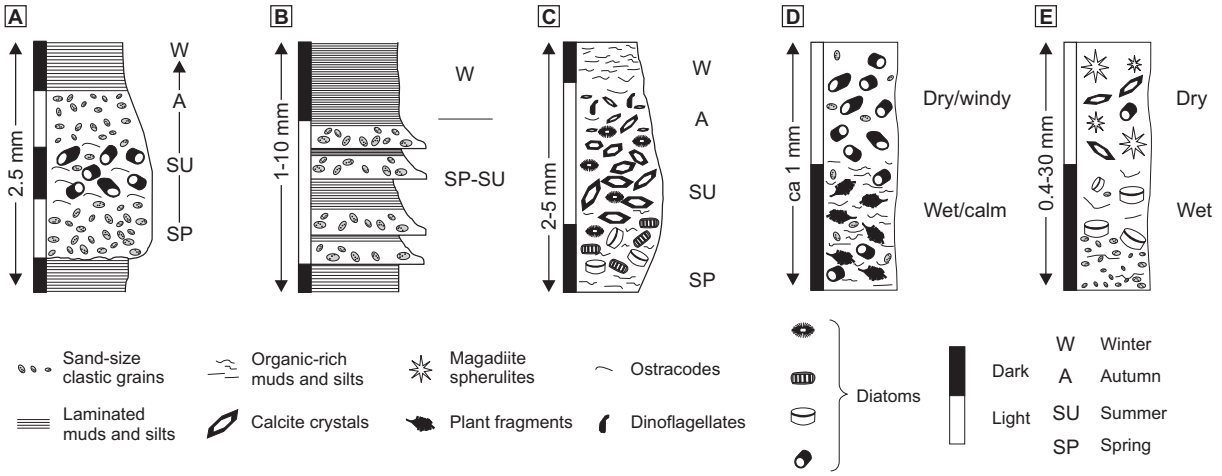

Figure 1.4. Some rhythmite types showing lithologies and relationships between compositional variations and seasonal or longer-term climate change (modified from Talbot and Allen, 1996). A) Varve from a subarctic Swedish lake (after Renberg, 1981); B) Varve from a glacial lake (after Smith and Ashley, 1985); C) non-glacial varve from a temperate hardwater lake (Lake Zürich, after Kelts and Hsü, 1978); D) non-glacial varve from Lake Malawi (after Pilskaln and Johnson, 1991); E) rhythmite from the Upper Pleistocene section in Lake Magadi, Kenya. Each couplet represents ca 2–3 years accumulation (after Damnati et al.,1992)

High-resolution lake records often display cyclical facies changes at different scales, indicative of fluctuations in productivity, lake level, and climate. Commonly, the seasonal sediment pulse is responsible for generating a rhythmic sedimentation pattern because the seasonal climate pulse governs the production, movement and deposition of sediment in the lacustrine system (Anderson and Dean, 1988; Brauer et al. 1999; Zolitschka et al. 2000). These rhythmites are termed varves. However, it is conceivable that rhythmites could represent a sediment cycle produced by other factors than the annual seasonal cycle. For example, they can record periodicities marking solar cycles (Kemp, 1996; Shunk et al. 2009) as well as climate cycles such as the ENSO phenomenon (Rittenour et al. 2000; Muñoz et al. 2002).

A great deal of research has focused on tracking the climate signal in sedimentary rhythmites (e.g. Grosjean et al. 1995; Zolitschka and Negendank, 1996; Brauer et al. 1999; Prasad et al. 2006; Kirilova et al. 2009). Hydroclimate cyclicities at different scales are evidenced by a variety of depositional trends that provide a linkage between the rhythmite pattern and climate. Laminae thickness patterns may change as a result of decadal-to centennial-scale trends in rainfall or temperature (Kelts and Hsü, 1978; Giralt et al. 1999; Romero-Viana et al. 2008). Furthermore, mineralogical and organic contrasts are also common as a result of changing moisture balance. Overall, the main problem is to distinguish the climate signals from those of catchment processes and, especially those, from human activities (Lotter and Birks, 1997).

1.2 Diatoms

Diatoms (Phyllum Heterokontophyta, Class Bacillariophyceae) are a widely distributed group of microscopic, unicellular and photosynthetic organisms that are characterised by cell walls composed of opalline or biogenic silica ($SiO_2 \cdot nH_2O$), which conforms to a particular type of skeleton called frustule (Round et al. 1990). Much of the uniqueness of diatoms is related to their silica composition (Battarbee et al. 2001). Diatoms live in lakes, oceans, rivers and streams, and many typically live as free-floating species, making up part of the ecological assemblage known as phytoplankton (Willén, 1991; Reynolds, 2006). Other species grow on various substrates forming part of the ecological assemblage known as periphyton (Theriot, 2001).

Before the emergence of diatoms about 250 Myrs ago in accordance with the estimates of the molecular-clock (Sorhannus, 2007), the phytoplankton in the seas consisted primarily of cyanobacteria and green algae that were slightly larger than bacteria (Falkowski et al. 2004). The appearance of diatoms and the emergence of other groups such as dinoflagellates and coccolithophorids led to a major shift in global organic carbon cycling. This ushered in an era of declining atmospheric CO_2 concentrations and increasing atmospheric O_2 (Armbrust, 2009). At present, the main importance of diatoms is that they contribute to 20-25% of global primary productivity (Saade and Bowler, 2009), which is equivalent to the photosynthetic activity of all the rainforests combined (Field et al. 1998; Saade and Boular, 2009).

The kind of diatoms found in lakes depends on the range and extent of habitats available for growth, and also on the combination of physical, chemical and biological conditions that prevail in the water column (Battarbee et al. 2001). Diatoms require dissolved inorganic nutrients, including CO_2, N, P, Si and a variety of metals and vitamins, to photosynthesise and reproduce (Werner, 1977). Diatom shape, form and physiology vary in ways that suggest that they have adapted to the different environments in which they occur (Theriot, 2001). They can survive in a wide gradient of pH values, concentrations of solutes, nutrients, and organic and inorganic contaminants, and across a range of water temperatures. Individual species are often restricted to specific ecological conditions which make them extremely valuable for palaeoenvironmental reconstructions (Stoermer and Smol, 1999; Battarbee et al. 2001; Crosta and Koç, 2007; Jones, 2007).

Most diatom silica is recycled through dissolution within the water column, but a fraction, typically 5–20%, is incorporated into lake sediments (Bootsma et al. 2003) and preserved as a record of environmental change. Good examples are the records of eutrophication (Hall and Smol, 1999), acidification (Birks et al. 1990) or climate change (Mackay, 2007). Diatoms do not, however, respond directly to the temperature of the atmosphere and the amount of rain (Fritz et al. 1999; Anderson, 2000). The water budget of endorheic lakes is mainly driven by changes in precipitation to evaporation balance (P/E) that bring about changes in ionic concentrations, causing a rise or a decrease in salinity and/or alkalinity, and in nutrient availability. In this way, diatoms can be used as indirect indicators of P/E in closed lake systems (e.g. Fritz et al. 1991, 1999; Gasse et al. 1997; Bao et al. 1999; Barker et al. 2002).

More recently, diatom frustules have also proved useful for chemical analysis (Swann and Leng, 2009). Stable isotopes such as $\delta^{13}C$, $\delta^{15}N$, $\delta^{18}O$ and $\delta^{30}Si$ can now be extracted from diatom silica or from the organic matter enclosed within, and used for palaenvironmental reconstructions (e.g. De La Rocha, 2002; Crosta and Shemesh, 2002; Robinson et al. 2004; Hurrell et al. 2009).

1.2.1 The diatom frustule

The cell wall of a diatom is made up of a silica-based scaffold and specific organic macromolecules (proteins and polysaccharides) (Kröger and Poulsen, 2008). Proteins located in the cell wall are believed to control the morphogenesis of the species-specific silica structure (Hecky et al. 1973; Kroger et al. 1994). Silica formation takes place in intracellular compartiments termed silica deposition vesicles (SDVs). The SDVs grow during cell division until valve formation is complete and the SDVs fuse with the cell membrane (Sumper and Kröger, 2004). Suggested functions for the siliceous cell wall include acting as an ultraviolet filter, as armour to protect against grazing by zooplankton, as ballast to control water column position, and as a buffer in the conversion of HCO_3^- to CO_2. It has also been proposed that the construction of a cell wall with silica is energetically cheaper than with organic carbon (Milligan and Morel, 2002; Hurrell, 2009).

The opalline diatom cell wall consists of two halves that are very similar in structure with one half (epitheca) that is slightly larger and overlaps the other half (hypotheca). The epitheca and hypotheca completely enclose the protoplast (Round et al. 1990). Diatoms can be divided into three major groups according to the shape and symmetry of their cell walls: radial centrics, polar centrics, and pennates (Kröger and Poulsen, 2008) (Fig. 1.5). Radial centrics have a Petri dish-like shape with a circular centre of symmetry (annulus) in the middle of the valve, and rows of pores (striae) radiating from the annulus. Polar centrics have bi- or multipolar valves with an elongated or distorted annulus. Pennate diatoms are bilaterally symmetrical and instead of an annulus they possess a rib (sternum) running along the longitudinal axis of each valve. In raphid pennates, the sternum contains a slit (raphe) that is obstructed by the central nodule in the middle of the valve (Edgar and Pickett-Heaps, 1984; Round et al. 1990).

The rigidity and architecture of the silica cell wall imposes restrictions on the mechanism of cell division and growth (Round et al. 1990). Diatom valves can only be formed during cell division, but new valves are usually smaller than the parental cell. Accordingly, the average cell size in a diatom population gradually decreases with continued vegetative growth (the MacDonald-Pfitzer rule) (Macdonald, 1869; Pfitzer, 1869; Battarbee et al. 2001). Ultimately, this reduction in size would result in cells that are too small to be viable with the result that the diatom population would die. The only way to escape this fate is by sexual reproduction (Chepurnov et al. 2004). During this process meiotic cell division takes place and the resulting gametes slough off their cell walls. Immediately after gamete fusion, a specialized zygote (auxospore) is formed, leading to a considerable increase in volume within a relatively short time (hours to a few days) (Fig. 1.6).

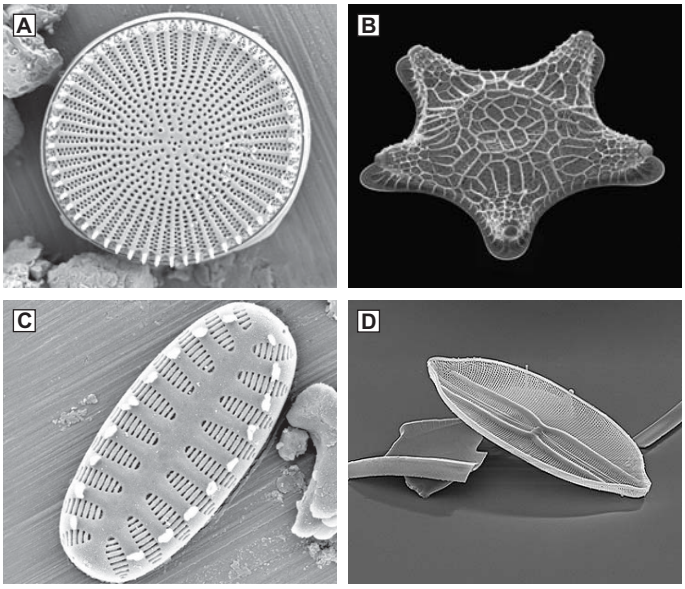

Figure 1.5. Scanning electron microscopy (SEM) images of the cell walls of four different diatom genera: A) *Cyclostephanos*, B) *Triceratium*, C) *Staurosira*, D) *Navicula*.

The silica frustules enclose the content of the cell (protoplast) which includes chloroplasts, cytoplasm, vacuoles, mitochondriae and SDVs (Sicko-Goad et al. 1984). The cell wall itself is enclosed in a brown/yellow organic biofilm (mucilage layer) that is not closely associated with the siliceous structure (Crawford et al. 2001). In a sedimentary setting, some or all of these components may be subject to diagenesis, thus altering the elemental composition and isotopic ratios required for environmental reconstructions (Hurrell, 2009). Alternatively, amino acids and long chain polyamines entombed within the structure of the silica cell wall contain carbon and nitrogen which may be independently preserved (Hecky et al. 1973; Volcani, 1981).

1.2.2 Ecology of diatoms

Despite the fact that diatoms display a wide species-specific range in their ecological preferences, they prefer aquatic environments with a turbulent regime or environments at the onset of stratification in conditions of low light, low temperature and with suficient nutrients (Willén, 1991). Although diatoms have been considered cosmopolitan (e. g. Kociolek and Spaulding, 2000), their distribution can also be due to historical constraints within geographical regions. Recent studies suggest that this distribution is regulated by the same processes that operate in macro-organisms, involving the existence of endemisms attaining unexpected high levels (Vanormelingen et al. 2008). Therefore, the study of the ecological preferences and historical distributions would help us to better understand diatom occurrences (Stoermer and Julius, 2003).

Diatoms are good competitors during periods of low light and comparatively low temperatures (Margalef, 1983). Most diatoms have temperature optima in the laboratory well above 10°C. However, they

are more abundant in lakes in spring when nutrients are in high concentration and temperatures are as low as 4°C (Werner, 1977; Theriot, 2001). Diatoms that develop during spring blooms have higher growth rates at lower light levels and lower temperatures than diatoms growing later in the year when temperature and light conditions are higher (Guillard and Kilham, 1977). Planktonic diatoms are as dense, or denser, than water, and lack all propulsion with the result that they will quickly sink in still water (Round et al. 1990). They therefore depend on the existence of a turbulent regime to avoid sinking (Margalef, 1978).

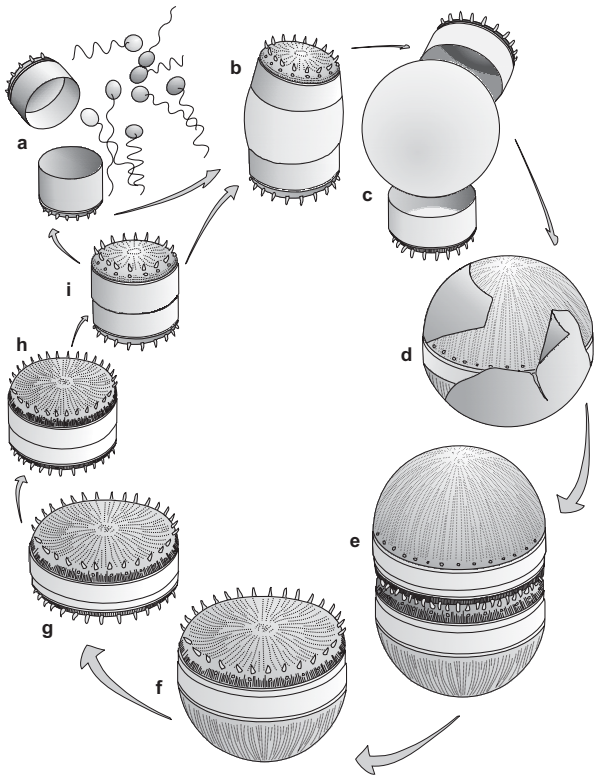

Figure 1.6. Life cycle of a diatom based on *Stephanodiscus* except that the position of the auxospore (c) and the formation of motile gametes (a) have not been seen in this particular genus; d) auxospore wall breaking open to reveal initial cell; e) first division of initial cell to form two new normal hypovalves back to back; f) one of the cells from stage (e) with a normal valve and an initial cell valve; g) a cell formed following several divisions of f) (the other valve is not illustrated but will be a replica of f); h) and i) vegetative size reduction; i) small cell which will give rise to either male or female gametes (Modified from Round et al., 1990).

Diatoms require dissolved inorganic nutrients including CO_2, N (NO_2^-, NO_3^- and/or NH_4^+), P (as PO_4^{3-} although uptake of organic phosphates may occur), Si (as dissolved $Si(OH)_4$) and a variety of metals (such as Fe) and vitamins (for instance vitamin B12) to photosynthesise and reproduce (Werner, 1977; Willén, 1991).

As stated above, C, N and P follow a more or less closely stochiometric relationship of 106:16:1 (by atoms) in healthy algae (Harris, 1986; Reynolds, 2006). Whether or not CO_2 is a limiting nutrient for diatoms in the ocean (Riebesell et al. 1993) remains a moot point (Vaulot, 2006). Si is essential for diatoms since it is necessary for the construction of the siliceous cell wall. Silica is less available in oceans than in lakes, and marine diatoms have four times less silica per cell than freshwater diatoms on average (Conley et al. 1989). In

a series of culture experiments, Tilman et al. (1982) reported the competition between different freshwater diatom specie as a function of the Si:P ratio. These authors found that large pennate diatoms were better competitors at high Si:P ratios and that small centrics required more P. Fe, which is a micronutrient, has also been found limiting in certain oceanic environments (Martin, 1992).

The complex interplay between light, temperature, nutrient concentration, turbulence, and biotic interactions throughout the annual cycle in aquatic ecosystems gives rise to a phytoplankton succession where diatoms are present (Margalef, 1983; Harris, 1986; Reynolds, 2006). A fundamental model of how phytoplankton succession proceeds is summarised in Theriot (2001). Phytoplankton generally occur in low numbers in the winter. The temperature of the water column is more or less uniform with the result that mixing is facilitated. On the other hand, there is little light for growth. Nutrient-rich deep waters circulate and are well mixed until spring, when thermal stratication commences and diatoms and other phytoplankton begin to grow. Phytoplankton reproduce at the same rate as they consume the nutrient supply. This is particularly true of silicate, which, being relatively insoluble, is transported to the sediments as diatoms die or are eaten. The freshwater and marine systems must await autumn turnover (during which nutrient-rich bottom waters are again mixed to the surface) and/or heavy runoff to return nutrients to the well-lit surface waters. In this dynamic system, nutrients are utilised and regenerated at different rates and from different sources. It may well be that absolute levels of nutrients and light do not determine diatom species. Rather, diatoms are determined by the rate at which nutrients are supplied (through regeneration by dissolution, runoff, rainfall, bacterial degradation, etc.), the ratios of nutrient concentrations and supply rates. In other words, a system with high N and high P may have the same dominant diatom as a lake with a smaller supply of these nutrients provided that the nutrient ratios are similar. This could account for the otherwise enigmatic distribution of some diatom species (Theriot, 2001).

1.3 Isotopes

Isotopes are atoms whose nuclei contain the same number of protons but a different number of neutrons (Urey, 1947). They can be divided into two main kinds: stable and radioactive species. The total number of known stable isotopes is about 300 although over 1,200 radioactive species have been discovered to date (Hoefs, 2004). Isotope exchange reactions and kinetic processes are the main phenomena that produce isotope fractionation, which is the partitioning of isotopes into two substances or two phases of the same substance (Bigeleisen and Wolfsberg, 1958; Melander and Saunders, 1980).

Differences in chemical and physical properties arising from variations in atomic mass of an element are called «isotope effects» (Bigeleisen and Mayer, 1947; Melander, 1960; Richet et al. 1977;

O'Neil, 1986; Fritz and Fontes, 1986; Clark and Fritz, 1997; Chacko et al. 2001; Schauble, 2004). These isotope effects give rise to certain differences in the physicochemical isotope properties because of mass differences. The replacement of any atom in a molecule by one of its isotopes leads to a very small change in chemical behaviour. In nature these slight differences result in isotopic fractionation according to biological, chemical and physical processes. This fractionation, which is indicated by the fractionation factor (α), is recorded in the sediments and may facilitate palaeoenvironmental reconstructions (Criss, 1999; Hoefs, 2004). This α is defined as the ratio of the numbers of any two isotopes in one chemical compound divided by the corresponding ratio of another chemical compound (Ito, 2001). However, in isotope geochemistry it is common to present isotope composition in terms of delta (δ) values and this is expressed as parts per thousand (per mil or ‰). Thus, isotopes are expressed as ratios relative to an internationally recognised standard (equation 1):

$$\delta = [(R_{compound}/R_{standard}) - 1] \cdot 10^3 \ (‰) \qquad (1)$$

where $R_{compound}$ is the absolute isotope ratio of the sample and $R_{standard}$ is the absolute isotope ratio of the laboratory standard (e.g. Ito, 2001; Schwalb, 2003; Leng and Barker, 2006). The stable isotopic composition of any compound reflects the relative proportions of the two stable isotopes. This composition shows the degree of depletion in the heavier isotope with respect to a specific standard (Fritz and Fontes, 1986; Clark and Fritz, 1997).

1.3.1 Stable isotopes in palaeoenvironmental research

Stable isotopes, such as δD, $\delta^{13}C$, $\delta^{15}N$, and $\delta^{18}O$ can be employed to better understand present and past environmental and climate evolutions of natural systems. There are several natural archives where the stable isotope analyses may be applied, such as water, marine and lacustrine sediments, bones and teeth, speleothems and tree rings (e.g. Gat, 1996; Eronen et al. 2002; Drucker et al. 2003; Leng and Marshall, 2004; Maslin and Swann, 2005; McDermott et al. 2005).

δD, $\delta^{13}C$ and $\delta^{18}O$ of the studied compound, organism or sediment reflect specific boundaries and/or environmental conditions of the water and carbon cycles at the time of their formation (Fig. 1.7). Therefore, the present isotopic behaviour of the chemical elements within these cycles must be well understood and characterised in order to interpret past isotopic oscillations recorded in the sedimentary sequences (Darling et al. 2005).

The measurement of $\delta^{18}O$ and $\delta^{13}C$ isotopes in marine sediments has played a major part in establishing stable isotopes as one of the most important sets of proxies within palaeoceanography. $\delta^{18}O$

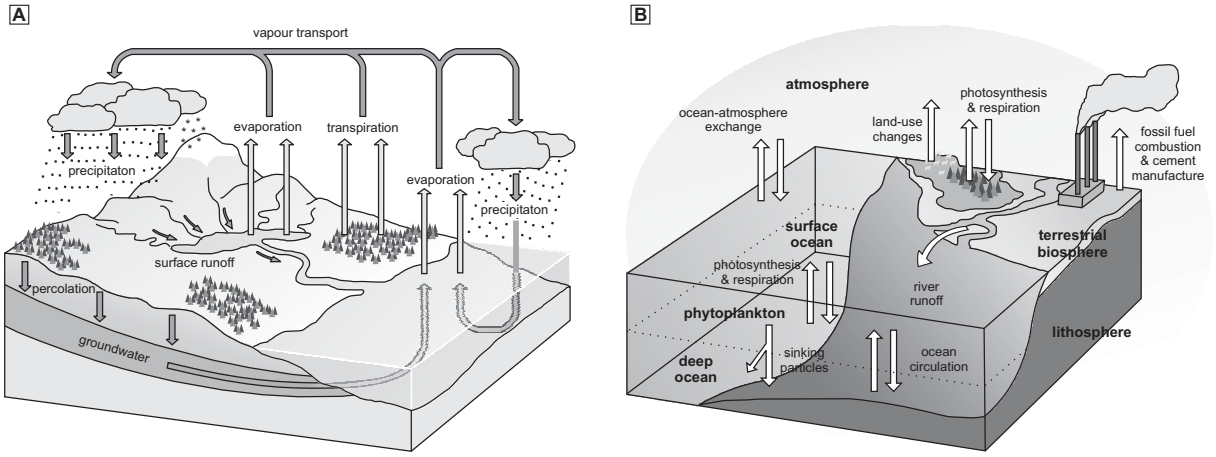

Figure 1.7. A) Block-diagram of the global water cycle. Evaporation of seawater leads to cloud formation with progressive rainout as temperature decreases. The moisture will eventually return to the sea mainly via surface runoff or groundwater flow though it may be delayed by recycling via evaporation from lakes or transpiration from vegetation. B) Block-diagram depiction of the Earth's carbon cycle, highlighting various sources and sinks for carbon. Note the arrows indicating the main relationships between the different sources and sinks

from marine sediments allow the reconstruction of past global ice volume, ocean temperatures, relative sea level, ocean circulation and structure, surface water salinity, iceberg melting, river discharge, and monsoonal intensity (e.g. Urey, 1947; Emilliani, 1955; Shackleton and Opdyke, 1973; Tiedemann et al. 1994; Shemesh et al. 1995; Shackleton et al. 1995; Niebler et al. 1999; Maslin and Burns, 2000; Zachos et al. 2001; Skinner et al. 2003; Maslin and Swann, 2005). $\delta^{13}C_{carbonates}$, $\delta^{13}C_{bulk}$ and $\delta^{13}C_{diatom}$ from marine sediments can provide information on the past carbon cycle over a range of time-scales, offering a useful insight into past marine productivity, ocean circulation, past surface water, atmospheric CO_2, and storage and exchange of carbon at both local and global scales (Berger et al. 1978; Sarnthein et al. 1994; Andersen et al. 1999; Ruhlemann et al. 1999; Rosenthal et al. 2000; Kennett et al. 2003).

Stable isotopes in palaeolimnology

Stable isotope composition of lacustrine sedimentary materials can yield a wide range of useful palaeoclimate information (Leng et al. 2005b). Stable isotope studies have become an essential part of palaeolimnology since McCrea (1950) and Urey et al. (1951) highlighted the potential of oxygen isotope composition for palaeotemperature reconstruction. $\delta^{18}O$ are the main isotopes used in palaeolimnology although other palaeoenvironmental information can be obtained from δD, $\delta^{13}C$ and $\delta^{15}N$ in lacustrine biogenic materials (Leng et al. 2005b). It is possible to measure several stable isotope ratios (e.g. δD, $\delta^{13}C$, $\delta^{15}N$, $\delta^{18}O$) from either bulk lake sediments or any organic and/or inorganic compound depending on the kind of material incorporated into the lake deposits (Fig. 1.8).

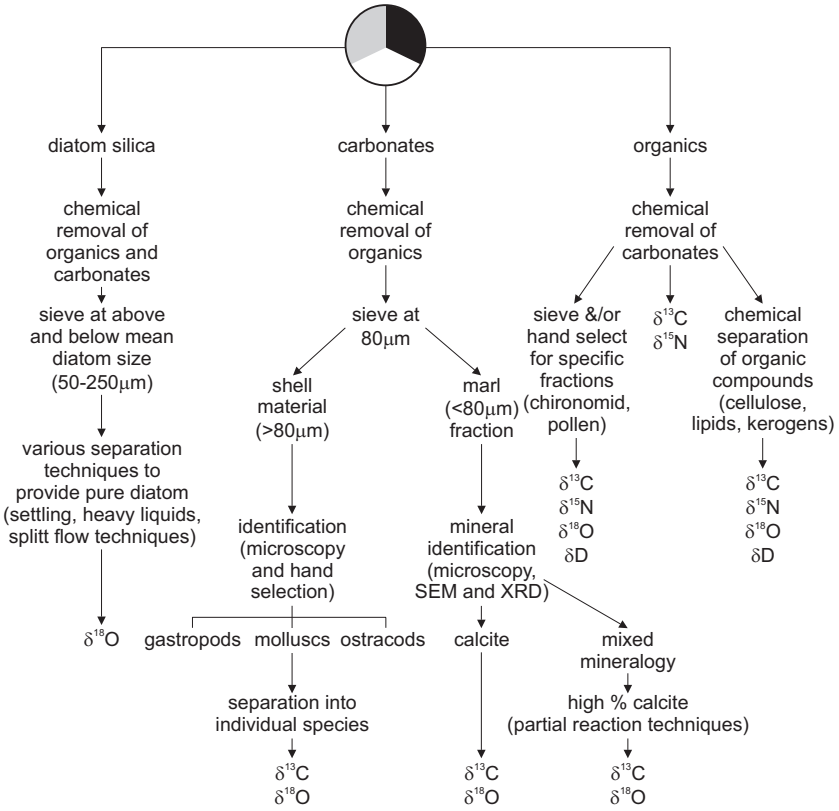

Figure 1.8. Flow diagram showing the most common materials analysed by isotope analysis in lake sediments, and the laboratory pretreatments required (Leng et al. 2005b).

The $\delta^{13}C_{bulk}$ in lake sediments are important for assessing organic matter sources, reconstructing past productivity rates and for identifying changes in the availability of nutrients in surface waters. Increases in the accumulation rates of organic matter and its $\delta^{13}C$ have been widely used as an indicator of enhanced aquatic productivity in lakes (Hollander and McKenzie, 1991; Brenner et al. 1999; Meyers, 2003). The $\delta^{13}C_{bulk}$ are proxies for palaeoenvironmental changes in lake watersheds as well as in the lakes themselves (Meyers and Teranes, 2001). Although the $\delta^{15}N_{bulk}$ are less used, they can also help to distinguish the sources of this material and reconstruct past productivity rates (Gu et al. 1996, Talbot and Laerdal, 2000). This proxy is particularly useful in identifying changes in the past availability of nitrogen used by aquatic primary producers. However, the dynamics of nitrogen biogeochemical cycling is very complicated. Changes in nitrogen cycling that accompany anthropogenic eutrophication of lakes can also exert a strong influence on the $\delta^{15}N_{bulk}$ (Brenner et al. 1999; Teranes and Bernasconi, 2000). This does not facilitate $\delta^{15}N$ interpretations of sedimentary records (Fogel and Cifuentes, 1993; Brenner et al. 1999; Talbot, 2001; Meyers, 2003). Despite their great potential for providing palaeolimnological information, oxygen and hydrogen isotopic compositions of organic matter have rarely been determined in sedimentary records because of practical difficulties in their analysis (Meyers and Teranes, 2001).

Isotope analyses in carbonates constitute an ideal tool for identifying the mechanisms that cause their accumulation in lake sediments, enabling the reconstruction of the history of a lake body (e.g. Schelske and Hodell, 1991; Thompson et al. 1997; Hodell et al. 1998; Ricketts and Anderson, 1998; Filippi et al. 1999). The ability to distinguish the carbonate sources archived in lacustrine carbonates through stable isotope analyses demand a thorough understanding of the local lake dynamics and the biology of the lake system (Gierlowski-Kordesch, 2010). Detailed studies of the climate, hydrology and the provenance of a lake are necessary for a reliable reconstruction and interpretation of the isotope signals archived in its sedimentary carbonates (Ito, 2001; Leng and Marshall, 2004). $\delta^{13}C$ of lake waters is influenced by the geochemical composition of input waters, atmospheric CO_2 exchange, gas mixing through bacterial methanogenesis in the degradation of organic matter, and pelagial photosynthesis (McKenzie, 1985; Talbot and Kelts, 1990). On the other hand, $\delta^{18}O$ is influenced by the isotopic composition of waters supplied to the lake, including rainfall, surface inflow, and groundwater inflow (Leng and Marshall, 2004). Temperature, and thus evaporation, also controls the output of the lighter oxygen (^{16}O), affecting the isotope ratio. Changes in temperature, rainfall sources (especially through seasonal changes), P/E, riverine influx, and even groundwater input are postulated to have been preserved as $\delta^{18}O_{carbonates}$ precipitating in lake waters (Teranes et al. 1999; Lamb et al. 2000; Schwalb and Dean, 2002; Leng and Marshall, 2004; Yansa et al. 2007).

Biogenic silica in lacustrine sediments is deposited by a variety of aquatic organisms, including diatoms and sponges, and its study is especially useful in lakes with no endogenic carbonates (Leng and Marshall, 2004; Leng and Barker, 2006). Measurements of $\delta^{18}O_{diatom}$ provide a potentially important source of palaeolimnological information equivalent to that from $\delta^{18}O_{carbonate}$. $\delta^{18}O_{diatom}$ has been used as a proxy for temperature change in some studies (e.g. Rietti-Shati et al. 1998; Rosqvist et al. 1999; Leng et al. 2001; Hu and Shemesh, 2003) although the temperature dependence of oxygen isotope fractionation between diatom silica and water continues to be controversial. The use of $\delta^{18}O_{diatom}$ in terms of variations in the isotope composition of the lake water due to changes in P/E or in the source of precipitation has become more rational (e.g. Barker et al. 2001, 2007; Shemesh et al. 2001; Jonsson et al. 2010). A new approach involving a combined methodology for analysing $\delta^{18}O_{diatom}$ and $\delta^{30}Si_{diatom}$ in the same sample has recently been implemented (Leng and Sloane, 2008; Swann et al. 2010). In conjunction with separate analyses on $\delta^{13}C_{diatom}$ and $\delta^{15}N_{diatom}$, this will permit a more detailed, isotope based reconstruction of carbon and nitrogen cycles (Hurrell et al. submitted). To date, few studies have focused on the combined analysis of $\delta^{18}O_{diatom}$, $\delta^{30}Si_{diatom}$, $\delta^{13}C_{diatom}$ and/or $\delta^{15}N_{diatom}$ at the same site (Hurrell, 2009; Swann et al. 2010; Hernández et al. submitted).

1.3.2 Stable oxygen isotopes

$\delta^{18}O$ can be obtained from a large range of organic and inorganic materials from different sources. It is essential to obtain accurate information about how rainfall isotope compositions are determined by climate in order to better understand the environmental signal contained within the isotope composition from different materials (Leng et al. 2005b). The water cycle is especially important, since it is the precursor back to which most $\delta^{18}O$ studies are attempting to relate (Clark and Fritz, 1997). While the concept of the water cycle may be simple in essence –water evaporates from the sea, falls as rain over land, and eventually returns to the sea mainly via river and groundwater discharge (Fig. 1.7)– there are a number of complicating factors at least where $\delta^{18}O$ are concerned, such as seasonal freeze-thaw, plant transpiration, soil evaporation and/or evaporation from surface waters (Dincer et al. 1974; Allison et al. 1984; Berner and Berner, 1987). In particular, lake sediments are an important archive for climate change, and it is therefore vital to improve our understanding of the often complex isotopic relationship between individual lakes and regional precipitation (Darling et al. 2005).

$\delta^{18}O_{carb/diatom}$ is controlled by water temperature and by the isotope composition of the lake water from which the mineral is formed (Stuiver, 1968)(Fig. 1.9). If the mineral is precipitated in isotope equilibrium with the lake water, then mineral–water fractionation equations may be used to estimate variations in past temperatures providing there is no change in the $\delta^{18}O_{lakewater}$ (Leng and Marshall, 2004). A thorough understanding of the factors that may have influenced the isotope composition of the lake water ($\delta^{18}O_{lakewater}$ on Fig. 1.9) is necessary to correctly interpret the $\delta^{18}O$ signal from the analysed mineral

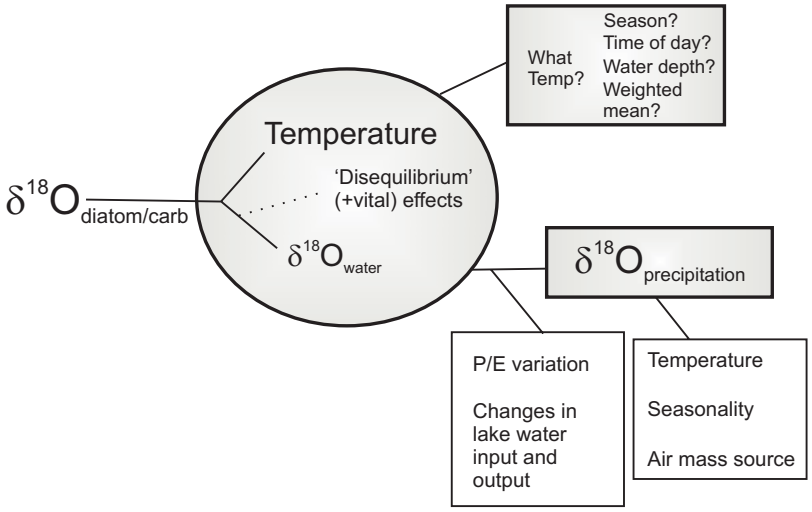

Figure 1.9. Controls on the oxygen isotope composition of lacustrine diatom silica and carbonates ($\delta^{18}O_{diatom/carb}$). If biogenic material is precipitated in isotopic equilibrium, $\delta^{18}O_{diatom/carb}$ depends entirely on temperature and on the isotopic composition of the lake water ($\delta^{18}O_{lakewater}$). Disequilibrium effects, commonly known as 'vital effects' in biogenic precipitates caused by local changes in microenvironment or by the rate of precipitation can induce systematic or non-systematic offsets in the $\delta^{18}O_{diatom/carb}$ signal (modified from Leng and Marshall, 2004 and Leng and Barker, 2006)

or organic compound. The $\delta^{18}O_{lakewater}$ in hydrologically open lakes usually reflects the isotope composition of precipitation ($\delta^{18}O_{precipitation}$), both rain and snowfall, received by the lake, whereas oscillations of $\delta^{18}O_{lakewater}$ in closed lakes respond predominantly to the P/E (Ito, 2001; Leng and Barker, 2006). Moreover, disequilibrium effects (vital effects in biogenic materials) (Fig. 1.9) should also be taken into account when the material analysed is composed by more than one taxon.

Stable oxygen isotopes from diatoms

All silicates, including diatom silica, are composed of silica tetrahedrons. Following the uptake and fractionation of oxygen, covalent Si–O–Si bonds are formed in the diatom frustule through the condensation of two Si–OH groups to form $(SiO_2)_n$ (Labeyre and Juillet, 1982) (Fig. 1.10). Within the centre of the diatom frustule the –Si–O–Si bonds form an isotopically homogeneous dense layer of silica, the $\delta^{18}O_{diatom}$ of which is assumed to reflect $\delta^{18}O$ from the water in which the silica precipitated at a given temperature (Juillet, 1980a,b).

Research on $\delta^{18}O_{diatom}$ was first developed in marine sedimentary records (e.g. Labeyrie, 1974; Labeyrie and Juillet, 1982, Labeyrie et al. 1984; Shemesh et al. 1993, 1995). Nonetheless, in the last decade, the $\delta^{18}O_{diatom}$ in lacustrine sediments has increased in number since carbonates may be rare (or absent) in non-alkaline, dilute, and/or open lakes (Leng and Marshall, 2004). Such lakes are common at high-altitudes and are ideal for investigating climate change using $\delta^{18}O$ because the isotope composition of the lake water is often similar to that of meteoric water (on either an annual or seasonal basis) (Leng and Barker, 2006).

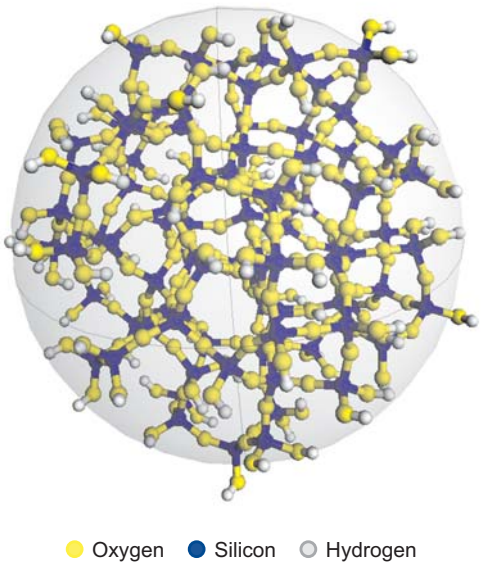

Figure 1.10. Structure of biogenic silica showing a 2nm particle. The core of the particle is the only part predominantly made up of Q4 and subsequent layers contain a mixture of Qn species. Q represents a silicon atom surrounded by four oxygen atoms and suffix n gives the number of surrounding oxygen atoms (out of 4) that are bonded to another silicon atom. Typically, the amount of Q1 and Q2 is small and therefore the level of hydration is studied as a ratio of Q4/Q3. A higher ratio implies lower hydration and a higher atomic organisation of biogenic silica (Leng et al. 2009).

The $\delta^{18}O_{diatom}$ record results from a) changes in P/E (e.g. Barker et al. 2007), b) changes in lake temperature assuming that the $\delta^{18}O_{diatom}$ does not vary (e.g. Hu and Shemesh, 2003), c) oscillations in $\delta^{18}O$ or temperature at the source of the precipitation (e.g. Swann et al. 2010) or d) changes in isotopic composition of $\delta^{18}O_{lakewater}$ related to fluctuations in the contribution of precipitation from different sources (e.g. Rosqvist et al. 2004). Naturally, more than one effect is possible, and different effects may predominate at different times with the result that identification is not easy (Jones et al. 2004; Morley et al. 2005; Leng and Barker, 2006).

1.3.3 Stable carbon isotopes

The carbon cycle is much more complex than the water cycle even if our attention is restricted to dissolved organic (DOC) and inorganic (DIC) carbon in water (Fig. 1.7). This is because there are several sources of carbon in contrast to the single source of water (precipitation). $\delta^{13}C$ are crucial for palaeoenvironmental reconstructions because they are affected by many factors that may be more or less related to climate. They have considerable potential for the interpretation of past environmental conditions where the overall geochemical conceptual model can be suitably constrained (Darling et al. 2005).

In particular, the lake carbon pool is a complex mixture of DIC and DOC derived from internal biological and chemical processes and inputs from the catchment (Fig. 1.11) (Meyers and Teranes, 2001; Duarte and Praire, 2005; Cole et al. 2007). Inorganic carbon isotope ratios from DIC in lake waters ($\delta^{13}C_{DIC}$) are useful as tracers of environmentally determined processes which are often attributed to climate change (Leng and Marshall, 2004). In general, there are three predominant processes that control $\delta^{13}C_{DIC}$: a) annual turnovers that mix low $\delta^{13}C_{DIC}$ from oxidised or respired organics from the lake bottom throughout the water column (Ito, 2001; Houser et al. 2003); b) extraction of low $\delta^{13}C_{DIC}$ from CO_2 by photosynthesis, atmosphere-water exchange or evasion of CO_2 from water (Cole et al. 1994); and c) input of DIC or DOC into the lake from surface runoff and groundwater inflow (Ito, 2001). Additionally, the release of methane from surface sediments by methanotrophic bacteria can also create an isotopically depleted DIC pool (Boschker and Middelburg, 2002) (Fig. 1.11).

Lacustrine DOC is derived from allochthonous organic material or through autochthonous productivity. Lake derived organic matter, such as phytoplankton and macrophytes, is added to the DOC pool (Meyers and Teranes, 2001). The $\delta^{13}C$ of the DOC ($\delta^{13}C_{DOC}$) in the lake water body reflects the isotopic composition of the source materials. Although DOC inputs from the catchment are large, they are often in a form not readily available to aquatic organisms (Pace et al. 2004; Brönmark and Hansson, 2005). However, oxidation of terrestrial DOC and respiration of bacteria that feed on DOC can contribute a considerable amount of DIC to lakes (Tranvik, 1988; Jonsson et al. 2001; Cole et al. 2002) (Fig. 1.11).

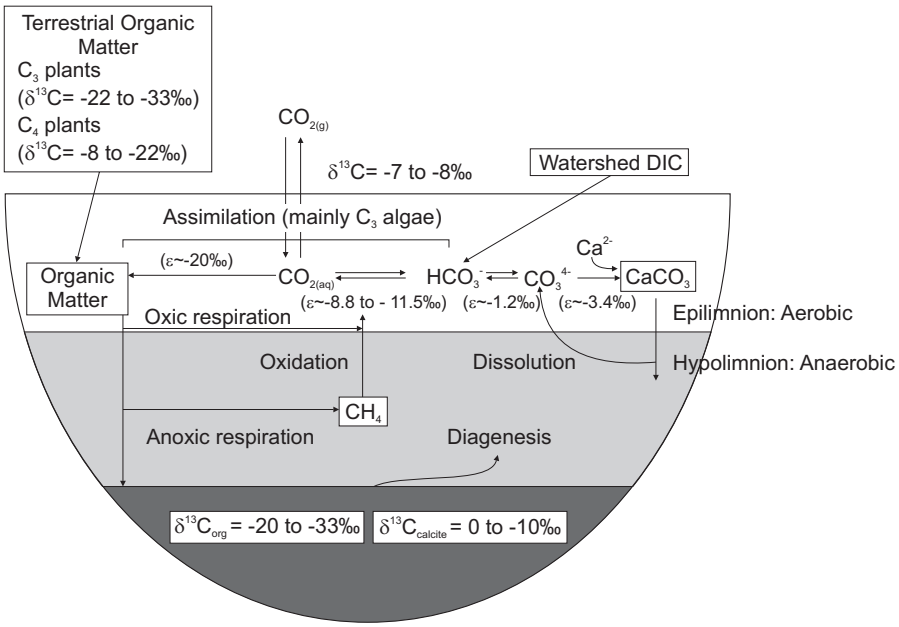

Figure 1.11. Idealised carbon isotope cycle in a small stratified lake. The isotopic composition of organic matter buried in sediments is determined by the proportions of different terrestrial and lacustrine organic matter, the carbon isotopic composition of dissolved inorganic carbon (DIC), and the rates of primary production and respiration within the water column. Isotope enrichment factors (ε), listed here as the difference between the product and the substrate, vary with the form of DIC, which is assimilated by lake algae (e.g. $CO_{2(aq)}$ or HCO_3^-). Inorganic carbonate ($CaCO_3$) typically forms in isotopic equilibrium with the DIC pool and, as such, is indirectly affected by organic matter sources and primary production and respiration rates (modified from Meyers and Teranes, 2001).

Stable carbon isotopes from diatoms

Although diatoms require carbon, usually in the form of CO_2, for photosynthesis (Werner, 1977), they are also able to utilise HCO_3^- through biophysical concentrating mechanisms (Johnston et al.2001; Milligan and Morel, 2002).

A complex set of biological and physical factors control $\delta^{13}C_{diatom}$. The literature suggests primary productivity and $CO_{2(aq)}$ concentration as the main factors that may determine the $\delta^{13}C_{diatom}$ (Shemesh et al. 1993, 2002; Singer and Shemesh, 1995, Crosta and Shemesh, 2002; Schneider-Mor et al. 2005). However, other factors such as diatom growth rate, carbon source, metabolic pathway, diatom shape and/or taxonomic composition can also influence the isotopic signal of organic matter (Fry, 1996; Laws et al. 1997; Gervais and Riebesell, 2001). Furthermore, this organic matter, which is enclosed in the diatom cell wall, is not altered by diagenesis with the result that it is useful in palaeoenvironmental reconstructions (Des Combes et al. 2008).

The interpretation $\delta^{13}C_{diatom}$ is not simple. The most common interpretation which relates higher $\delta^{13}C_{diatom}$ values to high productivity events in marine sediments is in apparent contradiction to the recent results found at other lacustrine sites (Hurrell et al. submitted). Alternatively, $\delta^{13}C_{diatom}$ in lacustrine sediments can also be used to interpret lake-catchment interactions (Hurrell et al. submitted). These findings have important implications for the understanding of the global carbon budget. They show that

the most productive lakes emit more CO_2 into the atmosphere than can be sequestered. This is because carbon inputs prevent carbon limitation (Talling, 1976).

1.4 Aims

The aims of this PhD Thesis are twofold: a) to explore the possibilities that the study of $\delta^{18}O_{diatom}$ and $\delta^{13}C_{diatom}$ can offer in palaeoenvironmental reconstructions, and b) to carry out high- and ultra-high resolution environmental and climate reconstructions in the Andean Altiplano during the Late Glacial-Early Holocene transition using these stable isotopes.

1.5 Thesis structure

This PhD thesis is concerned with an environmental reconstruction based on the study of stable isotopes in diatom silica from lake sediments. Chapter 1 provides a state-of-the-art introduction to lakes, diatoms and isotopes. The regional geographical and geological settings as well as the modern and ancient climates of the Central Andes and the studied site are presented in Chapter 2. This thesis forms part of a major work carried out by a multidisciplinary research group with scientists belonging to the Institut de Ciències de la Terra, 'Jaume Almera'- Consejo Superior de Investigaciones Científicas (ICTJA-CSIC), the Universities of A Coruña (UDC), Barcelona (UB) and Católica del Norte (UCN), the Instituto Pirenaico de Ecologia (IPE-CSIC), the NERC Isotopes Geosciences Laboratory (NIGL) and the Lancaster Environmental Center (LEC). Chapter 2 sets out the scientific context of the thesis. The methodological procedures employed are descibed in Chapter 3.

A detailed petrographical study is a prerequisite for verifying the reliability of the sedimentary record for a robust palaeoenvironmental reconstruction. This is developed in Chapters 4 and 6. The thesis also focuses on new and poorly documented fields where $\delta^{18}O_{diatom}$ and $\delta^{13}C_{diatom}$ can successfully be applied to lacustrine sediments. It shows how stable isotopes from diatom silica may be used a) to highlight the importance of reconstructing the different evolutionary stages of lake ontogeny given that climate derived palaeohydrological signals can be distorted by changes in lake morphology (Chapter 4); b) as a main proxy in ultra-high resolution moisture balance reconstructions forced by fluctuations in the intensity of the ENSO and solar activities (Chapter 5); c) to reveal the major biogeochemical processes that give rise to the formation of rhythmites (Chapter 6), and finally d) to reconstruct the regional environmental evolution at centennial-to-millenial time scales (Chapter 7).

The conclusions are grouped according to their methodological, limnological or climate implications and are presented in Chapter 8. Finally, the raw data obtained during the experimental processes, and the original published papers are contained in the appendices.

Chapter 2

Geological, geographical, limnological and climate framework

2.1 Geographical and geological setting

The Andes (8,000 km long and up to 750 km wide), the dominant landform of South America, extends along the entire western coast (Fig. 2.1). They are the result of the oblique subduction of the Nazca Plate (oceanic plate) beneath the South-American Plate (continental plate) (Dewey and Bird, 1970; James, 1971; Allmendinger and Jordan, 1997). Subduction began soon after the breakup of Rodinia in Late Proterozoic times, and since then it has been intermittently active up to the present (Ramos, 2009). The highest peaks in the southern tropical and subtropical Andes exceed altitudes of 6,000 m; ice caps and glaciers are present where the atmospheric circulation systems provide sufficient moisture for snow and ice accumulation (Zech et al. 2009) (Fig. 2.1).

The Andes constitute a unique physiogeographical setting with vertical gradients ranging from sea level up to peaks that exceed 6,000 m in less than 150 km. This mountain range resulted from a Cenozoic tectonic uplift in the forearc region of the active tectonic convergence zone (Stecker et al. 2007; Grosjean et al. 2007). A longitudinal tectonic segmentation that has been ascribed to dip variations in the flat subduction of the Nazca Plate is observed in the Andes. Structures involving the basement (thick-skinned) with no volcanism are developed in the low-angle subduction zones, whereas thin-skinned structures associated with volcanism are present in high-angle subduction zones (Carrera, 2009).

The geological features of this active orogen resulted from a succession of orogenic cycles that probably started during the Late Precambrian and continued during Phanerozoic times (Ramos, 1994, 2009). Two major tectono-sedimentary super-cycles are commonly distinguished in the Andes: the Pre-Andean Cycle (mostly Paleozoic-Early Triassic in age) and the Andean Cycle (mostly Permian-Early Triassic to Cenozoic), which is responsible for the present Andean uplift (Coira et al. 1982).

According to the main features of the subducted plate, the Andes has been sub-divided into different geological regions: Northern Andes (5-15° S), Central Andes (15-33.5° S), Southern Andes (33.5-47° S) and Austral Andes (47-56° S) (Tassara and Yañez, 2003).

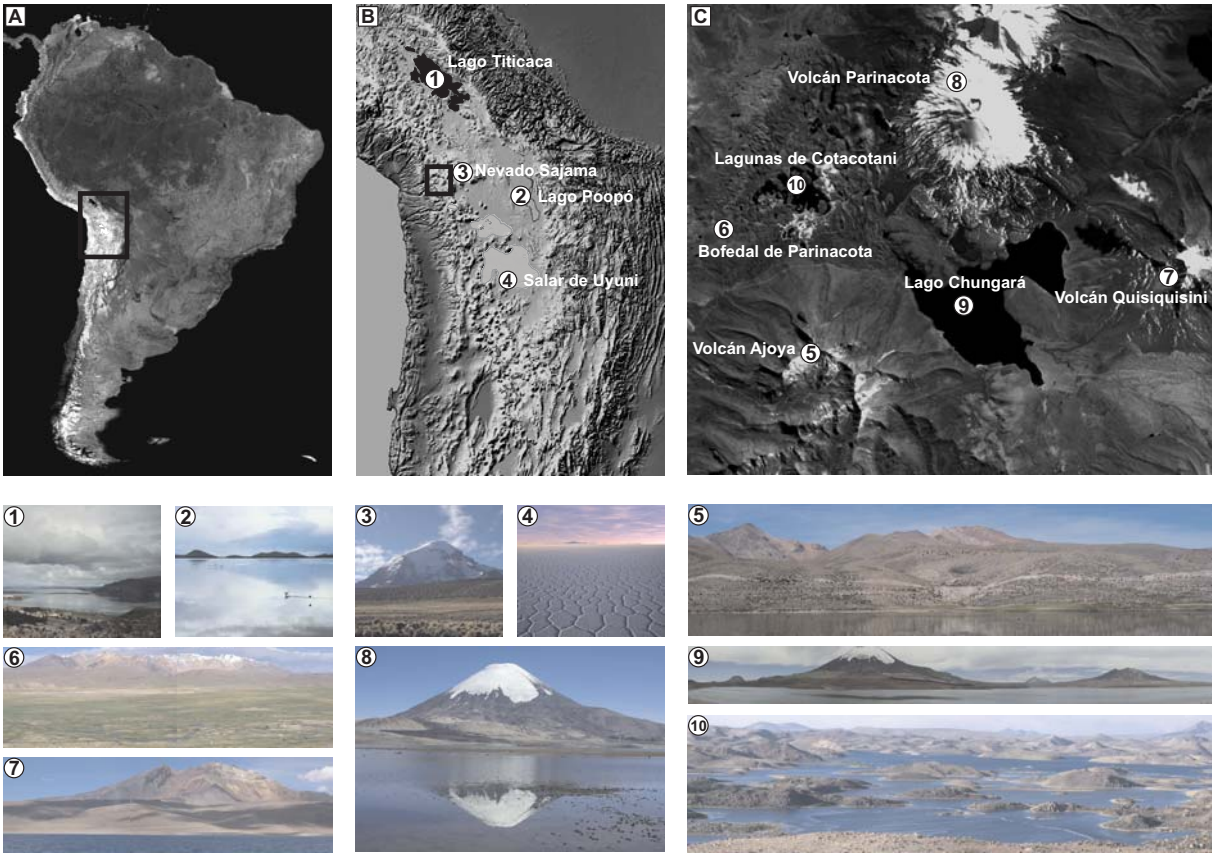

Figure 2.1. Satellite images of A) South America, B) Andean Altiplano, C) Lago Chungará. Square on the image depicts the position of the following image. Numbers indicate the position of the main geographical features shown in the pictures: 1) Lago Titicaca (Perú-Bolivia), 2) Lago Popoó (Bolivia), 3) Nevado Sajama (Bolivia), 4) Salar de Uyuni (Bolivia), 5) Volcan Ajoya (Chile), 6) Bofedal de Parinacota (Chile), 7) Vocan Quisiquisini (Chile-Bolivia), 8) Volcan Parinacota (Chile), 9) Lago Chungará (Chile), 10) Lagunas de Cotacotani (Chile).

2.1.1 The Central Andes

The geological region of the Central Andes is where the Andean orogen attains its maximum height and width. Tectonic, sedimentary and magmatic processes closely interplayed in the Central Andes, which can be sub-divided into different morphostructural units. From West to East, these include Cordillera de la Costa, Valle Longitudinal, Precordillera Andina, Cordillera Occidental, Altiplano or Puna, Cordillera Oriental, and in the easternmost part before reaching the Chaco, from North to South, the Sierras Subandinas, Sistema de Santa Bárbara or Sierras Pampeanas (Coutand et al. 2001) (Fig. 2.2).

The Andean Altiplano is a segment of the Andean orogenic belt between 14° and 27° S, which consists of Northern Chile and Argentina, Western Bolivia and Southern Perú (Isacks, 1988; Strecker et al. 2007) (Fig. 2.1). At present, this high-elevation Plateau (~3,500 – 4,100 m) is an area of inland drainage (endorheic) formed during an uplift ~30 Myrs ago (Gregory-Wodzicki, 2000; Orme, 2007) owing to the compression of the western rim of the South American Plate due to the subduction of the Nazca Plate

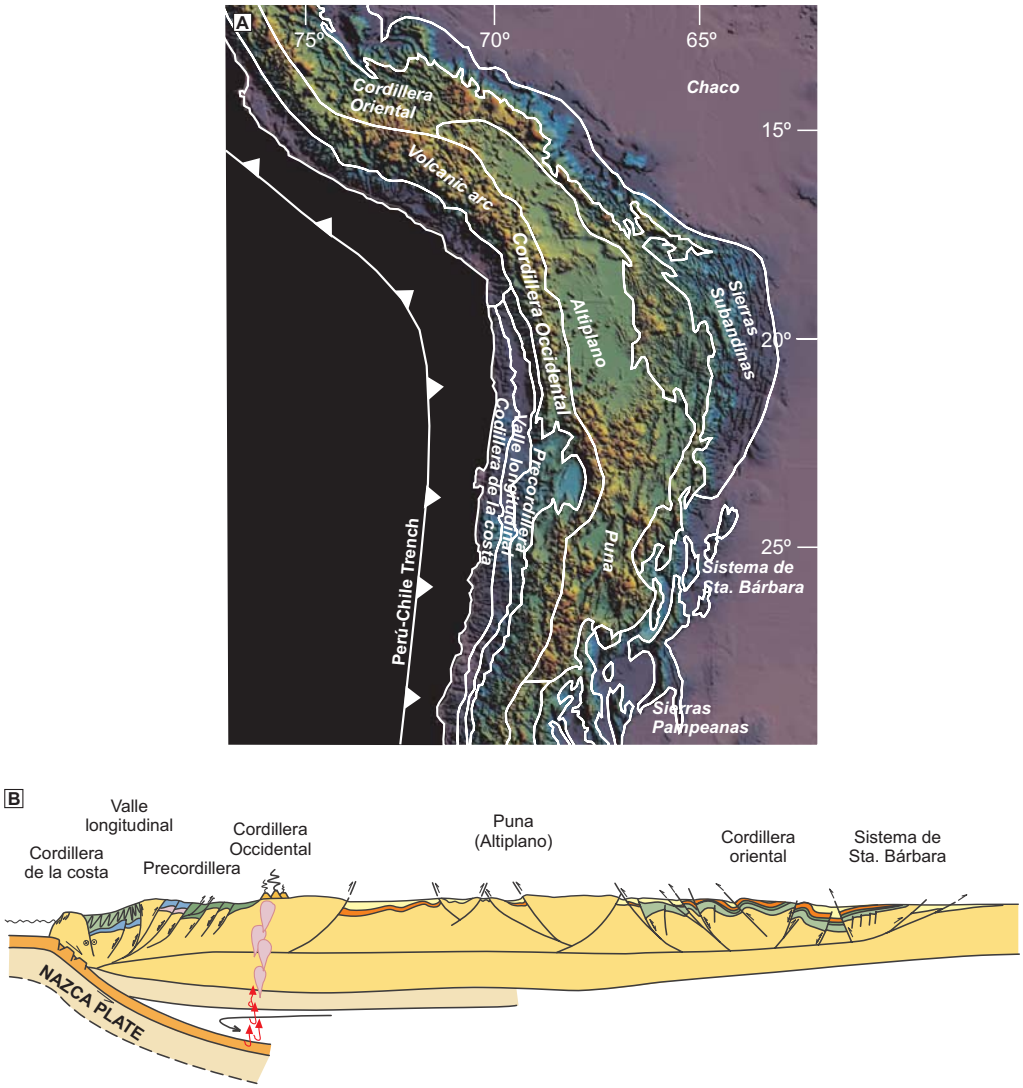

Figure 2.2. A) Main morphostructural units from the Central Andes (from West to East): Cordillera de la Costa, Valle Longitudinal, Precordillera Andina, Cordillera Occidental, Altiplano or Puna, Cordillera Oriental, and, from North to South, Sierras Subandinas, Sistema de Santa Bárbara or Sierras Pampeanas, and the Chaco. Note the position of Lago Chungará. Modified from Coutand et al. (2001) and Amilibia (2002). B) General cross-section of the Central Andes at 25.5º S. Modified from Muñoz et al. (2004).

and the Antarctic Plate (Allmendinger et al. 1997). It attains a width of 350–400 km and is dominated by massive active volcanoes (Wörner et al. 2000). The most prominent features that define this non-collisional orogen are the subducting Nazca plate and its associated trench, the present day active volcanic arc and the fold-and-thrust belt in the foreland (Whitman et al. 1996). The modern lithospheric thickness is roughly 150 km beneath the Altiplano (Whitman et al. 1996). The Andean Altiplano is characterised by the presence of thick syn-orogenic sediments (up to 3 km) lying directly over the Precambrian or Paleozoic basement (Carrera, 2009). These syn-orogenic sediments were deposited and preserved in intra-mountain basins. Their growth geometries and disconformities show that the development of the present thrusts began during the Paleogene and continued developing until the Present (Ramos, 1999; Coutand et al. 2001).

Lago Chungará region

Lago Chungará (18°15'S, 69°10'W, 4,520 m asl) is located on the Andean Altiplano (Central Andes, Chile) in a highly active tectonic and volcanic context (Clavero et al. 2002; Hora et al. 2007). It lies on the northeastern edge of the Lauca basin, which is the westernmost and also the highest fluvio-lacustrine basin of the Altiplano. Lago Chungará is filled with an Upper Miocene to Pliocene volcaniclastic alluvial and lacustrine sedimentary succession (> 120m thick) that rests unconformably on an Upper Cretaceous–Lower Miocene volcanic substrate (Kött et al. 1995; Gaupp et al. 1999). In particular, the lake forms part of the small hydrologically closed Chungará Sub-Basin. It came into existence as a result of a debris avalanche during the partial collapse of the Parinacota Volcano, which dammed the former Lauca River. Lago Chungará and Lagunas Cotacotani were formed almost immediately (Fig. 2.1). However, the age of this collapse is not well constrained, with estimates ranging from 13,000 to 20,000 years BP (Wörner et al. 2000; Clavero et al. 2002, 2004; Hora et al. 2007).

The area surrounding Lago Chungará and Lagunas Cotacotani has been characterised by intermittent volcanic activity since the Miocene until the present (Katsui and González-Ferrán, 1968; Wörner et al. 1988; Clavero et al. 2002). There are three main volcanoes surrounding the lake: Parinacota, Ajoya and Quisiquisini (Fig. 2.1). Parinacota volcano is a conic and symmetric stratovolcano (6,342 m asl) with excellent lava flows and dome preservation. The most distal lava flows of the southern volcano flank coincide with the northern boundary of Lago Chungará. Lagunas Cotacotani, which are located on debris avalanche deposits on the western volcano flank, formed during the collapse of Parinacota volcano (Clavero et al. 2002) (Fig. 2.1). The most recent lava flows of the Parinacota volcano are located on the southern and western flanks and are composed of dark grey-colour basaltic-andesitic lavas. Parinacota has been the only active volcano in the Lago Chungará watershed during the Holocene (Wörner et al. 1988; de Silva and Francis, 1991). The Miocene-age eroded Ajoya volcano is situated on the southern boundary of Lago Chungará (Fig. 2.1) and its grey-colour lavas are mainly andesitic with porphyritic textures of plagioclase, hornblende and pyroxene phenocrystals (Katsui and González-Ferrán, 1968). Despite the presence of an ancient crater at the top, it is not possible to identify the lava flows of this volcano. The Pleistocene-age Quisiquisini volcano is located along the eastern boundary of Lago Chungará. It is also very eroded and is largely made up of andesitic lavas and tuffs (Katsui and González-Ferrán, 1968).

2.2 Climate Framework

Given its vast extension across the equator from about 10°N to 55°S, South America displays a large distribution of tropical to extratropical climates. Superimposed on the mean north-to-south

variations are significant east–west asymmetries across the continent due to a) the presence of the Andes, b) changes in the continental width (broad at low- latitudes, narrow at mid-latitudes), and c) the boundary conditions imposed by the cold south-eastern Pacific and the warm south-western Atlantic oceans (Sylvestre, 2009). The sea surface temperature (SST) anomalies in association with the ENSO, the Pacific Decadal Oscillation (PDO), the Antarctic Oscillation (AAO), or the North Atlantic oscillation (NAO) significantly contribute to the climate variability of the continent (Garreaud et al. 2009).

2.2.1 Modern Climate

The InterTropical Convergence Zone (ITCZ) is a belt of low pressure created by the convergence of northeast and southeast trade winds over the equatorial oceans (Barry and Chorley, 1992; McGregor and Nieuwolt, 1998). This zone is east–west oriented over the tropical oceans (Fig. 2.3). The rainfall in South America exhibits the highest values along the ITCZ over the continent (Garreaud et al. 2009). This rainfall is mainly convective and is produced by deep cumulus–nimbus (Mitchell and Wallace, 1992). During summer months (December to February), strong surface heating in the Southern Hemisphere results in the southerly location of the ITCZ, whilst strong surface heating in the Northern Hemisphere between July and August causes the ITCZ to migrate north of the Equator (McGregor and Nieuwolt, 1998). Thus, during the austral winter the north of the equator experiences maximum rainfall in accordance with the oceanic ITCZ, whereas the central part of the continent (including southern Amazonia) undergoes its dry season (Garreaud et al. 2009). During the austral fall, the rainfall maximum gradually returns to northern South America. Such migration has led many scientists to describe the climate of the central part of South America as monsoon-like (Zhou and Lau, 1998; Vera et al. 2006). The climate is not fully monsoonal, however, because the low-level winds never reverse their direction. In contrast to the copious precipitation near the ITCZ, rainfall is almost absent over broad areas of the subtropical oceans owing to the large-scale mid-tropospheric subsidence (Garreaud et al. 2009).

At present, the seasonal rainfall cycle over South America is dominated in tropical latitudes by the so-called South American Summer Monsoon (SASM) (Zhou and Lau, 1998). Rainfall over the Andean Altiplano originates primarily from the Atlantic Ocean, and humidity is advected into the Amazon Basin by the north-easterly SASM, which is associated with the ITCZ (Zhou and Lau, 1998; Vuille and Werner, 2005). Humidity is then transported further south along the eastern slopes of the Andes by the South American Low Level Jet (Saulo et al. 2000; Marengo et al. 2004). The deep moist convection, especially during the austral summer, is ascribed to the distinctive atmospheric pressure systems known as the near-surface Chaco Low and the tropospheric Bolivian High (Aceituno and Montecions, 1993; Lenters and Cook, 1997). Ultimately, upper-tropospheric easterly anomalies, which are modulated by the Pacific

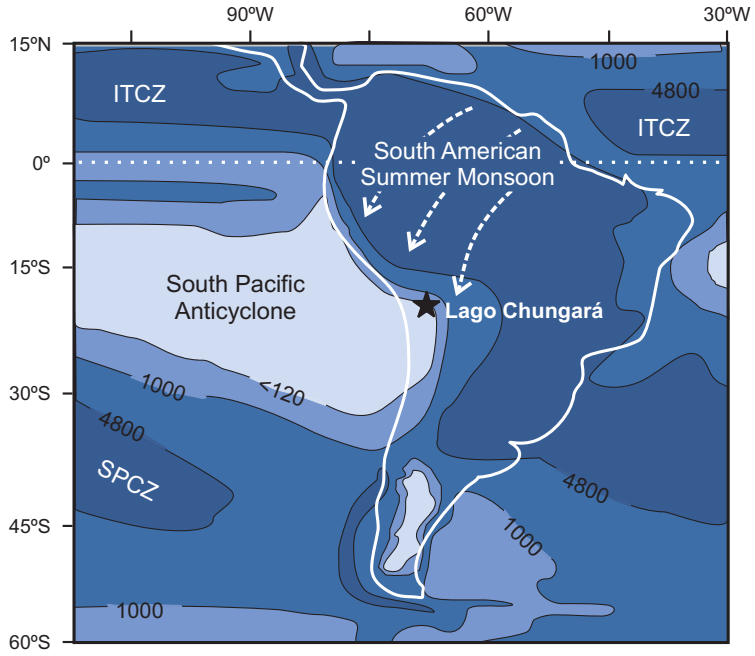

Figure 2.3. Location of Lago Chungará on a rainfall rate map (mm/year) of South America simplified from Negri et al. (2004). The main atmospheric systems are indicated. ICTZ: Intertropical Convergence Zone, and SPCZ: South Pacific Convergence Zone.

SSTs, transport the humidity to the Cordilleras and onto the Altiplano (e.g. Bradley et al. 2003; Garreaud et al. 2003; Vuille and Keimig, 2004; Falvey and Garreaud, 2005).

El Niño-Southern Oscillation-related climate variability

Among the many forcings that determine the interannual climate variability in South America (e.g. PDO, AAO), the ENSO plays a major role in many regions. The ENSO is a coupled ocean-atmosphere phenomenon rooted in the equatorial tropical Pacific Ocean and is characterised by irregular fluctuations between its warm (El Niño) and cold (La Niña) phases with a periodicity ranging from 2 to 7 years (Diaz and Markgraf, 1992; Cane, 2005; McPhaden et al. 2006) (Fig. 2.4). Rainfall and temperature anomalies associated with the occurrence of the El Niño and La Niña events are the major source of interannual variability over much of South America (e.g., Aceituno, 1988; Marengo, 1992; Antico, 2009; Hill et al. 2009). The overall pattern is that the El Niño episodes are associated with a) below normal rainfall over tropical South America, b) above normal precipitation over the southeastern part of the continent and central Chile, and c) warmer than normal conditions over tropical and subtropical latitudes. Contrasting rainfall and temperature anomalies are observed during the La Niña episodes (Garreaud et al. 2009). Otherwise, the most plausible forcing behind the low-frequency fluctuations is the PDO, an enduring pattern of Pacific climate variability (e.g. Mantua et al. 1997; Garreaud and Battisti, 1999; Villalba et al. 2001). The PDO is often described as ENSO-like because the spatial climate fingerprints of its warm and

cold phase bear a strong resemblance to those of the El Niño and the La Niña events, respectively (e.g. Garreaud and Battisti, 1999; Barichivich et al. 2009). However, the causes of the PDO and its links with the ENSO are not yet fully understood (Newman et al. 2003; Schneider and Cornuelle, 2005).

Present-day climate in the Lago Chungará region

The climate in the Chungará-Cotacotani lake district is dominated by arid conditions due to the influence of the South Pacific Anticyclone (Fig. 2.3). The modern mean annual temperature at Lago Chungará is +4.2°C (Figur3 2.5). The annual rainfall ranges from 100 to 750 mm year^{-1} (mean 411 mm year^{-1}) whereas the potential evaporation has been estimated at 1200 mm year^{-1}, which exceeds the precipitation (Valero-Garcés et al. 2000). The lake region shows pronounced seasonal contrasts owing to the dominance of the SASM (Garreaud et al. 2003; Vuille and Werner, 2005). This climate situation defines the wet season (December-March) in the Altiplano, accounting for more than 70% of the annual precipitation. Instrumental data from the Chungará area show a reduction of precipitation during moderate to intense El Niño years (Fig. 2.5). However, there is

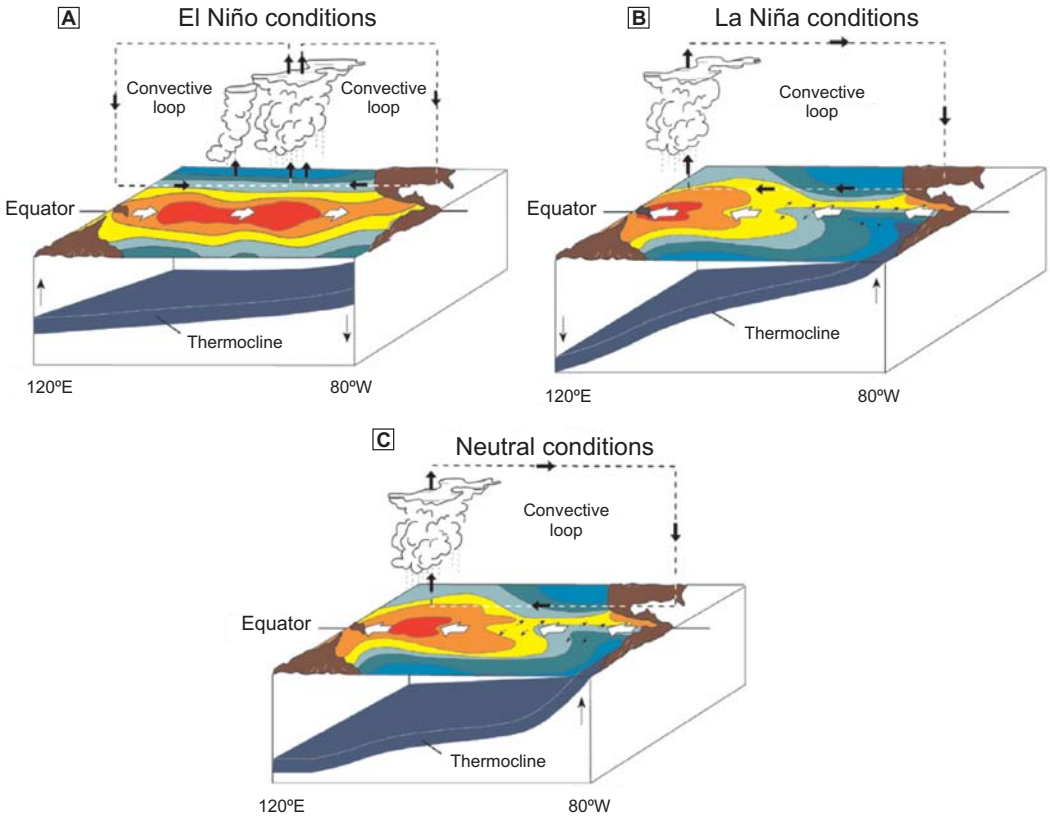

Figure 2.4. Atmospheric circulation and thermocline position in the Pacific Ocean zone between America and Australia during A) El Niño events; B) La Niña events; and C) Neutral conditions. Red and green colours represent warm and cold SST, respectively. Modified from http://www.pmel.noaa.gov/tao/elnino/nino-home.html

no direct relationship between the relative El Niño strength and the amount of rainfall reduction (Valero-Garcés et al. 2003). Furthermore, at longer timescales, it is postulated that changes in the tropical-Atlantic meridional SST gradients also govern rainfall variability on the Altiplano (Baker et al. 2001b).

The rainfall isotope composition in the Central Andes is characterised by a large variability in $\delta^{18}O$ (between +1.2 and −21.1‰) and of δD (between +22.5 and −160.1‰). The origin of the lightest oxygen isotope values is the strong fractionation in the air masses from the Amazon and is directly related to higher rainfall intensity ('amount effect') (Herrera et al. 2006). However, the rainfall oxygen isotope composition in the Chungará-Cotacotani lake district only shows a variation of 6‰, between −14‰ and −20‰, with a mean value of −14.3‰ (Fig.2.5).

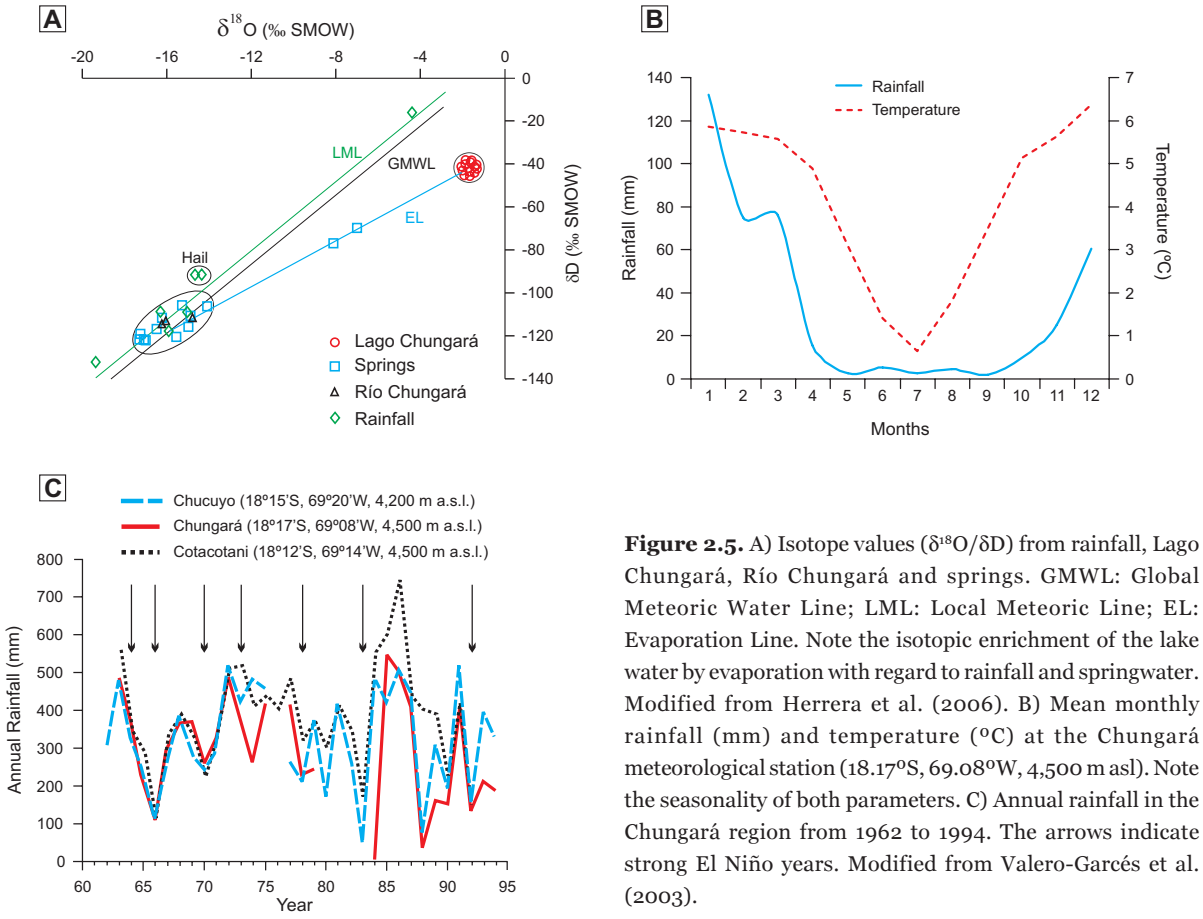

Figure 2.5. A) Isotope values ($\delta^{18}O$/δD) from rainfall, Lago Chungará, Río Chungará and springs. GMWL: Global Meteoric Water Line; LML: Local Meteoric Line; EL: Evaporation Line. Note the isotopic enrichment of the lake water by evaporation with regard to rainfall and springwater. Modified from Herrera et al. (2006). B) Mean monthly rainfall (mm) and temperature (ºC) at the Chungará meteorological station (18.17ºS, 69.08ºW, 4,500 m asl). Note the seasonality of both parameters. C) Annual rainfall in the Chungará region from 1962 to 1994. The arrows indicate strong El Niño years. Modified from Valero-Garcés et al. (2003).

2.2.2 Last Glacial-Holocene climate variability in the Central Andes

Until recently, few palaeoclimatic studies have been carried out in the Central Andes, and the basic character of climate change during the Late Quaternary was poorly documented. In the last two decades, important studies have been published (e.g. Thompson et al. 1995; Betancourt et al. 2000; Barker et al. 2001a,b) without reaching a consensus on some key questions (e.g. Rigsby et al. 2005; Villalba et al. 2009).

The Last Glacial Maximum (LGM) appears in several Altiplano records and is dated at approx. 21,000 cal years BP (e.g. Baker et al. 2001a; Placzek et al. 2006), but whether it was arid (e.g. Heine, 2000; Mourguiart and Ledru, 2003) or wet (e.g. Baker et al. 2001a,b; Tapia et al. 2003) remains unclear. A number of authors suggest a warmer and wet situation throughout the succeeding Late Glacial (e.g. Thompson et al. 1998; Baker et al. 2001a; Rigsby et al. 2005; Hyllier et al. 2009) (Fig. 2.6). Changes in the tropical circulation system are responsible for the massive precipitation increase in Late Glacial times. They are probably linked to a southward displacement of the ITCZ, which gives rise to an enhanced moisture transport onto the Altiplano (Rowe et al. 2002).

The Late Glacial-Early Holocene transition is generally presented as a period of change towards drier conditions with minor wet events (e.g. Abbot et al. 2003; Tapia et al. 2003; Rigsby et al. 2005). However, there is no clear consensus on whether climate periods such us the Northern Hemisphere's Bølling-Allerød-like or the Younger Dryas-like could have co-existed in the Central Andes. These short millennial events are reflected in Lake Titicaca (Perú-Bolivia), Salar de Uyuni (Bolivia) and Nevado Sajama (Bolivia) (e.g. Thompson et al. 1998; Baker et. al 2001a; Placzek et al. 2006) but there are no records of these events in other places (e.g. Abbott et al. 2003; Hillyer et al. 2009).

By contrast, there is a general agreement that a strong arid period throughout the last 30,000 cal years BP occurred during the Early-to-Mid Holocene (e.g. Wolfe et al. 2001; Grosjean et al. 2007; Giralt et al. 2008), but this period does not occur at the same time on the Andean Altiplano (Betancourt et al. 2000; Grosjean et al. 2003). Abbott et al. (2003) found an approximately 2000-year lag in the timing of this dry event, with more northerly lakes responding earlier. In the Lago Pachuca region (Perú), the driest period began earlier (at ~10,000 cal years BP) than in the southern region (Lago Chungará, Lago Poopó (Bolivia) and Salar de Uyuni), which did not begin earlier than 8,000 cal years BP (Fig. 2.6). The amplitude of this period also differs depending on the record (Abbott et al. 2003; Grosjean et al. 2003; Placzek et al. 2006). The most plausible explanation of the Mid-Holocene aridity does not seem to be an insolation minimum, which occurred earlier (Fig. 2.6), but the establishment of a weakening in the ENSO variability between ca 8,000 and 5,000 cal years BP (Rodbell et al. 1999; Rein, 2007). The additive effect of a weakened ENSO and the slowly increasing insolation during the wet season may have thrown the region into a drought-prone stage (Baker et al. 2001a; Abbott et al. 2003; Paduano et al. 2003).

Finally, the Late Holocene period showed a general return to moister conditions probably attributed to enhanced precipitation, decreased evaporation, a shorter dry season or a combination of all these factors (Marchant and Hooghiemstra, 2004). This period is however commonly considered highly oscillating because the lake water level increases are punctuated by minor lake level drops (e.g. Valero-Garcés et al. 1996; Grosjean et al. 1997; Baker et al. 2001a; Rigsby et al. 2005; Hyllier et al. 2009). These changes would be ascribed to orbital forcing, which resulted in a strengthening of wet-season convection

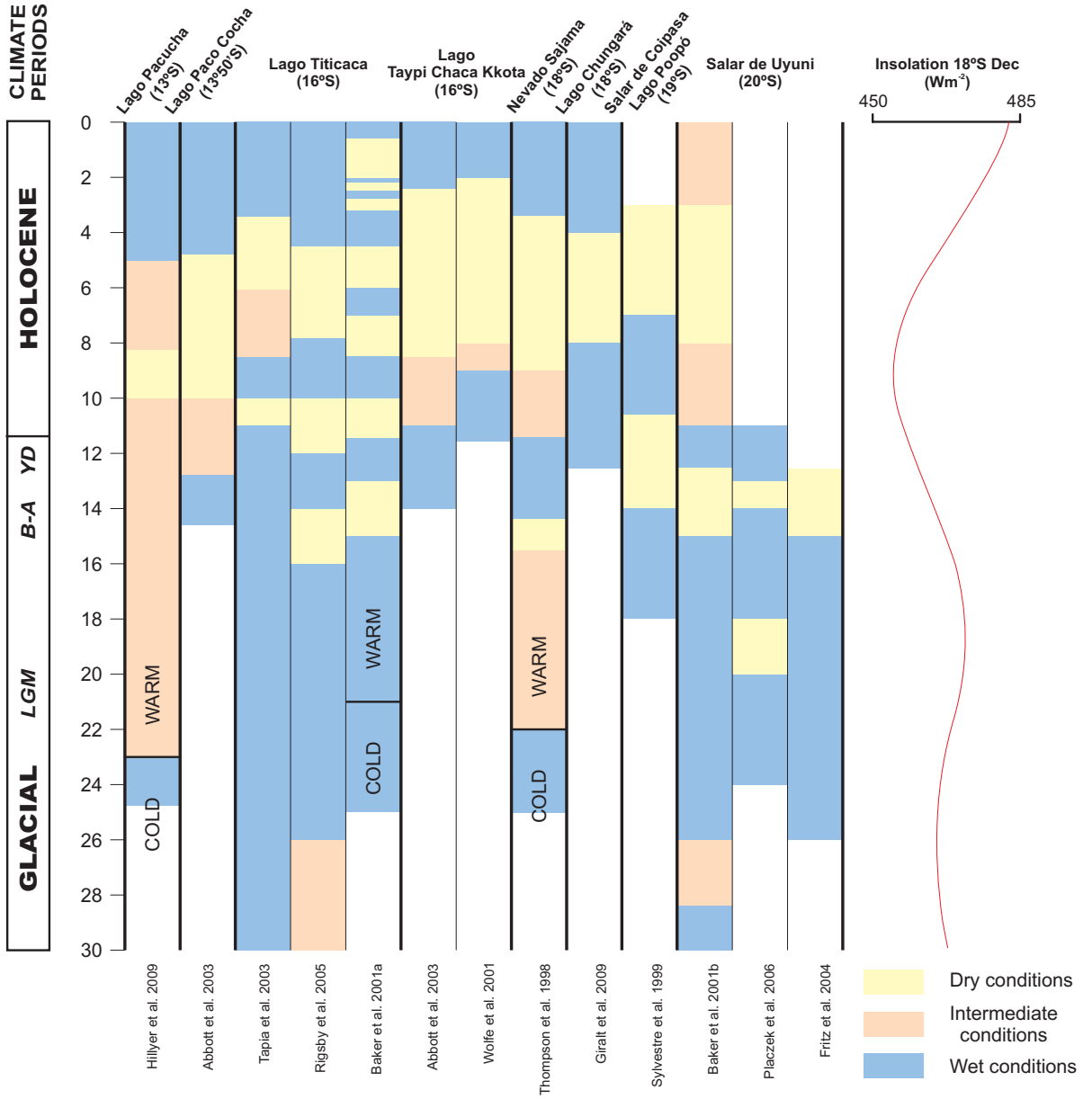

Figure 2.6. Compilation of palaeoclimatic records from the Andean Altiplano and insolation curve for the austral summer at 18ºS to account for the main climate patterns in terms of wet-dry conditions during the last 30,000 cal years BP. LGM: Last Glacial Maximum; B-A: Bølling-Allerød chronozone; YD: Younger Dryas chronozone

as summer insolation increased during the Late Holocene (Abbot et al. 2003). Overprinting these centennial- to millennial-scale climate shifts are higher-resolution changes that are not directly attributed to insolation forcing. These fluctuations in the regional water balance are due to changes in the tropical Pacific SST and are therefore linked to the ENSO activity. The pacific SST changes give rise in the Altiplano to dry conditions during the El Niño phase and to wet conditions during the La Niña phase (Vuille, 1999; Vuille et al. 2000; Valero-Garcés et al. 2003).

In summary, the timing of wet and dry periods over the Andean Altiplano is broadly consistent with the insolation inducing precipitation (e.g. Martin et al. 1997; Betancourt et al. 2000; Seltzer et al.

2000; Baker et al. 2001a,b; Cross et al. 2001)(Fig. 2.6). Maximum insolation during the austral summer (20,000 cal years BP and present) gave rise to the highest deep convection over southern tropical South America (maximum intensity of the SASM), which is consistent with wet conditions on the Altiplano during the LGM and the Late Holocene (Rigsby et al. 2005). Conversely, the summertime insolation minimum at 10,000 cal years BP ushered in an arid phase on the Altiplano (Seltzer et al. 2000; Tapia et al. 2003). Furthermore, the most extreme climate events over the Andean Altiplano did not occur during the terminal ice age, but during the Holocene. Hence, regardless of human influence, the rates of climate change appear to be faster in the Holocene than in Glacial or Deglacial times (Hillyer et al. 2009)

2.3 Limnological features of Lago Chungará

Lago Chungará has an irregular shape, with a maximum length of 8.75 km, maximum water depth of 40 m, a surface area of 21.5 km^2 and a water volume of ca 400 Hm^3 (Mühlhauser et al. 1995; Herrera et al. 2006) (Fig. 2.7). The western and northern lake margins are steep, constituted by the eastern slopes of the Ajoya and Parinacota volcanoes. The eastern and southern margins are gentle, formed by the distal fringe of recent alluvial fans and the River Chungará valley (Sáez et al. 2007). The morphology of the lake floor has been determined by bathymetric data (Villwock et al. 1985) and seismic profiles (Valero-Garcés et al. 2000). Six morphological components can be differentiated along a west-to-east profile (Fig. 2.7): a) a narrow western littoral platform, ca 175–300 m wide, 0–7 m deep (slope <1º); b) a western slope, 115 m wide and 7–20 m deep, dipping 10º; c) a 2–3º rise at the base of the slope, 115–235 m wide and 25–40 m deep; d) a central plain, 4 km wide and 25–40 m deep; e) an eastern slope of 3º, 200 m wide and between 7 and 25 m deep; and f) a subhorizontal (<1º) eastern platform, 450–850 m wide and between 0 and 7 m deep. The absence of high-level shorelines along the lake margins suggests that the current level of the lake is the highest since its formation (Sáez et al. 2007).

At present, the main inlet to the lake is the Chungará River (300-460 l s^{-1}) although small streams flow into the lake along the south-western margin. Water inputs to the lake have, on average, the following composition: 42 ppm HCO_3^-, 3 ppm Cl^-, 17 ppm SO_4^{2-}, 7 ppm Na^+, 4 ppm Mg^{2+}, 8 ppm Ca^{2+}, 3 ppm K^+ and 22 ppm Si. The Mg:Ca ratio of water inputs ranges from 0.22 to 0.71, depending on the local lithology of the catchment (Herrera et al. 2006, Sáez et al. 2007). Evaporation constitutes the main water loss (3.10^7 m^3 $year^{-1}$). There is no surface outlet, but groundwater outflow from Lago Chungará to Lagunas Cotacotani ($6\text{-}7{\cdot}10^6$ $m^3 year^{-1}$) (Dorador et al. 2003) represents about 20% of the total outflow. The calculated residence time for the lake water is approximately 15 years (Herrera et al. 2006).

The lake, which can be regarded as polymictic and oligo- to meso-eutrophic, contains 1.2 g l^{-1} TDS (total dissolved solids); its conductivity ranges between 1,500 and 3,000 µS cm^{-1} (Dorador et al. 2003),

and its water chemistry is of the Na^{+}-Mg_2^{+}-HCO_3-SO_4^{2-} type and alkaline (Table 2.1). The $\delta^{18}O$ and δD composition of the lake water revealed that it diverges from the Global Meteoric Water Line (GMWL) and the Regional Meteoric Line (RML) (Herrera et al. 2006). This divergence can be attributed to the enrichment of the lake water due to evaporation with regard to rainfall and springwater (Herrera et al. 2006; Hernández et al. 2008). The mean lake water values of $\delta^{18}O$ and δD are –1.1‰ SMOW and –39.2‰ SMOW, respectively (Table 2.1 and Fig. 2.5).

Present day primary productivity is mainly governed by diatoms and chlorophyceans during the cold and warm seasons, respectively (Dorador et al. 2003). Seasonal measurements of conductivity, nitrate, phosphate and chlorophyll reveal that these changes in productivity and in the composition of algal communities are mainly due to variations in water temperature and salinity (Dorador et al. 2003). Dense macrophytic vegetation patches and microbial colonies are present in the littoral zone, also contributing to primary productivity (Dorador et al. 2003). The local vegetation is dominated by tussock-like grasses, shrubs, *Polylepis*, dwarf trees of the Rosaceae family as well as extensive soligenous peatlands ("bofedales") (Schwalb et al. 1999; Earle et al. 2003). Finally, the fauna includes endemic cyprinodontid fish (e.g. 19 species of *Orestias*) (Villwock et al. 1985).

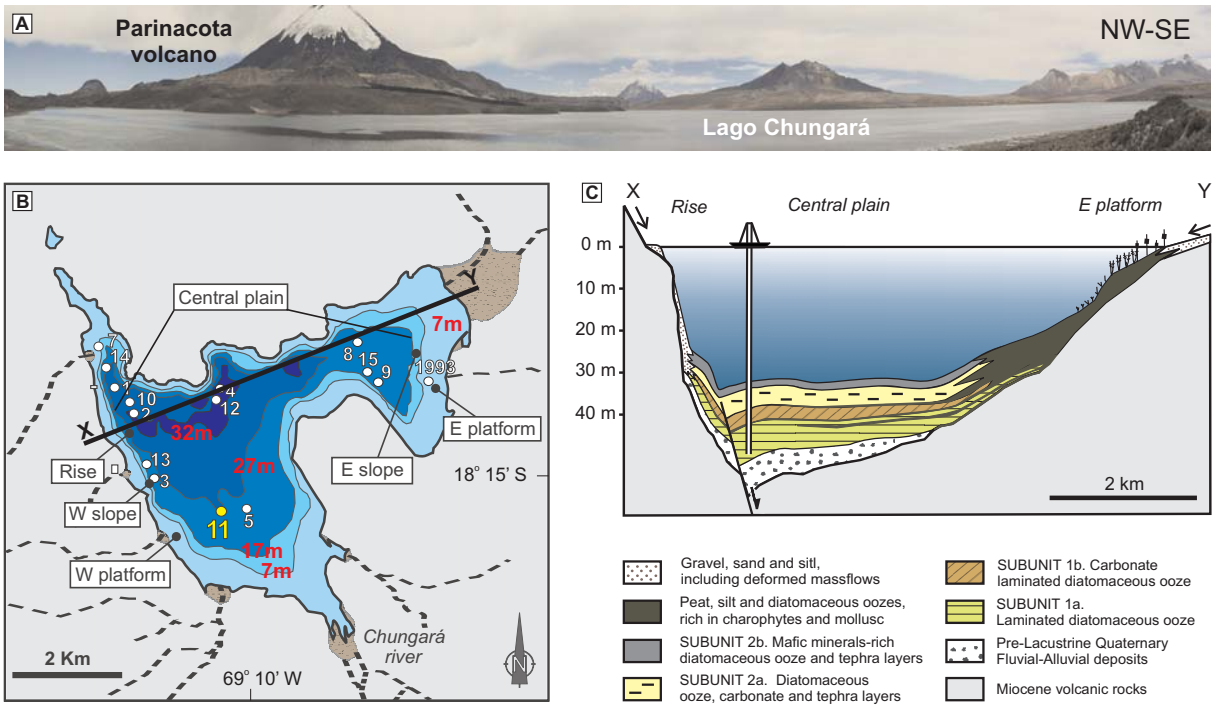

Figure 2.7. A) Panoramic view of Lago Chungará. B) Bathymetric map of Lago Chungará showing the main morphological units of the lake floor cited in the text, and the position of the recovered cores. Black line indicates the cross section (C) throughout the lake. C) Cross section of sediment infilling of Lago Chungará. Position of the studied core is shown. Note that the position of the core is projected in its equivalent position in the central plain. Arrows indicate major hydrological inputs and sedimentary contributions to the lake. Simplified from Sáez et al. (2007).

Table 2.1. Isotope and other chemical and physical data analysed from water samples collected in Lago Chungará, neighbouring small lakes and main surface water inflows. Samples were collected in December 2008. Position of the collected samples is indicated in Figure 3.1.

Sample	Temp air (ºC)	Temp water (ºC)	pH	Conductivity µs/cm)	Salinity (mg/l)	Cl (ppm)	SO_4 (ppm)	HCO_3 (ppm)	B (ppm)	Na (ppm)	K (ppm)	Ca (ppm)	Mg (ppm)	Si (ppm)	P (ppm)	Li (ppm)	δD (SMOW)	$\delta^{18}O$ (SMOW)
Lake																		
Chun1- 0m	9.7	12	9.19	1,501	743	81	422	365	0,9	162,9	32,2	50,6	105,4	0,6	0,7	0,2	-40,05	-1,85
Chun1- 2m	9.7	11.4	9.19	1,495	741	74	405	364	0,9	162,1	32,1	50,5	104,5	0,7	0,7	0,2	-38,8	-1,59
Chun1- 4m	9.7	10.5	9.18	1,496	741	74	406	356	0,9	160,2	32,0	49,9	102,8	1,0	0,7	0,2	-39,4	-1,81
Chun1- 6m	9.7	10	9.17	1,490	737	74	396	364	0,9	159,1	31,7	49,7	102,2	1,3	0,7	0,2	-39,9	-1,03
Chun1- 8m	9.7	9.8	9.15	1,490	735	74	405	363	0,9	159,0	31,7	50,0	102,0	1,3	0,7	0,2	-39,6	-0,29
Chun5- 0m	17	12.1	9.27	1,463	725	74	384	339	0,9	158,9	31,1	48,9	101,1	0,9	0,7	0,2	-41	-0,01
Chun9- 0m	14.2	11	9.18	1,505	746	79	403	359	0,9	163,4	31,9	50,6	105,2	0,6	0,8	0,2	-38,2	0,07
Chun9- 2m	14.2	11	9.16	1,498	742	79	400	364	0,9	163,7	32,1	50,9	105,3	0,6	0,7	0,2	-37,4	-1,69
Chun9- 4m	14.2	10.4	9.20	1,502	745	69	402	359	0,9	164,1	32,1	50,9	105,4	0,6	0,8	0,2	-38,3	-1,98
Chun9- 6m	14.2	10.6	9.18	1,502	744	75	391	364	0,9	164,4	32,2	50,6	105,3	0,6	0,8	0,2	-37,6	-1,68
Chun9- 8m	14.2	10.4	9.19	1,499	743	76	390	362	0,9	163,4	32,0	50,5	105,0	0,6	0,7	0,2	-38,4	-1,67
Chun9- 10m	14.2	10.2	9.19	1,505	746	75	396	361	0,9	164,8	32,3	51,2	106,4	0,6	0,8	0,2	-38	-1,48
Chun9- 12m	14.2	10	9.17	1,510	747	75	391	358	0,9	163,6	31,9	50,6	104,9	0,7	0,8	0,2	-37,5	0,14
Chun9- 14m	14.2	9.8	9.17	1,510	746	73	389	357	0,9	164,6	32,2	50,9	105,5	0,7	0,7	0,2	-36,8	0,07
Chun9- 16m	14.2	10.6	9.15	1,492	739	72	390	363	0,9	164,3	32,3	50,4	104,7	0,7	0,8	0,2	-36,6	-2,09
Chun9- 18m	14.2	9.8	9.13	1,487	731	74	387	364	0,9	162,3	32,2	50,2	104,7	0,8	0,8	0,2	-35,7	0,55
Chun9- 20m	14.2	9.5	9.15	1,507	747	74	388	363	0,9	162,5	32,2	50,2	103,8	0,8	0,7	0,2	-36,4	0,15
Chun10- 0m	10	18.8	9.06	1,068	523	63	239	246	0,8	113,7	25,9	39,9	66,3	10,8	1,0	0,2	-55,2	-3,12
Small Lakes																		
Chun2- 0m	17	14.9	10.76	1,830	914	117	543	231	1,3	229,5	43,0	29,2	138,7	0,1	0,4	0,3	-12,95	6,24
Chun7- 0m	11	11.8	8.85	323	153.9	14	55	105	0,4	30,5	6,6	19,8	13,9	25,9	<0.1	0,0	-108	-13,84
Chun8- 0m	na	11.4	8.62	761	371	46	118	182	0,8	69,7	9,9	43,7	45,5	10,6	0,3	0,1	-74,7	-6,26
River-Streams																		
Chun3- 0m	8.3	6.3	10.23	272	129.3	3	60	81	0,1	18,8	3,8	19,9	14,6	31,7	0,4	0,0	-101,4	-13,95
Chun4- 0m	na	8.4	8.48	269	127.9	3	68	73	0,1	17,5	3,5	19,2	13,7	33,1	0,4	0,0	-104	-16,37
Chun6- 0m	na	13.7	8.65	48.9	22.8	1	3	25	0,1	5,1	3,2	2,6	1,8	21,5	<0.1	0,0	-115,4	-15,07

2.4 Earlier work undertaken at Lago Chungará

Given that this PhD thesis was prompted by earlier multiproxy studies, some data employed here have been published by other authors from the same research group (Herrera et al. 2006; Moreno et al. 2007; Sáez et al. 2007; Giralt et al. 2008). Earlier studies have characterised the surface and underground waters from the Chungará and Cotacotani lake district (Section 2.3) as well as the sedimentary infill of Lago Chungará.

2.4.1 Sedimentary record

In November 2002 fifteen sediment cores (6.6 cm inner diameter and up to 8 m long) were recovered from Lago Chungará using a raft equipped with a Kullenberg coring system. All cores were cut in 1.5 m sections and physical properties (GRAPE-density, p-wave velocity and magnetic susceptibility) were measured in the laboratory using a GEOTEK™ Multi-Sensor Core Logger (MSCL) at 1 cm intervals. Thereafter, the cores were split into two halves, scanned using a DMT colour scanner, and the textures, colours and sedimentary structures were described. Smear slides were used to characterise the sediment composition in order to estimate the biogenic, clastic and endogenic mineral content (Moreno et al. 2007).

The uppermost sedimentary infill of Lago Chungará was characterised by the lithological description of the fifteen cores (Sáez et al. 2007) and by seismic imagery obtained in 1993 (Valero-Garcés et al. 2000). A 3D sedimentary model was obtained after the construction of correlation sedimentary panels (Sáez et al. 2007) (Fig. 2.8). These stratigraphic correlation panels allowed us to select cores 10 and 11, located offshore (Fig. 2.7 and 2.8) to carry out the palaeoenvironmental reconstruction. A composite core recording the whole sedimentary infill (minimum thickness of 10 m) of the offshore zone was constructed from the detailed description and correlation of these two cores. From the bottom to the top of the composite core, two sedimentary units (units 1 and 2) were identified and correlated over the offshore zone of the lake mainly using 14 tephra keybeds (Fig. 2.8).

Unit 1 is made up of diatomaceous ooze with variable types and quantities of carbonates (calcite, aragonite) and amorphous organic matter. This unit, which extends across the lake, is thicker in the NW sector of the central plain and thinner towards the south and west, probably overlapping the Miocene substrate. This unit lies in the central plain and on the steep flank of the lake (Fig. 2.8). It is divided into two subunits: subunit 1a and subunit 1b. Subunit 1a ranges in thickness between 0.58 m and 2.56 m and is composed of light-white and dark-green diatomaceous ooze couplets (Fig. 2.9). Subunit 1b (from 0.62 m to 1.87 m thick) is made up of centimetre-to decimetre-thick laminated brown diatomaceous ooze and endogenic carbonates that occur at low concentrations (Sáez et al. 2007) (Fig. 2.9).

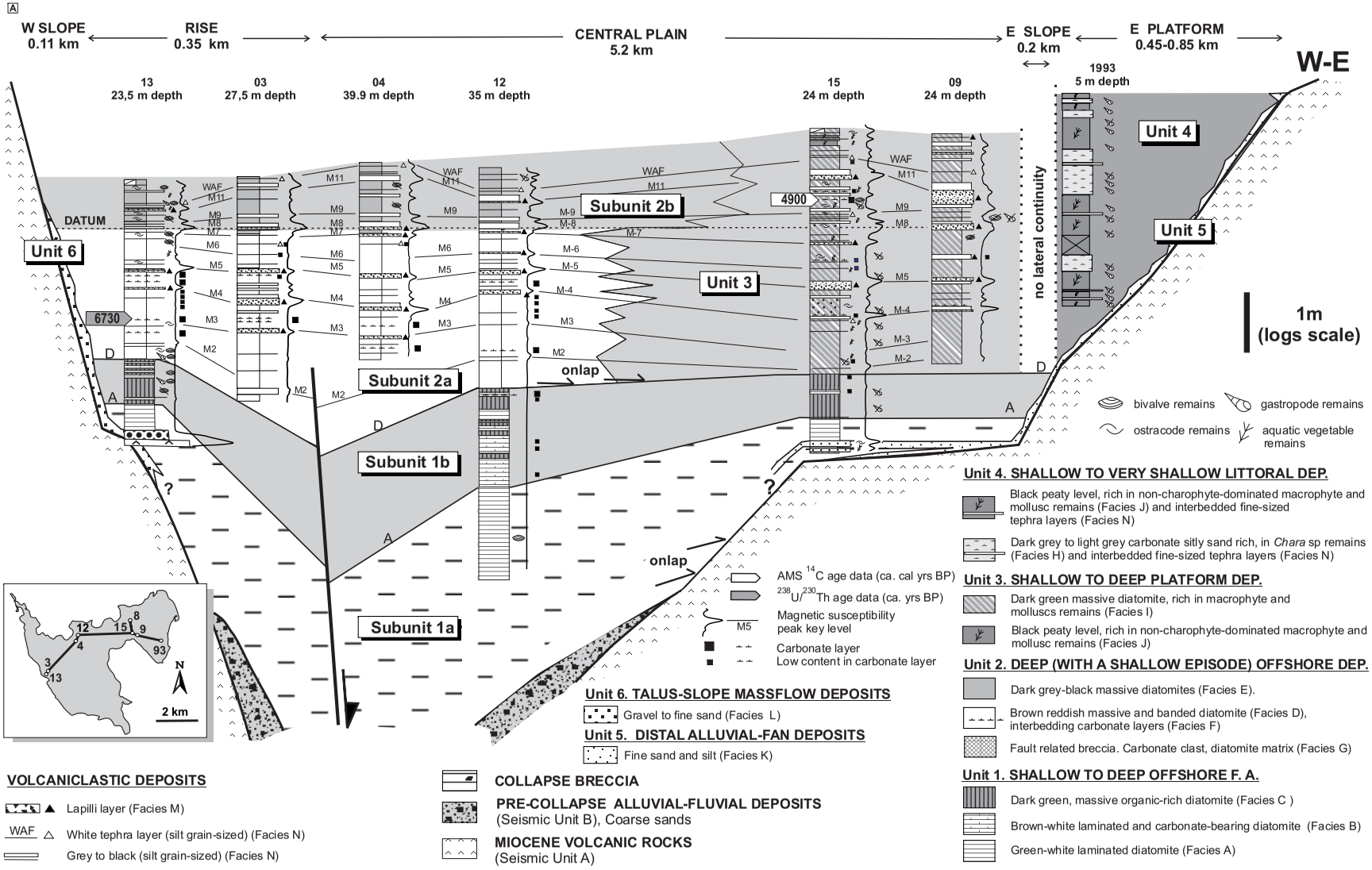

Figure 2.8. A) West–East stratigraphic cross-section; B) North–South stratigraphic cross-section. Stratigraphic correlations are based on lithostratigraphic and sedimentological criteria (limits between units and some key levels and facies) and magnetic susceptibility profiles. To improve clarity, the horizontal scales are not the same in the central trough as in the platforms (Sáez et al., 2007).

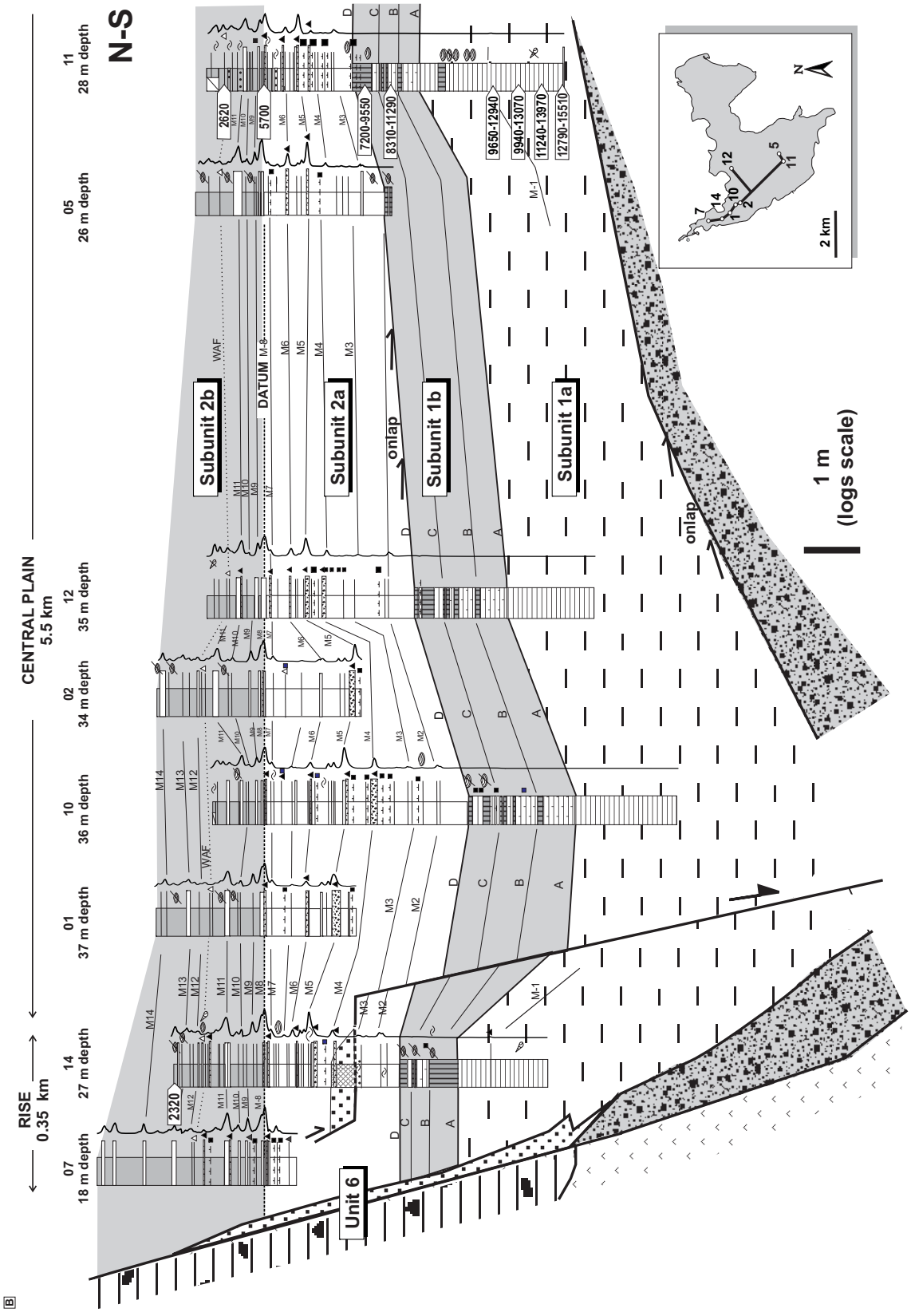

Figure 2.8. (continued).

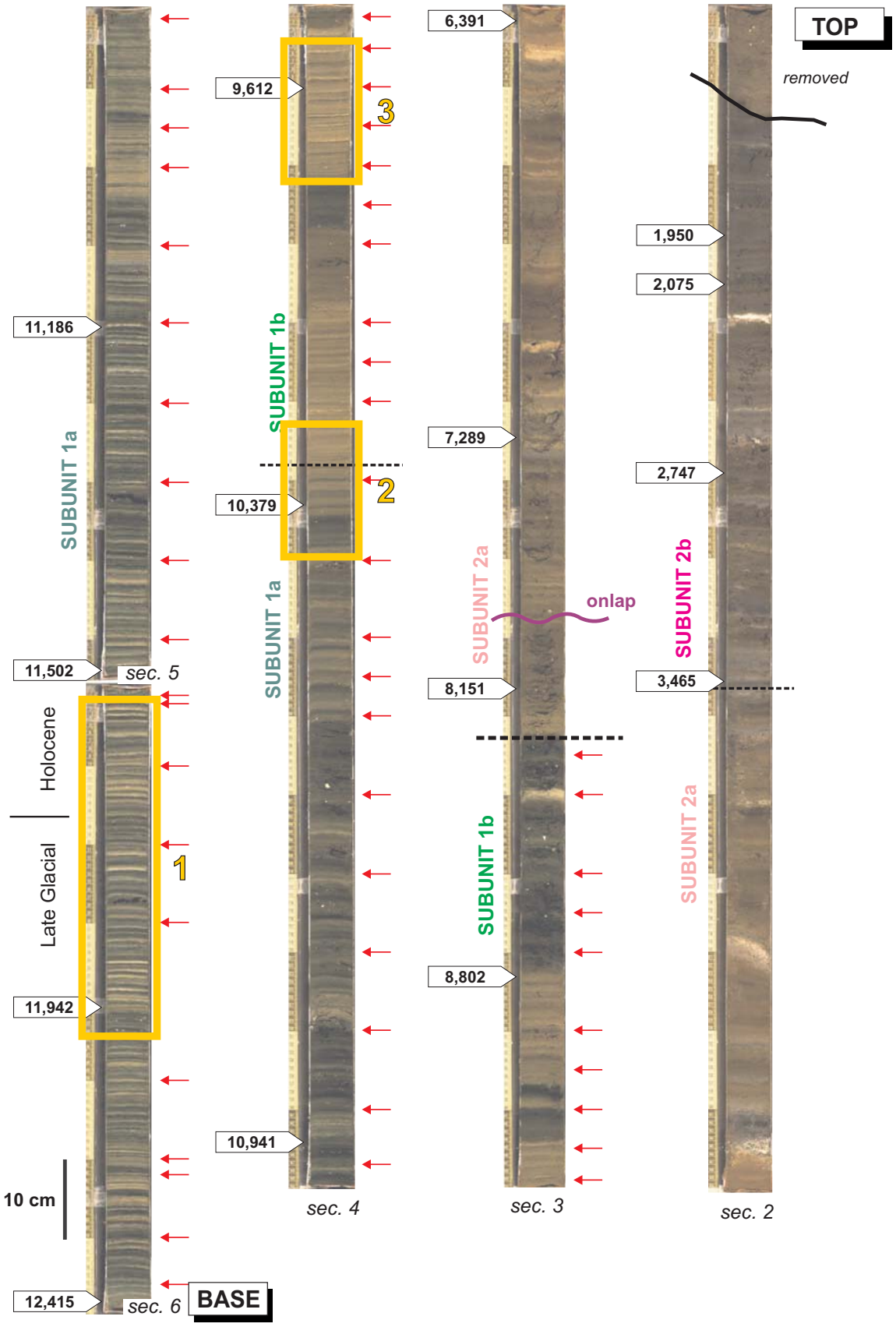

Figure 2.9. DMT scanner (LRC, Minnesota) image of core 11. Lithological units, ^{14}C AMS radiocarbon dates, intervals sampled for chapters 4, 5 and 6 (yellow squares), and the position of the samples analysed for chapter 7 (red arrows) are indicated.

Unit 2 is about 6 metres-thick and grades laterally to the west and south into alluvial and deltaic deposits, and towards the east into macrophyte, organic-rich facies (Fig. 2.8). It is mainly made up of massive to slightly banded diatomaceous ooze interbedded with 13 tephra layers. Unit 2 is also divided into two subunits: subunit 2a and subunit 2b. Subunit 2a (between 1.56 m and 3.44 m thick) is composed of massive brownish-red to slightly banded sapropelic diatomaceous ooze with abundant calcite crystals (silt grain-sized) and carbonate-rich layers (Fig. 2.9). The sediments of the uppermost subunit 2b range from 0.86 m to 3 m in thickness and consist of dark-grey diatomaceous ooze with frequent macrophyte remains alternating with massive black tephra layers, mainly constituted by plagioclase, glass and mafic minerals (Fig. 2.9) (for further details see Moreno et al. 2007 and Sáez et al. 2007).

The Lago Chungará sediments were analysed by X-Ray Fluorescence (XRF), X-Ray Diffraction (XRD), Total Carbon and Total Organic Carbon (TC and TOC), Biogenic Silica (BSi), pollen and diatoms (Fig. 2.10).

The XRD analyses indicated that offshore sediments of Lago Chungará are constituted by an amorphous and a crystalline fraction. The amorphous fraction, ranging from 40 wt% (towards the top of the composite core) to almost 100 wt% (in the lower two thirds of the composite core), is made up of organic matter and diatoms. The crystalline fraction, ranging between 1 wt% and 60 wt%, consists of Ca-plagioclase, carbonate (calcite and dolomite), muscovite, pyrite, quartz and an amphibole (probably riebeckite) (Fig. 2.10). In addition, XRF analysis of the distribution of chemical elements enabled us to detect three main components in the Lago Chungará sediments: a) lacustrine biological remains (mainly diatoms), b) volcanic minerals and c) endogenic offshore carbonates. The first component corresponds to the amorphous fraction revealed by the XRD and the other two correspond to the crystalline fraction (Fig. 2.10) (Moreno et al. 2007).

The geology of the Lago Chungará catchment (see Sáez et al. 2007 for further details) indicates that volcanic minerals have two main provenances: a) the erosion of former volcanic rocks and that of previous deposited fallout material from the catchment, and b) the ash fallout from the Parinacota volcano. Conversely, the origin of the carbonates is not so straightforward. The presence of large amounts of Ca of volcanic origin dissolved in the lake water together with a marked lake level decrease could have promoted the precipitation of these carbonates (see Giralt et al. 2008 for further details).

2.4.2 Chronological Framework

The chronological model for the sedimentary sequence of Lago Chungará is based on 17 AMS ^{14}C dates of bulk organic matter and aquatic plant macrofossils, and one $^{238}U/^{230}Th$ date from carbonates (Table 2.2 and Fig. 2.11). The radiocarbon dates were performed in the Poznan Radiocarbon Laboratory (Poland) whereas the $^{238}U/^{230}Th$ sample was analysed by high-resolution ICP-IRMS multicollector at the University of Minnesota (Edwards et al. 1987; Cheng et al. 2000; Shen et al. 2002). The main problems encountered in the construction

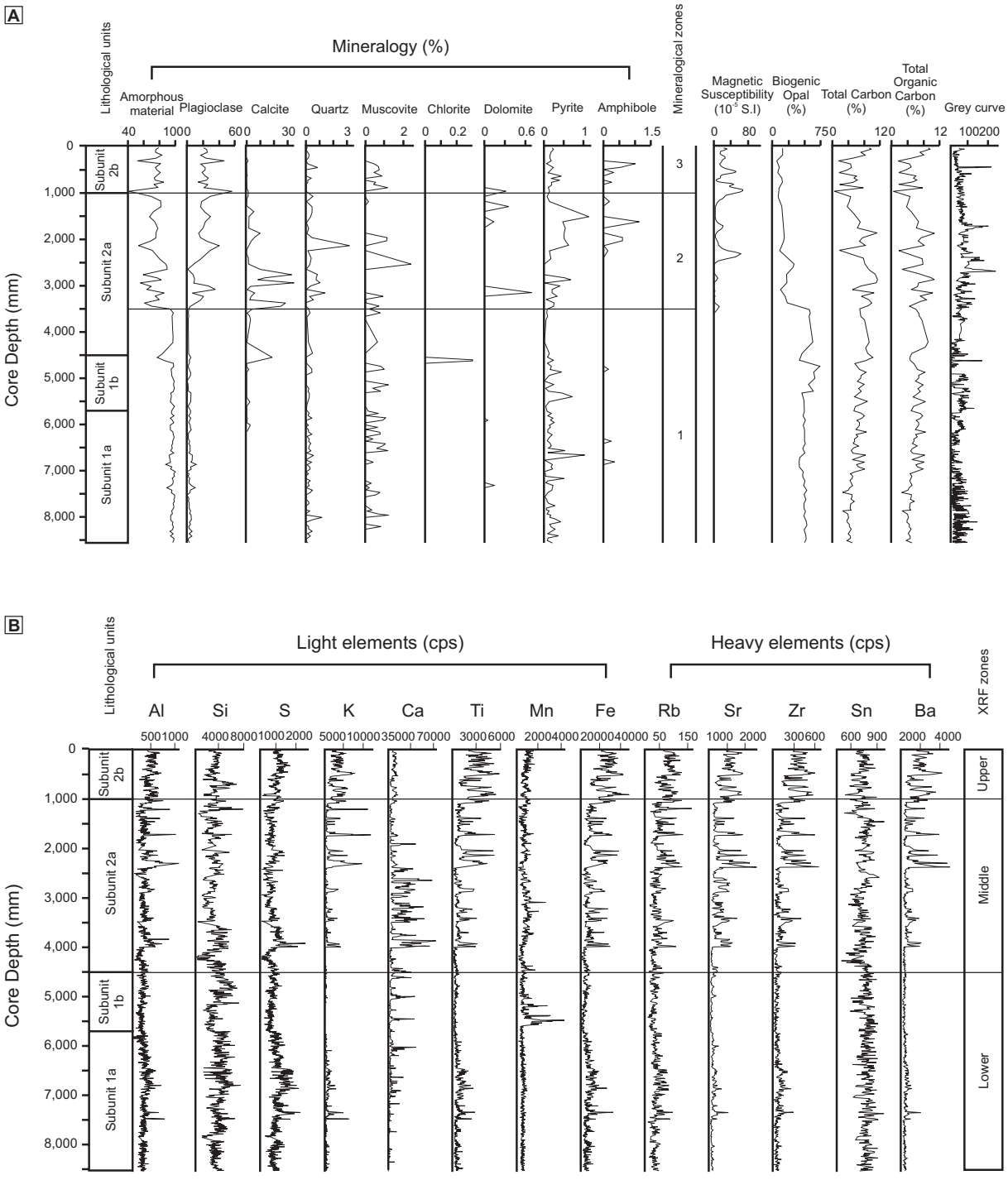

Figure 2.10. A) Mineralogy (expressed as percentages on total dry weight), magnetic susceptibility (expressed as standard units), Total Biogenic Silica (BSi), Total Carbon (TC), Total Organic Carbon (TOC) (expressed as percentages) and grey-colour curve of the Lago Chungará sediments (Giralt et al. 2008). B) Analysed light and heavy elements (expressed as counts per second) in the sediments of Lago Chungará. The zones correspond to those established in Moreno et al. (2007).

of reliable chronological frameworks for the lacustrine sedimentary infill of most lakes in the Andean Altiplano were: a) the determination of the large and variable radiocarbon reservoir effect (Geyh et al. 1999; Geyh and Grosjean, 2000; Grosjean et al. 2001), and b) the temporal evolution of this radiocarbon reservoir effect.

The modern reservoir effect in lakes must be calculated as the difference between the ^{14}C age of the water and that of the atmospheric $^{14}CO_2$ measured at the same time (Giralt et al. 2008). Radiocarbon dating of the modern DIC resulted in 2,320 ± 40 ^{14}C years BP (Table 2.2), but this value must be corrected owing to the atmospheric thermonuclear bomb tests carried out during the late 1950s–early 1960s. These nuclear tests doubled the amount of ^{14}C in the atmosphere (Reimer et al. 2004b). The effects of these thermonuclear tests on the modern carbon cycle of a lake depend on a) the year in which the sample was taken and b) the residence time of the lake (Hua and Barbetti, 2004; Goslar et al. 2005). The Lago Chungara water residence time is about 15 years (Herrera et al. 2006) and the DIC sample was obtained and dated in 2004. Therefore, the real present-day reservoir effect of this lake is 3,260 years BP: 2,320 years BP (radiocarbon date of the DIC) minus –920 years (apparent radiocarbon age of the atmospheric $^{14}CO_2$ for the period 1988–2002) (Hua and Barbetti 2004; Goslar et al. 2005) (see Giralt et al. 2008 for further details).

The reservoir effect in the Altiplano lakes proved to be highly variable over time. One of the factors that could influence the reservoir effect is the change in the volume/surface ratio of the lake, which is a function of the water depth (Geyh et al. 1998; Grosjean et al. 2001). According to these authors, the

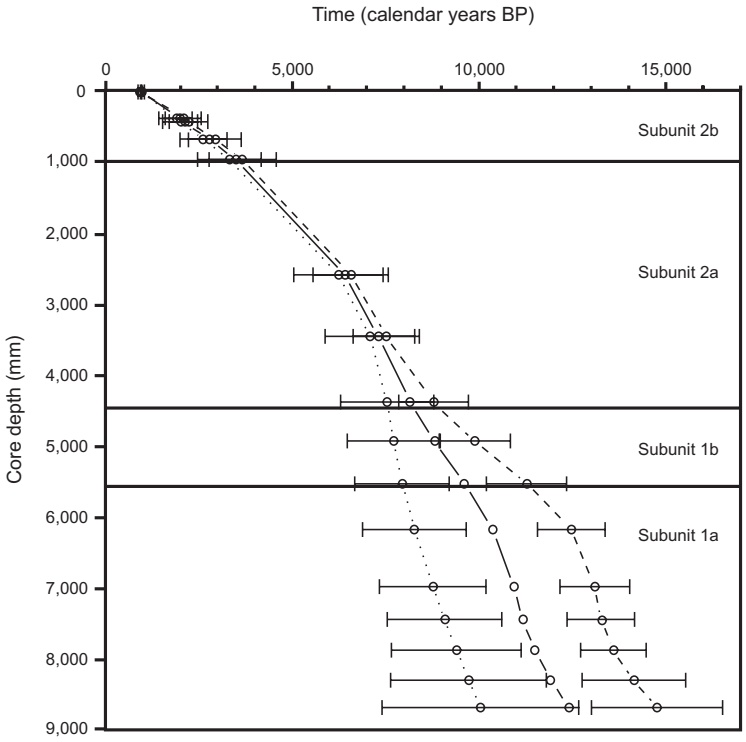

Figure 2.11. Chronological framework of Lago Chungará was constructed using 15 ^{14}C AMS dates and after applying Heegaard's method (Heegaard et al. 2005) in calendar years BP (modified from Moreno et al. 2007). The dotted line represents the chronological model constructed considering a constant reservoir-effect of 3,260 years. The dashed line depicts the chronological model considering a reservoir effect of 3,260 years for the upper sedimentary unit and 0 years for the lower unit. The intermediate continuous line represents the average model of the two earlier ones and is applied to Lago Chungará. Horizontal bars are the confidence error of the radiometric dates after applying the method of Heegaard. Reproduced from Giralt et al. (2008).

reservoir effect decreases when the lake level diminishes, and viceversa. Therefore, the approach followed in Moreno et al. (2007) and Giralt et al. (2008) to correct the dates for the variable reservoir effect was based on two assumptions: a) the Lago Chungará ecosystem had an environmental status during the deposition of Unit 2b akin to the one existing at present and b) the present-day lake level is at its highest position. Accordingly, a different correction of the reservoir effect was applied to Units 1 and 2. A constant reservoir effect of 3,260 years was substracted from the radiocarbon dates present in Unit 2. However, it is only possible to speculate about the variations over time of the reservoir effect in Unit 1. Given that it was not possible to estimate the reservoir effect by applying the methodology of Geyh et al. (1998), the ages of the two extreme reservoir values (a minimum of 0 and a maximum of 3,260 years) were calculated (Table 2.2 and Fig. 2.11). A theoretical mid point between the two extreme reservoir effect points was calculated for Unit 1 and this theoretical value was employed to construct the final chronological model (Fig. 2.11). All the corrected radiocarbon dates were calibrated using the CALIB 5.02 software package (Reimer et al. 2004a) selecting the mid-point of 95.4% of the distribution. The upper and lower limits of the chronological model were calculated employing the Cagedepth software (Heegaard et al. 2005).

Table 2.2. A) AMS ^{14}C datings carried out to construct the chronological framework of the Lago Chungará sedimentary sequence. B) Results of $^{238}U/^{230}Th$ datings. Reproduced from Giralt et al. (2008).

Lithological Units	Composite depth (mm)	Lab ID	Sample reference	Sample material	Uncalibrated ^{14}C (years BP)	Calibrated age[a] (calendar years BP)	Calibrated age[b] (calendar years BP)	$\delta^{13}C$ (‰PDB)
Unit 2	-	Beta-188745	-	Lake water	2,320 ± 40	-	-	-
	375	Poz-8726	14 A-1, 5	Bulk organic remains	4,620 ± 40	1,850 ± 454	2,050 ± 500	-13.6 ± 0.2
	420	Poz-8720	11 A-2, 39	Bulk organic remains	4,850 ± 40	1,964 ± 460	2,185 ± 520	-12.9 ± 0.4
	670	AA56904	15 A-2, 48	Aquatic plants	6,635 ± 39	2,590 ± 630	2,900 ± 710	-25.46
	951	Poz-8721	11 A-2, 84	Bulk organic remains	7,290 ± 50	3,290 ± 860	3,645 ± 910	-14.8 ± 0.2
	2,573	Poo-8723	11 A-3, 2	Bulk organic remains	8,920 ± 50	6,227 ± 1,200	6,555 ± 1,010	-16.1 ± 0.1
	3,440	AA56903	15 A-4, 27	Aquatic plants	9,999 ± 50	7,070 ± 1,200	7,505 ± 890	-
	4,361	Poz-8724	11 A-3,86	Bulk organic remains	10,860 ± 60	7,530 ± 1,250	8,775 ± 940	-16.9 ± 0.1
Unit 1	4,909.1	Poz-7170	11 A-3, 123	Bulk organic remains	8,570 ± 50	7,705 ± 1,230	9,900 ± 950	-16.8 ± 0.1
	5,504.8	Poz-8647	11 A-4, 10	Bulk organic remains	9,860 ± 60	7,940 ± 1,260	11,290 ± 1,080	-14.1 ± 0.3
	6,152	Poz-7171	11 A-4, 63	Bulk organic remains	11,070 ± 70	8,270 ± 1,400	12,490 ± 910	-13.6 ± 0.2
	6,650	**AA56905**	**15 A-5, 77**	**Aquatic plants**	**4,385 ± 101**	**-**	**-**	**-**
	6,750	**Poz-8725**	**13 A-4, 66**	**Bulk organic remains**	**8,810 ± 50**	**-**	**-**	**-22.9 ± 0.1**
	6,962	Poo-11891	11 A-4, 145.5	Bulk organic remains	11,460 ± 60	8,765 ± 1,420	13,120 ± 930	-16.2 ± 0.4
	7,442	Poz-13032	11 A-5, 41	Bulk organic remains	10,950 ± 80	9,080 ± 1,540	13,290 ± 910	-22.7 ± 2.3
	7,852	Paz-11982	11 A-5, 84	Bulk organic remains	11,180 ± 70	9,400 ± 1,740	13,605 ± 880	-28.7 ± 3.7
	8,272	Poz-13033	11 A-6, 41	Bulk organic remains	12,120 ± 80	9,730 ± 2,090	14,155 ± 1,390	-19.6 ± 1.7
	8,652	Poz-7169	11 A-6, 79	Bulk organic remains	13,100 ± 80	10,040 ± 2,640	14,795 ± 1,760	-23.1 ± 0.2

Bolded radiocarbon dates were not taken into account in the construccition of the chronological framework

Composite depth (mm)	Sample reference	Carbonate Type	^{238}U (ppb)	^{232}Th (ppm)	$\delta^{234}U$ measured	$^{230}Th/^{238}U$	$^{230}Th/^{232}Th$	Calendar age (years BP)
3,440	13 A-2, 105	Crystalline	467,4	35.2	413.5	0.1036	23	-6,728 ± 974

Chapter 3

Methods

3.1 Hydrochemical and isotopic water analyses

Water samples were collected from Lago Chungará in December 2009 in order to complement samplings carried out by the research team in 2002 and 2004 (Herrera et al. 2006). Water samples were taken each 2 metres in vertical profiles up to water depths of 8 and 20 metres in the lake. These water samples were complemented by additional samplings from the nearby smaller lakes, rivers and streams (Table 2.1 and Fig. 3.1). The variables measured in situ were conductivity, oxygen concentration, pH, temperature and salinity. A total of 24 samples were collected for isotope analyses. The samples for the $\delta^{18}O$ and δD analyses were stored in 50 ml polythene tubes. For the $\delta^{18}O$ analysis, the waters were equilibrated with CO_2 prior to mass spectrometry measurements, whereas for δD analysis the samples were reduced to H_2 using Pt before mass spectrometry. The isotope analyses were conducted using a Finnigan MAT Delta S IRMS. Isotopic standards employed as reference were VSMOW, SLAP and GISP for δD and $\delta^{18}O$ in water samples. Replicate analysis of all the samples indicated a precision of $\pm<0.1‰$ (1 σ) (for $\delta^{18}O$) and 1.5‰ (1σ) (for δD).

All these samples were also analysed by means of Ion-exchange chromatography, volumetric analysis and Inductively Coupled Plasma (ICP-OES) in order to measure the concentrations of the main chemical components (Cl^-, SO_4^{2-}, NO_3^-, HCO_3^- and cations). The water samples were previously filtered (0.45 μm) during the field sampling.

All the water samples were analysed at the Serveis Científico-Tècnics de la Universitat de Barcelona.

3.2 Sediment sampling

The Lago Chungará sediments were sampled following different strategies in accordance with three main objectives:

a) To characterise the climate and environmental changes, at different resolutions, taking place in the Late Glacial-Early Holocene transition (12,000-9,400 cal years BP). Three short intervals consisting

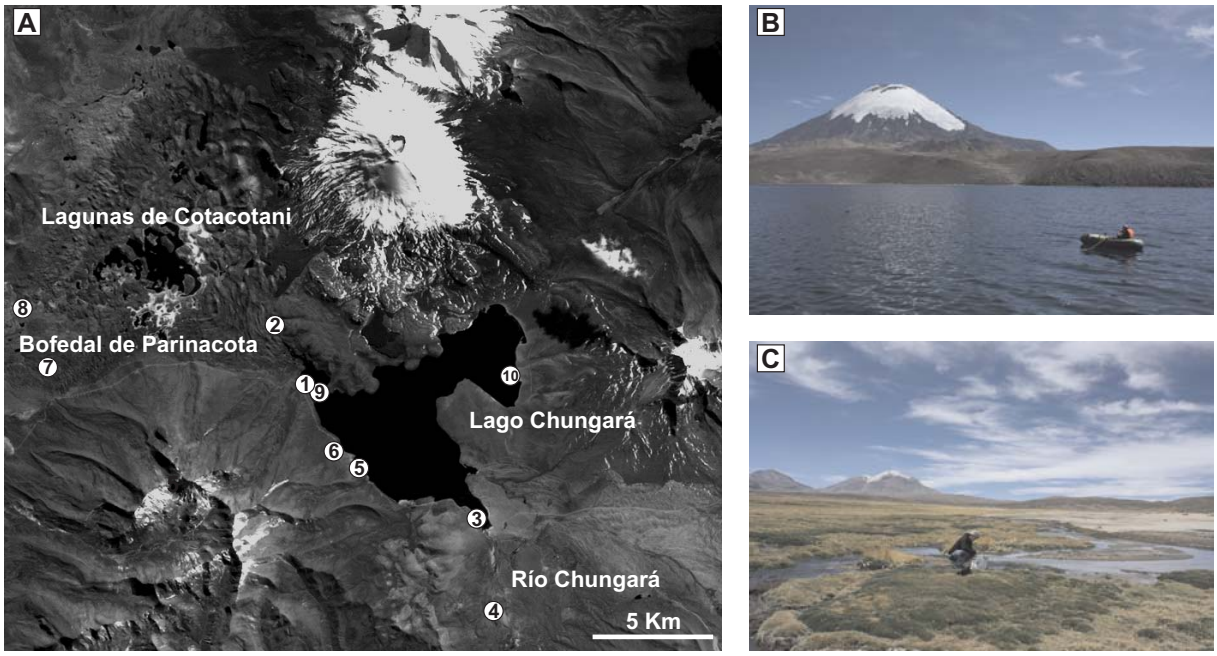

Figure 3.1. A) Aerial-view of the Lago Chungará region with the position of water sampling sites. B) and C) pictures of water sampling in Lago and Río Chungará, respectively.

of light and dark finely-laminated sediments were selected. Light laminae were formed by the accumulation of massive short-term diatom blooms, probably lasting only days or weeks, whereas dark laminae would represent a normal annual cycle of the lake with alternating phases of stratification and mixing over several years. Interval 1 (11,990–11,450 cal years BP) was located at subunit 1a. Interval 2 (10,430–10,260 cal years BP) was located at the transition between subunit 1a and subunit 1b. Interval 3 (9,890–9,430 cal years BP) was located at subunit 1b. Individual laminae within the three intervals were sampled with a blade for isotope analyses. A total of 190 samples (111 samples from interval 1, 37 samples from interval 2, and 42 samples from interval 3) were obtained. A selection of 37 samples from dark laminae of these 3 intervals was selected to investigate the baseline hydrological evolution of Lago Chungará by means of $\delta^{18}O_{diatom}$ analysis. Additionally, 40 samples of dark laminae from a stretch of 46.5 cm corresponding to the interval 1 (11,990-11,450 cal years BP) were analysed by an ultra-high resolution $\delta^{18}O_{diatom}$ reconstruction to track the influence of the ENSO and solar activity at this time interval.

b) To characterise the biogeochemical changes taking place at ultra-high frequency. To this end, 102 samples of both light and dark laminae from the interval 1 were selected for $\delta^{18}O_{diatom}$. Additionally, 11 samples from interval 1 were also analysed for $\delta^{13}C_{diatom}$ and $\%C_{diatom}$.

c) To characterise the high-frequency environmental changes recorded in laminated unit 1 (12,400-8,400 cal years BP). A total of 51 bulk samples were selected for $\delta^{18}O_{diatom}$ and $\delta^{13}C_{diatom}$ analyses (Fig. 2.9). The sampling was carried out every 10 cm except where the sediments were either carbonate or tephra-rich.

3.3 Light and Scanning Electron Microscope sample preparation

Each interval from unit 1 (Intervals 1, 2, 3) was continuously covered by thin sections. Thin sections of 120 mm x 35 mm (30 μm in thickness), with an overlap of 1 cm at each end, were obtained after freeze-drying and balsam-hardening (Fig. 3.2). Detailed petrographical descriptions and lamina thickness measurements were performed with a Zeiss Axioplan 2 Imaging petrographic microscope.

A number of representative samples were also selected for observation with the Jeol JSM-840 and the Hitachi H-4100FE field emission Scanning Electron Microscopes (SEM) to complement the petrographical study using the thin sections and to check the purity of the samples for isotopic analyses. The samples were dried in two steps because of the high absorbed water content: a) most of the water was eliminated by capillary action using filter paper, and b) samples were freeze-dried and vacuum stored prior to being carbon coated.

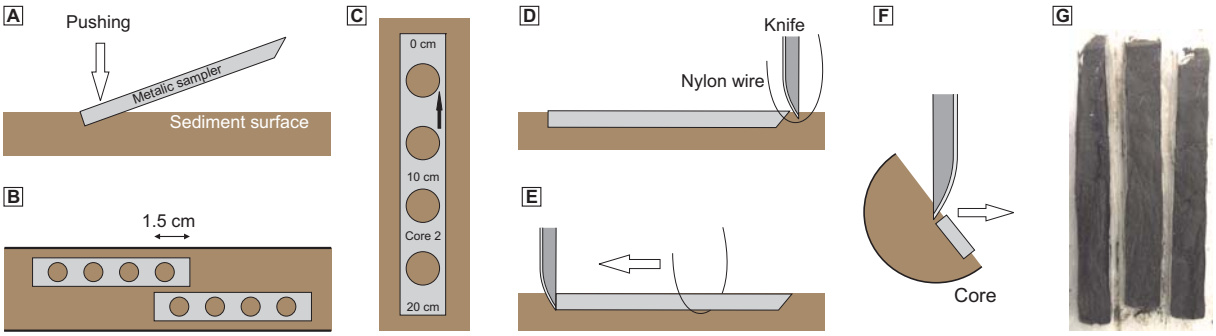

Figure 3.2. Sampling procedure to obtain the material of the thin sections in soft sediment cores. A) Insertion of a metallic sampler into one side of the core. B) If more than one metallic sampler is used for the same core, a minimum overlapping of 1.5 cm is performed. C) Annotation of the bottom depth, the top depth, and some middle depths, indicating the polarity of the sample as well as the name of the core. D) Nylon wire cutting the sediment with the aid of a knife at the top end. E) To avoid horizontal displacement, the bottom of the metallic sampler is secured with the knife. Nylon wire is then pulled along to the end of the metallic sampler. F) Inclination of the core 45 degrees and extraction of the metallic sampler. G) Samples prepared for freezing for subsequent study of thin sections. All thin sections were performed at GFZ in Potsdam.

3.4 Isotope analyses in sediments

3.4.1 Cleaning of diatom frustules

Analysis of $\delta^{18}O_{diatom}$ requires the material to be almost pure diatomite since fluorination techniques following Clayton and Mayeda (1963) will release oxygen from all the components in the sediment; i.e. silt, clay, tephra, carbonates and organic matter (Juillet-Leclerc, 1986). Hence, samples were treated in

accordance with the four clean-up stage method proposed by Morley et al. (2004) with some variations (Fig. 3.3). Sample purity was checked after each stage using light microscopy:

Stage 1: Organic and carbonate removal. Standard methods were used to remove organic and carbonate material (Battarbee et al. 2001). A few grams of sediment were heated at 90°C in 30% H_2O_2 until all reaction ceased. Carbonate was then removed using 10% HCl for 12h. A stronger oxidising agent (concentrated HNO_3 heated at approximately 80°C for 1h) was used to eliminate any remaining organic matter. The samples were washed in a centrifuge three times in distilled water between each step and before the next stage.

Stage 2: Sieving. The samples were first sieved using a 125 µm sieve. This eliminated resistant charcoal and terrigenous particles >125 µm. The samples were then sieved again to obtain a fraction between 38 and 63 µm to remove clay and the remaining detrital grains. A diatom concentrate made up almost exclusively of valves of the large centric diatom *Cyclostephanos andinus* was obtained, thereby eliminating any species-specific effect variability in the samples. At this stage all diatoms of <38 µm were removed, an insignificant number of diatoms remained in the >63 µm fraction.

Stage 3: Differential settling. Gravity settling in a water column during the sieving process also helped to remove any remaining tephra and clay particles. The 38–63 µm sieved fraction was placed in glass beakers. Differential settling occurred since faster settling coarser silt grains were deposited under the slower settling diatoms. The diatom layer was carefully removed using a pipette. Excess water was decanted away but samples were kept wet.

Stage 4: Gravitational split-flow lateral-transport thin (SPLITT). The fourth stage was an alternative approach to heavy liquid separation. SPLITT was developed by J.C. Giddings at the University of Utah (Giddings, 1985) and first applied to the separation of diatoms at the University of Jülich (Schleser et al. 2001; Rings et al. 2004) (Fig. 3.4). SPLITT utilises the different densities and hydrodynamic properties of diatoms and contaminants to produce two distinct end fractions. Samples are passed along a narrow channel in a laminar flow at a constant velocity. Sediments of different density and hydrodynamic properties settle differently to create two distinct end fractions (Leng and Barker, 2006). A sample (A') is introduced into a thin channel where it meets a carrier fluid (usually water for diatom samples) in a laminar flow (Fig. 3.4). The velocity of the flow is controlled to separate the sample into two streams: the upper stream and the lower stream. The former stream, which contains finer, less dense and more hydrodynamic particles, passes through an outlet (A). The latter stream enables the collection of the remaining particles to pass through another outlet (B) (Leng and Barker, 2006) (Fig. 3.4). SPLITT was employed at Lancaster University (UK). The SPLITT technique was only applied to the 38-63 µm fraction which contained clays and fine tephra particles after the previous settling stage.

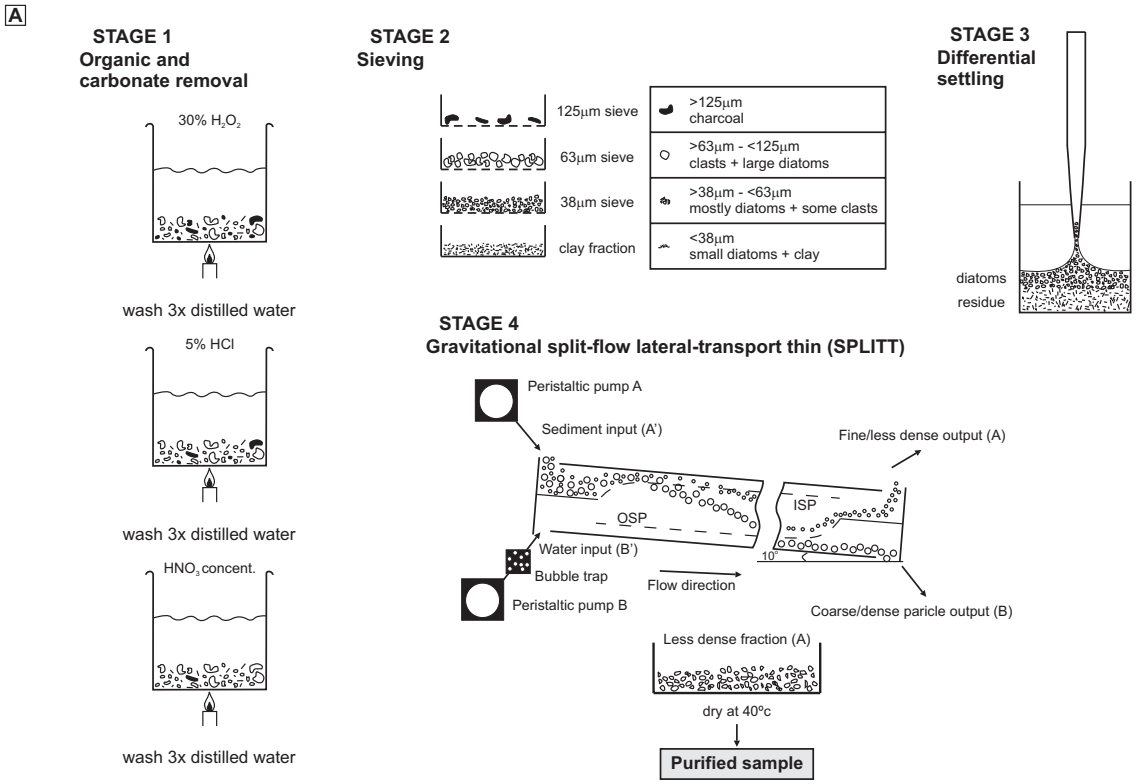

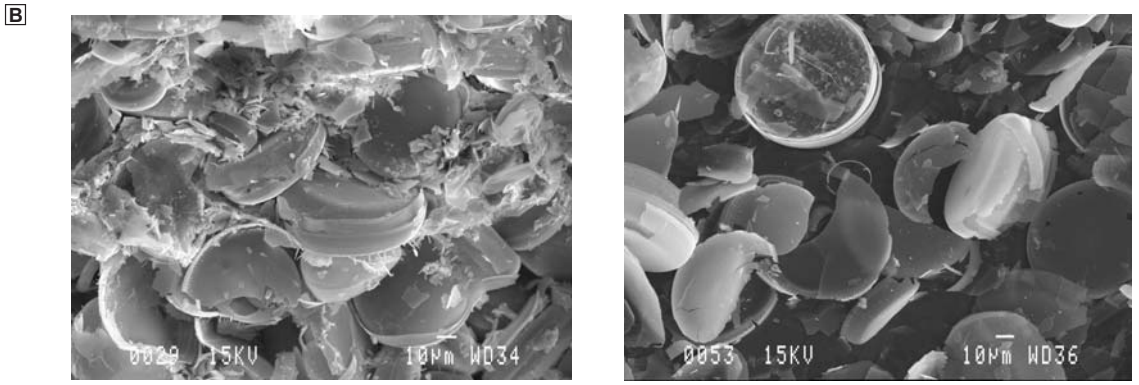

Figure 3.3. A) Diagram showing the four-stage laboratory pretreatment before $\delta^{18}O_{diatom}$ analysis. Stage 1 chemically removes organic matter and carbonates. Stages 2, 3 and 4 eliminate mineral contaminants that may contribute to the $\delta^{18}O_{diatom}$ signal. The duration of the treatment varies from sample to sample (modified from Morley et al. 2004). B) SEM images of two samples before cleaning (left) and after cleaning (right)

Finally, the purified diatom samples were dried at 40ºC between 24h and 48h. After the cleaning process all the samples were checked under a light microscope and a number of random samples were verified with XRD, TC analysis and SEM observations. This verification process confirmed that the samples did not contain significant amounts of terrigenous matter. TC values were below 0.5 wt% and the terrigenous content (clays or tephra) was less than 1 wt% (Fig. 3.3). The final isotope data were not affected despite the fact that a large number of diatoms were broken during the cleaning process.

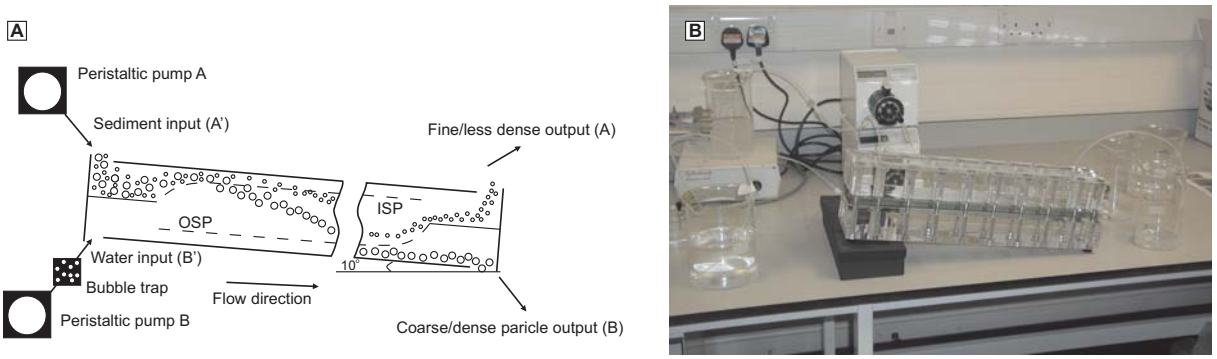

Figure 3.4. A) The SPLITT system utilises the different properties of sediment for separation into two fractions. Sediments with a higher density will settle faster than sediments with a lower density. Similarly, oval-shaped sediments will have greater drag than needle-shaped sediments. These properties create two distinct end fractions. The process can be repeated several times to further purify samples. B) Image of the SPLITT from the Lancaster Environment Centre at Lancaster University.

3.4.2 Oxygen isotope extraction

Diatom frustules consist of an inner tetrahedrally bonded silica skeleton (Si–O–Si) with an outer hydrous layer (Labeyrie and Juillet,1982) (Fig. 1.10). The distribution of these two components is more complex than simple layering and is related to the mode of formation of the frustule and its differential porosity. Through the dissolution of the hydrous parts of the frustule, Juillet (1980) demonstrated that the internal dense silica is isotopically homogenous whereas the outer hydrous layer freely exchanges with any water that the diatom silica comes into contact with. Knauth (1973) considered that biogenic opal has 7–12 wt% water, compared to 1 wt% for quartz, although Leng et al. (2001) suggested that 20–30% of diatom oxygen needs to be removed before stable values for $\delta^{18}O$ are reached. Thus, prior to analysis it is essential to remove the –Si–OH layer of the diatom frustule when attempting to obtain environmental records from δ18Odiatom (Swann and Leng, 2009). The extraction of the –Si–OH layer, however, which may require the removal of 7–40% of all oxygen within diatoms (Leng and Sloane, 2008), is technically challenging and requires specialised equipment, hazardous reagents and highly trained operators (Swann and Leng, 2009).

The internal Si–O bond needs considerable energy to break and requires the use of an extremely powerful oxidising reagent (i.e., a fluorine based compound such as ClF_3 or BrF_5) or high temperatures (Leng and Barker, 2006; Leng and Sloane, 2008). The classic fluorination approach using the step wise approach method described here (Fig.3.5) is the standard methodology employed for extracting oxygen from diatom silica prior to mass spectrometry at the NERC Isotope Geosciences Laboratory (NIGL), UK. All isotope analyses described in this PhD thesis (with the exception of the water O and H) were analysed at NIGL.

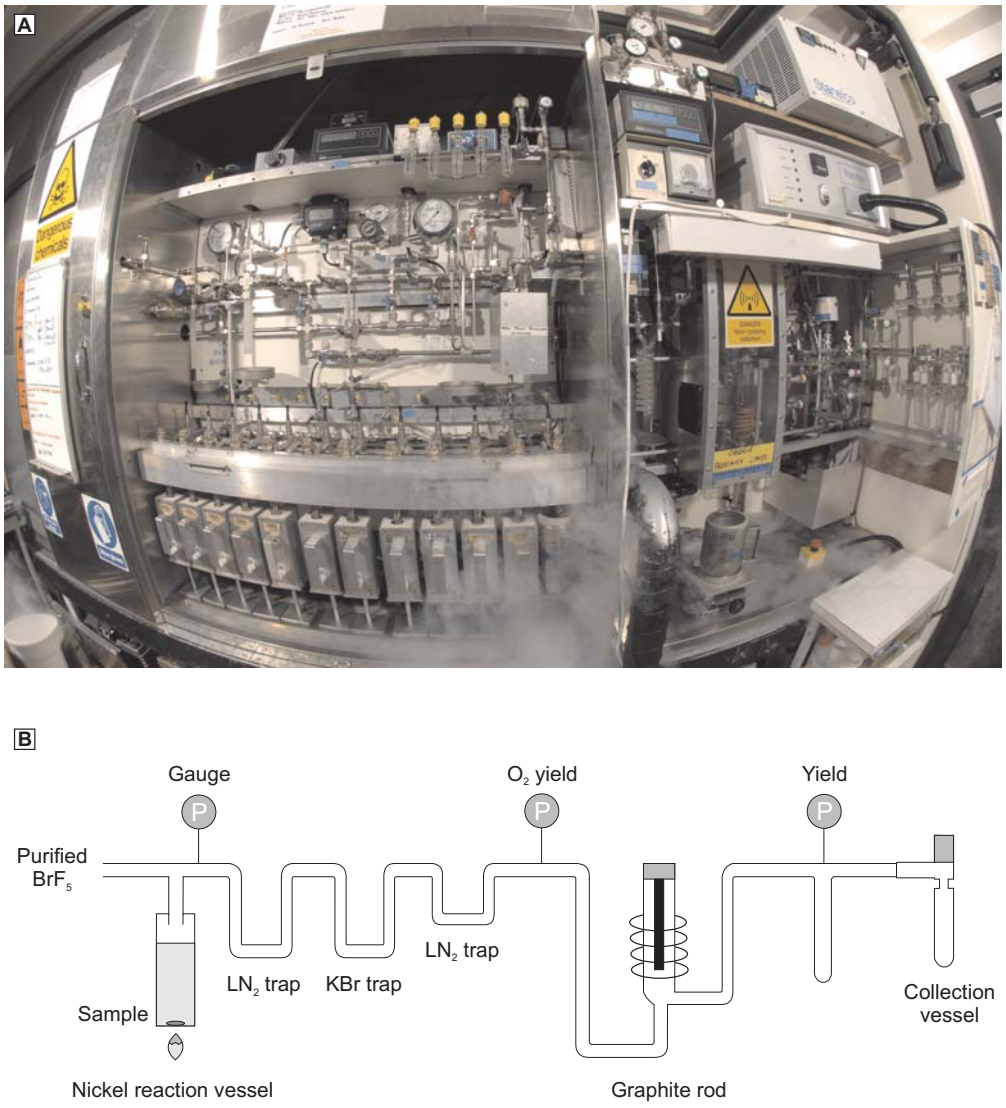

Figure 3.5. The fluorination line used at the NERC Isotope Geosciences Laboratory for the extraction of oxygen (as CO_2) from biogenic silica for IRMS. A) Fish-eye lens image; B) schematic. Modified from Leng and Sloane (2008).

Stepwise Fluorination (SWF) involves a three-stage process (Haimson and Knauth, 1983; Matheney and Knauth, 1989). First, samples between 5 and 10 mg were outgassed in nickel reaction tubes at room temperature to remove the hydrous layer and excess water. Given that the first fluorination stage of the SWF methodology removed some non-diatom contamination (e.g. highly reactive clays) in the sample (Matheney and Knauth, 1989), the SWF method provides $\delta^{18}O_{diatom}$ data that is less distorted by contamination when sample purity is less than 100% (Swann and Leng, 2009). The second fluorination stage was used to release oxygen from the outer –Si–O–Si layer. This involved prefluorination using a stoichiometric deficiency of the reagent BrF_5 at a low temperature. The third stage involved a full reaction at 450°C for 12 hours with an excess of BrF_5 to release the oxygen (gas) from the structurally bound component (Leng and Barker, 2006; Leng and Sloane, 2008). The oxygen liberated was then converted

into CO_2 by exposure to graphite using the method of Clayton and Mayeda (1963). The CO_2 was measured with a Finnigan MAT 253 dual inlet mass spectrometer and normalised against a NBS-28 quartz international standard.

During oxygen extraction, oxygen yields were monitored for every sample and compared with their calculated theoretical yield for SiO_2. Most samples had mean yields of 69% - 70% of their theoretical yield based on silica. This suggests that around 30% of the material including hydroxyl and loosely bonded water (both OH^- and H_2O) was removed during prefluorination.

A random selection of more than 50 samples were analysed in duplicate or in triplicate, giving a reproducibility between 0.01‰ and 0.6‰ (1σ) with a mean value of 0.15‰. The standard laboratory quartz and a diatomite control sample (BFC) had a mean reproducibility over the period of analysis of 0.2‰. The oxygen isotope composition of diatom silica is expressed on the delta-scale in terms of per mil (Equation 1). For diatom oxygen the reference is VSMOW (Vienna Standard Mean Ocean Water, which is specially-prepared distilled seawater).

3.4.3 Analyses of $\delta^{13}C_{diatom}$ and $\%C_{diatom}$

$^{13}C/^{12}C$ ratios and %C of organic matter within the diatom frustules were analysed by combustion in an elemental analyser (Costech ECS4010) interfaced with a VG dual inlet isotope ratio mass spectrometer (Fig. 3.6).

Samples containing 1 to 2 mg of pure diatomite were loaded into tin capsules and placed on the carousel of the elemental analyser. The samples were sequentially dropped into a continuous flow of helium carrier gas into a 1020°C furnace. A pulse of oxygen gas promoted an exothermal flash oxidation of the tin, ensuring full combustion of the sample, and the product gases were further oxidised by chromium and cobaltous oxides in the lower part of the furnace. The excess oxygen and water were removed by passing them through hot copper and magnesium perchlorate. The remaining N_2 and CO_2 were then passed through a Gas Chromatrography column and a thermal conductivity detector. This generated an electrical signal proportional to the concentrations of N_2 and CO_2 present in the helium stream. The Costech software station acquired and evaluated this information, producing %C data for the sample. As a result, it was possible to calibrate the instrument and to quantify the content of carbon of the unknown sample by analysing a standard sample of a given composition under the same operating conditions.

Meanwhile the helium stream had carried the CO_2 through a trap at –90°C (for complete removal of water), before reaching the Triple Trap held at –196°C. Here the CO_2 was frozen, allowing the N_2 and helium to vent to the atmosphere. The TripleTrap was then evacuated before warming the CO_2 trap and discharging the sample CO_2 into the inlet of the Optima (Fig. 3.6).

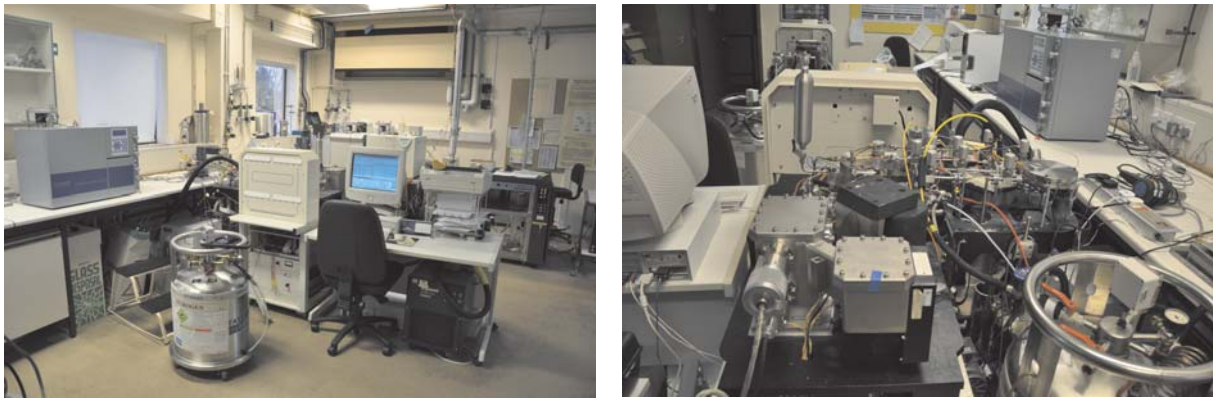

Figure 3.6. Images of the carbon isotope analyser used at the NERC Isotope Geosciences Laboratory for the extraction of carbon (as CO_2) from biogenic silica and for analysis by means of an Optima mass spectrometer.

The Optima mass spectrometer had triple collectors allowing simultaneous monitoring of CO_2 ion beams at the mass-to-charge ratio (m/e) = 44, 45 and 46 and a dual-inlet allowing rapid comparison of sample CO_2 compared with a reference CO_2. 45/44 molecular mass ratios were converted to $^{13}C/^{12}C$ ratios after correction for common ion effects (Craig correction). Samples were measured against a within-run laboratory standard (BROC1). Based on the knowledge of the $\delta^{13}C$ values obtained from the lab standard (derived from regular comparison with international calibration and reference materials NBS-19 and NBS-22), the $^{13}C/^{12}C$ ratios of the unknown samples were converted into $\delta^{13}C$ values versus VPDB (Leng, pers comm.). Replicate analyses of well-mixed samples indicated a precision of ±<0.1‰ (1 σ) (for $\delta^{13}C$) and 0.1 (1 σ) (for %C).

3.5 Statistical analyses and Grey-colour curve

The Multi-Taper Method (MTM) and the Time-Frequency (TF) analysis were employed to examine the periodic components in the $\delta^{18}O$ values from interval 1. These spectral analyses enabled us to examine statistically significant modes in the time series in both the frequency and time domains. MTM provided a means of spectral estimation (Thompson, 1982) and a signal reconstruction (e.g. Park, 1992) for time series with spectra that contain both singular and continuous components (Theissen et al. 2008). MTM has been widely employed in the analysis of geophysical data including data from palaeoclimate studies (e.g. Mann et al. 1995; Mann and Park, 1996). The TF analysis is a hybrid tool constituted by the Fourier Transform and wavelets to examine non-stationary phenomena that decompose a time series into time-frequency space. As a result, the dominant modes of variability and the manner in which these modes vary in time can be determined (Lau and Weng, 1995; Torrence and Compo, 1998). For this reason, this analysis does not use a fixed-size Gaussian window but a Gaussian window that adapts to the spectrum

(Stockwell et al. 1996). All the statistical treatments of the datasets were performed using the R software package (R Development Core Team, 2008).

Grey-colour curve was calculated using the ImageJ software package (Rasband, 1997–2009). A surface from the interval studied was selected in order to obtain a digital image which was a two-dimensional array of pixels. Every pixel presented a value related to the light reflection from a grey-scale variation. The image was an 8-bit grey-scale, and each pixel represented a value ranging from 0 (black) to 255 (white). Thus, it was possible to calculate a curve showing the variations along every pixel in a row. The results are presented in a 21 running mean curve.

Chapter 4

The palaeohydrological evolution of Lago Chungará (Andean Altiplano, northern Chile) during the Late Glacial and Early Holocene using oxygen isotopes in diatom silica*

4.1 Introduction

Oxygen isotopes of diatom silica have been widely used in palaeoenvironmental reconstructions from lake sediments in the last decade (see Leng and Barker, 2006 for a comprehensive review). Using $\delta^{18}O$ in palaeoenvironmental reconstruction is however not easy, because the sedimentary record can be influenced by a wide range of interlinked environmental processes ranging from regional climate change to local hydrology. The oxygen isotopic composition of diatom silica depends on the isotope composition of the water when the skeleton of the siliceous micro-organisms is secreted, and also on the ambient water temperature (Shemesh et al. 1992). Therefore, knowledge of all the environmental factors that may have influenced the isotope composition of the lake water is vital for the interpretation of the $\delta^{18}O_{diatom}$ signal (Leng et al. 2005b). One of these environmental factors is evaporation, which has a major influence on the isotope composition of any standing water body (Leng and Marshall, 2004). The $\delta^{18}O$ record can therefore be used, at least in closed lakes, as an indicator of changes in the P/E related to climate changes (Leng and Marshall, 2004). Yet, before any palaeoclimatic interpretation of the isotope records from a lake is considered, other local palaeohydrological intervening factors from the basin need to be taken into account (Sáez and Cabrera, 2002; Leng et al. 2005b).

The sedimentary records of high-altitude, Andean Altiplano lakes, are good candidates for carrying out oxygen isotope studies to reconstruct the Late Quaternary palaeoclimatology of the region, because they preserve an excellent centennial- to millennial-scale record of effective moisture fluctuations and source changes during the Late Glacial and Holocene although the interpretation not always strength forward (Abbot et al. 1997; Argollo and Mourguiart, 2000; Valero-Garcés et al. 2000, 2003; Baker et al.

**Chapter based on the paper published in:*
Journal of Quaternary Science *(2008) vol. 23(4) 351-363. Armand Hernández, Roberto Bao, Santiago Giralt, Melanie J. Leng, Philip A. Barker, Alberto Sáez, Juan J. Pueyo, Ana Moreno, Blas L. Valero-Garcés and Hilary J. Sloane.*

2001a,b;Grosjean et al. 2001; Tapia et al. 2003; Fritz et al. 2004, 2006; Placzek et al. 2006). The $\delta^{18}O$ analyses of carbonates, cellulose and biogenic silica have successfully been used to reconstruct the hydrological responses to climate change in different Andean lacustrine systems (Schwalb et al. 1999; Abbott et al. 2000, 2003; Seltzer et al. 2000; Wolfe et al. 2001; Polissar et al. 2006).

Up to now, only stable isotopes in carbonates have been examined in Lago Chungará (Valero-Garcés et al. 2003), although its sedimentary record is made up of rich diatomaceous ooze ideal for diatom silica oxygen isotope studies. Lago Chungará currently behaves as a closed lake, without any surface outlet and evaporation as the dominant water loss process (Herrera et al. 2006); however it has shown a complex depositional history since the Late Glacial (Sáez et al. 2007) and the relative role of other factors (groundwater versus evaporation) should be evaluated.

Here we examine a high resolution $\delta^{18}O_{diatom}$ record of three selected sections belonging from the Late Glacial to Early Holocene (ca 12,000 – 9,400 cal years BP) from Lago Chungará. We emphasise the role that some local factors such as sedimentary infill and palaeohydrology can play on the interpretation of the $\delta^{18}O_{diatom}$ record and therefore the need to discriminate between the climate and local environmental signals.

4.2 Results: Petrography and isotope composition of diatoms

Smear slide, SEM, and several analyses (XRD, TC, biogenic silica) of the lake sediments before they were prepared for isotope analysis showed that the samples were composed of both amorphous and crystalline material. The amorphous fraction comprises biogenic silica (between 47-58 wt%), organic matter and volcanic glass. The crystalline fraction represented <10% of the sediments.

4.2.1 Interval 1 (11,990 – 11,530 cal years BP)

Diatom concentration range from 108.3 to 633.8 million valves g^{-1}. The interval is dominated by euplanktonic diatoms ranging from 79.1% to 93.9% of the diatom assemblage. The thicknesses of the laminae are between 0.9 and 10.3 mm (Fig. 4.1.A). Smear slide, thin section and SEM observations showed that light laminae were quasi-monospecific layers of large *Cyclostephanos andinus* (diameter > 50 μm). The upper contact of the light laminae with the dark laminae is transitional, showing an increase in diatom diversity with subdominant tychoplanktonic (*Fragilaria* spp.) and benthic diatoms (mainly *Cocconeis* spp., *Achnanthes* spp., *Navicula* spp. and *Nitzschia* spp.) (Fig. 4.2.C) whereas the lower contact is abrupt (Fig. 4.2.A). Diatom valves show good preservation with no preferred orientation in the lower part, but increasingly orientated upwards. The content of the organic matter also increases upwards. Dark laminae comprise a more diverse mixture of diatoms, including the euplanktonic (those having a strict planktonic character) smaller *Cyclostephanos andinus* (diameter < 50 μm) than those found in light laminae, and diatoms of the *Cyclotella*

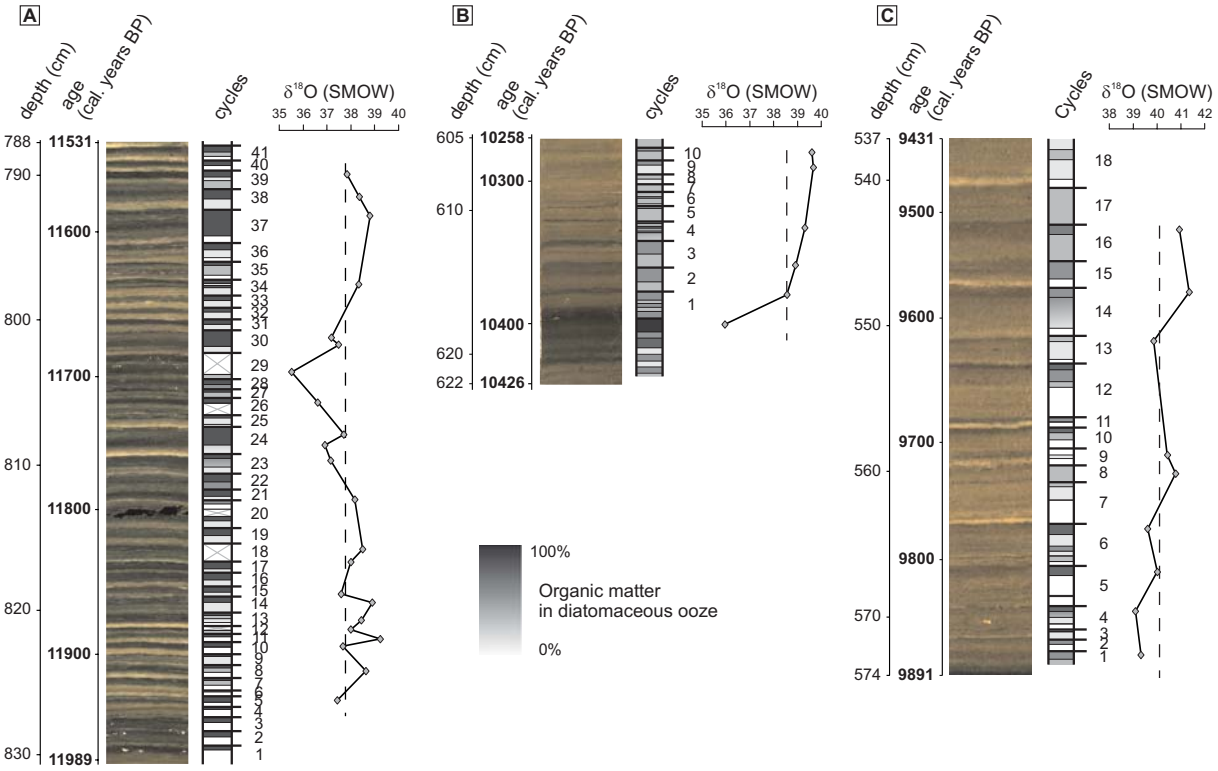

Figure 4.1. Digital images of the three intervals selected according to its depth and timescale. The identified couplets and the $\delta^{18}O$ values from diatom silica have been plotted for interval 1 (A), interval 2 (B) and interval 3 (C). Stippled line shows mean values.

stelligera complex, as well as tychoplanktonic (those usually having a benthic life form but which can occasionally be facultatively planktonic) and benthic diatoms (bottom dwelling forms). These dark laminae are also enriched in organic matter probably from diatoms and other algal groups. Up to 41 light and dark laminae couplets were defined. The thickness of these couplets ranges between 4.2 mm and 22.5 mm and, according to the chronological model they are pluriannual (mean about 10 years). The rhythmite starts with the dominance of light laminae progressively changing to a dominance of dark laminae.

The $\delta^{18}O_{diatom}$ values of the purified diatoms in interval 1 range from +35.5‰ to +39.2‰ (Fig. 4.1.A). Higher $\delta^{18}O_{diatom}$ occur in the lower part of the interval (around 822 cm of core depth). There is an upwards decreasing trend (~1.9‰/100 years) attaining a minimum of +35.5‰ around 803 cm depth. This stretch is followed by an increasing shift of ~2.9‰/100 years towards the upper part of the interval where a relative maximum of +38.8‰ is reached at 793 cm depth. The uppermost two samples show a light depletion. The mean $\delta^{18}O_{diatom}$ value of this interval is +37.8±0.85‰.

4.2.2 Interval 2 (10,430 – 10,260 cal years BP)

Diatom concentration ranged from 95.2 to 218 million valves g^{-1} in interval 2. Almost 94% of the diatom assemblages of this interval were made up of euplanktonic diatoms. Benthic taxa show the

minimum values for the three analysed intervals. The thickness of diatomaceous ooze laminae ranged from 1.8 mm to 16 mm (Fig. 4.1.B). Light laminae were dominated by large *Cyclostephanos andinus* (diameter > 50 μm) with some tychoplanktonic (*Fragilaria* spp.) and benthic diatoms, as well as minor amounts of siliciclasts and organic matter. Dark laminae are composed of a mixture of small and large *Cyclostephanos andinus* valves, with more abundant tychoplanktonic and benthic diatoms (as well as organic matter) compared to light laminae. Diatom valves are not so well preserved as in interval 1 sometimes showing a high degree of fragmentation and a preferred orientation. The contact between the laminae is similar to those found in interval 1. Clear couplets were only observed in the upper two thirds of the interval and only 10 couplets could be identified (Fig. 4.1.B). They are pluriannual (mean couplet represents about 10 years of sedimentation) and their thicknesses range between 5.5 and 19 mm. Light laminae were more abundant in the upper part of the interval 2, whereas dark laminae are more abundant in the lower part.

The $\delta^{18}O_{diatom}$ curve shows a clear increasing trend during this interval (Fig. 4.1.B). The lowest $\delta^{18}O_{diatom}$ value (+36‰) was recorded at the bottom of the interval (617 cm depth) and the maximum at the two uppermost samples (+39.7‰ and +39.6‰; 606-605 cm of core depth). The magnitude of the increasing trend is much higher between the two lowermost samples (~18.5‰/100 years) than for the rest of the interval (~0.6‰/100 years). The mean $\delta^{18}O_{diatom}$ value of this interval is +38.7±1.4‰.

4.2.3 Interval 3 (9,890 – 9,430 cal years BP)

Diatom concentration ranges between 163.8 and 255.8 million valves g^{-1} for interval 3. Euplanktonic diatoms (68.6% - 98.1%) also dominate this interval, and have the minimum values for the three intervals. On the contrary, benthic diatoms show moderate values (up to 31.4%), being the highest for the three intervals.

Light diatomaceous ooze laminae ranged between 0.9 and 12.3 mm in thickness (Fig. 4.1.C), and they comprise *Cyclostephanos andinus* (diameter > 50 μm) increasing upwards in both taxonomic diversity and organic matter content. The lower contact with dark laminae shows an abrupt change in diatom size whereas the upper one is gradual. Diatom valves show good preservation with no orientation in the lower part but are preferentially oriented upwards. Dark laminae comprise a mixture of smaller *Cyclostephanos andinus* (diameter < 50 μm), with subdominant tychoplanktonic and benthic diatoms, as well as a high organic matter content. The lower contact is gradual whereas the upper one abrupt. Up to 18 light and dark pluriannual couplets were defined (mean couplet represent around 12 years). These couplets are 3 to 18 mm thick. The rhythmite starts with light laminae progressively changing to dark laminae.

The $\delta^{18}O_{diatom}$ curve for interval 3 (Fig. 4.1.C) shows an overall continuous increasing trend of ~0.9‰/100 years from +39.1‰ (570 cm of core depth) to +41.3‰ (548 cm of core depth). Superimposed over the general trend are short-term fluctuations. The mean $\delta^{18}O_{diatom}$ value of this interval is +40.1±0.77‰.

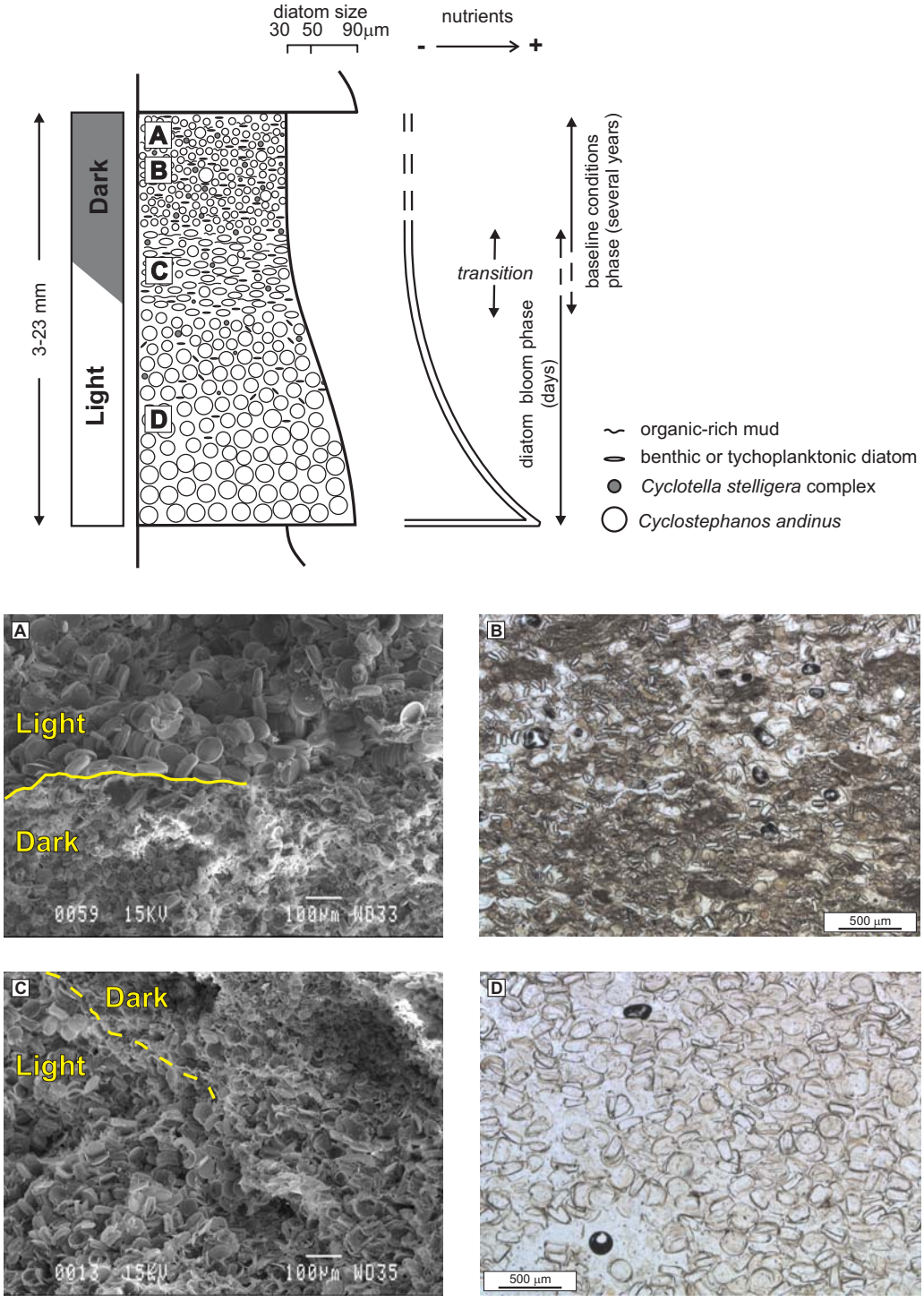

Figure 4.2. Rhythmite type showing thickness, colour, ecological succession and temporal scale. (A) SEM image showing the contact between dark (bottom) and light lamina (top). (B) Petrographical microscope image of the dark lamina. (C) SEM image showing the transitional contact between light (bottom) and dark lamina (top). (D) Petrographical microscope image of the light lamina. See text for details.

The three intervals have different $\delta^{18}O_{diatom}$ averages displaying a progressive low-frequency enrichment from the interval 1 (+37.8±0.85‰) to interval 3 (+40.1±0.77‰). The overall isotopic enrichment is 2.1‰ throughout these intervals.

4.3 Discussion

4.3.1 The sedimentary model of diatom rhythmites

Laminated diatomaceous oozes in the sedimentary record of Lago Chungará comprise variable thickness couplets of alternating light and dark laminae. These couplets display different features (colour and mean thickness) in the three intervals described here although they exhibit similar diatom assemblages and textural characteristics and therefore it is assumed that their formation is by similar environmental processes. Rhythmite types have been established (Fig. 4.2); light laminae are formed almost exclusively by diatom skeletons of a quasi-monospecific assemblage of *Cyclostephanos andinus,* while dark laminae, with a high organic matter content, comprise a mixture of a more diverse diatom assemblage including the euplanktonic *Cyclostephanos andinus* although diatoms of the *Cyclotella stelligera* complex are the dominant taxa. Subdominant groups are some tychoplanktonic (*Fragilaria* spp.) and benthic taxa (*Cocconeis* spp., *Achnanthes* spp., *Navicula* spp., *Nitzschia* spp.).

Each couplet was deposited during time intervals ranging from 4 to 24 years according to our chronological model. Couplets are therefore not a product of annual variations in sediment supply but due to some kind of pluriannual processes. The good preservation and size of diatom valves in the light laminae suggest accumulation during short-term extraordinary diatom blooms, perhaps of only days to weeks in duration. These diatom blooms could have been triggered by climatically driven strong nutrient inputs to the lake and/or to nutrient recycling under extreme turbulent conditions and mixing affecting the whole water column. On the contrary, the baseline conditions are represented by the dark laminae. Each of these laminae is made up of the remains (organic matter and diatom skeletons) of a diverse planktonic community deposited throughout several years under different water column mixing regimes. The preserved remains are therefore a reflection of different stages in the phytoplankton succession throughout several years (Reynolds, 2006).

4.3.2 Lake level and $\delta^{18}O_{diatom}$ changes

A preliminary lake level reconstruction of Lago Chungará was undertaken employing the variations of euplanktonic diatoms, *Botryoccocus* and macrophyte remains (see Sáez et al. 2007). This reconstruction shows a general deepening trend during the Late Glacial and Early Holocene. This overall increase in lake level is punctuated by one deepening (D1; Fig. 4.3) and by two shallowing episodes (S1 and S2; Fig. 4.3). According to Sáez et al. (2007) the three selected intervals described here represent two different lacustrine conditions. Intervals 1 and 3 are likely shallower episodes that ocurred in different

climate periods, whereas interval 2 occurred during a period between two shallow intervals, and likely with higher lake level conditions. However, the resolution of the lake level reconstruction provided by Sáez et al. (2007) does not preclude the occurrence of other shallowing episodes than those previously detected. The isotope analyses presented here of these three intervals have allowed us to characterise the hydrological evolution of the lake for these different lacustrine conditions during the Late Glacial and Early Holocene. Dark laminae were selected for $\delta^{18}O_{diatom}$ analyses to investigate the baseline hydrological evolution of Lago Chungará. These dark laminae would represent a normal annual cycle of the lake with alternating phases of stratification and mixing. These conditions would lead to the development of a complex diatom community, among other algal groups (Hernández et al. 2007). The $\delta^{18}O_{diatom}$ variation can result from a variety of processes (Jones et al. 2004; Leng et al. 2005a) but for closed lakes, particularly in arid regions where water loss is mainly through evaporation, measured $\delta^{18}O_{lakewater}$ values are always more enriched than those of ambient precipitation since the oxygen lighter isotope (^{16}O) is preferentially lost via evaporation. Under these circumstances, the $\delta^{18}O_{diatom}$ record can be used as an indicator of changes in the P/E related to climate changes (Leng and Marshall, 2004).

Lago Chungará is a hydrologically closed lake and its main water loss is currently via evaporation, thus meaning that changes in $\delta^{18}O$ values should be directly related to shifts in the P/E. The lake level change from the deeper water conditions recorded during the sedimentation of interval 2 to the shallower conditions occurred during the deposition of interval 3 according to the Sáez et al. (2007) reconstruction, is

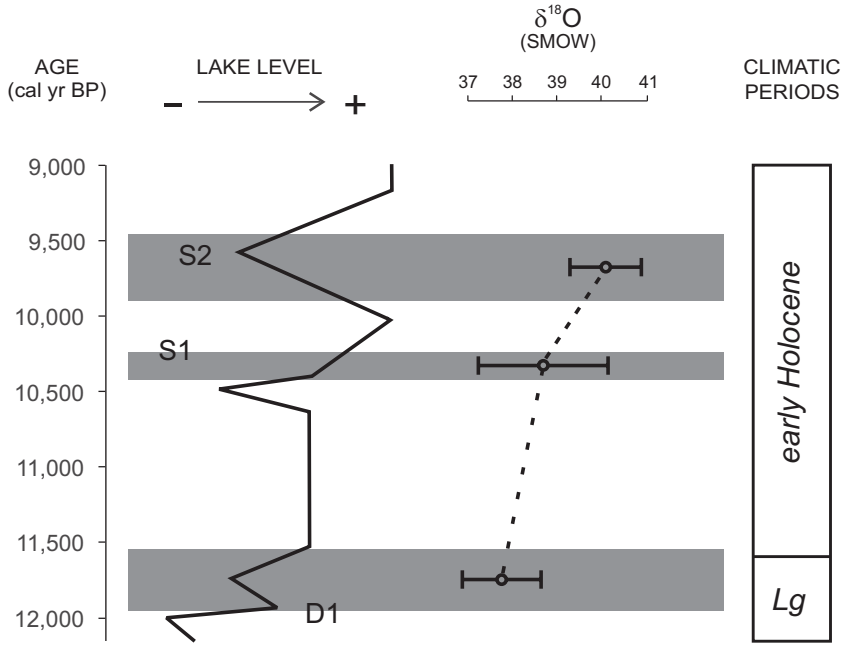

Figure 4.3. Lake-level evolution curve based on biological indicators (modified from Sáez et al. 2007). Deepening–shallowing episode (D1) and shallowing–deepening episodes (S1 and S2) are indicated. The lake followed an overall deepening trend (see Sáez et al. 2007 for further details). Shaded bands mark the three studied intervals. On the right corresponding mean values of $\delta^{18}O$ from diatom silica of the studied intervals are shown.

compatible with the observed increase in $\delta^{18}O$ values. However, the isotope values and the lake level reconstruction do not agree over the transition from interval 1 to interval 2. The isotope values suggest a reduced P/E (shallower) stage, whereas several proxy indicators suggest deeper conditions (Fig. 4.3). A possible explanation for this could involve shifts in $\delta^{18}O_{diatom}$ related to other environmental circumstances, such as variations in the morphometrical parameters and changes in the groundwater outflow. Changes in the surface to volume ratio and in groundwater outflow of Lago Chungará from the Late Glacial to Early Holocene are the factors likely to account for most of the shifts found in the $\delta^{18}O_{diatom}$ values.

Besides fluctuations in the P/E, another factor to take into account is basin morphology. During the lake's evolution the lake's surface to volume ratio would have changed. A tentative palaeobathymetric reconstruction of Lago Chungará based on the lake level curve from Sáez et al. (2007) (Fig. 4.4) shows that during the Late Glacial the lake only occupied the present central plain area. The rise in the lake level during the Early Holocene, although punctuated by some oscillations, flooded the extensive eastern and southern margins of the basin. Under these circumstances, the lake underwent a significant increase in its surface area (Fig. 4.4). Because the eastern margin is much shallower than the central plain (Fig. 2.7), the whole lake's surface area to volume ratio would have significantly increased, and also concurrently the relative importance of evaporation. So the observed $\delta^{18}O_{diatom}$ high values of the interval 3 could be explained not only by the shallowing trend from interval 2 to interval 3, but also by the increasing of the lake's surface to volume ratio between both intervals.

There are no signs of subaerial exposure in the recovered sediments of the eastern platform, which indicates that lake water level did not drop significantly afterwards. Although the lake was deeper during interval 3 than during the interval 1, the mean isotope value is higher during interval 3. This fact could be explained by the increase of the surface to volume ratio and by the reduction of groundwater losses. Hence, the morphology of the lake, and not only water depth, must be considered as a key factor in any interpretation of the $\delta^{18}O_{diatom}$ in terms of changes in P/E.

Furthermore, changes in the groundwater fluxes in Lago Chungará could have been a significant factor in the shifts found in the $\delta^{18}O_{diatom}$ values from the Late Glacial to Early Holocene. The groundwater outflow from the lake during the Late Glacial was probably higher than during the Holocene. This condition would progressively change with the sedimentary infill of the basin. Drainage, through the breccia barrier would progressively become less efficient as the groundwater outflows silted-up (Leng et al. 2005b). Thus, evaporative losses would have predominated over groundwater during the Early Holocene. This highlights the fact that stable isotopes would not have, in this case, a direct correspondence with changes in the lake water level.

In summary, the relative increase in evaporation due to the increase in the lake's surface to volume ratio between the studied intervals could have played a significant role. Superimposed onto this situation, the increase in the $\delta^{18}O_{diatom}$ values from the Late Glacial (when the lake was at its shallowest) to the Early

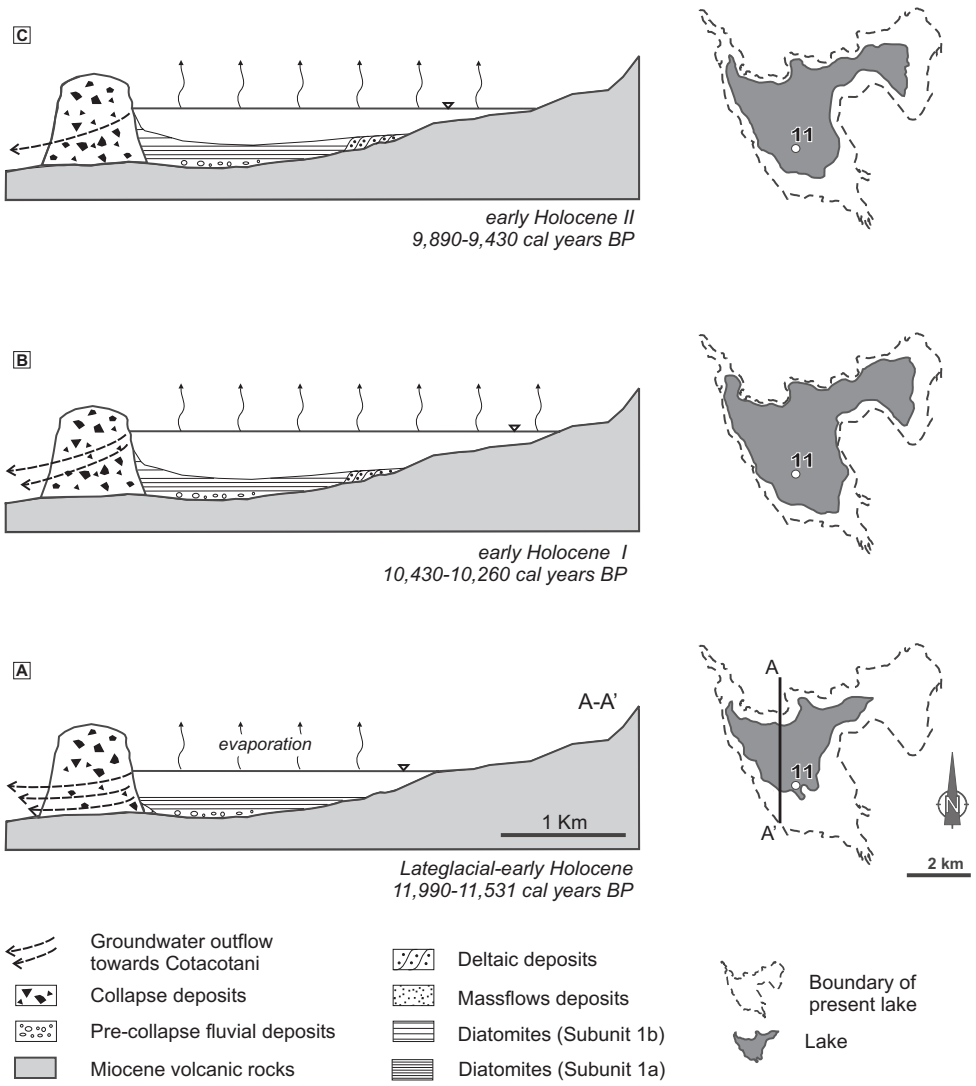

Figure 4.4. Hydrological evolution of the Lago Chungará in the Lateglacial–early Holocene. North–South cross-section of the lake (left) and water lake surface area (right) for the sedimentation of interval 1 (11,990–11,530 cal. years BP (A)), interval 2 (10,430–10,260 cal. years BP (B)) and interval 3 (9,890–9,431 cal. years BP (C)).

Holocene (when the overall deepening trend started) is also likely to have been related to a change to a predominantly evaporative lake as the lake's bottom became more impermeable due to sediment basin sealing.

4.4 Conclusions

The thin section study of the diatomaceous laminated sediments shows that the rhythmites are made up of light quasi monospecific lamina of the euplanktonic diatom *Cyclostephanos andinus* and a pluriannual dark lamina rich in organic matter and a mixture of a more diverse diatom assemblage. The formation of light laminae is apparently related to short term (days to weeks) diatom blooms whereas dark laminae represent baseline conditions lasting several years.

The oxygen isotope record of the dark laminae diatoms of Lago Chungará indicates a progressive $\delta^{18}O$ enrichment from the Late Glacial to Early Holocene. Besides changes in the P/E, two other factors could have governed shifts in the Lago Chungará $\delta^{18}O_{diatom}$ record. The basin's stepped morphology forced the expansion of the lake towards the eastern and southern shallow margins during the rising trend. These changes could have caused an increase in the lake's surface to volume ratio thus enhancing the evaporation which caused isotope enrichment during the Early Holocene. In addition, changes in the groundwater/evaporation loss ratio and changes in the lake's extent. The hydrology of the lake was probably modified during the Late Glacial to Early Holocene transition as the lake's groundwater outflow became progressively sealed by sediments, thereby increasing lake water residence time and potential evaporation.

Previous work has focused on issues of diagenesis, contamination and host-water interactions that can all influence $\delta^{18}O_{diatom}$ whereas local hydrological factors have been largely neglected. These results point to the complex interplay among the different factors which intervene in the diatom oxygen isotope record of closed lakes and how interpretation needs to be adapted to the different evolutionary stages of the lake's ontogeny. This study highlights the importance of reconstructing local palaeohydrology as this may be only indirectly related to palaeoclimate.

Chapter 5

ENSO and solar activity signals from oxygen isotopes in diatom silica during the Late Glacial-Holocene transition in Central Andes (18ºS)*

5.1 Introduction

The study of Andean Altiplano lacustrine records plays a prominent role for interpreting the Quaternary palaeoclimatic history of the South American tropics and therefore for understanding the function of the tropics in the Earth's climate system (Grosjean et al. 2001; Valero-Garcés et al. 2003; Placzek et al. 2006) (Fig. 2.3). For this reason, studies on the sedimentary records from this area have increased in the last few decades. Most of these studies have focussed on the reconstruction of climate events at millennial time scales, especially since the Last Glacial Maximum (Baker et al. 2001a). There is a general consensus that orbital forces are the main factor triggering the climate conditions at a millennial-scale (Rowe et al. 2002; Placzek et al. 2006), and are therefore responsible for those climate events. Superimposed onto this long term variability, changes in the hydrologic balance at a sub-millennial scale in the Andean Altiplano, have been attributed to the variability of the Pacific SSTs and the strength of the zonal winds (Rowe et al. 2002; Garreaud et al. 2003). Both factors are controlled by ENSO and changes in the solar activity (Theissen et al. 2008). A number of studies have detected multidecadal- to centennial-scale hydrological balance shifts, suggesting that these relationships have been active since, at least, the Mid-Holocene (Valero-Garcés et al. 2003; Theissen et al. 2008).

$\delta^{18}O_{diatom}$ are increasingly being used for palaeoenvironmental reconstructions in lacustrine sedimentary records (Rietti-Shati et al. 1998; Barker et al. 2001). However, application of this proxy to high-resolution centennial to millennial lacustrine records is still in its infancy (Barker et al. 2007). $\delta^{18}O_{diatom}$ in decadal-to-centennial resolution palaeoclimatic reconstructions has not been utilised, mainly due to the difficulty in obtaining high resolution samples from sites with sufficient variation in $\delta^{18}O_{diatom}$ (outside of analytical error) that can be characterised at this fine temporal scale. Additional difficulties

*Chapter based on the paper published in:
Journal of Paleolimnology *(In press). Armand Hernández, Santiago Giralt, Roberto Bao, Alberto Sáez,Melanie J. Leng, Philip A. Barker.*

in using $\delta^{18}O_{diatom}$ are related to the difficulty in obtaining monospecific diatom samples in order to eliminate any species-specific effect variability, to acquire the necessary amount of sample from these short periods of time, and to have pure diatom samples, since significant contaminants can produce excursions in $\delta^{18}O_{diatom}$ that are similar to those produced by climate variations (Brewer et al. 2008).

The diatomaceous ooze from Lago Chungará has previously been the subject of a preliminary diatom oxygen isotope study at low resolution. This earlier study was aimed at three non consecutive stretches of the sedimentary record, and did not include all the dark-green laminae (Hernández et al. 2008). For the present study we have analysed 40 consecutive dark-green laminae, corresponding to the Late Glacial and Early Holocene, which represent a continuous record of the background limnological conditions (Hernández et al. 2008) (see the sedimentary model in the sedimentary sequence and rhythmite type section below). The excellent preservation and high diatom content of the record of Lago Chungará allow a detailed study of the regional moisture balance at decadal and centennial timescales.

Here, we present the decadal to centennial time scale moisture balance reconstruction for the Andean Altiplano during the Late Glacial-Holocene transition (11,990-11,450 cal years BP) based on high-resolution analysis of $\delta^{18}O_{diatom}$. This analysis was performed on successive and continuous 40 dark-green laminae of lacustrine sediments present in a core located in the offshore zone of Lago Chungará. In order to support the interpretation, isotope data are compared with the reconstructions of the terrigenous inputs and inferred regional effective moisture in the Lago Chungará performed in the same core by Giralt et al. (2008).

5.2 Results

5.2.1 Oxygen isotopes

The $\delta^{18}O_{diatom}$ record (Fig. 5.1.E) shows both short-term (decadal) and long-term oscillations (centennial time scales) ranging from +35‰ to +39.2‰ (mean= +37.4 ± 0.8‰). From the bottom to the top, the studied record can be subdivided into three phases. These intervals correspond to three enrichment/depletion phases (Fig. 5.1.D). Each phase starts with a continuous centennial isotope enrichment which abruptly ends with a sharp depletion:

Phase 1. Lower interval (11,990 to 11,800 cal years BP). It shows the maximum and minimum $\delta^{18}O_{diatom}$ values (+39.2‰ and +35.1‰ respectively, with a mean value of +37.7 ± 1‰) throughout the whole record. It starts with an increasing trend of ~3.3‰/100 years which finishes at 11,860 cal years BP. This trend is followed by a shift to lighter values of ~8.1‰/100 years with a sharp final decrease in the $\delta^{18}O_{diatom}$ values of 3.5‰ in less than 10 years, acquiring the minimum value for the whole record at ca 11,800 cal years BP. Both trends are interrupted by ca 5 to 20 years depletion/enrichment excursions ranging between ±0.9 and ±1.7‰.

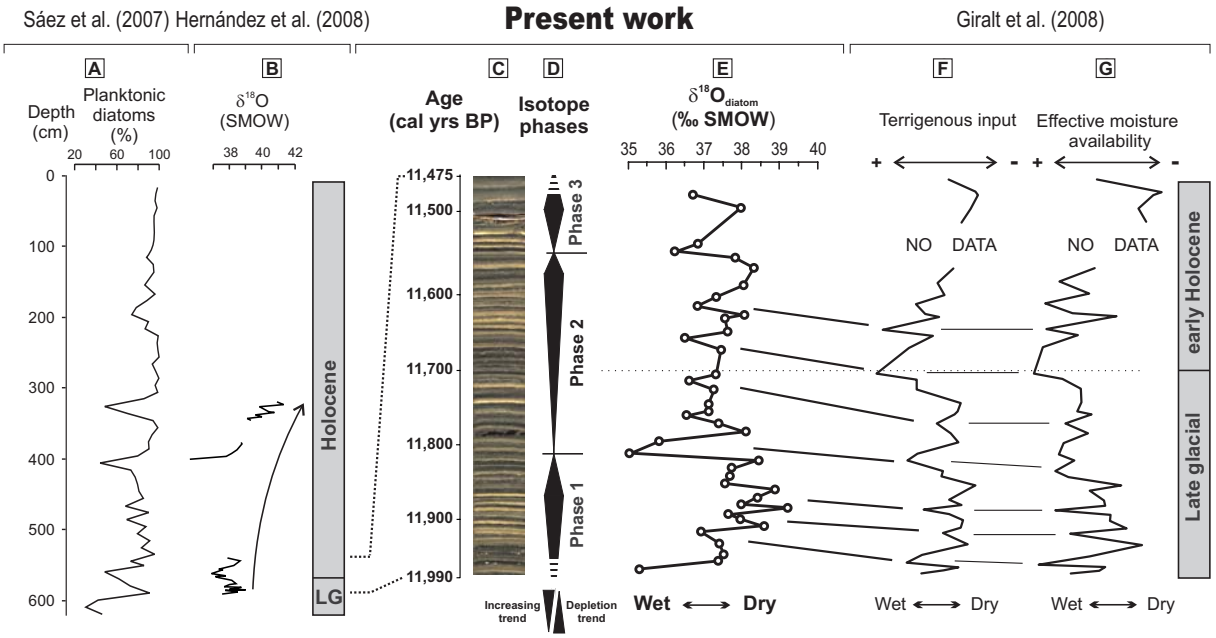

Figure 5.1. $\delta^{18}O_{diatom}$ data for the period 11,990–10,475 cal year BP from Lago Chungará, compared with other paleoenvironmental records of the lake. A) Planktonic diatoms percent abundance curve for the whole Lago Chungará sequence (Sáez et al. 2007). B) $\delta^{18}O_{diatom}$ data of non-consecutive dark-green laminae from three intervals of the record (Hernández et al. 2008). C) Photography of laminated sediments corresponding to the sampled interval of subunit 1a in core 11. D) Oxygen isotope enrichment/depletion phases, in the studied interval, interpreted from the data. E) $\delta^{18}O_{diatom}$ data from the present study and interpretation in terms of wet and dry conditions. The values correspond to 40 consecutive dark-green laminae throughout the whole selected interval. F) Terrigenous input variations derived from the first eigenvector of PCA on magnetic susceptibility, XRF, XRD, TC and TOC, BSi (Giralt et al. 2008). G) Effective moisture availability variations from the second eigenvector of the mentioned PCA (Giralt et al. 2008). Correlation lines correspond to the main oxygen isotope depletion peaks. Note that the main trends of the three curves are similar but there is a systematic temporal disagreement between them.

Phase 2. Middle interval (11,800 to 11,550 cal years BP). This section (mean values +37.3 ± 0.7‰) starts with an enrichment trend showing an upwards gradient of ~1.3‰/100 years which finishes at 11,570 cal years BP with a +38.3‰ $\delta^{18}O_{diatom}$ value. This trend is however punctuated by one sudden rise (+2.3‰) and up to four minor depletions (ranging from -0.6 to -1.3‰.) of the $\delta^{18}O_{diatom}$ values on a 40 to 55 years basis. The enrichment trend is followed by a shift of ~9.1‰/100 years to lighter values reaching a minimum value of +36.2‰.

Phase 3. Upper interval (11,550 to 11,450 cal years BP). This interval (mean values +37.2 ± 0.7‰) also starts with an enrichment trend but, because the section only comprises three samples, this enrichment has not been estimated. This trend is also followed by depletion of 1.3‰ in 10 years.

5.2.2 Spectral analyses of the diatom oxygen isotope record

MTM performed on the $\delta^{18}O_{diatom}$ values shows a number of clear periodicities (Fig. 5.2). Almost all identified periodicities (7.2, 8.9, 11.1, 13, 18.6, 22.3 and 39.4 years) exceed the 99% confidence interval

whereas only two (3.7 and 8 years) lie between 95-99% confidence interval (Fig. 5.2). Most of the sub-decadal identified frequencies are close to the minimum temporal resolution of the sampling (4.1 years), which explains in great part the weaker intensity of the short periodicities between 3 and 8 years. Therefore, only the most significant frequencies and above the minimum temporal sampling resolution have been taken into account in the discussion.

TF analysis reveals the strongest energy for the lower values of frequency, mainly focussed on the 35-years cycles, whereas it decreases towards higher frequency values, i. e., the higher periodicities (Fig. 5.3). This fact can mostly be explained by the decadal sampling resolution, making periodicities lower than ten years less significant. Additionally, TF analysis indicates that the highest energies of the significant frequencies are located in the Late Glacial period between ca 11,950 and 11,700 cal years BP, decreasing just from the onset of the Holocene until, at least, approximately 11,550 cal years BP (Fig. 5.3). TF diagram also highlights that the identified frequencies did not have the same intensity (energy) during all the studied period. For instance, the shortest significant periodicity observed in the MTM (7.2 years) was mainly active during the first 150 years of the record, whereas it was only active during three short time windows in the following 500 years. A similar pattern is also observed for the rest of the significant periodicities (8.9, 11.1, 13, 18.6, 22.3 and 39.4 years). The maximum energy areas correspond to depletions in the $\delta^{18}O_{diatom}$ values, i.e. 11,800 and 11,550 cal years BP (Fig. 5.3).

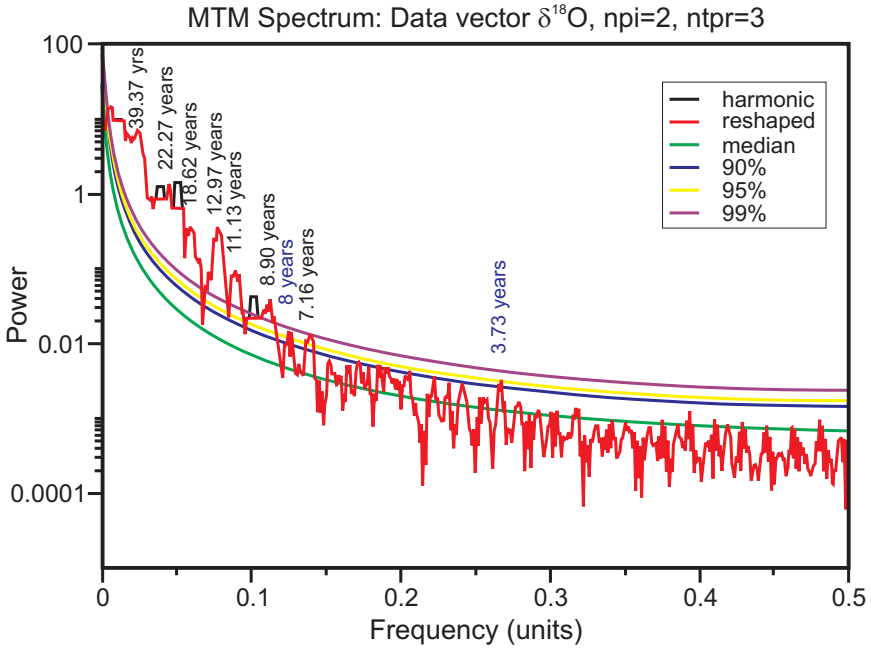

Figure 5.2. Multi-taper analysis of the $\delta^{18}O_{diatom}$ values. The 90, 95 and 99% confidence levels are indicated and significant periodicities are shown. Note that periodicities with more than 99% of significance are shown in black and those with more than 95% significance in blue.

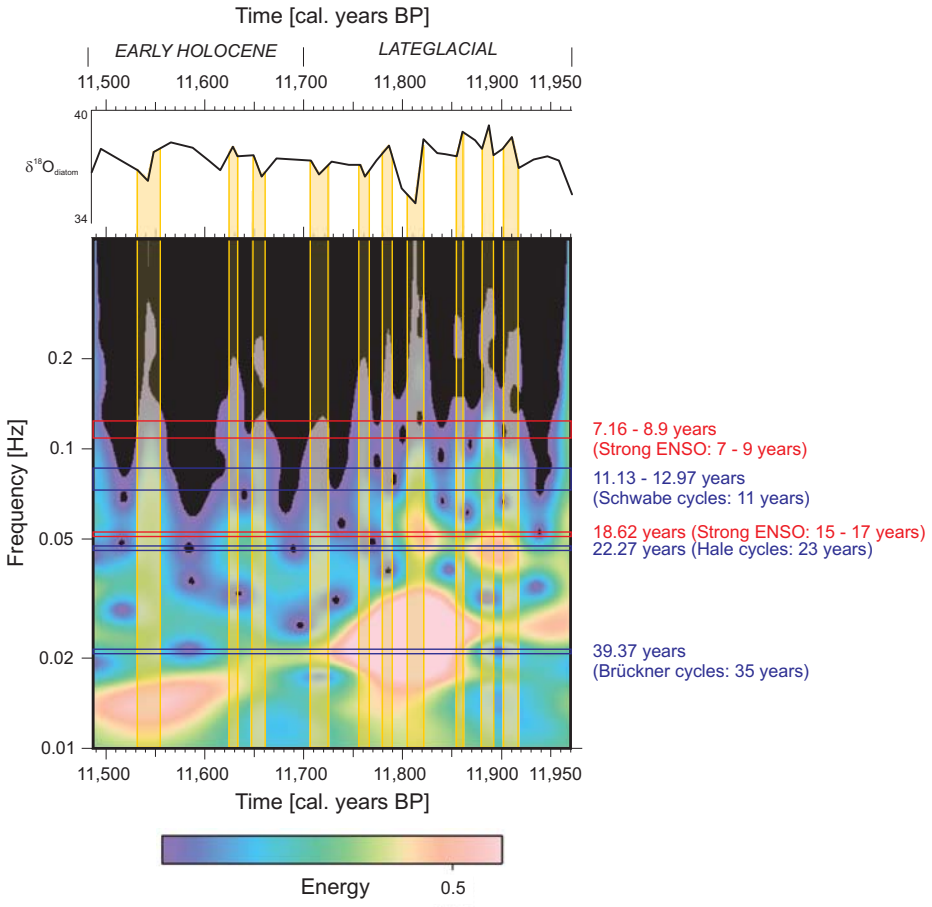

Figure 5.3. Time–Frequency analysis of the $\delta^{18}O_{diatom}$ values. Pink indicates high energy whereas blue displays low energy areas. Energies below 0.03 were clipped in order to facilitate understanding of the graph. Red and blue horizontal bands mark different frequency bands of the ENSO and solar activity forcings. Yellow vertical bands show zones with $\delta^{18}O_{diatom}$ shifts and their corresponding power values for each frequency. A weakening pattern in ENSO and solar activity energies can be observed through the Late Glacial-Early Holocene transition.

5.3 Discussion

5.3.1 Controlling factors of $\delta^{18}O_{diatom}$ in Lago Chungará

$\delta^{18}O_{diatom}$ in lake sediments is controlled by the $\delta^{18}O_{lakewater}$, temperature, and the possible disequilibrium by vital effects or diagenesis (Leng and Barker, 2006). We discount vital effects and diagenesis as analyses were made on near-monospecific diatom samples and preservation of the diatom frustules is excellent (Fig. 5.4).

$\delta^{18}O_{lakewater}$ depends on the balance between the isotope composition of water inputs (including the source and amount of precipitation, surface runoff and groundwater inflow) and outputs (evaporation and groundwater loss) in the lake. The measured $\delta^{18}O$ of the inputs (springs, Río Chungará and rainfall) in the Lago Chungará is homogeneous, giving values close to the $\delta^{18}O_{precipitation}$ (Fig. 2.5.A). $\delta^{18}O_{precipitation}$ is

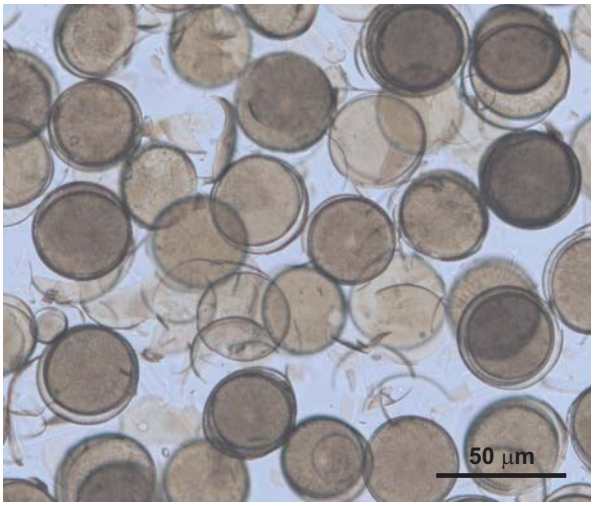

Figure 5.4. Diatom-rich sediment from Lago Chungará after the cleaning process. Large *Cyclostephanos andinus* valves are the unique component.

a function of the isotope composition of the moisture source and air-mass trajectory, but in the Lago Chungará there are no changes in the moisture source composition since the air masses always come from the Atlantic Ocean throughout the Amazon basin (Grosjean et al. 1997). During moisture transport from the Atlantic to the lake area, three processes are directly responsible for the low and variable values of the present $\delta^{18}O_{precipitation}$ throughout the Andean Altiplano (Aravena et al. 1999). These processes include interaction of the air masses within the Amazon basin, an altitude effect due to the ascent of the air masses along the eastern slope of the Andes, and the convective nature of the storms in the Altiplano region. Nevertheless, in the Lago Chungará region the values obtained for the measured $\delta^{18}O_{precipitation}$ are relatively stable with almost all values around –14 and –20‰ (Herrera et al. 2006) (Fig. 2.5.A) , whereas $\delta^{18}O_{lakewater}$ is much higher (Fig. 2.5.A). This result is in accordance with a $\delta^{18}O_{lakewater}$ enrichment via evaporation. Thus, any isotopic variation of $\delta^{18}O_{lakewater}$ will be more related to changes in the amount of precipitation («amount effect») and evaporation rather than to the variability of $\delta^{18}O_{precipitation}$. Evaporation enriches $\delta^{18}O_{lakewater}$ by 14‰ relative to the inlets (precipitation, springs and river) in the present day (Fig. 2.5.A). During the Late Glacial and Early Holocene the water residence time of the lake was shorter than present because of the different palaeohydrological context, but even so it can be considered closed for that period (Hernández et al. 2008).

Accordingly, the variations in the $\delta^{18}O_{diatom}$ must be mainly derived from changes in the $\delta^{18}O_{lakewater}$ resulted from shifts in the P/E, rather than dominated by temperature. However, two factors should be considered in the interpretation of the $\delta^{18}O_{diatom}$ values in terms of temperature oscillations. The first factor is related to $\delta^{18}O_{precipitation}$ that correlates directly with changes in the air temperature. The global relationship between changes in $\delta^{18}O_{precipitation}$ with air temperature is commonly referred to as the 'Dansgaard relationship', and it implies changes between +0.2 and +0.7‰/°C (Dansgaard, 1964). The second is the water of the lake temperature dependence of oxygen isotope fractionation between diatom

silica and the lake water (Brandriss et al. 1998). Nevertheless, the fractionation factor value of this temperature dependence is still controversial. Published fractionation factors range from –0.2‰ and –0.5‰/ºC (Brandriss et al. 1998; Moschen et al. 2005).

The two temperature factors have opposing effects on $\delta^{18}O_{diatom}$ but, owing to its larger variability, the effects of the first factor (air temperature) usually dominate over the second. However, even in the case of the largest change due to the Dansgaard relationship, its magnitude will be greatly damped by the effect of the isotope fractionation between diatom silica and lake water. Moreover, it is known that most of the tropical rainfall isotope datasets exhibit a far stronger correlation with total precipitation than with air temperature (Leng et al. 2005b), indicating in the Lago Chungará case a magnification of the P/E in wetter periods.

Hence, we can assume that in the Lago Chungará the effects of precipitation variability and temperature oscillations in the $\delta^{18}O_{diatom}$ values will be small in comparison to evaporative concentration, as pointed by other authors for closed lakes in general (Gat 1980; Gasse and Fontes 1992).

5.3.2 Variations of the P/E in the lake

Oxygen isotopes have widely been used to carry out lake level reconstructions and to establish consequent palaeoclimatic interpretations (Barker et al. 2001; Valero-Garcés et al. 2003).

There is a relationship between lake level change and the P/E for Lago Chungará during the Late Glacial and Early Holocene, but this dependency is hampered by local palaeohydrological factors such as changes in the groundwater outflow and shifts in the lake surface/volume ratio which produce a background long term enrichment trend (Hernández et al. 2008). This effect is however negligible when considering isotopic changes at a decadal to centennial time scale. Both present (Fig. 2.5.A) and past (Thompson et al. 1998) rainfall isotope values in the Lago Chungará region are much lighter than those measured for the water of the lake, and the magnitude of the long-term enrichment trend is very small compared to them. Therefore, depletions of $\delta^{18}O_{diatom}$ would directly be related to wet episodes in the Andean Altiplano, whereas exceptionally high values, which stand out over the general enrichment trend, would indicate arid episodes.

The observed $\delta^{18}O_{diatom}$ enrichment trends agree with periods where light-white laminae are more common, whereas depletion episodes coincide with poorly developed and less abundant light-white laminae (Fig. 5.1.C and D). These light-white laminae are most likely the result of exceptional periods of mixing of the shallow water column during lowstands, which recycle nutrients from the hypolimnion and therefore trigger extraordinary diatom blooms (Hernández et al. 2007). This interpretation is also supported by terrigenous input and regional effective moisture reconstructions previously performed

on the Lago Chungará sedimentary record (Giralt et al. 2008) (Fig. 5.1 .F and G). These reconstructions were carried out by applying multivariate statistical analyses (Cluster, Redundancy Analysis (RDA) and PCA) to magnetic susceptibility, XRF, XRD, TC, TOC, TBSi and grey-colour curve data. The terrigenous inputs curve was derived from the first eigenvector of the PCA, whereas the regional effective moisture reconstruction was obtained from the second eigenvector. For the lower part of Chungara sequence (Unit 1), the more positive values of the terrigenous inputs were interpreted, as increasing erosion rate of catchment volcanic sediments, suggesting humid conditions. Similarly, the effective moisture availability proxy depends on the P/E, with positive values corresponding to drier conditions (Giralt et al. 2008). The comparison of the three proxies (Fig. 5.1.E, F and G) shows that the hydrological response of the diatom silica oxygen isotopes (a biological proxy) and of the other two reconstructions to the environmental variations is not the same.

The main trends in the three curves (Fig. 5.1.E, F and G) are similar but there is a systematic temporal disagreement (ranging between ca 5 and 50 cal years BP) between the terrigenous inputs and the regional effective moisture availability (which both react first) and the $\delta^{18}O_{diatom}$ (reacting afterwards). This time lag between the two proxies highlights the complex and non-linear response of the lacustrine ecosystem to environmental forcings (Fritz, 2008). After rainfall the increased runoff and input of terrigenous material is almost immediate. On the contrary, the oxygen isotope homogenisation of the water of the lake which later will be incorporated on the diatom frustule, has a delayed time of response. This depends on the epilimnion water residence time and, furthermore, whether the lake is hydrologically closed or not. Hence, the observed time lag can be showing these different responses of the system to the same forcing. However, we cannot discount the poorly understood concept of silica maturation, where pores in the silica matrix close through early diagenesis creating differences in the $\delta^{18}O$ between living diatoms and sediment assemblages (Schmidt, 2001) and therefore a lag in the $\delta^{18}O_{diatom}$ record.

At centennial-scale, the Lago Chungará isotopic values show a general pattern of increasing $\delta^{18}O_{diatom}$ (Fig. 5.1.B), with an enhanced enrichment period at the bottom, but interrupted by three major depletion events. The depletion events, accentuated by the «amount effect», correspond to heavy rainfall conditions, whereas enriched values would indicate exceptionally dry conditions favouring the evaporation. This interpretation is reinforced by the terrigenous input and effective regional moisture availability independent reconstructions.

Three wet/dry phases have been identified in the $\delta^{18}O_{diatom}$ record (Fig. 5.1.D). Phase 1 (11,990 – 11,800 cal years BP) shows a significantly increased gradient in $\delta^{18}O_{diatom}$ suggesting that dominantly dry climate conditions played a key role triggering this isotope enrichment. Because of this drier situation the lake level would be lower, as also indicated by the important development and major presence of light-white laminae in this part of the interval. Three low-intensity and short-term wet episodes punctuate

the established Late Glacial arid period (Fig. 5.1.E). These episodes can also be recognised and correlated with events of increased terrigenous inputs and effective moisture availability (Fig. 5.1.E, F and G).

The much weaker isotope enrichment for phase 2 (11,800 and 11,550 cal years BP) can be mainly ascribed to the general low magnitude palaeohydological background trend towards heavier isotope conditions of the Late Glacial-Early Holocene transition (Hernández et al. 2008). This fact, together with the poorer development and minor presence of the light-white laminae with respect to the previous interval, suggests that the enrichment via evaporation was much less important than during the sedimentation of phase 1, corresponding to a more humid period. Furthermore, the terrigenous inputs and effective regional moisture availability curves show relatively wetter conditions for this period (Fig. 5.1.F and G). This trend is also punctuated by a sudden rise in the lowest part of the interval indicating a short dry event and slight depletions in $\delta^{18}O_{diatom}$ indicating wet decadal-scale events (Fig. 5.1.E).

In phase 3 any clear trend is difficult to identify (Fig. 5.1.E). Although the $\delta^{18}O_{diatom}$ record seems to show a new trend towards drier conditions after the sudden wet event dated at 11,550 cal years BP, the lack of suitable samples has hampered any firm conclusions.

5.3.3 Long-term, centennial- to millennial-scale palaeoclimatic implications

There are many Late Quaternary palaeoclimatic reconstructions from the Andean Altiplano region (Sylvestre et al. 1999; Rigsby et al. 2005) but the climate context for the Late Glacial-Holocene transition still remains unclear. Some authors have defined a cold period (12,600-11,500 cal years BP) coincident with the Northern hemisphere's Younger Dryas event (Baker et al. 2001b). The wet («Coipasa phase», Thompson et al. 1998; Placzek et al. 2006) or dry (Maslin and Burns 2000; Weng et al. 2006) character of this event remains controversial. On the contrary, other authors consider this period just the final part of the deglaciation towards the present Interglacial («Ticaña phase», Sylvestre et al. 1999), as part of a long-term dry pattern (Rowe et al. 2002; Abbott et al. 2003).

The previous lake level reconstruction, mainly based on the abundance of planktonic diatoms, shows a shallowing followed by a long term rising trend for the interval presented here (Sáez et al. 2007). Additionally, recent data on the Lago Chungará record, mainly based on XRF core scanner analysis, has established the Late Glacial to Holocene transition as a relatively wet period (Giralt et al. 2008). The centennial scale $\delta^{18}O_{diatom}$ record is congruent with the lake level reconstruction performed by Saéz et al. (2007) which represents the palaeoclimatic evolution related to the major lake level variations (Fig. 5.1.B). The non continuous isotopic data (Fig. 5.1.B) also displays a persistent, but minor, background isotope enrichment trend. This enrichment is related to changes in the lake morphology due to shifts in its surface/volume ratio, as well as changes in the groundwater outflow during the lake ontogeny

(Hernández et al. 2008). In any case, the new $\delta^{18}O_{diatom}$ data presented here highlights that the Glacial-Interglacial transition in the central Andean Altiplano was punctuated by abrupt and high-frequency centennial climate variability.

5.3.4 Short-term, decadal- to centennial-scale palaeoclimatic implications

Millennial-scale shifts in the Atlantic-Amazon-Altiplano hydrologic system have been attributed to orbitally induced changes in solar insolation, coupled with long-term changes in the ENSO variability (Rowe et al. 2002; Abbott et al. 2003; Servant and Servant-Vildary 2003). However, higher-resolution changes are not directly related to orbitally induced insolation forcing (Abbott et al. 2003). The interannual climate variability in the Andean Altiplano is most likely related to changes in the Pacific Tropical SSTs, and the sign and strength of the zonal winds above the Altiplano (Garreaud et al. 2003). Both factors would affect the strength and position of the Bolivian high and, hence, the moisture distribution over the region. The main force controlling the SSTs is the ENSO variability, involving dry or wet situations in the Altiplano during El Niño- or La Niña-like conditions respectively (Garreaud et al. 2003; Vuille and Werner, 2005). This is consistent with instrumental data from the Chungará area where precipitation is reduced during moderate to intense El Niño years (1965, 1972, 1983, and 1992) (Fig. 2.5.C). Additionally, the sign and strength of the zonal winds above the Altiplano would be modulated by decadal and multidecadal variations in solar activity, possibly related to the mode of the ENSO system (Theissen et al. 2008). Although ENSO modulation by solar activity has been suggested (Velasco and Mendoza, 2008), no clear relationship has been demonstrated between both forcings. Nevertheless, there is broad agreement that ENSO events are the main control governing the moisture distribution in the Altiplano (Servant and Servant-Vildary, 2003), and that decadal-scale changes in the effective moisture could be related to the solar activity during the Mid-Holocene (Theissen et al. 2008).

The results presented here would suggest a similar pattern during the Late Glacial-Holocene transition over the Andean Altiplano (Fig. 5.3). The identified frequencies can be attributed to different periodicities of the solar activity cycles such as Schwabe 11 years (identified as 11.1 and 13 years), Hale 23 years (22.3 years) and Brückner 35 years (39.4 years), and of the ENSO frequency (main frequency at 7-9 years (7.2 and 8.9 years) and its decadal frequency 15-17 years (18.6 years)). The influence of solar activity and ENSO variability on the isotope record is supported by the fact that several periodicities concordant with both forces were identified. The time-frequency analysis suggests that the driest period (11,950 - 11,800 cal years BP) was ruled by high solar activity, mainly represented by a Brückner cycle, and strong ENSO-like conditions.

The ENSO and solar activity signals remain present for the Early Holocene period (between 11,750 until 11,500 cal years BP), although they show a weakening pattern through this period (Fig. 5.03). This fact is congruent with the progressive weakening of the ENSO suggested by other authors for the Late Glacial-Holocene transition (Rodbell et al. 1999; Moy et al. 2002; Rodó and Rodriguez-Arias, 2004). In Lago Chungará, the onset of the Holocene was characterised by minor $\delta^{18}O_{diatom}$ enrichment by evaporation and by the occurrence of multi-decadal weak depletions that would be governed by the more humid La Niña-like conditions. This would agree with previous observations that suggest a reduction in the El Niño intensity within the region during the Early-Holocene in favour of long-term La Niña-like conditions in the tropical Pacific (Betancourt et al. 2000; Koutavas et al. 2002).

5.4 Conclusions

The Late Glacial to Holocene transition from the Lago Chungará record is made up of laminated diatom-rich sediments which provide excellent material for the application of oxygen isotope analysis in biogenic silica. $\delta^{18}O_{diatom}$ data have for the first time provided palaeoclimatic reconstruction at decadal-to-centennial resolution. The well-laminated nature of these sediments allowed a lamina by lamina continuous sampling, giving one of the highest resolution records available for $\delta^{18}O_{diatom}$. It has also revealed important insights into the usefulness of this method, as well as provided decisive palaeoenvironmental information for this critical period.

$\delta^{18}O_{diatom}$ from dark-green diatom laminae represent the baseline in the environmental evolution of Lago Chungará, and show decadal to centennial variability in the moisture conditions of the Andean Altiplano. The isotopic record displays a persistent background isotope enrichment trend related to changes in the lake morphology and groundwater outflow during the Late Glacial and Early Holocene. Overprinted onto this long-term (centennial to millennial) trend there are cyclically short-term (decadal to centennial) shifts which are not related to changes in temperature or isotopic composition of the source of precipitation, but to the P/E variability in the Altiplano.

The record shows two major isotope depletions, occurring at a centennial time scale (11,800 and 11,550 cal years BP) indicating a long-term increase in moisture conditions, and one major isotope enrichment above the background levels that occurred between 11,990 and 11,800 cal years BP indicating a short dry phase during the Late Glacial. Minor depletions at a decadal time scale are associated with weaker rainfall short-term events. The comparison with terrigenous input and effective moisture availability reconstructions previously performed for Lago Chungará shows agreement, but includes a systematic lag time (up to 50 years) among these proxies and $\delta^{18}O_{diatom}$. This is mainly due to the time necessary to change the $\delta^{18}O_{lakewater}$ values and its subsequent incorporation into the diatom frustules,

but other factors should not be completely disregarded. The time lag highlights the fact that not all the proxies react at the same time to environmental forcing and this needs to be more often recognised in high resolution palaeolimnological reconstructions.

Sub-millennial shifts in the hydrological balance of Lago Chungará are hypothesised to be the result of changes in the strength and position of the Bolivian High. Spectral analyses of $\delta^{18}O_{diatom}$ suggest that these changes in the atmospheric conditions over the Altiplano during the wet events were triggered by both ENSO and solar activity. The change from the Late Glacial dry period to a wetter Early Holocene period confirms a weakening of El Niño intensity in the Andean Altiplano region in favour of La Niña-like conditions found elsewhere. Nested upon the underlying climate dynamics are the different cyclicities of solar activity (Schwabe, Hale and Brückner) that were active during different time windows. There is undoubtedly an interaction between these and ENSO at the decadal and greater scales and it is likely that apparent solar forcing of the Lago Chungará record is transmitted via ENSO modulation of the South American monsoon. The complexity of Andean Altiplano palaeoenvironmental conditions, and the absence of other high resolution studies for this time interval, does not allow us to establish any clear conclusion on the existence of significant climate events synchronous to the Younger Dryas in the northern hemisphere. While many studies have demonstrated ENSO-like forcing during the Glacial-Interglacial transition, this highly resolved record is one of the few that preserves key ENSO frequencies, therefore further implicating this major climate process with events governing the transition to the Holocene.

Chapter 6

Biogeochemical processes controlling oxygen and carbon isotopes of diatom silica in lacustrine rhythmites*

6.1 Introduction

Rhythmites are finely laminated sequences (millimetre- to submillimetre thick) made up of regular alternations of two or three contrasting sediment types called couplets or triplets (Talbot and Allen, 1996). Rhythmite formation is generally associated with seasonally heterogeneous sediment supply and a lack of physical or biological reworking processes (Grimm et al. 1996). Thus, laminated sediments indicate high-frequency environmental change through time. A number of studies have described laminated lacustrine sediments, but they have mainly dealt with annual-rhythmites (varves) with different clastic grain-size and/or biogenic content deposited over different seasons (e.g. Bird et al. 2009). At mid- to high latitudes the processes that lead to rhythmite formation are often well constrained (e.g. Chang et al. 2003), whereas the biogeochemical processes and climate events which prompt laminated sediments in tropical lacustrine sediments are often less understood. In these cases, tropical rainfall regimes associated with intense storms and wind may be responsible for extraordinary external nutrient loading or upwelling of nutrient rich-waters which trigger phytoplankton blooms (Talbot and Allen, 1996). These tropical climate regimes follow a seasonal behaviour (e.g. monsoons), but they can also be highly influenced by climate multiannual phenomena (e.g. ENSO).

Changes in $\delta^{18}O_{diatom}$ in lacustrine sediments are used to infer hydrological variations. For closed lakes in the tropics, these variations are mostly related to the P/E, which is generally directly linked to lake level change (Leng and Barker, 2008). The isotope-inferred reconstructions can thus be used to unreveal the climate history of the region (e.g. Barker et al. 2007) although this may be mitigated by biological and sedimentary processes. Besides $\delta^{18}O_{diatom}$, the $\delta^{13}C_{diatom}$, can give other relevant palaeoenvironmental information, including insights on the lakes' carbon cycle. There are few studies of

*Chapter based on the paper submitted in:
Palaeogeography, Palaeoclimatology, Palaeoecology *(submitted). Armand Hernández, Roberto Bao, Santiago Giralt, Philip A. Barker, Melanie J. Leng, Hilary J. Sloane, Alberto Sáez.*

carbon isotopes from organic inclusions within diatom frustules, and of those published, most have dealt with marine sedimentary records (e.g. Crosta and Shemesh, 2002). Studies on $\delta^{13}C_{diatom}$ in lake sediments are now emerging and providing valuable insights into the complex carbon cycle of lakes (Hurrell et al. submitted).

The aim of this paper is to understand high frequency biological, chemical and sedimentary processes which cause the laminae formation in the sedimentary record of Lago Chungará, a high altitude tropical lake located in the Central Andes. $\delta^{18}O_{diatom}$ and $\delta^{13}C_{diatom}$ data from individual lamina are presented for a period between 11,990 and 11,530 cal years BP. High frequency environmental perturbations brought about by interannual-decadal climate events are rarely recorded in lake sediments, and therefore, the laminated sediments here are a good record of their intensity and their effect on lacustrine hydrological and carbon cycles.

6.2 Results

6.2.1 Laminae biogenic composition

The present study extends the petrographical examination of the diatomaceous laminated sediments of Lago Chungará for the Late Glacial to Early Holocene transition (11,990 - 11,530 cal years BP) described in Hernández et al. (2008). A hundred laminae have been differentiated and grouped under the white, light-green and dark-green laminae categories according to their diatom composition, organic matter content and colour. Additionally, nine laminae were undifferentiated due to their mixed features between the three groups (Figure 6.1).

White laminae are formed almost exclusively by diatom frustules of the large (diameter > 50 μm) euplanktonic diatom *Cyclostephanos andinus* (Fig. 6.2.G). Dark-green laminae, which contain a higher organic matter content, probably derived from diatoms and other algal groups, are made up of a mixture of different diatom species. This mixture is mainly composed of smaller (diameter < 50 μm) *Cyclostephanos andinus* valves, with diatoms of the Discostella stelligera species complex as co-dominant taxa. Subdominant diatom taxa comprise a number of tychoplanktonic (mainly *Staurosira construens* aff. *venter* and *Fragilaria* spp.) and benthic life forms (including Cocco*neis placentula, Gomphonema minutum, Nitzschia tropica* and *Opephora* spp. aff. *mutabilis*) (Fig. 6.2.C). The light-green laminae are made up of components from the white laminae progressively grading upwards to the typical constituents of the dark-green laminae. Diatoms of the light-green laminae are usually embedded in an organic matrix creating a preferential orientation of the valves (Fig. 6.2.B and E). Thus, a lower white lamina, an intermediate light-green lamina and an upper dark-green lamina form a typical sedimentary triplet. These light-green laminae may be variable in thickness or even absent. The transition between well-defined laminae within the triplets (from here on called intra-cycle relationships) is gradual, whereas the transition between different triplets is abrupt (from here on called inter-cycle relationships) (Fig. 6.2.B, D, F and H).

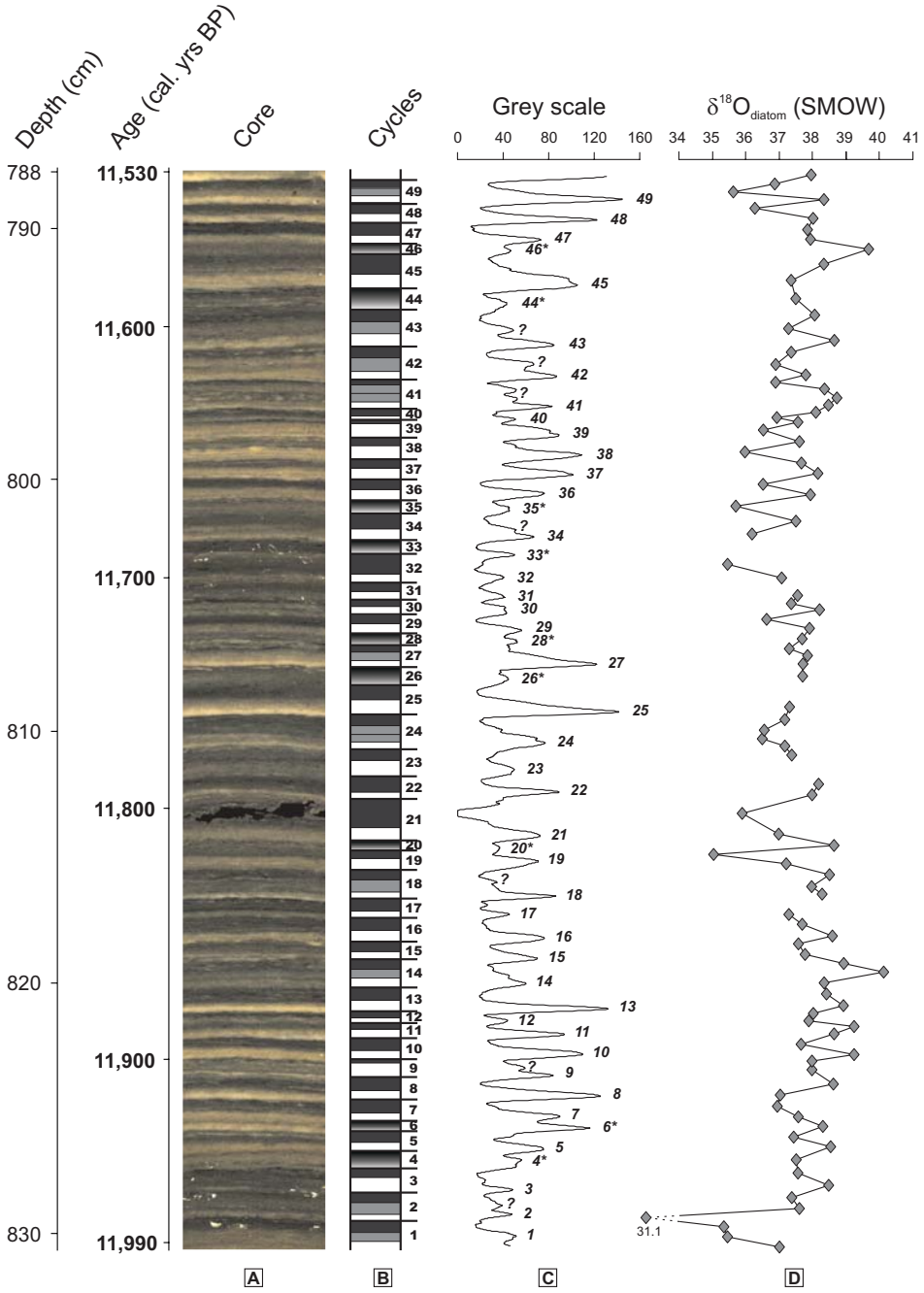

Figure 6.1. A. Digital XRF ITRAX core scanner image from the selected and sampled interval indicating the age and its correspondent core depth. B. The 49 defined cycles composed by couplet/triplets from 102 sampled laminae. C. The smoothed grey-colour curve D. $\delta^{18}O_{diatom}$ values associated to each lamina. Note the diatom super-blooms are indicated by thicker white laminae and the higher values of the curve.

6.2.2 Laminae isotope composition

In spite of the very high sampling resolution (mean=4 years, sd=1.5, n=101) $\delta^{18}O_{diatom}$ values display a large variability, ranging between +40.1‰ and +31.1‰ with a mean value of +37.5‰ for the whole record (sd=1.1, n=97) (Fig. 6.1). The studied interval shows three $\delta^{18}O_{diatom}$ major enrichment trends which

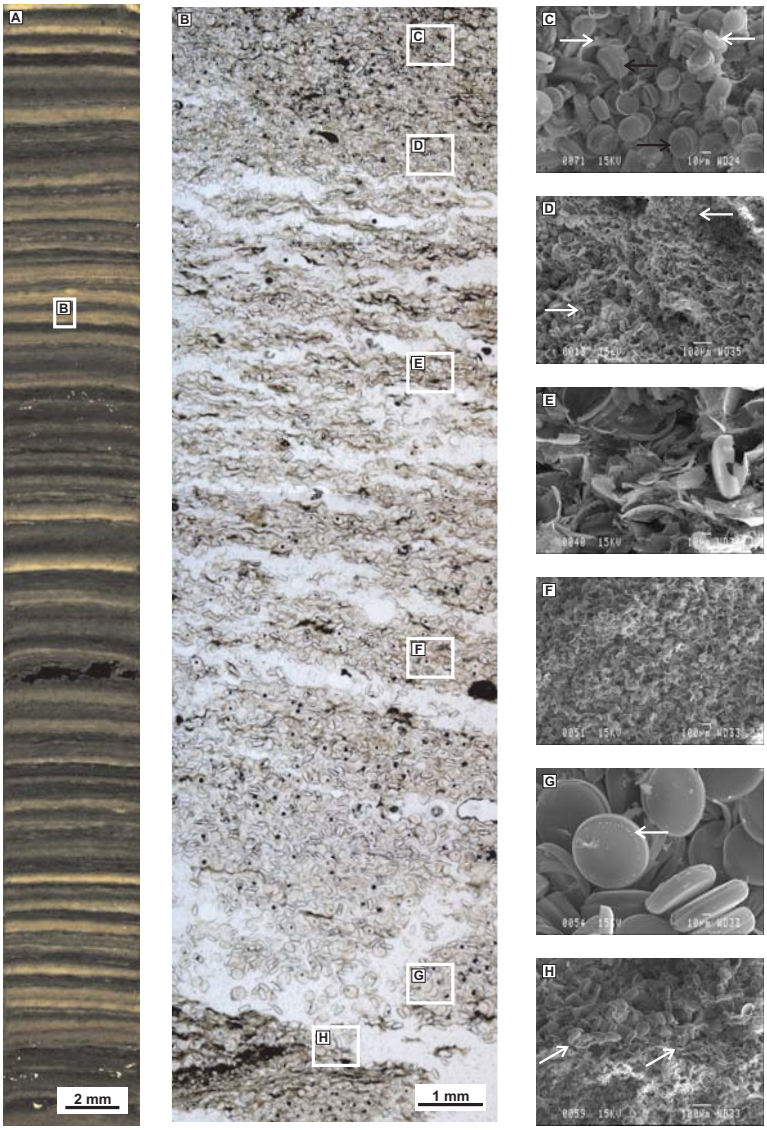

Figure 6.2. A. Digital XRF ITRAX core scanner image of laminated sediments of core 11 corresponding to the sampled interval of Subunit 1a. Note that the lamination is composed by millimetre thick white lamina and green lamina forming rhythmites.

B. Photomosaic from a thin-section showing an ideal triplet rhythmite sequence made up of (from base to top): *(H)* Abrupt contact between dark-green and white laminae; *(G)* A white lamina formed by skeletons of the large diatom *Cyclostephanos andinus* (> 50 µm); *(F)* Gradual contact between white and light-green laminae; *(E)* A light-green lenticular and discontinous lamina which is made up of a mixture of white and dark-green lamina; *(D)* Gradual contact between light- and dark- green laminae; *(C)* A dark-green lamina made up of diatoms embedded in an organic matter matrix.

C. SEM image of dark-green lamina mainly made up by *Cyclostephanos andinus* (black arrows) and diatoms of the *Discostella stelligera* species complex (white arrows). Note the smaller *Cyclostephanos andinus* size (diameter < 50 µm).

D. SEM image showing the decreasing upwards size of the diatoms throughout an intra-cycle contact between a light-green lamina and a dark-green lamina. Arrows indicate the different size of the diatoms.

E. SEM image of a light-green lamina. The lamina is made up of complete valves and fragments of *Cyclostephanos andinus* valves, both showing a preferential orientation.

F. SEM image showing an intracycle contact between the white and light-green laminae. Note the preferential orientation of de diatoms placed at the top of the image (light-green lamina).

G. SEM image of a white lamina. The lamina is exclusively composed by large *Cyclostephanos andinus* (diameter > 50µm). The excellent preservation of the diatom frustules can be observed in the image (white arrow). There are no signs of dissolution.

H. SEM image showing an intercycle contact between a dark-green and a white lamina. The arrows indicate the exact position of the contact which can be perfectly followed. Note the different size of the diatoms.

coincide with similar trends in the grey-colour curve (Fig. 6.3). The $\%C_{diatom}$ values range from 0.63% in the uppermost sample (rhythmite 48) to 0.32% in the lowermost sample (rhythmite 8) (mean=0.42%, sd=0.10, n=11) whereas $\delta^{13}C_{diatom}$ values oscillate between –26.1‰ and –29.5‰ (mean=–28.1‰, sd=0.95, n=11). The white laminae generally display lower $\%C_{diatom}$ and $\delta^{13}C_{diatom}$ values than the dark laminae from the same rhythmite, in addition there is an increase in C/Si ratios and $\delta^{13}C_{diatom}$ values throughout the 5 studied intra-cycle relationships (Table 6.1).

$\delta^{18}O_{diatom}$ inter-cycle relationships have been studied in 49 cases. From these, 12 cases could not be taken into account due to the absence of $\delta^{18}O_{diatom}$ data or because the difference between the two consecutive isotopic values was below the mean analytical error. Valid $\delta^{18}O_{diatom}$ inter-cycle relationships (n=37) are characterised by higher oxygen isotope values. The most common inter-cycle relationship is the dark-green to white laminae (n=25), and it shows isotope enrichment (i.e. values increase) in 60% of the cases. Likewise, the difference between dark-green laminae to undifferentiated laminae shows similar levels of increasing $\delta^{18}O_{diatom}$, whereas relationships between undifferentiated and white laminae show both increases and decreases in $\delta^{18}O_{diatom}$ (Table 6.2.A).

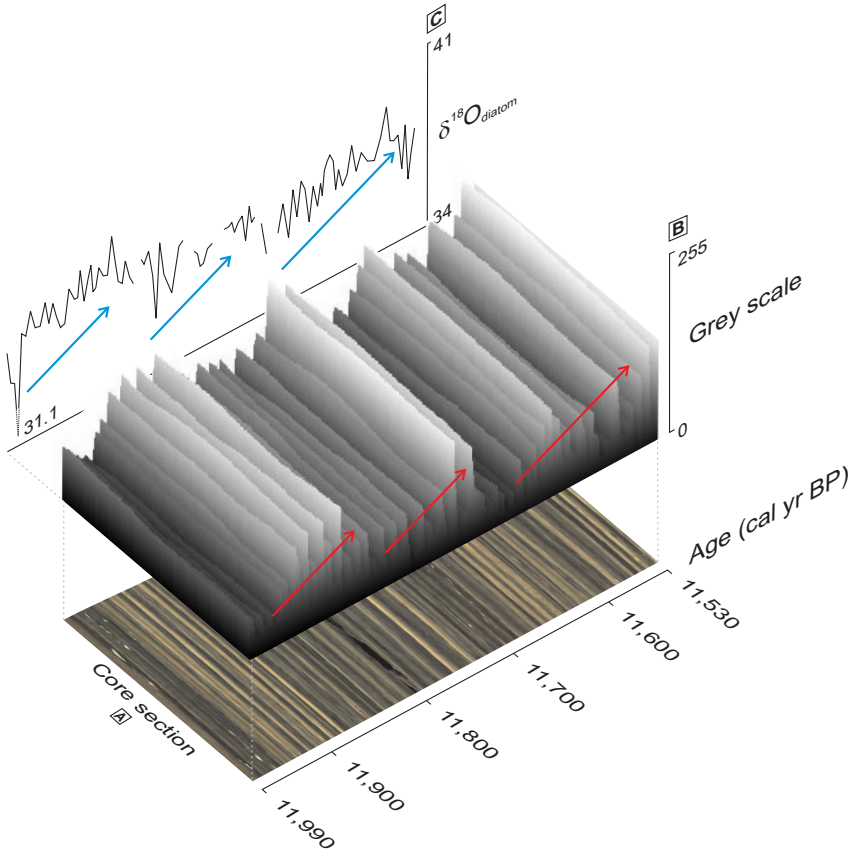

Figure 6.3. A. Digital XRF ITRAX core scanner image from the selected interval. B. Grey-colour surface plot elaborated from the digital image. Decadal-scale main grey-colour trends to whiter values are indicated by means of red arrows. C. $\delta^{18}O_{diatom}$ record. Decadal-scale main $\delta^{18}O_{diatom}$ trends to higher values are indicated by means of blue arrows. Note the good agreement between both proxies.

Table 6.1. Analysed samples and their features (number, cycle, colour, depth, age, $\delta^{18}O_{diatom}$, $\delta^{13}C_{diatom}$ and $\%C_{diatom}$. Dark grey stripes indicate not available (na) samples.

Sample	Cycle	Colour	Depth (cm)	Age (cal yr BP)	$\delta^{18}O_{diatom}$ (SMOW)	$\delta^{13}C_{diatom}$ (PDB)	$\%C_{diatom}$
1		White	787.8	11,529	38.97		
2	49	Dark-green	788.1	11,532	36.87		
3	49	Light-green	788.5	11,537	35.63		
4	49	White	788.8	11,540	38.35		
5	48	Dark-green	789.1	11,543	36.27	-28,99	0,63
6	48	White	789.5	11,547	38.01	-28,51	0,47
7	47	Dark-green	789.7	11,549	37.85		
8	47	White	790.2	11,554	37.93		
9	46	Undifferentiated	790.6	11,559	39.67		
10	45	Dark-green	791.3	11,566	38.35		
11	45	White	792	11,573	37.37		
12	44	Undifferentiated	792.6	11,580	37.50		
13	43	Dark-green	793.4	11,588	38.07	-26,05	0,57
14	43	Light-green	794.1	11,595	37.29	-28,30	0,38
15	43	White	794.5	11,599	38.65	-28,46	0,39
16	42	Dark-green	794.9	11,604	37.36		
17	42	Light-green	795.4	11,609	36.91		
18	42	White	795.8	11,613	37.79		
19	41	Dark-green	796.1	11,616	36.86		
20	41	Light-green	796.3	11,618	38.35		
21	41	Light-green	796.6	11,621	38.73		
22	41	White	797	11,626	38.49		
23	40	Dark-green	797.3	11,629	38.10		
24	40	White	797.5	11,631	36.93		
25	39	Dark-green	797.7	11,633	37.58		
26	39	White	798	11,636	36.52		
27	38	Dark-green	798.5	11,641	37.62		
28	38	White	799	11,647	35.96		
29	37	Dark-green	799.3	11,650	37.67	-27,87	0,40
30	37	White	799.6	11,653	38.16	-29,01	0,33
31	36	Dark-green	800	11,657	36.51		
32	36	White	800.4	11,661	37.92		
33	35	Undifferentiated	801	11,668	35.70		
34	34	Dark-green	801.5	11,673	37.49		
35	34	White	802	11,678	36.18		
36	33	Undifferentiated	802.5	11,683	na		
37	32	Dark-green	803.4	11,693	35.46		
38	32	White	804	11,699	37.05		
39	31	Dark-green	804.3	11,702	na		
40	31	White	804.6	11,705	37.57		
41	30	Dark-green	804.8	11,707	37.35		
42	30	White	805.1	11,711	38.20		
43	29	Dark-green	805.5	11,715	36.62		
44	29	White	805.9	11,719	37.91		
45	28	Undifferentiated	806.3	11,723	37.70		
46	27	Dark-green	806.7	11,727	37.30		
47	27	Light-green	807	11,730	37.84		
48	27	White	807.3	11,734	37.72		
49	26	Undifferentiated	807.7	11,738	37.71		
50	25	Dark-green	808.4	11,745	na		
51	25	White	809	11,751	37.30		
52	24	Dark-green	809.5	11,757	37.16		
53	24	Light-green	809.9	11,761	36.53		
54	24	Light-green	810.3	11,765	36.50		
55	24	White	810.5	11,767	37.18		

Table 6.1. Continued.

Sample	Cycle	Colour	Depth (cm)	Age (cal yr BP)	$\delta^{18}O_{diatom}$	$\delta^{13}C_{diatom}$	$\%C_{diatom}$
56	23	Dark-green	811	11,772	37.39		
57	23	White	811.7	11,780	na		
58	22	Dark-green	812.2	11,785	37.16		
59	22	White	812.6	11,789	37.99		
60	21	Dark-green	813.4	11,798	35.86		
61	21	White	814	11,804	36.98		
62	20	Undifferentiated	814.5	11,809	38.70		
63	19	Dark-green	814.8	11,812	35.06		
64	19	White	815.2	11,816	37.19		
65	18	Dark-green	815.6	11,821	38.49		
66	18	Light-green	816.2	11,827	37.99		
67	18	White	816.5	11,830	38.28		
68	17	Dark-green	816.9	11,834	na		
69	17	White	817.2	11,837	37.30		
70	16	Dark-green	817.6	11,842	37.70		
71	16	White	818.2	11,848	38.66		
72	15	Dark-green	818.7	11,853	37.59		
73	15	White	819	11,856	37.81		
74	14	Dark-green	819.3	11,859	38.92		
75	14	Light-green	819.6	11,862	40.13		
76	14	White	820	11,867	38.34		
77	13	Dark-green	820.5	11,872	38.44	-27,21	0,44
78	13	White	820.9	11,876	38.91	-29,53	0,32
79	12	Dark-green	821.2	11,879	38.02		
80	12	White	821.4	11,881	37.90		
81	11	Dark-green	821.8	11,886	39.24		
82	11	White	822	11,888	38.66		
83	10	Dark-green	822.3	11,891	37.67		
84	10	White	822.8	11,896	39.24		
85	9	Dark-green	823.1	11,899	37.98		
86	9	White	823.4	11,902	38.00		
87	8	Dark-green	824	11,909	38.62	-27,69	0,38
88	8	White	824.3	11,912	37.03	-28,89	0,32
89	7	Dark-green	824.7	11,916	37.95		
90	7	White	825.3	11,922	37.57		
91	6	Undifferentiated	825.6	11,925	38.31		
92	5	Dark-green	826.1	11,931	37.43		
93	5	White	826.5	11,935	38.54		
94	4	Undifferentiated	827	11,940	37.50		
95	3	Dark-green	827.4	11,945	37.57		
96	3	White	827.9	11,951	38.50		
97	2	Dark-green	828.3	11,956	37.38		
98	2	Light-green	828.8	11,962	37.60		
99	2	White	829.2	11,967	31.14		
100	1	Dark-green	829.5	11,971	35.34		
101	1	Light-green	830	11,977	35.45		
102	1	White	830.3	11,981	37.05		

There are 51 valid (out of 62) relationships between laminae that take place within a rhythmite (intra-cycle relationships). These intra-cycle relationships are dominated by isotope depletion (values decrease). The most usual case shows changes from white to dark-green laminae (n=23) where isotope decreases occur in 67% of the cases (Table 6.2.B).

6.3 Discussion

6.3.1 Biological and sedimentary processes forming rhythmites

White laminae features (relatively thick, good diatom preservation and monospecific diatom composition) suggest accumulation during short-term massive diatom blooms, perhaps of only days to weeks in duration. According to the chronological model rhythmites are not a product of annual variations in sediment supply, but due to some kind of multiannual processes (Hernández et al. 2008). Causes of super-blooms can be different to regular seasonal blooms which occur as part of the normal phytoplankton succession (Reynolds, 2006). We suggest that our diatom super-blooms may have been triggered by abnormally high nutrient concentrations coupled with hydrological conditions prompting diatom population growth. Low lake level stages and/or strong wind episodes would favour upwelling of nutrient-rich hypolimnion waters (Talbot and Allen, 1996). Strong mixing would also select diatoms over other types of phytoplankton due to their relative buoyancy. Alternatively, the increase in nutrient external loading due to exceptional catchment erosion during wet events could also have had the same effect (Bradbury et al. 2002). ENSO cyclicity signals recorded at this time in the Lago Chungará record (Hernández et al. in press) provide support to the existence of those two contrasting dry (El Niño) and wet (La Niña) conditions (Vuille et al. 2000; Valero-Garcés et al. 2003).

Dark-green laminae (made up of a mixture of diatom valves belonging to several planktonic and benthic taxa, all embedded in an organic matter matrix) represent the baseline lake conditions where the complete phytoplankton successions over several years are preserved. These laminae therefore record the 'normal' intra- and inter-annual changes in the water column mixing regime characterised by the shifting species composition throughout general annual phythoplankton cycles. Preservation occurs as skeletons belonging to several diatom taxa, or simply as the organic matter mainly belonging to other algal groups (likely Chlorophycean, Cyanobacteria, etc.) that embed the valves in the dark-green laminae. Regular seasonal diatom blooms, are likely manifested in the dark-green laminae by the abundance of the small *Cyclostephanos andinus* (<50 μm), a large centric diatom whose buoyancy depends on the existence of a turbulent regime. Seasonal *Cyclostephanos andinus* (<50 μm) blooms reflected in the dark-green laminae would therefore be triggered by the same process during the super-blooms of the larger *Cyclostephanos andinus* (>50 μm) that make up the white laminae (i.e. water stratification breakdown). The dark-green laminae are sometimes preceded by light-green laminae. This observation indicates that recovery of the baseline conditions from the super-blooms can be more or less gradual (forming couplets or triplets, respectively).

Flocculation of diatoms by extracellular polymeric substances is a common feature in the marine realm (Thornton, 2002). This phenomenon occurs towards the end of a diatom bloom, due to the onset of

Table 6.2. A. Intercycle isotope relationships between the defined rhythmites. B. Intracycle isotope relationships between the defined rhythmites. Relationship types are established according to the colour of the laminae that are in contact.

Intercycle relationship types	Enrichments (%)	Depletions (%)	*n*
Dark-green to white laminae	60	40	25
Dark-green to undifferentiated laminae	67	33	6
Undifferentiated to white laminae	50	50	6
Total			37

Intracycle relationship types	Enrichments (%)	Depletions (%)	*n*
White laminae to light-green laminae	33	67	9
Light-green to light-green laminae	0	100	1
Light-green to dark-green laminae	56	44	9
White laminae to dark-green laminae	35	65	23
White laminae to dark-green laminae *(non-consecutive laminae, base to top of the rhythmite)*	33	67	9
Total			51

nutrient limitation. Diatom aggregation and subsequent rapid sedimentation of species having any kind of resting cell stages would favour future recruitment once nutrient resources were again available (Smetacek, 1985). Biosiliceous laminae in marine sediments have been interpreted as the product of changes in the mass sedimentation of diatoms by means of the formation of aggregates (Grimm et al. 1996, 1997). At Lago Chungará a similar phenomenon could have taken place in the formation of the light-green laminae once the super-blooms of the large (>50 μm) *Cyclostephanos andinus* come to an end. Aggregation of cells enclosed in a gelatinous matrix could therefore have taken place, being rapidly deposited in the form of the transitional light-green laminae. Although the life cycle details of *Cyclostephanos* are far from fully known, the closely related genera *Stephanodiscus*, to which *Cyclostephanos* once belonged (Round et al. 1990), is known to produce resting cells (Sicko-Goad et al. 1989), whose aggregation and rapid sedimentation represents a transition to a resting phase (Smetacek, 1985; Alldredge et al. 1995). It is therefore likely that the mechanism of formation of triplets is mediated by processes of self-sedimentation triggered by *Cyclostephanos andinus* (Grimm et al. 1997).

6.3.2 $\delta^{18}O_{diatom}$ and $\delta^{13}C_{diatom}$ interpretation

Variation in $\delta^{18}O_{diatom}$ can result from a variety of processes, such as $\delta^{18}O_{lakewater}$, temperature, vital effects and post depositional diagenesis (Leng and Barker, 2006). In hydrologically closed lakes under arid climate conditions evaporative concentration processes have a much larger effect on $\delta^{18}O_{lakewater}$

than any other process (Gasse and Fontes, 1992; Leng and Marshall, 2004; Hernández et al, in press). In these circumstances, the $\delta^{18}O_{diatom}$ record can be used as an indicator of changes in the P/E related to climate change (Leng and Barker, 2006).

At present, Lago Chungará can be considered a closed lake due to its water residence time (ca 15 years), and the fact that $\delta^{18}O_{lakewater}$ is enriched by 14‰ relative to $\delta^{18}O$ of the inputs (precipitation, springs and river) (Herrera et al. 2006). This was probably also the case in the Late Glacial-Early Holocene transition described here because $\delta^{18}O_{diatom}$ values are similar (around +37.5‰) to other diatom-isotope sequences in tropical sites (e.g. Lakes from Mount Kenya (Kenya), Barker et al. 2001; Lake Malawi (Malawi, Mozambique, Tanzania), Barker et al. 2007; Lake Tilo (Ethiopia); Lamb et al. 2005). Thereby the variations in the $\delta^{18}O_{diatom}$ from Lago Chungará sediments must be mainly derived from changes in the $\delta^{18}O_{lakewater}$ resulting from shifts in the balance between P/E, rather than other factors.

The organic matter enclosed within diatom frustules contains polysaccharides, proteins and long-chain polyamines (Kröger and Poulsen, 2008). These substances host carbon which is protected from post-depositional diagenetic alteration (Des Combes et al. 2008). As these carbon compounds will be synthesised from the surrounding waters, isotope analysis of the carbon contained in the diatom frustules can be used as a proxy for reconstructing the lake's carbon cycle. Previously published studies suggest primary productivity and $CO_{2(aq)}$ concentration as the main factors which determine $\delta^{13}C_{diatom}$ in marine environments (Schneider-Mor et al. 2005), although lake $\delta^{13}C_{diatom}$ is likely controlled by more complex environmental conditions (Hurrell et al. submitted). $\delta^{13}C_{diatom}$ variations due to the species effect, cell size, growth rate or/and metabolic pathway are neglected here since in our case the $\delta^{13}C_{diatom}$ analysis was always carried out on similar sized-cells (38-62 μm) and on the same diatom species (*Cyclostephanos andinus*).

In lakes, it is usually assumed that the carbon pool in the water becomes enriched in ^{13}C during the periods of enhanced productivity (Leng et al. 2005b; Singer and Shemesh, 1995) since phytoplankton preferentially use the lighter isotope. However, the maximum productivity events found here, associated with the white laminae (short-term diatom super-blooms), show the lowest $\delta^{13}C_{diatom}$ values. Therefore, although the diatom blooms will have preferentially incorporated ^{12}C, this cannot have been sufficient to positively shift the isotope value of the dissolved carbon. Instead, the supply of carbon available to the diatoms must have been sufficient not to lead to limiting conditions.

The $\delta^{13}C_{bulk}$ in the Lago Chungará laminated unit range from –21‰ to –19‰ (J.J. Pueyo, unpublished data), yielding a difference of more than 5‰ when compared to the measured $\delta^{13}C_{diatom}$ values. Nevertheless, the C/N ratio from bulk sediments of the laminated unit have values ranging between 7 and 11 (J.J. Pueyo, unpublished data), indicating that the $\delta^{13}C_{bulk}$ signal would have a mainly algal origin (Meyers and Terranes, 2001). For this reason, it seems that the $\delta^{13}C_{diatom}$, rather than being mainly affected by changes in the source of organic matter, is mostly conditioned by changes in dissolved carbon concentration. Mineralisation of terrestrial or previously deposited carbon through microbial

decomposition could create a pool of isotopically lighter carbon available to the diatoms. Release of this through respiration ($CO_{2(aq)}$ and possible also CH_4) would be partly controlled by lake dynamics under the control of external forcing factors. Lake water dynamics are mainly governed by two contrasting situations (Hernández et al. 2008): (1) a water column subjected to episodes of very strong mixing, which is represented by the white laminae, and (2) a more stable condition, including periods of lake water stratification, and represented by the dark-green laminae. During the stratified periods, concentrations of oxygen and other electron acceptors typically decrease in the hypolimnion, while $CO_{2(aq)}$, CH_4, and nutrients accumulate (Bedard and Knowles, 1991). These dissolved nutrients, as well as the accumulated $CO_{2(aq)}$ and CH_4, are released into the entire lake during mixis (Houser et al., 2003), when the diatom blooms occur, being the carbon incorporated into the diatom frustules.

6.3.3 $\delta^{18}O_{diatom}$ inter-cycle relationships (white laminae formation)

The characterisation of $\delta^{18}O_{diatom}$ values through the inter-cycle relationships gives clues to understand the underlying processes involved in the formation of the white laminae. The massive diatom blooms that produce the white laminae have to be triggered by an exceptional injection of nutrients into the water column which may or may not be associated with a water mass change. The start of the rhythmite is usually accompanied by $\delta^{18}O_{diatom}$ enrichment (Table 6.2.A), indicating a decrease in the P/E ratio, a drop in the lake water level and a remobilization of nutrients from the hypolimnion as the more likely scenario during the white laminae formation (Fig. 6.4.A and B, transition 1).

Episodes of diatom super-blooms occur throughout the whole studied section, but their formation is a time scale-dependent process. At decadal-centennial scales white laminae are more marked (higher values in the grey colour curve) and thicker (around 6 mm) with higher isotope oxygen values (up to 39.2‰) than during other laminae deposition periods (Hernandez et al. in press). Deposition of these white laminae stretches are related to low-stand conditions, as shown in the uppermost part of the three shallowing upwards trends observed in the $\delta^{18}O_{diatom}$ record (Fig. 6.3). However, at interannual scales the inter-cycle isotope relationships reveal that both changes to drier or wetter conditions may trigger the formation of the white laminae, but falls in lake level were more likely responsible for the development of the massive diatom blooms (Table 6.2).

6.3.4 $\delta^{18}O_{diatom}$ and $\delta^{13}C_{diatom}$ intra-cycle relationships (green laminae formation)

The intra-cycle relationship between $\delta^{18}O_{diatom}$ and $\delta^{13}C_{diatom}$ provides a means of better understanding of the environmental processes involved in the origin of the green laminae. The $\delta^{18}O_{diatom}$

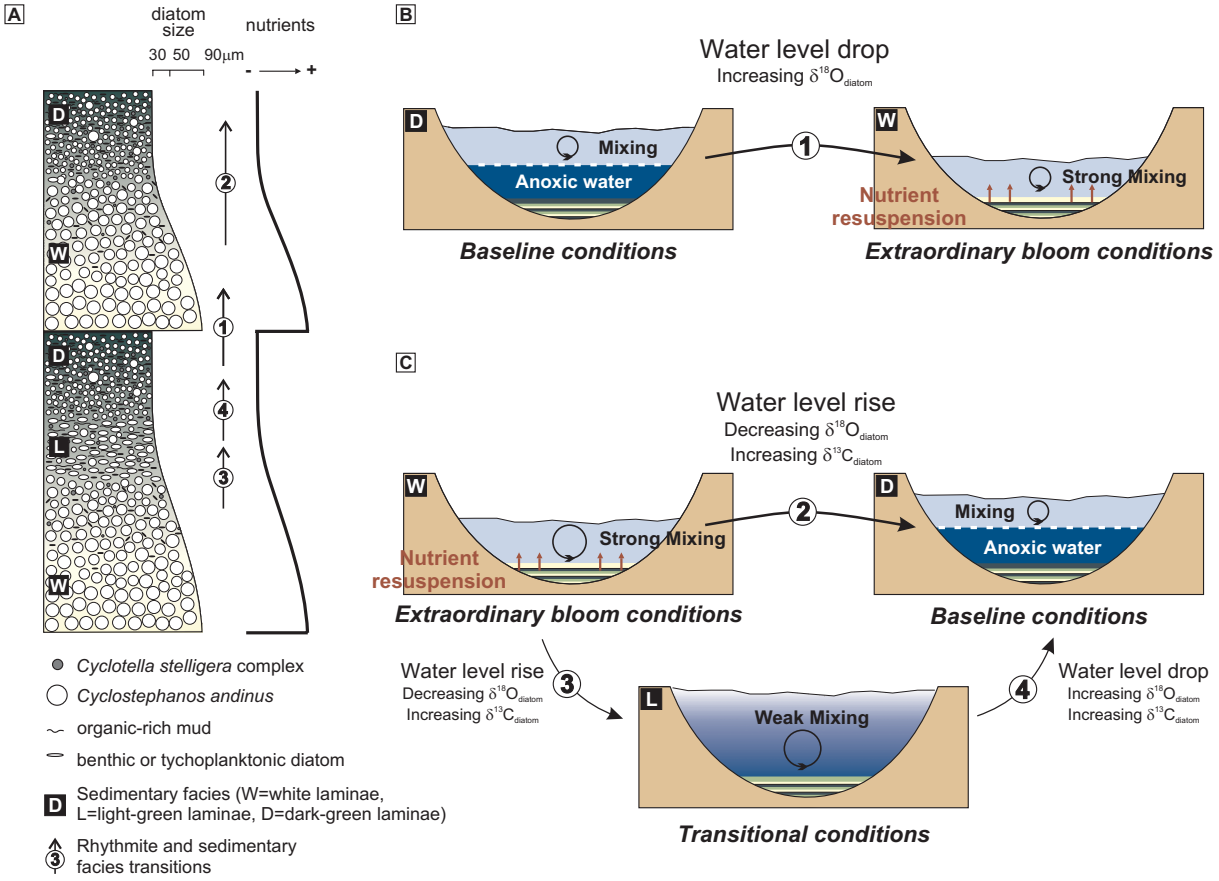

Figure 6.4. A. Rhythmite log succession showing facies and transitions (indicated by letters and numbers, respectively). B. The most frequent intercycle relationship scenarios. Transition case 1: From dark-green to white laminae, the white laminae formation (diatom super-blooms) is more often favoured by drops of the lake water level (increases in $\delta^{18}O_{diatom}$ values) and therefore related to recycled nutrients from the hypolimnion. C. The most common intracycle relationship scenarios. Transition case 2: From white to dark-green laminae, the dark-green lamina formation is usually favoured by rises of the lake level water (decreases in $\delta^{18}O_{diatom}$ values). Transition case 3: From white to light-green laminae, the light-green laminae formation is usually favoured by rises of the lake water level (lower $\delta^{18}O_{diatom}$ values). Transition case 4: From light-green to dark green laminae, the dark-green laminae formation is almost indistinctly favoured by drops or rises of the lake water level, with a slight predominance of the former as the $\delta^{18}O_{diatom}$ show.

intra-cycle relationships show that transitions from white to dark-green laminae are mainly governed by $\delta^{18}O_{diatom}$ depletions by up to –2.7‰ (65%; n=23), although there are also a significant percentage of enrichments (Table 6.2). As in the case of the white laminae formation, green laminae can be formed under both lake-water level drops and rises, but their formation is clearly favoured by increasing P/E ratios with subsequent lake-water level rises (Fig. 6.4.A and C, transitions 2 and 3).

Green laminae record the baseline conditions in the water column mixing regime including water table stratification periods. The intra-cycle relationships which show $\delta^{18}O_{diatom}$ depletions indicate that the lake tended to progressively recover the previous environmental conditions by means of a gradual increase in water availability (Fig. 6.4.A and C, transition 2 and 3). Conversely, the intra-cycle relationships which show $\delta^{18}O_{diatom}$ enrichments would indicate the recovery to a lower lake level after a super-bloom caused by a massive allochthonous nutrient input associated to enhanced rainfall. This is

suggested by the prevalence of $\delta^{18}O_{diatom}$ depletions that precede those super-blooms (90%; n=10) (Table 6.1). This model suggests that the green laminae occurred most of the time as a result of the recovery phase favoured by lake water rises. Finally, when the lake is already in the recovery phase (transitional and baseline conditions) it may evolve, indistinctly, towards rise or fall lake water level stands, as indicated by the light- to dark-green isotope transitions (enrichments= 56%; n=9) (Fig. 6.4.A and C, transition 4).

Comparison between $\delta^{13}C_{diatom}$ and $\delta^{18}O_{diatom}$ in the intra-cycle relationships show that the former can be associated to either $\delta^{18}O_{diatom}$ enrichments or depletions. However, $\delta^{13}C_{diatom}$ values show that all intra-cycle relationships yield carbon isotope enrichment during the formation of the organic-rich green laminae (Table 6.1). This occurs because during the white laminae formation, the strong mixing necessary for the formation of the massive diatom blooms break the lake water stratification. Transport of $CO_{2(aq)}$ and CH_4 from an hypolimnion enriched in these compounds is then allowed, depleting the $\delta^{13}C$ of the total carbon pool.

6.3.5 Climate forcing of the laminae formation

The biogeochemical reconstruction presented above suggests that laminae are formed by the occurrence of diatom super-blooms. These are directly affected by nutrient availability which, in turn, is mainly controlled by the lake level fluctuations and mixing as stable isotopes ($\delta^{13}C_{diatom}$ and $\delta^{18}O_{diatom}$) demonstrate. Hence, the laminae formation in Lago Chungará seems to be mainly induced by environmental forcing such as short-term climate variability.

ENSO and solar activity, as well as interactions between both phenomena, have been key factors prompting changes in the atmospheric conditions over the Altiplano region during the Late Glacial to Early Holocene at decadal and longer term time scales (Hernandez et al. in press). ENSO and solar activity, as responsible for the more accentuated sub-millennial wet or dry conditions over the Andean Altiplano (Theissen et al. 2008), are very likely the main environmental factors in the frequency and production of the white laminae. In the Central Andes, there is a weak trend towards wet conditions during La Niña phase and to dry conditions during El Niño phase (Valero-Garcés et al. 2003). According to our depositional model, white laminae formation could be triggered by both phases. However, El Niño events seem most likely to be responsible, since the white laminae formation is usually favoured by changes from wet-to-dry conditions, which is seen in the isotope enrichments. It is important to point out that white laminae are more intense (higher intensity grey colour values) and better developed (thicker) during periods showing higher isotope values which point to their formation during drier conditions (Hernández et al. in press). Thus, the diatom super-blooms likely occurred during El Niño-like periods. The presence of exceptionally intense and thick white laminae could, on the other hand, be indicative of the overlapping of both ENSO and solar activity phenomena during such periods. Isotope data show that high intensity of ENSO and solar activities can be recorded beyond the white laminae deposition.

The short duration (days) of extreme blooms in relation to lake water residence time gives an isotope signature that will remain for longer periods (years) being recorded in the dark laminae (Hernández et al. in press).

6.4 Conclusions

Lago Chungará rhythmites record multiannual diatom super-blooms lasting from days to weeks (white laminae) and the lake hydrology recovery towards the baseline conditions throughout several years (dark-green laminae). Self-sedimentation phenomena taking place immediately after the diatom super-blooms cannot be discarded as a sign of the end of the super-bloom (light-green laminae). The diatom super-blooms are favoured episodes of extreme turbulent conditions affecting the whole water column, and/or by strong runoff during wet episodes. In the first case upwelling from nutrient-rich hypolimnion waters allowed an extraordinary nutrient availability, whereas in the second case allochthonous nutrient enrichment would be implicated.

In Lago Chungará, the $\delta^{18}O_{diatom}$ record can be used as an indicator of changes in the P/E related to climate changes, whereas the $\delta^{13}C_{diatom}$ variability would be mainly influenced by changes in $CO_{2(aq)}$ concentration. $\delta^{18}O_{diatom}$ values show that both white and green laminae formation may occur in either dry or wet conditions, but the diatom super-blooms were more intense (thicker white laminae) during decadal-centennial lowstands. $\delta^{18}O_{diatom}$ composition shows that the white laminae formation was mainly favoured by low lake levels, whereas the green laminae formation was especially prompted by lake level rises.

ENSO and solar activity are the most likely main climate forcing mechanisms triggering the white laminae formation. Both El Niño and La Niña phases could be responsible for this, but geochemical data indicate that dry conditions associated to El Niño could have the primary role since the white laminae formation was usually favoured by changes from wet-to-dry conditions in the Altiplano region. Moreover, the periods where the white laminae present major thickness and whiter colours might be indicative of phases with overlapping El Niño and solar activity. On the contrary, green-laminae were deposited during the baseline climate phases, when the normal plankton succession throughout several years and associated regular diatom blooms occur.

High resolution isotope analysis of the oxygen and carbon isotopes in diatom silica in this uniquely laminated sequence has displayed links between limnology, catchment runoff variations, hydrology and climate forcing at different time scales. Strong El Niño phases have triggered nutrient and carbon release from the hypolimnion and sediments that has led to diatom super-blooms. Such phenomena may be found in many lakes but few preserve evidence in their sedimentary architecture. Further work on other parts of this record and in similarly laminated sites may reveal the full impact of these multi-annual events on lake ecosystems and biogeochemical cycles.

Chapter 7

Oxygen and carbon diatom isotope records from the Lago Chungará laminated unit (12,400 to 8,400 cal years BP)

7.1 Introduction

A sound grasp of the tropical circulation and its temporal evolution is essential for characterising moisture transport mechanisms towards extratropical areas. Long-term response and climate variability of tropical systems is therefore crucial for understanding future climate change (e.g. Barker et al. 2007; Giralt et al. 2008; Chiang, 2009). However, there are currently few data on the frequency and amplitude of abrupt climate changes in tropical latitudes of South America, and the forcings responsible for this climate variability at different temporal scales are poorly documented (e.g. Moreno et al. 2007; Hyllier et al. 2009). Although it is believed that orbital parameters are the most important drivers of tropical precipitation at millennial-time scales (Baker et al. 2001a; Clement et al. 2001; Plazeck et al. 2006), a growing body of evidence suggests that climate variability is also governed by other centennial- to millennial-scale forcings such as the ENSO (Rowe et al. 2002; Baker, 2002). Despite the fact that many studies have focused on the period from the LGM until the present, a number of questions such as whether or not the Younger Dryas-like conditions arose in the Central Andes (Clapperton et al. 1997; Rodbell and Seltzer, 2000; Lowell and Kelly, 2008) or whether or not the ENSO weakening in the Early Holocene had a major effect on the lake levels (Rodbell et al.1999; Moy et al. 2002; Hernández et al. in press) remain unresolved. One way to answer these questions could be to undertake multiproxy studies of high-resolution lacustrine sequences.

Recent palaeoenvironmental studies conducted at Lago Chungará have shown a clear response of this lake to regional climate changes, evidenced by shifts in the lake water level (Valero-Garcés et al. 2003; Moreno et al. 2007; Sáez et al. 2007; Giralt et al. 2008). The laminated unit of the Lago Chungará sedimentary infill is made up almost exclusively of diatom frustules that are exceptionally well preserved. Such a sedimentary record enables us to apply the well-established technique of $\delta^{18}O_{diatom}$ (e.g. Shemesh et al. 2001; Leng and Barker, 2006) as well as the recent and much less developed technique of analysis

of $\delta^{13}C_{diatom}$ (Hernández et al. submitted; Hurrell et al. submitted). The combination of both $\delta^{18}O_{diatom}$ and $\delta^{13}C_{diatom}$ proxies provides valuable insights into the nutrient input and carbon cycle during the Late Glacial-Early Holocene transition.

The consumption and production of CO_2 and CH_4 by microorganisms exert an influence both on the concentration of these gases and on the atmospheric heat budget (Tranvik et al. 2009). Lakes play an important role in the global carbon cycle, potentially affecting regional climate and global change (Cole et al. 2007). Changes in the lacustrine carbon cycle may be revealed by $\delta^{13}C_{diatom}$ from lacustrine sediments, as has been reported in marine environments (e.g. Rosenthal et al. 2000; Crosta and Shemesh, 2002; Schneider-Mor et al. 2005). Diatom frustules contain polysaccharides and proteins (pleuralins, silaffins and long chain polyamines) enclosed within the silica cell wall structure (Kroger and Polusen, 2008). This organic matter is protected by silica against diagenetic processes that might affect the sediments (Des Combes et al. 2008). Therefore, it may reflect the features of dissolved carbon in water during cell formation. However, the $\delta^{13}C_{diatom}$ has not been widely applied to lake sediments where the complexity of sedimentary conditions such as the existence of different carbon sources and highly dynamic aquatic food webs raise further questions for interpretation (Hurrell et al. submitted).

In this study, we present records of $\delta^{18}O_{diatom}$ and $\delta^{13}C_{diatom}$ from the Lago Chungará diatom-rich laminated sedimentary unit which spans from 12,400 to 8,400 cal years BP. These records provide evidence of significant palaeoenvironmental changes at local and regional scales in the Central Andes over this time window.

7.2 Results

Isotopic values of the $\delta^{18}O_{diatom}$ record range from 34.7 to 40.3‰. This proxy displays a long-term enrichment trend (~+3‰) between 12,400 and 10,100 cal years BP. This trend is however punctuated by short-term depletions centered at ca 11,500, 11,200 11,000, 10,700, 10,400 and 10,200 cal years BP. Subsequently, a period with maximum isotope values (ca +40‰) lasts for approximately one thousand years. Finally, a progressive depletion trend (–3‰) characterises the last 800 years of the record (Fig. 7.1).

The $\delta^{13}C_{diatom}$ values range from -30.3‰ (12,400 cal years BP) to -22.6‰ (10,100 cal years BP). The record shows considerable fluctuation with excursions to lower values that match the $\delta^{18}O_{diatom}$ record. Changes in $\delta^{13}C_{diatom}$ reveal a pattern that is similar to that of $\delta^{18}O_{diatom}$ from 12,400 to 10,100 cal years BP (Fig. 7.1). The following millennium is characterised by a depletion of $\delta^{13}C_{diatom}$ whereas the $\delta^{18}O_{diatom}$ values remain high. The uppermost part of the record displays a $\delta^{13}C_{diatom}$ enrichment trend that is particularly pronounced in the last 200 years. This trend is however interrupted by a large depletion reversal (–5‰) at 9,200 cal years BP.

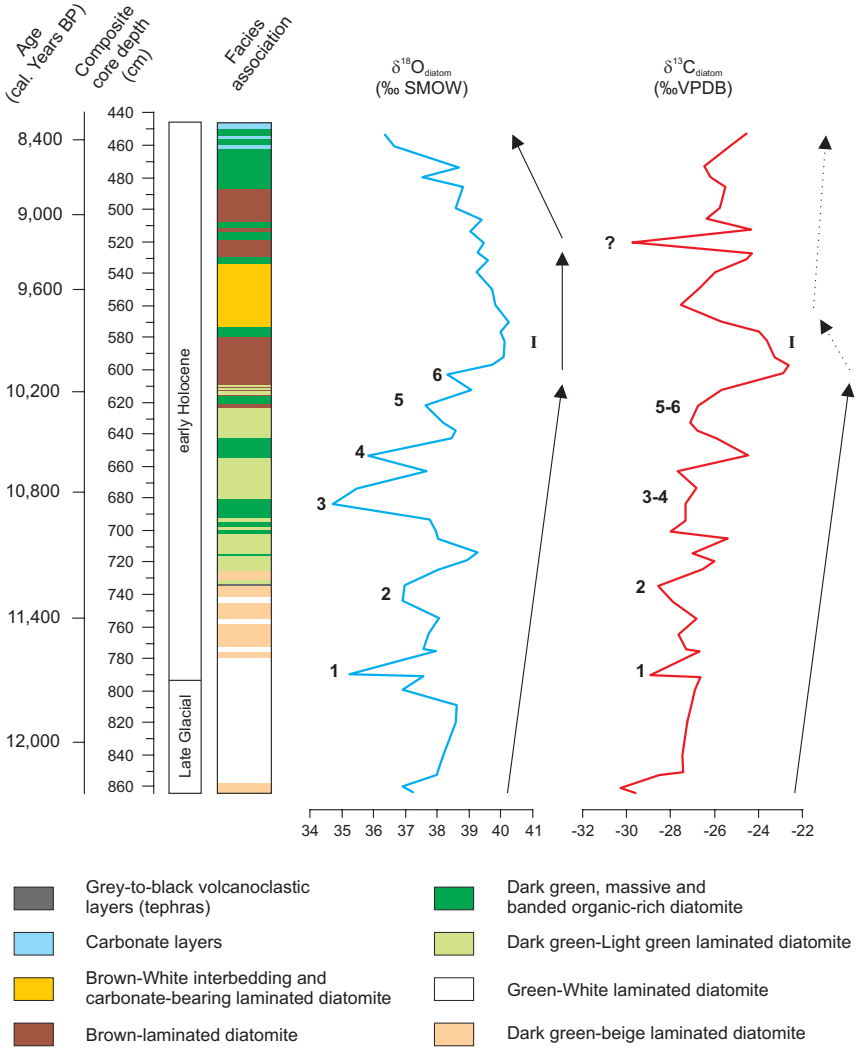

Figure 7.1. Facies association, $\delta^{18}O_{diatom}$ and $\delta^{13}C_{diatom}$ records for the period 12,400–8,400 cal years BP from Lago Chungará. Arabic numerals indicate the main humid events as revealed by the $\delta^{18}O_{diatom}$ record and the related $\delta^{13}C_{diatom}$ depletions during the Late Glacial-Early Holocene transition. The Roman numeral indicates the maximum dry phase associated with the highest $\delta^{13}C_{diatom}$ values. Arrows show the main trends during the established climate stages: Late Glacial-Early Holocene humid phase (12,400-10,100 cal years BP), Early Holocene dry phase (10,100-9,100 cal years BP) and Early Holocene dry-to-wet transition phase (9,100-8,400 cal years BP).

7.3 Discussion

7.3.1 Controlling factors in $\delta^{18}O_{diatom}$ and $\delta^{13}C_{diatom}$

Diatoms are autotrophic organisms containing a shell or frustule made up of biogenic silica ($SiO_2 \cdot nH_2O$) and various specific organic macromolecules such as proteins and polysaccharides (Round et al. 1990; Kröger and Poulsen, 2008). Diatoms, like plants, require CO_2 for photosynthesis. However, they also have the ability to utilise HCO_3^- through biophysical concentrating mechanisms (Johnston et al. 2001). Thus, the interpretation of changes in the stable isotope composition of diatom silica is not straightforward since a number of influential factors cannot be ruled out.

A good grasp of the processes that govern the $\delta^{18}O_{diatom}$ signal is therefore required to interpret the past oscillations of this proxy (Leng et al. 2005b). $\delta^{18}O_{diatom}$ depends on both the water temperature and the isotopic composition of the lake water when the shell is secreted (Shemesh et al. 1992). The $\delta^{18}O_{diatom}$ record may thus result from one or more of the following factors: a) changes in the P/E (e.g. Barker et al. 2007), b) oscillations in water temperature (e.g. Hu and Shemesh, 2003), c) fluctuations in $\delta^{18}O$ or in temperature at the source of the precipitation (e.g. Swann et al. 2010), and/or d) variations in the $\delta^{18}O_{lakewater}$ attributed to changes in the contribution of precipitation from different air masses (e.g. Rosqvist et al. 2004).

The interpretation of $\delta^{18}O_{diatom}$ may be complicated by changes in the specific composition of diatom assemblages, diatom dissolution, and silica maturation (Swann et al. 2010, Jonsson et al. 2010). Despite the fact that little is known about these factors, our analyses, which were performed in an exceptionally well preserved single species (*Cyclostephanos andinus)* with no signs of diagenetic alteration, show that these factors exert little influence on the $\delta^{18}O_{diatom}$ record of Lago Chungará (Fig. 5.4).

In closed lakes, oscillations in $\delta^{18}O_{lakewater}$ will usually be far greater than fluctuations due to temperature or isotope changes in rainfall (Leng and Barker, 2006). Oxygen isotope records in tropical regions have also proved to be sensitive to the amount of precipitation (Cole et al. 1999), and it is likely that this relationship is important in tropical lake records (Barker et al. 2001; Hernández et al. in press). Under these circumstances, the $\delta^{18}O_{diatom}$ record can be used as an indicator of change in the P/E related to climate change (Leng and Marshall, 2004). A modern day calibration was carried out to determine the environmental forcings governing changes in $\delta^{18}O_{diatom}$ from Lago Chungará (Herrera et al. 2006; Table 2.1). At present, evaporation enriches the lake by ~14‰ with respect to precipitation. It may be assumed therefore that significant changes in water isotope values in the past mainly resulted from shifts in the P/E. Although the P/E is usually governed by climate oscillations, non-climate effects such as the ontogeny of the lake can also exert an influence on the $\delta^{18}O$ signal. Changes in the residence time of the lake caused by variations in basin hydrology or in groundwater fluxes will also influence the degree of enrichment (Leng et al. 2005b; Hernández et al. 2008). During transgressive periods, the stepped morphology of Lago Chungará forced the expansion of the lake towards the shallow margins (Fig. 4.4), resulting in an increase in the lake surface/volume ratio that enhanced evaporation. This caused a background isotope enrichment during the Late Glacial-Early Holocene transition. Nevertheless, oscillations in the P/E seem to be mainly responsible for changes in the $\delta^{18}O_{diatom}$ in Lago Chungará (Hernández et al. 2008).

As photosynthesisers, diatoms offer a more reliable substrate for reconstructing past changes in $\delta^{13}C$ than bulk sediment organic matter, which often includes a mixture of both autotrophs and heterotrophs (Rosenthal et al. 2000). In addition, organic carbon from diatom frustules is less likely to be affected by diagenesis (Des Combes et al. 2008). However, most of the information about how $\delta^{13}C_{diatom}$

isotopes records are interpreted is mainly derived from the marine realm (e.g. Schneider-Mor et al. 2005; Singer and Shemesh, 1995). Productivity plays a major role in determining the isotopic signature of oceanic DIC because reduced phytoplankton productivity increases the availability of ^{12}C with the result that diatoms yield lower $\delta^{18}O_{diatom}$ values (Singer and Shemesh, 1995; Schneider-Mor et al. 2005). Consequently, $\delta^{18}O_{diatom}$ from marine records has commonly been used as a proxy for primary production and $CO_{2(aq)}$ concentration (Des Combes et al., 2008). Nevertheless, there are other factors that influence $\delta^{13}C_{diatom}$, such as taxonomic composition, pH, cell growth rate, size, shape and $CO_{2(aq)}$ permeability and biochemical metabolic pathways (Popp et al. 1998, Hurrell, 2009). These obstacles could be overcome if a previous physical selection of single-size diatom species is undertaken (e.g. Singer and Shemesh, 1995; Hernandez et al. submitted).

In addition to the factors previously mentioned as major influences, the scant literature on lacustrine sediments highlight other factors given that $\delta^{13}C_{diatom}$ in lakes is controlled by more complex environmental conditions (Hurrell et al. submitted). The larger catchment carbon pool of lakes in relation to their water mass exerts a considerable influence, whereas the significance of inputs of terrestrial organic matter to the ocean basins can be considered low. $\delta^{13}C_{diatom}$ from lakes can thus indicate changes in the nature and concentration of lake carbon apart from productivity oscillations. Therefore, the $\delta^{13}C_{diatom}$ signal is not only a function of in-lake processes but also of the catchment characteristics that influence carbon (Hurrell et al. submitted). External loadings would increase the carbon inputs to the lake of terrestrial isotopically depleted carbon-rich materials which would become an important source of carbon and would therefore produce lower $\delta^{13}C_{diatom}$ signals (Hurrell et al. submitted). Isotope values from Lago Chungará terrestrial plants range between –26 and –23‰, whereas planktonic algae values are higher than –15‰ (Pueyo JJ, unpublished data). Thus, even small external loadings could produce significant excursions in $\delta^{13}C_{diatom}$ values.

Climate drives soil and vegetation dynamics in the watershed as well as stratification and mixing patterns in lakes. Thus, the transport of organic matter from catchments to lakes and its subsequent $CO2_{(aq)}$ concentration are ultimately controlled by climate (Catalan and Fee, 1994; Catalan et al. 2009). $\delta^{13}C_{diatom}$ depletions in Lago Chungará are consistent with humid events in Lago Chungará as indicated by the $\delta^{18}O_{diatom}$ record. External loadings favoured by these humid periods introduce isotopically depleted carbon from the terrestrial organic matter in the lake water.

On the other hand, periods of enhanced mixing of the water column also prompt influx of CO_2 enriched waters from the hypolimnion to the photic zone, causing isotopic depletion in DIC (Houser et al. 2003). The $\delta^{13}C_{diatom}$ in the Lago Chungará sedimentary record seems to corroborate this explanation. Major trends in $\delta^{13}C_{diatom}$ are in agreement with a rough indicator of water column mixing derived from the multivariate statistical analysis of the diatom assemblages (Bao et al. in prep) (Fig. 7.2).

Another concordance is found between the $\delta^{13}C_{diatom}$ record and the BSi flux to the sediments (Bao et al. in prep), an indicator of past biosiliceous productivity conditions (Conley, 2001) (Fig. 7.2). All these observations suggest that the $\delta^{13}C_{diatom}$ signature in the sediments are due to changes in the carbon input from the catchment, degree of mixing, biosiliceous productivity or to a combination of some of these factors.

7.3.2 Palaeoenvironmental reconstructions

The palaeonvironmental reconstruction of Lago Chungará during the Late Glacial and Early Holocene is based on a) the $\delta^{18}O_{diatom}$ record as an indicator of changes in the P/E and hence of the moisture balance, and b) the $\delta^{13}C_{diatom}$ record, which reveals changes in productivity, carbon inputs from the catchment and in $CO_{2(aq)}$ concentration.

Late Glacial-Early Holocene transition humid phase (12,400-10,100 cal years BP)

The Late Glacial-Early Holocene transition in the Andean Altiplano was a humid period (e.g. Wolfe et al. 2001; Giralt et al. 2009) coeval with the Coipasa humid phase found elsewhere (Sylvestre et al. 1999; Placzek et al. 2006). The $\delta^{18}O_{diatom}$ record in Lago Chungará however displays a slight enrichment trend during the first half of this period (12,400-11,000 cal years BP) and a higher enrichment trend during the second half (11,000-10,100 cal years BP), which would suggest a lake level decline (Fig. 7.1). Contrary to expectations, this increasing trend can be ascribed to the flooding of the shallow eastern and southern margins after ca 11,000 cal years BP (Sáez et al. 2007). The reason for this apparent contradiction is that the surface area to volume ratio of the lake significantly increased because these flooded margins were much shallower than the central plain (Fig. 2.7). As a result the relative importance of evaporation was enhanced. This induced an unexpected enrichment trend of $\delta^{18}O_{diatom}$ in a transgressive phase (Hernández et al. 2008). Therefore, the six major isotope depletions of the $\delta^{18}O_{diatom}$ curve at this time would be the real indicators of the overall humid character of this period. The magnitude of these six $\delta^{18}O_{diatom}$ depletions decreased from 10,500 to 10,100 cal years BP when the surface/volume ratio was probably at its maximum prior to a gradual shift towards arid conditions.

There is a general consensus that millennial-scale shifts in moisture conditions in tropical South America are orbitally induced by changes in solar insolation (e.g. Baker et al. 2001b; Clement et al. 2001) although the ENSO long-term changes also play a major role (e.g. Rowe et al. 2002; Abbott et al. 2003). The Late Glacial-Early Holocene transition is a period where the summer insolation decreases towards an insolation minimum at 10,000 cal years BP (Berger and Loutre, 1991). This insolation decrease

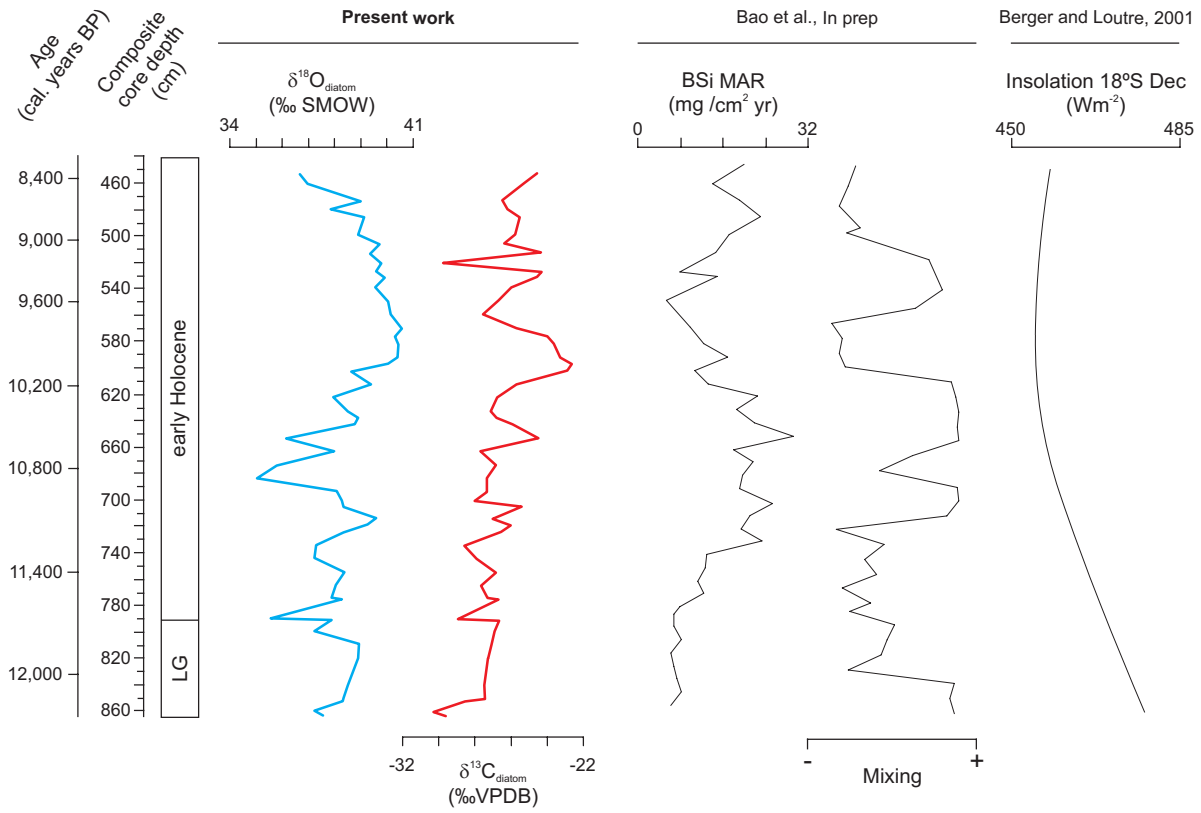

Figure 7.2. Comparison between $\delta^{18}O_{diatom}$ and $\delta^{13}C_{diatom}$ records obtained in this work with the data of Biogenic Silica (BSi) mass accumulation rates in the sediments and the mixing intensity in the lake water column as deduced from the multivariate analysis of diatom assemblages (Bao et al. in prep). The insolation curve in the austral summer at 18ºS for this period is also shown.

induces a diminution in the convective activity with clearer skies and less rainfall (Rowe et al. 2002; Hillyer et al. 2009), triggering a reduction in the P/E and lake level falls. However, the evidence for a highstand in Lago Chungará during this period suggests a humid phase. The most plausible explanation for this apparent contradiction would be the establishment of long-term La Niña-like conditions in the tropical Pacific (Betancourt et al. 2000; Koutavas et al. 2002), giving rise to a humid phase over the Altiplano during the Early Holocene (Hernández et al. in press). In addition, a regional effective moisture reconstruction was previously performed using the Lago Chungará sedimentary record (Giralt et al. 2008). This reconstruction was carried out by applying multivariate statistical analyses (Cluster, RDA and PCA) to magnetic susceptibility, XRF, XRD, TC, TOC, BSi and grey-colour curve of the sediment data. For the lower part of Chungará sequence (Unit 1), the effective moisture availability proxy depends on the P/E, with positive values corresponding to drier conditions (Giralt et al. 2008) (Fig. 7.3). The data obtained from this reconstruction were filtered for the ENSO (0.19-0.27 Hz) and solar activity cycles (0.075-0.11 Hz) frequency bands (Fig. 7.3) (Giralt et al. in prep). The moisture balance reconstruction shows a good agreement with a humid period between 11,000 and 10,500 cal years BP, and with a transition towards drier conditions for the next ca 500 years. Moreover, the ENSO intensity displays the highest values for this period, indicating an enhanced ENSO activity. This activity was mainly

governed by the La Niña conditions, which are characterised by a humid situation over the Andean Altiplano (Valero-Garcés et al. 2003) in accordance with the $\delta^{18}O_{diatom}$ values.

$\delta^{13}C_{diatom}$ data are consitent with this interpretation. $\delta^{13}C_{diatom}$ values also show an increasing trend with depletions that generally match the $\delta^{18}O_{diatom}$ drops (Fig. 7.1). The long-term increasing upwards trend agrees with the increase in productivity as revealed by the BSi flux to the sediments, suggesting a depletion of the available ^{12}C and hence higher values of $\delta^{13}C_{diatom}$. On the other hand, the coincidence of negative excursions in $\delta^{13}C_{diatom}$ with $\delta^{18}O_{diatom}$ drops suggests that increased organic matter transported by runoff could have added light carbon to the carbon pool, resulting in lower isotope values.

There is no clear evidence of a Younger Dryas-like event between 12,400 and 11,000 cal years BP in Lago Chungará, which is consistent with other tropical Andean records, e.g. Lakes Pacucha (Hillyer et al. 2009), Titicaca (Paduano et al. 2003) and Junin (Seltzer et al. 2000).

Early Holocene dry phase (10,100-9,100 cal years BP)

The driest period recorded during the Early Holocene corresponds to the highest values of $\delta^{18}O_{diatom}$ (Fig. 7.1). The reduction in the relative abundance of planktonic diatoms (Sáez et al. 2007; Bao et al. in prep) and XRF data (Moreno et al. 2007; Giralt et al. 2008) indicate a fall in the water availability in Lago Chungará (Fig. 7.3). The brown-white interbedding and carbonate-bearing laminated diatomite facies (Fig. 7.1) are also indicative of low lake levels and hence of a reduction in the moisture of the region (Sáez et al. 2007). Although this dry event seems to follow a heterogeneous spatial and temporal pattern, it appears in most of the records from the Andean Altiplano (e.g. Seltzer et al. 2000; Baker et al. 2001a; Abbott et al. 2003; Hyllier et al. 2009). This event coincides with the minimum values of the summer insolation precessional curve, favouring drier conditions and the lowest lake levels throughout the Holocene (Rigsby et al. 2005; Hyllier et al. 2009). During this insolation minimum, the ITCZ experienced a northward shift with a reduction in the moisture transport and in the precipitation over the South American tropics (McGregor and Nieuwolt, 1998). Moreover, the ENSO and solar activity intensities show the minimum values for this period (Fig. 7.3). When the ENSO forcing is weak, small northward shifts of the ITCZ or the establishment of a tropical North Atlantic warm pool can induce periods of drought in Amazonia (Baker, 2002; Marengo, 2004; Marengo, 2007; Vuille et al., 2000). Thus, the Andean Altiplano region would fall in the most arid period of the Holocene (Hyllier et al. 2009).

A thick stretch of mostly white laminae was deposited during this lowstand (Fig. 7.1). These white laminae accumulated during massive short-term diatom blooms and were triggered by high nutrient

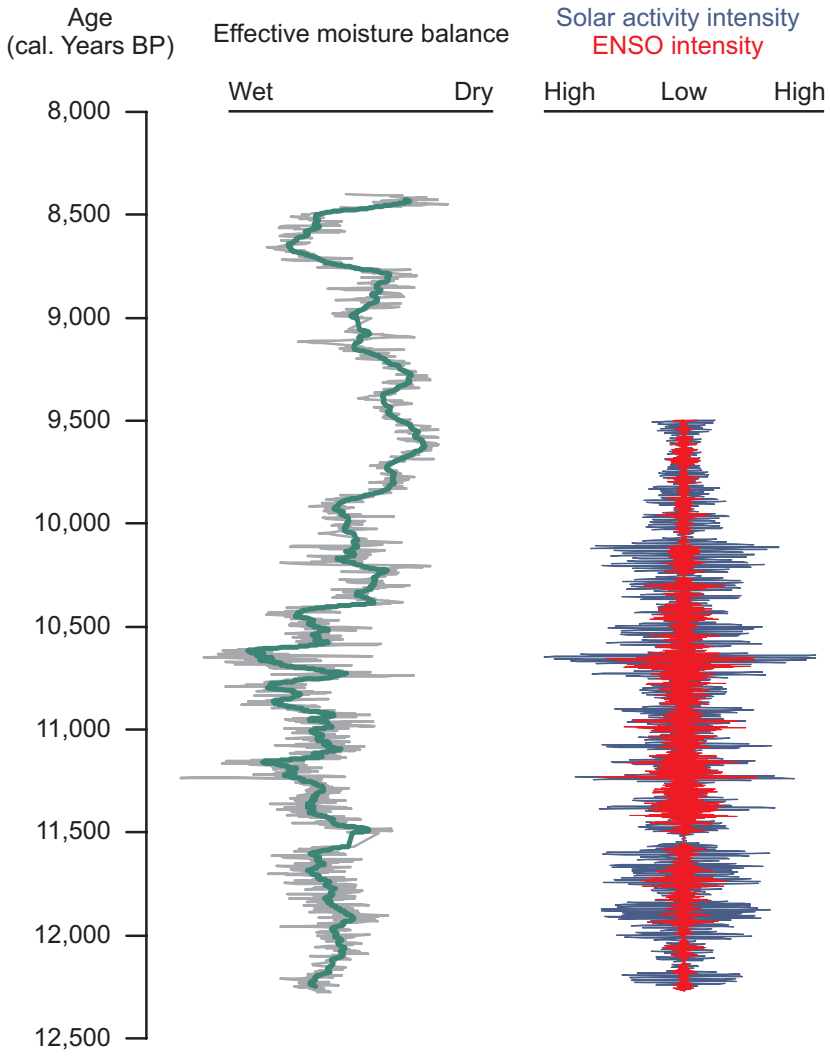

Figure 7.3. A) Effective moisture balance derived from the second eigenvector of PCA from magnetic susceptibility, XRF, XRD, TC and TOC, BSi (Giralt et al. 2008) for the laminated unit of Lago Chungará. The raw data are shown in grey and the smoothed data in yellow. B) Intensity of ENSO and solar activity signals (red and green, respectively) from the effective moisture balance curve filtered at 0.19-0.27 Hz and 0.075-0.11 Hz frequency bands (Giralt et al. in prep).

availability as a result of strong mixing periods (Hernández et al. submitted). Although lake productivity decreases in this period the $\delta^{13}C_{diatom}$ record displays high values followed by a sudden depletion (Fig. 7.1). This indicates either an increase in terrestrial organic matter inputs or in dissolved $CO_{2(aq)}$ concentration from the hypolimnion. Reduced loadings to the lake, which are associated with dry conditions, make the latter hypothesis the most plausible explanation. Enhanced mixing conditions governing this period (Bao et al. in prep.) (Fig. 7.2) would have released the $CO_{2(aq)}$ available in the hypolimnion, depleting the carbon pool and the $\delta^{13}C_{diatom}$ values (Hernandez et al. submitted). Bacterial induced methanogenesis providing CH_4 to the lake water must not be ruled out (J.J. Pueyo, pers comm.). However, the decreasing trend of $\delta^{13}C_{diatom}$ after this maximum could be ascribed to a depletion of the available $CO_{2(aq)}$ and to the subsequent depletion of ^{12}C in the carbon pool.

Early Holocene dry-to-wet transition phase (9,100-8,400 cal years BP)

A transition towards moister conditions is recorded by $\delta^{18}O_{diatom}$ between 9,100 and 8,400 cal years BP. This proxy displays a slight decreasing upwards trend to the top of the unit. These moister conditions are consistent with an increase in the summer insolation, and with the effective moisture reconstruction (Giralt et al. 2008) that indicates a shift to more humid conditions between 9,000 and 8,500 cal years BP (Fig. 7.3). Moreover, this humid phase is well known elsewhere over the Andean Altiplano (Baker et al. 2001a; Grosjean et al. 2001).

On the other hand, $\delta^{13}C_{diatom}$ values display a slight enrichment trend in this period. This indicates that the $\delta^{13}C_{diatom}$ values are more influenced by lake productivity (which also increases) than by the terrestrial organic matter inputs from an increased runoff. The transition to more humid conditions from a severe drought situation, when vegetation coverage of the catchment was scarce, reduced external organic matter inputs to the lake. This would have limited the carbon pool, resulting in the subsequent $\delta^{13}C_{diatom}$ enrichment during this enhanced productivity period. Furthermore, the reduced mixing (Fig. 7.2) also affected the availability of isotopically light carbon for diatoms living in the photic zone. Intensification of the stratification conditions prevented the release of $CO_{2(aq)}$ from the hypolimnion to surface waters, thereby stimulating the $\delta^{13}C_{diatom}$ enrichment.

7.4 Conclusions

Measurements of $\delta^{18}O_{diatom}$ and $\delta^{13}C_{diatom}$ are useful proxies for understanding regional climate patterns and lake-catchment processes in Lago Chungará. The interpretation of the $\delta^{18}O_{diatom}$ record is based on the hydrology of the lake, and reflects the centennial-to-millennial regional moisture balance, whereas the interpretation of $\delta^{13}C_{diatom}$ is probably conditioned by changes in productivity, $CO_{2(aq)}$ concentration and the source of carbon in the lake.

Three main climate phases were identified during the Late Glacial and Early Holocene: a) a humid phase during the Late Glacial-Early Holocene transition (12,400-10,100 cal years BP), b) a dry phase in the Early Holocene (10,100-9,100 cal years BP), and c) a dry-to-humid phase in the latter part of the Early Holocene period (9,100-8,400 cal years BP). Although the Late Glacial to Early Holocene wet phase coincides with a trend to an insolation minimum, the establishment of long-term La Niña-like conditions in the tropical Pacific, as indicated by the high values in the ENSO activity intensity, seems to have overcome the precessional forcing. Evidence of the Younger Dryas-like event was not obtained in Lago Chungará. The insolation minimum at ca 10,000 cal years BP played a key role during the Early Holocene (10,100-9,100 cal years BP), giving rise

to the probable northward migration of the ITCZ. This, in addition to the ENSO weakening, would have plunged the tropical Andes into a severe drought. The return to more humid conditions began around 9,000 cal years BP, following a slight increase in summer insolation. This period was probably brief since many Andean Altiplano records show the start of a major dry period at ca 8,000 cal years BP as a result of an ENSO weakening. Further analyses throughout the non-laminated unit 2 from the Lago Chungará record would be required to confirm this hypothesis.

Isotope analysis of $\delta^{13}C_{diatom}$ reveals that several factors, such as productivity, carbon source and carbon concentration account for the $\delta^{13}C_{diatom}$ oscillations. Furthermore, these oscillations reveal interactions between the lake water carbon pool and the catchment. During wet periods $\delta^{13}C_{diatom}$ shows that the relative contribution of external loadings, in addition to lake productivity, significantly enriched the carbon pool, whereas dry periods favoured the in-lake lacustrine carbon accumulation and the subsequent enrichment of the $\delta^{13}C_{diatom}$ values. The release of CO_2 from the hypolimnion during mixing conditions can also deplete the $\delta^{13}C_{diatom}$ values. Both $\delta^{18}O_{diatom}$ and $\delta^{18}O_{diatom}$ analyses can help us to gain a better understanding of the role of lakes in the carbon cycle in the context of global change.

Chapter 8

Conclusions

8.1 Concluding remarks

The isotope analyses and the petrographical study of diatomaceous laminated sediments from the Lago Chungará record yield the following methodological, limnological and climate conclusions:

8.1.1 Methodological conclusions

- Analysis of $\delta^{18}O_{diatom}$ shows that a number of factors in addition to climate forcings can exert an influence on the $\delta^{18}O_{diatom}$ signal. Given that $\delta^{18}O$ records cannot only be interpreted in terms of changes in wet–dry conditions, it is essential to investigate the hydrology of each system. The $\delta^{18}O_{diatom}$ records can provide valuable insights into the sedimentological processes that trigger the input, transport and accumulation of sedimentary particles, and into the ontogeny of the lake apart from palaeoclimatic issues.

- Analysis of $\delta^{13}C_{diatom}$ has proved to be a useful tool to reconstruct the carbon cycle in lakes and to improve our understanding of the global carbon cycle. The $\delta^{13}C_{diatom}$ record yields information on lake lacustrine productivity, carbon sources, lake-catchment relationships and changes in the concentration of $CO_{2(aq)}$.

- The Lago Chungará laminated diatom-rich sediments demonstrated that $\delta^{18}O_{diatom}$ and $\delta^{13}C_{diatom}$ can be used to reconstruct abrupt and rapid climate and enviromental changes. The well laminated nature of the Lago Chungará sediments has enabled us to conduct a continuous sampling lamina by lamina in accordance with the sedimentary structures. This sampling has provided one of the highest resolution records for the study of isotopes in diatom silica. The ultra-high resolution of this record showed significant high-frequency climate and limnological changes which would not otherwise have been identified. As a result, this technique can be used to characterise key climate and environmental events at an ultra-high temporal resolution, complementing the usual lower resolution studies in which these techniques are commonly applied.

8.1.2 Limnological conclusions

- The laminated sedimentary unit of Lago Chungará is made up of millimetric (3-23 mm) rhythmites composed of multiannual (4-24 years) triplets of white, light-green and dark-green laminae. White laminae consist almost exclusively of very large valves of the euplanktonic diatom *Cyclostephanos andinus*. Dark-green laminae are constituted by a mixture of diatoms (mainly smaller valves of smaller *Cyclostephanos andinu*s and diatoms of the *Discostella stelligera* complex) and organic matter. Light-green laminae are made up of components from the white laminae progressively grading upwards into the typical constituents of the dark-green laminae. The typical rhythmite starts with the white laminae deposition changing to dark-green laminae, and occasionally presenting interbedded light-green laminae. The contacts within the rhythmites are transitional, whereas contacts between rhythmites are abrupt.

- White laminae were formed during extraordinary short-term diatom blooms (days to weeks). These extraordinary diatom blooms were favoured by episodes of extreme turbulent conditions affecting the water column and/or by episodes of exceptional erosion of the top soil of the catchment. In the former case, upwelling from nutrient-rich hypolimnetic waters gave rise to an extraordinary nutrient availability whereas, in the latter case, allochthonous nutrient inputs would be implicated. Light-green laminae were formed during the end of the diatom super-blooms probably by self-sedimentation processes. Finally, dark-green laminae were deposited over several years under different water column regimes representing baseline lake conditions.

- Values of $\delta^{18}O_{diatom}$ showed that although both white and green laminae formations occurred in either dry or humid conditions, the extraordinary diatom blooms were more intense (thicker white laminae deposition) during decadal-to centennial-lowstands (i.e. in enhanced $\delta^{18}O_{diatom}$ periods). On the other hand, $\delta^{13}C_{diatom}$ values indicated that the carbon availability was higher during diatom super-blooms owing to the release of accumulated $CO_{2(aq)}$ from the hypolimnion in the mixing periods. In most cases, the $\delta^{18}O_{diatom}$ composition showed that the white laminae formation was mainly due to falls in the lake level, whereas the green laminae formation was mainly caused by rises in the lake level.

- High resolution isotope analysis of the diatoms in this laminated sequence showed complex links between limnology, catchment processes, hydrology and climate forcings. The $\delta^{18}O_{diatom}$ and $\delta^{13}C_{diatom}$ results highlight the importance of using both proxies in combination. Changes in carbon and biogeochemical cycles indicated by $\delta^{13}C_{diatom}$ are linked to hydrological changes evidenced by $\delta^{18}O_{diatom}$. During wet events indicated by $\delta^{18}O_{diatom}$, low values of $\delta^{13}C_{diatom}$ show that the relative contribution of

external loadings, in addition to lake productivity, significantly increased the carbon pool. By contrast, dry periods favoured the in-lake lacustrine carbon accumulation and an increase in $\delta^{13}C_{diatom}$ values. However, the release of the $CO_{2(aq)}$ from the hypolimnion during the mixing periods could also favour the depletion of the $\delta^{13}C_{diatom}$ values. Therefore, in this region, periods with enhanced precipitation led to a larger productivity, a greater exportation of CO_2 to the atmosphere, or both.

8.1.3 Climate conclusions

- This record clearly shows, that depending on the temporal-scale, one forcing type could prevail over the others when interpreting $\delta^{18}O_{diatom}$ and $\delta^{13}C_{diatom}$ in Lago Chungará:

- At centennial-to millennial-scales, in addition to climate, hydrological factors such as changes in the groundwater/evaporation loss ratio and in the lake size can also play a major role. This must be borne in mind when interpreting the $\delta^{18}O_{diatom}$ results. Nevertheless, the long-term evolution of the diatom oxygen isotope record from the Lago Chungará laminated unit reflects long-term changes in the regional moisture balance that are related to orbital forcing (insolation) and ENSO-like conditions. Three main climate stages were identified during Late Glacial and Early Holocene:

  a) A wet phase during Late Glacial-Early Holocene transition (12,400-10,100 cal years BP)

  b) A dry phase during the Early Holocene (10,100-9,100 cal years BP)

  c) A dry-to-wet phase throughout the last years of the Early Holocene period (9,100-8,400 cal years BP)

- At decadal scales, this proxy was used as an indicator of high-frequency climate phenomena. The $\delta^{18}O_{diatom}$ analysis of the dark-green laminae present in the Late Glacial-Early Holocene transition (11,990-11,450 cal years BP) showed two major events marked by an increase in moisture conditions (11,800 and 11,550 cal years BP) and one major dry event (between 11,990 and 11,800 cal years BP). Apart from this, several minor depletions at a decadal time scale were associated with short-term events with more rainfall. These abrupt and rapid shifts in the hydrological balance of Lago Chungará may due to changes in the strength and position of the Bolivian High. Changes in the atmospheric conditions over the Altiplano at this time scale, and hence in the position of the Bolivian High were triggered by both the ENSO and solar activity. Therefore, the shift from Glacial to Interglacial conditions in the tropical latitudes of South America consisted in see-saw

moisture oscillations rather than in a progressive moisture increase, which has been reported in other low-resolution environmental reconstructions.

- The comparison of $\delta^{18}O_{diatom}$ values from the Late Glacial-Early Holocene transition with terrigenous input and water availability reconstructions (previously performed for Lago Chungará) shows a good agreement. Nevertheless, it is necessary to consider a systematic time lag of up to 50 years since the terrigenous inputs and the effective moisture availability react earlier than $\delta^{18}O_{diatom}$. This is mainly due to the time needed to change the values of $\delta^{18}O_{lakewater}$ and its subsequent incorporation into the diatom frustules. The time lag highlights the fact that the proxies do not always react at the same time to environmental forcings. This should be recognised in high resolution palaeolimnological reconstructions.

8.2 Perspectives and future work

The results obtained provide valuable insights into isotope research and into the use of lacustrine sediments in palaeonvironmental reconstructions. As the study of isotopes in biogenic silica has developed mainly in the last decade, further work is required to improve this technique and its interpretation. The Isotopes in Biogenic Silica (IBiS) group is currently developing a number of new approaches to the use of different isotopes and different organisms. These approaches include the new analyses of $\delta^{13}C_{diatom}$, $\delta^{15}N_{diatom}$ and $\delta^{30}Si_{diatom}$, which will assume greater importance in the near future. Some of these new isotopes were employed in this PhD Thesis with promising results. In addition, studies on diatom cultures would provide new opportunities to control diatom-environment relationships or even species specific comparisons.

In the present work, isotope analyses were successfully applied to the well preserved diatoms of the laminated sedimentary unit from Lago Chungará. The samples contained little organic matter and few carbonates, and the diatoms showed no signs of dissolution or diagenesis. Nevertheless, the upper sedimentary unit is made up of diatoms, organic matter and tephra clasts. This non siliceous and/or non diatomitic material hampers the direct application of $\delta^{18}O_{diatom}$ as environmental and climate proxies. The study of this upper unit would offer fresh insights into the methodology, especially in sample purification and in the effect of early-diagenesis on $\delta^{18}O_{diatom}$ signal. Local and regional palaeoclimate patterns for the period spanning from 8,400 to 1,300 cal years BP would also be obtained. This would probably include the long- and short-temporal scale evolution of local and regional moisture, the main forcings that govern it and the impact of abrupt climate phenomena, such as the ENSO.

Bibliography

Abbott MB, Seltzer GO, Kelts K, Southon J. 1997. Holocene paleohydrology of the tropical Andes from Lake Records. *Quaternary Research* **47**: 70–80.

Abbott MB, Wolfe PW, Aravena R, Wolfe AP, Seltzer GO. 2000. Holocene hydrological reconstructions from stable isotopes and paleolimnology, Cordillera Real, Bolivia. *Quaternary Science Reviews* **19**: 1801–1820.

Abbott MB, Wolfe BB, Wolfe AP, Seltzer GO, Aravena R, Mark BG, Polissar PJ, Rodwell DT, Rowe HD, Vuille M. 2003. Holocene paleohydrology and glacial history of the central Andes using multiproxy lake sediment studies. *Palaeogeography, Palaeoclimatology, Palaeoecology* **194**: 123–138.

Aceituno P. 1988. On the functioning of the Southern Oscillation in the South American sector. Part I: surface climate. *Monthly Weather Review* **116**: 505–524.

Aceituno P, Montecinos A. 1993. Circulation anomalies associated with dry and wet periods in the South American Altiplano. *Proccedings Fourth International Conference on Southern Hemisphere Meteorology*, American Meteorological Society: Hobart, Australia; 330–331.

Alldredge AL, Gotschalk C, Passow U, Riebesell U. 1995. Mass aggregation of diatom blooms: Insights from a mesocosm study. *Deep Sea Research Part II: Topical Studies in Oceanography* **42**: 9–27.

Allison GB, Barnes CJ, Hughes MW, Leaney FWJ. 1984. Effect of climate and vegetation on oxygen-18 and deuterium profiles in soils. In Isotope Hydrology. *Proccedings Symposium Vienna*: IAEA, Vienna, Austria; 105–122.

Allmendinger RW, Jordan TE. 1997. The Central Andes. In *Earth structure, An introduction to Structural Geology and Tectonics*, Van der Pluijm VA, Marshak S. (Eds.). WCB/McGraw-Hill: 430–434.

Allmendinger RW, Jordan TE, Kay SM, Isacks BL. 1997. Evolution of the Puna- Altiplano Plateau of the central Andes. *Annual Review of Earth and Planetary Sciences* **25**: 139–74.

Amilibia A. 2002. Inversion tectónica en la Cordillera de Domeyko, Andes del Norte de Chile. *PhD Thesis*, Universitat de Barcelona: Barcelona.

Amilibia A, Sàbat F, McClay KR, Muñoz JA, Roca E, Chong G. 2008. The role of inherited tectono-sedimentary architecture in the development of the central Andean mountain belt: Insights from the Cordillera de Domeyko. *Journal of Structural Geology* **30**: 1520–1539.

Anderson NJ. 2000. Diatoms, temperature and climatic change. *European Journal of Phycology* **35**: 307–314.

Anderson RY, Dean WE. 1988. Lacustrine varve formation through time. *Palaeogeography, Palaeoclimatology, Palaeoecology* **62**: 215–135.

Antico PL. 2009. Relationships between autumn precipitation anomalies in southeastern South America and El Nino event classification. *International Journal of Climatology* **29**: 719–727.

Aravena R, Suzuki O, Peña H, Pollastri A, Fuenzalida H, Grilli A. 1999. Isotopic composition and origin of the precipitation in northern Chile. *Applied Geochemistry* **14**: 411–422.

Argollo J, Mourguiart P. 2000. Late Quaternary climate history of the Bolivian Altiplano. *Quaternary International* **72**: 37–51.

Armbrust EV. 2009. The life of diatoms in the world's oceans. *Nature* **459**: 185–192.

Ashley GM, Moritz LE. 1979. Determination of lacustrine sedimentation rates by radioactive fallout (^{137}Cs), Pitt Lake, British Columbia. *Canadian Journal of Earth Science* **16**: 965–970.

Baker P. 2002. Trans-Atlantic climate connections. *Science* **296**: 67–68.

Baker PA, Seltzer GO, Fritz SC, Dunbar RB, Grove MJ, Tapia PM, Cross, SL, Rowe HD, Broda JP. 2001a. The history of South American tropical precipitation for the past 25,000 years. *Science* **291**: 640–643.

Baker PA, Rigsby CA, Seltzer GO, Fritz SC, Lowenstein TK, Bacher NP, Veliz C. 2001b. Tropical climate changes at millennial and orbital timescales on the Bolivian Altiplano. *Nature* **409**: 698–701.

Bao R, Saez A, Servant-Vildary S, Cabrera L. 1999. Lake-level and salinity reconstruction from diatom analysis in Quillagua Formation (Late Neogene, Central Andean Forearc, Nothern Chile). *Paleogeography, Paleoclimatology, Paleoecology* **153**: 309–335.

Barichivich J, Sauchyn DJ, Lara A. 2009. Climate signals in high elevation tree-rings from the semiarid Andes of north-central Chile: responses to regional and largescale variability. *Palaeogeography, Palaeoclimatology, Palaeoecology* **281**: 320–333.

Barker PA, Street-Perrott FA, Leng MJ, Greenwood PB, Swain DL, Perrott RA, Telford RJ, Ficken KJ. 2001. A 14 ka oxygen isotope record from diatom silica in two alpine tarns on Mt Kenya. *Science* **292**: 2307–2310.

Barker P, Telford R, Gasse F, Thévenon F. 2002. Late Pleistocene and Holocene palaeohydrology of Lake Rukwa, Tanzania, inferred from diatom analysis. *Palaeogeography Palaeoclimatology Palaeoecology* **187**: 295–305.

Barker PA, Leng MJ, Gasse F, Huang Y. 2007. Century-to-millennial scale climatic variability in Lake Malawi revealed by isotope records. *Earth and Planetary Science Letters* **261**: 93–103.

Barry RG, Chorley RJ. 1992. *Atmosphere, weather and climate*. 6th ed. Publisher Routledge: London.

Battarbee RW, Flower RJ. 1984. The inwash of catchment diatoms as a source of error in the sediment-based reconstruction of pH in an acid lake. *Limnology and Oceanography* **29**: 1325–1329.

Battarbee RW, Carvalho L, Jones VJ, Flower RJ, Cameron NG, Bennion H, Juggins S. 2001. Diatoms. In *Tracking Environmental Change Using Lake Sediments,Terrestrial, Algal, and Siliceous Indicators*, vol. 3. Last WM, Smol JP. (Eds.). Kluwer Academic Publishers: Dordrecht, The Netherlands; 155–202.

Bedard C, Knowles R. 1991. Hypolimnetic O_2 consumption, denitrification, and methanogenesis in a thermally stratified lake. *Canadian Journal of Fisheries and Aquatic Sciences* **48**: 1048–1054.

Berger A, Loutre MF. 1991. Insolation values for the climate of the last 19 million years. *Quaternary Science Reviews* **10**: 297–317.

Berger WH, Killingley JS, Vincent E. 1978. Stable isotopes in deep-sea carbonates. *Oceanologica Acta* **1**: 203–316.

Berner EK, Berner RA. 1987. *The Global Water Cycle: Geochemistry and Environment*. Prentice-Hall, Inc.: Englewood Cliffs, NJ; 142–155.

Betancourt JL, Latorre C, Rech JA, Quade J, Rylander KA. 2000. A 22,000-year record of monsoonal precipitation from northern Chile's Atacama desert. *Science* **289**: 1542–1546.

Bigeleisen J, Mayer MG. 1947. Calculation of equilibrium constants for isotopic exchange reactions. *Journal of Chemical Physics* **15**: 261–267.

Bigeleisen J, Wolfsberg M. 1958. Theoretical and experimental aspects of isotope effects in chemical kinetics. *Advances in Chemical Physics* **1**: 15–76.

Bird BW, Abbott MB, Kutchko B, Finney BP. 2009. A 2000-year Varve-Based Climate Record from the Central Brooks Range, Alaska. *Journal of Paleolimnology* **41**: 25–41.

Birks HJB, Line JM, Juggins S, Stevenson AC, Ter Braak CJF. 1990. Diatoms and pH reconstruction. *Philosophical Transactions of the Royal Society of London*, Series B.

Bootsma HA, Hecky RE, Johnson TC, Kling HJ, Mwita J. 2003. Inputs, outputs, and internal cycling of silica in a large, tropical lake. *Journal of Great Lakes Research* **29**: 121– 138.

Bos DG, Cumming BF, Smol JP. 1999. Cladocera and Anostraca from the interior plateau of British Columbia, Canada, as paleolimnological indicators of salinity and lake level. *Hydrobiologia* **392**: 129–141.

Boschker HTS, Middelburg JJ. 2002. Stable isotopes and biomarkers in microbial ecology. *Fems Microbiology Ecology* **40**: 85–95.

Bradbury P, Cumming B, Laird K. 2002. A 1500-year record of climatic and environmental change in Elk Lake, Minnesota III: measures of past primary productivity. *Journal of Paleolimnology* **27**: 321–40.

Bradley R, Vuille M, Hardy DR, Thompson LG. 2003. Low latitude ice cores record Pacific sea surface temperatures. *Geophysical Research Letters* **30**: 1174.

Brandriss ME, O'Neil JR, Edlund MB, Stoermer EF. 1998. Oxygen isotope fractionation between diatomaceous silica and water. *Geochimica et Cosmochimica Acta* **62**: 1119–1125.

Brauer A, Endres C, Gu¨nter C, Litt T, Stebich M, Negendank JFW. 1999. High resolution sediment and vegetation responses to Younger Dryas climate change in varved lake sediments from Meerfelder Maar, Germany. *Quaternary Science Reviews* **18**: 321–329.

Brenner M, Whitmore TJ, Lasi MA, Cable JE, Cable PH. 1999. Stable isotope $\delta^{13}C$, $\delta^{15}N$ signatures of sedimented organic matter as indicators of historical lake trophic state. *Journal of Paleolimnology* **22**: 205–221.

Brewer TS, Leng MJ, Mackay AW, Lamb AL, Tyler JJ, Marsh NG. 2008. Unravelling contamination signals in biogenic silica oxygen isotope composition: the role of major and trace element geochemistry. *Journal of Quaternary Science* **23**: 321–330.

Brönmark C, Hansson LA. 2005. *The Biology of Lakes and Ponds*. Oxford University Press: Oxford.

Cabrera L, Gierlowski-Kordesch EH, Alonso-Zarza AM, Arenas-Abad C. 2009. Limnogeology: Ancient and modern tales of an evolving Earth. *Sedimentary geology* **222**: 1–2.

Cane MA. 2005. The evolution of El Niño, past and future. *Earth and Planetary Science Letters* **230**: 227–240.

Carrera N. 2009. Inversió tectònica i evolució estructural de la Cordillera Oriental Meridional (Valls Calchaquís, NW d'Argentina). *PhD Thesis*, Universitat de Barcelona: Barcelona.

Catalan J, Fee EJ. 1994. Interannual variability in limnic ecosystems: origin, patterns and predictability. In *Limnology Now: A Paradigm of Planetary Problems*. Margalef R. (Ed.). Elsevier: Armsterdam, The Netherlands; 81–97.

Catalan J, Pla S, Garcia J, Camarero L. 2009. Climate and CO_2 saturation in an alpine lake throughout the Holocene. *Limnology and Oceanography* **54**: 2542–2552.

Chacko T, Cole DR, Horita J. 2001. Equilibrium oxygen, hydrogen, and carbon isotope fractionation factors applicable to geologic systems. In Stable Isotope Geochemistry, Valley JW, Cole DR. (Eds.). *Reviews in Mineralogy and Geochemistry* **43**: Mineralogical Society of America, Washington, D.C.; 1–81.

Chalié F, Gasse F. 2002. Late-Glacial–Holocene diatom record of water chemistry and lake-level change from the tropical East African Rift Lake Abiyata (Ethiopa). *Palaeogeography, Palaeoclimatology, Palaeoecology* **187**: 259–283.

Chang AS, Patterson RT, McNeely R. 2003. Seasonal sediment and diatom record from late Holocene laminated sediments, Effingham Inlet, British Columbia, Canada. *Palaios* **18**: 477–494.

Chepurnov VA, Mann DG, Sabbe K, Vyverman W. 2004. Experimental studies on sexual reproduction in diatoms. *International Review of Cytology* **237**: 91–154.

Chiang JCH. 2009. The tropics in Paleoclimate. *Annual Review in Earth and Planetary Sciences* **37**: 263–297.

Chikita K, Joshi SP, Jha J, Hasegawa H. 2000. Hydrological and thermal regimes in a supraglacial lake: Imja, Khumbu, Nepal Himalaya. *Hydrological Sciences Journal* **45**: 507–521.

Chu G, Liu J, Schettler G, Li J, Sun Q, Gu Z, Lu H, Liu Q, Liu T. 2005. Sediment fluxes and varve formation in Sihailongwan, a maar lake from northeastern China. *Journal of Paleolimnology* **34**: 311–324.

Clapperton CM. 1997. Late Quaternary glacier advances and paleolake high-stands in Bolivian Altiplano. *Quaternary International* **34**: 39–49.

Clark I, Fritz P. 1997. *Environmental isotopes in Hydrogeology*. Lewis Publishers: New York.

Clavero JE, Sparks SJ, Huppert HE. 2002. Geological constraints on the emplacement mechanism of the Parinacota debris avalanche, northern Chile. B*ulletin of Volcanology* **64**: 40–54.

Clavero JE, Sparks SJ, Polanco E, Pringle M. 2004. Evolution of Parinacota volcano, Central Andes, northern Chile. *Revista Geológica Chile* **31**: 317–347.

Clayton RN, Mayeda TK. 1963. The use of bromine pentafluoride in the extraction of oxygen from oxide and silicates for isotope analysis. *Geochimica et Cosmochimica Acta* **27**: 43–52.

Clement AC, Cane MA, Seager R. 2001. An orbitally driven tropical source for abrupt climate change. *Journal of Climate* **14**: 2369–2375.

Cohen AS. 1990. Tectono-stratigraphic model for sedimentation in Lake Tanganyika, Africa. In Lacustrine Basin Exploration-Case Studies and Modern Analogs, Katz BJ. (Ed.). *American Association of Petroleum Geologists* **50**: 137–150.

Cohen AS. 2003. *Paleolimnology: the history and evolution of lake systems*. Oxford University Press: New York.

Coira B, Davidson J, Mpodozis C, Ramos V. 1982. Tectonic and magmatic evolution of the Andes of Northern Argentina and Chile. *Earth-Science Reviews* **18**: 303-332.

Cole JE, Rind D, Webb RS, Jouzel J, Healy R. 1999. Climatic controls on interannual variability of precipitation delta O-18: simulated influence of temperature, precipitation amount, and vapor source region. *Journal of Geophysical Research—Atmospheres* **104**: 14223–14235.

Cole JJ, Caraco NF, Kling GW, Kratz TK. 1994. Carbon-dioxide supersaturation in the surface waters of lakes. *Science* **265**: 1568–1570.

Cole JJ, Carpenter SR, Kitchell JF, Pace ML. 2002. Pathways of organic carbon utilization in small lakes: Results from a whole-lake ^{13}C addition and coupled model. *Limnology and Oceanography* **47**: 1664–1675.

Cole JJ, Prairie Y T, Caraco NF, McDowell WH, Tranvik LJ, Striegl RG, Duarte CM, Kortelainen P, Downing JA, Middelburg JJ, Melack J. 2007. Plumbing the global carbon cycle: Integrating inland waters into the terrestrial carbon budget. *Ecosystems* **10**: 171–184.

Colman SM, Peck JA, Karabanov EB, Carter SJ, Bradbury JP, King JW, Williams DF. 1995. Continental climate response to orbital forcing from biogenic silica records in Lake Baikal. *Nature* **378**: 769–771.

Conley DJ, Kilham SS, Theriot E. 1989. Differences in silica content between marine and freshwater diatoms. *Limnology and Oceanography* **34**: 205–213.

Conley DJ, Schelske CL. 2001. Biogenic silica. In *Tracking Environmental Change Using Lake Sediments: Biological Methods and Indicators*, Smol J P, Birks HJB, Last WM. (Eds.). Kluwer Academic Press: 281-293.

Coutand I, Cobbold PR, de Urreiztieta M, Gautier P, Chauvin A, Gapais D, Rossello E, Lopez- Gamundi O. 2001. Style and history of Andean deformation, Puna plateau, northwestern Argentina. *Tectonics* **20**: 210–234.

Crawford SA, Higgins MJ, Mulvaney P, Wetherbee R. 2001. Nanostructure of the diatom frustule as revealed by atomic force and scanning electron microscopy. *Journal of Phycology* **37**: 543–554.

Criss RE. 1999. *Principles of Stable Isotope Distribution*. Oxford University Press: Oxford.

Cross SL, Baker PA, Seltzer GO, Fritz SC, Dunbar RB. 2001. Late Quaternary climate and hydrology of tropical South America inferred from an isotopic and chemical model of lake Titicaca, Bolivia and Peru. *Quaternary Research* **56**: 1–9.

Crosta X, Koç N. 2007. Diatoms:frommicropaleontologytoisotope geochemistry. In *Proxies in Late Cenozoic Paleoceanography, Developments in Marine Geology Series*, Vol.1. Hilaire-Marcel C, de Vernal A. (Eds.). Elsevier: Amsterdam, The Netherlands; 327–369.

Crosta X, Shemesh A. 2002. Reconciling down core anticorrelation of diatom carbon and nitrogen isotopic ratios from the Southern Ocean. *Paleoceanography* **17**: 1010.

Damnati B, Taieb M, Williamson D. 1992. Laminated deposits from Lake Magadi (Kenya); climatic contrast effect during the maximum wet period between 12,000-10,000 yrs BP. *Bulletin de la Societe Geologique de France* **163**: 407–414.

Dansgaard W. 1964. Stable isotopes in precipitation. *Tellus* **16**: 436–468.

Darling WG, Bath A, Gibson JJ, Rozanski K. 2005. Isotopes in water. In *Isotopes in Palaeoenvironmental Research*, Leng MJ (ed.). Springer: Dordrecht, Netherlands;1–66.

Davison W. 1993. Iron and manganese in lakes. *Earth-Science Reviews* **34**: 119–163.

Dean WE, Gorham E. 1998. Magnitude and significance of carbon burial in lakes, reservoirs, and peatlands. *Geology* **26**: 535–538.

De Batist M, Imbo Y, Vermeesch P, Klerkx J, Giralt S, Delvaux D, Lignier V, Beck C, Kalugin I, Abdrakhmatov KE. 2002. Bathymetry and sedimentary environments of Lake Issyk-Kul, Kyrgyz Republic (Central Asia): a large, high altitude, tectonic lake. In *Lake Issyk-Kul: Its Natural Environment*, Klerkx J, Imanackunov B. (eds.). NATO Science Series, IV. Earth and Environmental Sciences, Vol. 13. Kluwmer Academic Publisher: Dordrecht; 101–123.

De la Rocha CL. 2002. Measurement of silicon stable isotope natural abundances via multicollector inductively coupled plasma mass spectrometry (MC-ICP-MS). *Geochemistry Geophysics Geosystems* **3**: 1–8.

Des Combes HJ, Esper O, De la Rocha CL, Abelmann A, Gersonde R, Yam R, Shemesh A. 2008. Diatom $\delta^{13}C$, $\delta^{15}N$, and C/N since the Last Glacial Maximum in the Southern Ocean: Potential impact of species composition. *Paleoceanography* **23**: PA4209.

De Silva S, Francis P. 1991. *Volcanoes of the Central Andes*. Springer-Verlag: Berlin.

Devevey E, Bitton G, Rossel D, Ramos LD, Guerrero LM, Tarradellas J. 1993. Concentration and bioavailability of heavy-metals in Lake Yojoa (Honduras). *Bulletin of Environmental Contamination and Toxicology* **50**: 253–259.

Dewey JF, Bird JM. 1970. Mountain belts and the new global tectonics. *Journal of Geophysical Research* **75**: 2625–2647.

Diaz HF, Markgraf V. 1992. *El Niño*. Cambridge University Press, Cambridge.

Dincer T, Al-Mugrin A, Zimmermann U. 1974. Study of the infiltration and recharge through sand dunes in arid zones with special reference to the stable isotopes and thermonuclear tritium. *Journal of Hydrology* **23**: 79–87.

Dinsmore WP, Scrimgeour GJ, Prepas EE. 1999. Empirical relationships between profundal macroinvertebrate biomass and environmental variables in boreal lakes of Alberta, Canada. *Freshwater Biology* **41**: 91–100.

Dorador C, Pardo R, Vila I. 2003. Variaciones temporales de parámetros físicos, químicos y biológicos de un lago de altura: el caso del Lago Chungará. *Revista Chilena de Historia Natural* **76**: 15–22.

Drucker DG, Bocherens H, Billiou D. 2003. Evidence of shifting environmental conditions in southwestern France from 33,000 to 15,000 years ago derived from carbon-13 and nitrogen-15 natural abundances in collagen of large herbivores. *Earth and Planetary Science Letters* **216**: 163–173.

Duarte CM, Prairie YT. 2005. Prevalence of heterotrophy and atmospheric CO_2 emissions from aquatic ecosystems. *Ecosystems* **8**: 862–870.
Durand A. 1982. Oscillations of Lake Chad over the past 50,000 years: new data and new hypothesis. *Palaeogeography, Palaeoclimatology, Palaeoecology* **39**: 37–53.
Dussart B. 1961. Proprietes utiles de certains sediments lacustres. *Comptes rendus hebdomadaires des seances de l'academie des sciences* **252**: 2581.
Earle LR, Warner BG, Aravena R. 2003. Rapid development of an unusual peat-accumulating ecosystem in the Chilean Altiplano. *Quaternary Research* **59**: 2–11.
Edgar LA, Pickett-Heaps JD. 1984. Diatom Locomotion. In *Progress in Phycological Research*. Round FE, Chapman DJ. (Eds.). Biopress Ltd: Bristol; 47–88.
Emiliani C. 1955. Pleistocene Temperatures. *Journal of Geology* **63**: 538–78.
Emiliani C. 1991. Planktic/Planktonic, Nektic/Nektonic, Benthic/Benthonic. *Journal of Paleontology* **65**: 329.
Encyclopedia Britannica. 1962. William Benton: London, 23 vols.
Eronen M, Zetterberg P, Briffa KR, Lindholm M, Meriläinen J, Timonen M. 2002. The supra-long Scots pine tree-ring record for Finnish Lapland: Part 1, chronology construction and initial inferences. *The Holocene* **12**: 673–680.
Eugster HP, Hardie LA. 1978. Saline lakes. In *Lakes: Chemistry, Geology. Physics*, Lerman A (Ed.). Springer-Verlag: New York; 237–293.
Falkowski, P. G., Katz, M. E., Knoll, A. H., Quigg, A., Raven, J. A., Schofield, O. and Taylor, F. J. R. 2004. The Evolution of Modern Eukaryotic Phytoplankton. *Science* **305**: 354-360.
Falvey M, Garreaud R. 2005. Moisture variability over the South American Altiplano during the SALLJEX observing season. *Journal Geophysical Research* **110**: D22105.
Field CB, Behrenfeld MJ, Randerson JT, Falkowski P. 1998. Primary production of the biosphere: integrating terrestrial and oceanic components. *Science* **281**: 237–240.
Filippi ML, Lambert P, Hunziker J, Kübler B, Bernasconi S. 1999. Climatic and anthropogenic influence on the stable isotope record from bulk carbonates and ostracodes in Lake Neuchâtel, Switzerland, during the last two millennia. *Journal of Paleolimnology* **21**: 19–34.
Fogel ML, Cifuentes LA. 1993. Isotope fractionation during primary production. In *Organic Geochemistry*, Engel MH, Macko SA. (Eds.). Plenum Press: New York; 73–98.
Francus P, Bradley RS, Lewis T, Abbott M, Retelle M, Stoner JS. 2008, Limnological and sedimentary processes at Sawtooth Lake, Canadian High Arctic, and their influence on varve formation. *Journal of Paleolimnology* **40**: 963–985.
Fritz P, Fontes JCh. 1986. *Handbook of Environmental Isotope Geochemistry*, Vol 2. Elsevier: Amsterdam.
Fritz SC. 2008. Deciphering climatic history from lake sediments. *Journal of Paleolimnology* **39**: 5–16.
Fritz SC, Junggins F, Battarbee RW, Engstrom DR. 1991. Reconstruction of past changes in salinity and climate using a diatom-based transfer function. *Nature* **352**: 706–708.
Fritz SC, Cumming BF, Gasse F, Laird KR. 1999. Diatoms as indicators of hydrologic and climatic change in saline lakes. In *The Diatoms: Applications for the Environmental and Earth Sciences*, Stoermer EF, Smol JP. (Eds.). Cambridge University Press: Cambridge; 41–72.
Fritz SC, Baker PA, Lowenstein T K, Seltzer GO, Rigsby CA, Dwyer GS, Tapia PM, Arnold KK, Ku TL, Luo S. 2004. Hydrologic variation during the last 170,000 years in the southern hemisphere tropics of South America. *Quaternary Research* **61**: 95–104.
Fritz SC, Baker PA, Tapia P, Garland J. 2006. Spatial and temporal variation in cores from Lake Titicaca, Bolivia/Peru during the last 13 000 years. *Quaternary International* **158**: 23–29.
Fry B. 1996. $^{13}C/^{12}C$ fractionation by marine diatoms. Marine Ecology-Progress Series 134: 283–294.
Garreaud RD, Battisti DS. 1999. Interannual (ENSO) and interdecadal (ENSO-like) variability inthe Southern Hemisphere tropospheric circulation. *Journal of Climate* **2**: 2113–2123.
Garreaud RD, Vuille M, Clement AC. 2003. The climate of the Altiplano: observed current conditions and mechanisms of past changes. *Palaeogeography, Palaeoclimatology, Palaeoecology* **194**: 5–22.
Garreaud R, Vuille M, Compagnucci R, Marengo J. 2009. Present-day South American climate. *Palaeogeography, Palaeoclimatology, Palaeoecology* **281**: 180–195.
Gasse F. 2000. Hydrological changes in the African tropics since the Last Glacial Maximum. *Quaternary Science Reviews* **19**: 189–211.
Gasse F, Fontes JC. 1992. *Climatic changes in northwest Africa during the last deglaciation (16–7 ka BP)*. NATO ASI Series 12: Kluwer, Dordrecht; 295–325.
Gasse F, Barker P, Gell PA, Fritz SC, Chalié F. 1997. Diatom-inferred salinity in paleolakes: an indirect tracer of climate change. *Quaternary Science Reviews* **16**: 547–563.
Gat JR. 1980. Isotope hydrology of very saline lakes. In *Hypersaline brines and evaporitic environments*, Nissenbaum A. (Ed.). Elsevier: Amsterdam; 1–8.
Gat JR. 1996. Oxygen and hydrogen isotopes in the hydrologic cycle. *Annual Review of Earth and Planetary Sciences* **24**: 225–262.
Gaupp R, Kött A, Wörner G. 1999. Palaeoclimatic implications of Mio-Pliocene sedimentation in the highaltitude intra-arc Lauca Basin of northern Chile. In *Ancient and Recent Lacustrine Systems in Convergent Margins*, Cabrera L, Sáez A. (Eds.) *Paleogeography, Paleoclimatology, Paleoecology* **151**: 79–100.
Gervais F, Riebesell U. (2001) Effect of phosphorus limitation on elemental composition and stable carbon isotope fractionation in a marine diatom growing under different CO_2 concentrations. Limnology and Oceanography 46: 497–504.
Geyh MA, Grosjean M. 2000. Establishing a reliable chronology of lake level changes in the Chilean Altiplano: a result of close collaboration between geochronologists and geomorphologists. Zentralblatt für Geologie und Paläontologie: Teil I 7/8; 985–995.
Geyh MA, Schotterer U, Grosjean M. 1998. Temporal changes of the ^{14}C reservoir effect in lakes. Radiocarbon 40: 921–931.
Geyh MA, Grosjean M, Núñez L, Schotterer U. 1999. Radiocarbon reservoir effect and the timing of the Late-Glacial/early Holocene Humid phase in the Atacama desert (Northern Chile). *Quaternary Research* **52**: 143–153.

Giddings JC. 1985. A system based on split-flow lateral-transport thin (SPLITT) separation cells for rapid and continuous particle fractionation. *Separation Science and Technology* **20**: 749–768.

Gierlowski-Kordesch EH. 2010. Lacustrine carbonates. In *Carbonates in Continental Settings: Processes, Facies, and Application, Developments in Sedimentology* **61**. Alonso-Zarza AM, Tanner LH. (Eds.). Elsevier, Amsterdam; 1–101.

Giralt S, Burjachs F, Roca JR, Julià R. 1999. Late glacial to early Holocene environmental adjustment in the Mediterranean semi-arid zone of the Salines playa-lake (Alicante, Spain). *Journal of Paleolimnology* **21**: 449–460.

Giralt S, Moreno A, Bao R, Sáez A, Prego R, Valero BL, Pueyo JJ, González-Sampériz P, Taberner C. 2008. Statistical approach to disentangle environmental forcings in a lacustrine record: the Lago Chungará case (Chilean Altiplano). *Journal of Palaeolimnology* **40**: 195–215.

Goslar T, van der Knaap WO, Hicks S, Andric M, Czernik J, Goslar E, Räsänen S, Hyötylä H. 2005. Radiocarbon dating of modern peat profiles: pre- and post-bomb ^{14}C variations in the construction of age–depth models. *Radiocarbon* **47**: 115–134.

Gosling WD, Bush MB, Hanselman JA, Chepstow-Lusty A. 2008. Glacial–Interglacial changes in moisture balance and the impact on vegetation in the southern hemisphere tropical Andes (Bolivia/Peru). *Palaeogeography Palaeoclimatology Palaeoecology* **259**: 35–50.

Gregory-Wodzicki KM. 2000. Uplift history of the Central and Northern Andes: a review. *Geological Survey of America Bulletin* **112**: 1091–1105.

Grimm KA, Lange CB, Gill AS. 1996. Biological forcing of hemipelagic sedimentary laminae: evidence from ODP site 893, Santa Barbara Basin, California. *Journal of Sedimentary Research* **66**: 613–624.

Grimm KA, Lange CB, Gill AS. 1997. Self-sedimentation of phytoplankton blooms in the geologic record. *Sedimentary Geology* **110**: 151–161.

Grosjean M, Geyh MA, Messerli B, Schotterer U. 1995. Late-glacial and early Holocene lake sediments, groundwater formation and climate in the Atacama Altiplano 22-24°S. *Journal of Paleolimnology* **14**: 241–252.

Grosjean M, Núñez L, Cartajena I, Messerli B. 1997. Mid-Holocene climate and culture change in the Atacama Desert, northern Chile. *Quaternary Research* **48**: 239–246.

Grosjean M, van Leeuwen JFN, van der Knaap WO, Geyh MA, Ammann B, Tanner W, Messerli B, Núñez L, Valero-Garcés BL, Veit H. 2001. A 22,000 ^{14}C year BP sediment and pollen record of climate change from Laguna Miscanti (23°S), northern Chile. *Global and Planetary Change* **28**: 35–51.

Grosjean M, Cartajena I, Geyh MA, Núñez L. 2003. From proxy data to paleoclimate interpretation: the mid-Holocene paradox of the Atacama Desert, northern Chile. *Palaeogeography, Palaeoclimatology, Palaeoecology* **194**: 247–258.

Grosjean M, Santoro CM, Thompson LG, Núñez L, Standen VG. 2007. Mid-Holocene climate and cultural change in the South-Central Andes. In *Climate Change and Cultural Dynamics: A Global Perspective on Holocene Transitions*, Anderson G, Sandweiss DF, Maasch KA. (eds.). Academic Press: San Diego, CA; 51–115.

Grottoli A, Eakin CM. 2007. A review of modern coral $\delta^{18}O$ and $\delta^{14}C$ proxy records. *Earth-Science Reviews* **81**: 67–91.

Gu B, Schelske GL, Brenner M. 1996. Relationship between sediment and plankton isotope ratios ($\delta^{13}C$ and $\delta^{15}N$) and primary productivity in Florida lakes. *Canadian Journal of Fisheries and Aquatic Sciences* **53**: 875–883.

Guillard RRL, Kilham P. 1977. The ecology of marine planktonic diatoms. In *The Biology of Diatoms*. Werner D. (ed.). Oxford: Blackwell Scientific Publications; 372–469.

Gustavson TC. 1975. Bathymetry and sediment distribution in proglacial Malaspina Lake, Alaska. *Journal of Sedimentary Petrology* **45**: 450–461.

Haimson M, Knauth LP. 1983. Stepwise fluorination – a useful approach for the isotopic analysis of hydrous minerals. *Geochimica et Cosmochimica Acta* **47**: 1589–1595.

Hall RI, Smol JP. 1999. Diatoms as indicators of lake eutrophication. In *The Diatoms: Applications for the Environmental and Earth Sciences*, Stoermer EF, Smol JP. (Eds.). Cambridge University Press: Cambridge; 128–168.

Hamilton-Taylor J, Davison W. 1995. Redox-driven cycling of trace elements in lakes. In *Physics and Chemistry of Lakes*, Lerman A, Imboden D, Gat J. (Eds.). Springer-Verlag: 217–263.

Hamilton-Taylor J, Smith EJ, Davison W, Sugiyama M. 2005. Resolving and modeling the effects of Fe and Mn redox cycling on trace metal behaviour in a seasonally anoxic lake. *Geochimica et Cosmochimica Acta* **69**: 1947–1960.

Harris GP. 1986. *Phytoplankton Ecology*. Chapman and Hall: London.

Hecky RE, Mopper K, Kilham P, Degens ET. 1973. Amino-acid and sugar composition of diatom cell-walls. *Marine Biology* **19**: 323–331.

Heegaard E, Birks HJB, Telford RJ. 2005. Relationships between calibrated ages and depth in stratigraphical sequences: an estimation procedure by mixed-effect regression. *The Holocene* **15**: 612–618.

Heine K. 2000. Tropical South America during the Last Glacial Maximum: evidence from glacial, periglacial and fluvial records. *Quaternary International* **72**: 7–21.

Hernández A, Bao R, Giralt S, Leng MJ, Barker PA, Pueyo JJ, Sáez A, Moreno A, Valero-Garcés B, Sloane HJ. 2007. A high-resolution study of diatom oxygen isotopes in a Late Pleistocene to early Holocene laminated record from Lake Chungará (Andean Altiplano, Northern Chile). *Geochimica et Cosmochimica Acta* **71**: A398.

Hernández A, Bao R, Giralt S, Leng MJ, Barker PA, Sáez A, Pueyo JJ, Moreno A, Valero-Garcés BL, Sloane HJ. 2008. The palaeohydrological evolution of Lago Chungará (Andean Altiplano, northern Chile) during the Lateglacial and early Holocene using oxygen isotopes in diatom silica. *Journal of Quaternary Science* **23**: 351–363.

Hernández A, Giralt S, Bao R, Leng MJ, Barker PA. In press. ENSO and solar activity signals from oxygen isotopes in diatom silica during late glacial-Holocene transition in Central Andes (18°S). *Journal of Paleolimnology*.

Hernández A, Bao R, Giralt S, Barker PA, Leng MJ, Sloane HJ, Sáez A. Submitted. Biogeochemical processes controlling oxygen and carbon isotopes of diatom silica in lacustrine rhythmites. *Palaeogeography, Palaeoclimatology, Palaeoecology*.

Herrera C, Pueyo JJ, Sáez A, Valero-Garcés BL. 2006. Relación de aguas superficiales y subterráneas en el área del lago Chungará y lagunas de Cotacotani, norte de Chile: un estudio isotópico. *Revista Geológica de Chile* **33**: 299–325.

Hill WR. 1996. Effects of light. In *Algal Ecology: Freshwater Benthic Ecosystems*, Stevenson RJ, Bothwell ML, Lowe RL. (Eds.). Academic Press: New York; 122–149.

Hill KJ, Taschetto AS, England MH. 2009. South American rainfall impacts associated with inter-El Niño variations. *Geophysical Research Letters* **36**: L19702.
Hillyer R, Bush M, Valencia BG, Steinitz-Kannan M, Silman MR. 2009. A 24,000-year paleolimnological history from the Peruvian Andes. *Quaternary Research* **71**: 71–82.
Hodell DA, Schelske CL, Fahnenstill GL, Robbings LL. 1998. Biologically-induced calcite and its isotopic composition in Lake Ontario. *Limnology and Oceanography* **43**: 187–199.
Hoefs J. 2004. Stable isotope geochemistry. 5th edition. Springer: Berlin Heidelberg.
Hollander DJ, MacKenzie JA. 1991. CO_2 control on carbon-isotope fractionation during aqueous photosynthesis: A paleo-pCO_2 barometer. *Geology* **19**: 929–932.
Hora J, Singer B, Wörner G. 2007. Volcan eruption and evaporative flux on the thick curst of the Andean Central Volcanic Zone: $^{40}Ar/^{39}Ar$ constrains from Volcán Parinacota, Chile. *Geological Survey of America Bulletin* **119**: 343–362.
Horne AJ, Goldman CR. 1994. *Limnology*, Second Edition. McGraw-Hill: New York, NY.
Houser JN, Bade DL, Cole JJ, Pace ML. 2003. The dual influences of dissolved organic carbon on hypolimnetic metabolism: organic substrate and photosynthetic reduction. *Biogeochemistry* **64**: 247–269.
Hu FS, Shemesh A. 2003. A biogenic-silica $\delta^{18}O$ record of climatic change during the last glacial–interglacial transition in southwestern Alaska. *Quaternary Research* **59**: 379–385.
Hua Q, Barbetti M. 2004. Review of tropospheric bomb C-14 data for carbon cycle modeling and age calibration purposes. *Radiocarbon* **46**: 1273–1298.
Huc AY, Le Fournier J, Vandenbroucke M, Bessereau G. 1990. Northern Lake Tanganyika: an example of organic sedimentation in an anoxic rift lake. In Lacustrine basin exploration. Case studies and modern analogs. A*merican Association of Petroleum Geologists* **50**: 169–185.
Hurrell ER. 2009. Climate change and biogeochemical cycles on East African mountains by stable isotopes of diatom frustules. *PhD Thesis*. Lancaster Environment Center, Lancaster University: Lancaster.
Hurrell ER, Barker PA, Leng MJ, Vane CH, Wynn P, Kendrick CP, Verschuren D, Street-Perrott FA. Submitted. Developing a methodology for carbon isotope analysis of lacustrine diatoms. *Journal of Palaeolimnology*.
Hutchinson GE. 1969. Eutrophication, past and present. In *Eutrophication: Causes, Consequences, Correctives*. National Academy of Sciences: Washington DC; 17–26.
Hutchinson GE, Loffler J. 1956. The thermal classification of lakes. *Proceedings of the National Academy of Sciences* **42**: 84–86.
Imboden DM, Wüest A. 1995. Mixing mechanisms in lakes. In *Physics and chemistry of lakes*, Lerman A, Imboden D, Gat J (Eds.). Springer-Verlag: Berlin; 83–138.
Isacks BL. 1988. Uplift of the central Andean plateau and bending of the Bolivian orocline. *Journal of Geophysical Research* **93**: 3211–3231.
Ishihara S, Kato M, Tanimura Y, Fukusawa H. 2003. Varved lacustrine sediments and diatom assemblages of Lake Fukami, central Japan. *Quaternary International* **105**: 21–24.
Ito E. 2001. Application of stable isotope techniques to inorganic and biogenic carbonates. In *Tracking Environmental Change Using Lake Sediments*, *Physical and Geochemical Techniques*, vol. 2. Last WM, Smol JP. (Eds.). Kluwer Academic Publishers: Dordrecht, The Netherlands; 351–371.
Jacque JMS, Cumming BF, Smol JP. 2009. A 900-yr diatom and chrysophyte record of spring mixing and summer stratification from varved Lake Mina, west-central Minnesota, USA. *The Holocene* **19**: 537–547.
James DE. 1971. Plate-tectonic model for the evolution of the central Andes. *Geological Society of America Bulletin* **82**: 3325–3346
Johnson RK, Weiderholm T. 1989. Classification and ordination of profundal macroinvertebrate communities in nutrient poor, oligo-mesohumic lakes in relation to environmental data. *Freshwater Biology* **21**: 375–386.
Johnston AM, Raven JA, Beardall J, Leegood RC. 2001. Carbon fixation-photosynthesis in a marine diatom. *Nature* **412**: 40–41.
Jones V. 2007. Diatom introduction. In *Encyclopedia of Quaternary Science*, Elias SA. (ed.). Amsterdam: Elsevier, 476-484.
Jones VJ, Leng MJ, Solovieva N, Sloane HJ, Tarasov P. 2004. Holocene climate of the Kola Peninsula; evidence from the oxygen isotope record of diatom silica. *Quaternary Science Reviews* **23**: 833–839.
Jonsson A, Meili M, Bergstrom AK, Jansson M. 2001. Whole-lake mineralization of allochthonous and autochthonous organic carbon in a large humic lake (Ortrasket, N. Sweden). *Limnology and Oceanography* **46**: 1691–1700.
Jonsson C, Andersson S, Rosqvist GC, Leng MJ. 2010. Reconstructing past atmospheric circulation changes using oxygen isotopes in lake sediments from Sweden. *Climate of the Past* **6**: 49–62.
Juillet A. 1980a. *Structure de la silice biogenique: nouvelles donnes apportees par l'analyse isotopique de l'oxygene*. C.R. Academy of Science: Paris 290D; 1237–1239.
Juillet A. 1980b. *Analyse isotopique de la silice des diatomees lacustres et marines: fractionnement des isotopes de l'oxygene en fonction de la temperature*. Diss. Paris XI These de 3e cycle.
Juillet-Leclerc A. 1986. Cleaning process for diatomaceous samples. In *8th Diatom Symposium*, Ricard M (Ed.). Koeltz Scientific: Koenigstein, Germany; 733–736.
Karlsson J, Byström P, Ask J, Persson L, Jansson M. 2009. Light limitation of nutrient-poor lake ecosystems. *Nature* **460**: 506–9.
Katsui Y, González-Ferrán O. 1968. *Geología del área neovolcánica de los Nevados de Payachata*. Publicación 29: Universidad de Chile, Facultad de Ciencias Físicas y Matemáticas, Departamento de Geología, Santiago.
Kelts K, Hsü KJ. 1978. Freshwater carbonate sedimentation. In *Lakes: Chemistry, Geology*. *Physics*, Lerman A (Ed.). Springer-Verlag: New York; 294–323.
Kemp AES. 1996. *Laminated sediments as palaeo-indicators. In Palaeoclimatology and palaeoceanography from laminated sediments*. Kemp AES (Ed.). The Geological Society: London; 1–12.
Kennett J, Cannariato KG, Hendy IL, Behl RJ. 2003. M*ethane Hydrates in Quaternary Climate Change: The Clathrate Gun Hypothesis*. American Geophysical Union, Washington: DC, USA.
Kirilova E, Heiri O, Enters D, Cremer H, Lotter AF, Zolitschka B, Hübener T. 2009. Climate-induced changes in the trophic status of a Central European lake. *Journal of Limnology* **68**: 71–82.

Kitchell JF, Carpenter SR. 1993. Variability in lake ecosystems: complex responses by the apical predator. In *Human as Components of Ecosystems*, McDonnell M, Pickett S. (Eds.). Springer Verlag: New York; 111–124.
Knauth LP. 1973. Oxygen and hydrogen isotope ratios in cherts and related rocks. *PhD thesis*, California Institute of Technology.
Kociolek JP, Spaulding SA. 2000. Freshwater diatom biogeography. Nova Hedwigia 71:223–241.
Kooistra WHCF, De Stefano M, Mann DG, Medlin LK. 2003. The phylogeny of diatoms. *Progress in Molecular and Subcellular Biology* **33**: 59–97.
Kött A, Gaupp R, Wörner G. 1995. Miocene to Recent history of the western Altiplano in northern Chile revealed by lacustrine sediments of the Lauca Basin (18°15'-18°40' S/69°30'-69° 05' W). *Geologische Rundschau* **84**: 770–780.
Koutavas A, Lynch-Stieglitz J, Marchitto T, Sachs J. 2002. El Niño-like pattern in ice age tropical Pacific sea surface temperature. *Science* **297**: 226–230.
Kröger N, Poulsen N. 2008. Diatoms: from Cell Wall Biogenesis to Nanotechnology. *Annual Review of Genetics* **42**: 83–107.
Kröger N, Bergsdorf C, Sumper M. 1994. A new calcium-binding glycoprotein family constitutes a major diatom cell wall component. *EMBO Journal* **13**: 4676–4683.
Kull C, Imhof S, Grosjean M, Zech R, Veit H. 2008. Late Pleistocene glaciation in the Central Andes: temperature versus humidity control. A case study from the eastern Bolivian Andes (17°S) and regional synthesis. *Global and Planetary Change* **60**: 148–164.
Labeyrie LD. 1974. New approach to surface seawater paleotemperatures using $^{18}O/^{16}O$ ratios in silica of diatom frustules. *Nature* **248**: 40–42.
Labeyrie L. 1984. Paléoclimatologie, des squelettes d'organisme marins pour reconstruire le climat. *Echos du CEA* **2**: 8–11.
Labeyrie LD, Juillet A. 1982. Oxygen isotopic exchangeability of diatom valve silica; interpretation and consequences for palaeoclimatic studies. *Geochimica et Cosmochimica Acta* **46**: 967–975.
Lamb AL, Leng MJ, Lamb HF, Mohammed MU. 2000. A 9000-year oxygen and carbon isotope record of hydrological change in a small Ethiopian crater lake. *The Holocene* **10**: 167–177.
Lamb AL, Leng MJ, Sloane HJ, Telford RJ. 2005. A comparison of $\delta^{18}O$ data from calcite and diatom silica from early Holocene in a small crater lake in the tropics. *Palaeogeography, Palaeoclimatology, Palaeoecology* **223**: 290–302.
Lambert A, Giovanoli F. 1988. Records of riverborne turbidity currents and indications of slope failures in the Rhone and Lake Geneva. *Limnology and Oceanography* **33**: 458–468.
Lau KM, Weng H. 1995. Climate signal detection using wavelet transform: how to make a time series sing. *Bulletin of the American Meteorological Society* **76**: 2391–2406.
Laws EA, Bidigare RR, Popp BN. 1997. Effect of growth rate and CO_2 concentration on carbon isotopic fractionation by the marine diatom Phaeodactylum tricornutum. *Limnology and Oceanography* **42**: 1552–1560.
Leland HV, Berkas WR. 1998. Temporal variation in plankton assemblages and physicochemistry of Devils Lake, North Dakota. *Hydrobiologia* **377**: 57–71.
Lemoalle J, Dupont B. 1976. Iron-bearing oolites and the present conditions of iron sedimentation in Lake Chad. In *Ores in Sediments*, Amstutuz GC, Bernard AJ. (Eds.). International Union of Geological Science Vol. A3, Springer: Berlin; 167–178.
Leng MJ, Barker PA. 2006. A review of the oxygen isotope composition of lacustrine diatom silica for palaeoclimate reconstruction. *Earth-Science Reviews* **75**: 5–27.
Leng MJ, Marshall JD. 2004. Palaeoclimate interpretation of stable isotope data from lake sediment archives. *Quaternary Science Reviews* **23**: 811–831.
Leng MJ, Sloane HJ. 2008. Combined oxygen and silicon isotope analysis of biogenic silica. *Journal of Quaternary Science* **23**: 313–319.
Leng MJ, Barker PA, Greenwood P, Roberts N, Reed J. 2001. Oxygen isotope analysis of diatom silica and authigenic calcite from Lake Pinarbasi, Turkey. *Journal of Paleolimnology* **25**: 343–349.
Leng MJ, Metcalfe SE, Davies SJ. 2005a. Investigating late Holocene climate variability in Central Mexico using carbon isotope ratios in organic materials and oxygen isotope ratios from diatom silica within lacustrine sediments. *Journal of Palaeolimnology* **34**: 413–431.
Leng MJ, Lamb AL, Heaton THE, Marshall JD, Wolfe BB, Jones MD, Holmes JA, Arrowsmith C. 2005b. Isotopes in lake sediments. In *Isotopes in Palaeoenvironmental Research*, Leng MJ (ed.). Springer: Dordrecht, Netherlands; 147–184.
Leng MJ, Swann GEA, Hodson MJ, Tyler JJ, Patwardhan SV, Sloane HJ. 2009. The potential use of silicon isotope composition of biogenic silica as a proxy for environmental change. *Silicon* **1**: 65–77.
Lenters JD, Cook KH. 1997. On the origin of the Bolivian high and related circulation features of the South American climate. *Journal Atmospheric Sciences* **54**: 656–677.
Lewis WM Jr. 1983. A revised classification of lakes based on mixing. *Canadian Journal of Fisheries and Aquatic Sciences* **40**: 1779–1787.
Lindqvist JK, Lee DE. 2009. High-frequency paleoclimate signals from Foulden Maar, Waipiata Volcanic Field, southern New Zealand: An Early Miocene varved lacustrine diatomite deposit. *Sedimentary Geology* **222**: 98–110.
Livingstone DA, Melack JM. 1984. Some lakes of subsaharan Africa. In *Lakes and reservoirs*, Taub FB. (Ed.). Elsevier: Amsterdam; 467–497.
Lotter AF, Birks HJB. 1997. The separation of the influence of nutrients and climate on the varve time-series of Baldeggersee, Switzerland. *Aquatic Sciences* **59**: 362–375.
Lowell T V, Kelly MA. 2008. Was the Younger Dryas Global? *Science* **321**: 348–349.
MacDonald JD. 1869. On the structure of the diatomaceous frustule, and its genetic cycle. *Annals and Magazine of Natural History* **4**: 1–8.
Mackay AW. 2007. The paleoclimatology of Lake Baikal: a diatom synthesis and prospectus. *Earth-Science Reviews* **82**: 181–215.
Mackay AW, Karabanov E, Leng MJ, Sloane HJ, Morley DW, Panizzo VN, Khursevich G, Williams D. 2008. Reconstructing hydrological variability in Lake Baikal during MIS 11: an application of oxygen isotope analysis of diatom silica. *Journal of Quaternary Science* **23**: 365–374.
Mann ME, Park J. 1996. Greenhouse warming and changes in the seasonal cycle of temperature: model versus observations. *Geophysical Research Letters* **23**: 1111–1114.

Mann ME, Park J, Bradley RS. 1995. Global interdecadal and century-scale climate oscillations during the past five centuries. *Nature* **378**: 266–270.
Mantua NJ, Hare S, Zhang Y, Wallace JM, Francis RC. 1997. A Pacific interdecadal climate oscillation with impacts on salmon production. *Bulletin of the American Meteorological Society* **78**: 1069–1079.
Marchant RA, Hooghiemstra H. 2004. Rapid environmental change in tropical Africa and Latin America about 4000 years before present: a review. *Earth Science Reviews* **66**: 217–260.
Marengo J. 1992. Interannual variability of surface climate in the Amazon basin. *International Journal of Climatology* **12**: 853–863.
Marengo J. 2004. Climatology of the LLJ east of the Andes as derived from NCEP reanalyses. *Journal of Climate* **17**: 2261–2280.
Marengo J. 2007. Climate change and the hydrological modes of the wet tropics. In *Tropical Rainforest Responses to Climate Change*, Bush MB, Flenley JR. (Eds.). Praxis: Chichester; 237–268.
Marengo J, Soares W, Saulo C, Nicolini M. 2004. Climatology of the LLJ east of the Andes as derived from the NCEP reanalyses. *Journal of Climate* **17**: 2261–2280.
Margalef R. 1978. Life forms of phytoplankton as survival alternatives in an unstable environment. *Oceanologica Acta* **1**: 493–509.
Margalef R. 1983. *Limnología*. Ediciones Omega: Barcelona.
Martin L, Bertaux J, Correge T, Ledru M-P, Mourguiart P, Sifeddine A, Soubiès F, Wirrmann D, Suguio K, Turcq B. 1997. Astronomical forcing of contrasting rainfall changes in tropical South America between 12,400 and 8800 cal yr B.P. *Quaternary Research* **47**: 117–122
Martin JH. 1992. Iron as a limiting factor in oceanic productivity. In *Primary Productivity and Biogeochemical cycles in the Sea*, Falkowski PG, Woodhead AD. (eds.). New York: Plenum Press, 123–137.
Martin P, Granina L, Martens K, Goddeeris B. 1998. Oxygen concentration profiles in sediments of two ancient lakes: Lake Baikal (Siberia, Russia) and Lake Malawi (East Africa). *Hydrobiologia* **367**: 163–174.
Maslin MA, Burns, SJ. 2000. Reconstruction of the Amazon basin effective moisture availability over the last 14,000 years. *Science* **290**: 2285–2287.
Maslin MA, Swann GEA. 2005. Isotopes in Marine Sediments. In *Isotopes in Palaeoenvironmental Research*, Leng MJ (ed.). Springer: Dordrecht, Netherlands; 227–290.
Matheney RK, Knauth LP. 1989. Oxygen-isotope fractionation between marine biogenic silica and seawater. *Geochimica et Cosmochimica Acta* **53**: 3207–3214.
McCrea JM. 1950. On the isotopic chemistry of carbonates and palaeo-temperature scale. *Journal of Chemical Physics* **18**: 849–857.
McDermott F, Schwarcz H, Rowe PJ. Isotopes in Speleothems. In *Isotopes in Palaeoenvironmental Research*, Leng MJ (ed.). Springer: Dordrecht, Netherlands; 185–225.
McGregor GR, Nieuwolt S. 1998. *Tropical climatology: an introduction to the climates of the low latitudes*. 2nd ed. Wiley. New York.
McKenzie JA. 1985. Carbon isotopes and productivity in the lacustrine and marine environment. In *Chemical Processes in Lakes*, Stumm W. (Ed.). Wiley: New York; 99–118.
McPhaden MJ, Zebiak SE, Glantz MH. 2006. ENSO as an integrating concept in earth science. *Science* **314**: 1740–1745.
Melander LCS. 1960. *Isotope Effects on Reaction Rates*. Ronald Press Co: New York.
Melander L, Saunders WH. 1980. *Reaction Rates of Isotopic Molecules*. Wiley Interscience: New York, NY.
Merkel U, Prange M, Schulz M. 2010. ENSO variability and teleconnections during glacial climate. *Quaternary Science Reviews* **29**: 86–100.
Meybeck M. 1995. Global distribution of lakes. In *Physics and chemistry of lakes*, Lerman A, Imboden D, Gat J (Eds.). Springer-Verlag: Berlin; 1–35.
Meyers PA. 2003. Applications of organic geochemistry to paleolimnological reconstructions: A summary of examples from the Laurentian Great Lakes. *Organic Geochemistry* **34**: 261–289.
Meyers PA, Teranes JL. 2001. Sediment organic matter. In *Tracking Environmental Change Using Lake Sediments, Physical and Geochemical Techniques*, vol. 2. Last WM, Smol JP. (Eds.). Kluwer Academic Publishers: Dordrecht, The Netherlands; 239–270.
Milligan AJ, Morel FMM. 2002. A proton buffering role for silica in diatoms. *Science* **297**: 1848–1850.
Mitchell TP, Wallace JM. 1992. The annual cycle in the equatorial convection and sea surface temperature. *Journal of* Climate **5**: 1140–1156.
Moreno A, Giralt S, Valero-Garcés BL, Sáez A, Bao R, Prego R, Pueyo JJ, González-Sampériz P, Taberner C. 2007. A 13 kyr high-resolution record from the tropical Andes: the Chungará Lake sequence (18º S, northern Chilean Altiplano). *Quaternary International* **161**: 4–21.
Morley DW, Leng MJ, Mackay AW, Sloane HJ, Rioual P, Battarbee RW. 2004. Cleaning of lake sediment samples for diatom oxygen isotope analysis. *Journal of Paleolimnology* **31**: 391–401.
Morley DW, Leng MJ, Mackay AW, Sloane HJ. 2005. Late glacial and Holocene environmental change in the Lake Baikal region documented by oxygen isotopes from diatom silica. *Global and Planetary Change* **46**: 221–233.
Moschen R, Lücke A, Schleser G. 2005. Sensitivity of biogenic silica oxygen isotopes to changes in surface water temperature and palaeoclimatology. *Geophysical Research Letters* **32**: L07708.
Mourguiart P, Ledru M-P. 2003. Last glacial maximum in an Andean cloud forest environment (Eastern Cordillera, Bolivia). *Geology* **31**: 195–198.
Moy CM, Seltzer GO, Rodbell DT, Anderson DM. 2002. Variability of El Niño/Southern Oscillation activity at millenial timescales during the Holocene epoch. *Nature* **420**: 162–165.
Mühlhauser H, Hrepic N, Mladinic P, Montecino V, Cabrera S. 1995. Water-quality and limnological features of a high-altitude Andean lake, Chungará in northern Chile. *Revista Chilena de Historia Natural* **68**: 341–349.
Muñoz A, Ojeda J, Sanchez-Valverde B. 2002. Sunspot-like and ENSO/NAO-like periodicities in lacustrine laminated sediments of the Pliocene Villarroya Basin (La Rioja, Spain). *Journal of Paleolimnology* **27**: 453–463.

Muñoz JA, Amilibia A, Carrera N, Mon R, Roca E, Sàbat F. 2005. A geological cross-section of the Andean orogen at 25.5ºS. International Andean Geodynamics Syposium: Barcelona.

Negri AJ, Adler RF, Shepherd JM, Huffman G, Manyin M, Neklin EJ. 2004. A 16-year climatology of global rainfall from SSM/I highlighting morning versus evening differences. 13th Conference on Satellite Meteorology and Oceanography, American Meteorological Society: Norfolk, VA.

Newman M, Compo GP, Alexander MA. 2003. ENSO-forced variability of the Pacific Decadal Oscillation. *Journal of Climate* **16**: 3853–3857.

Niebler HS, Hubberten HW, Gersonde R. 1999. Oxygen isotopes values of planktic foraminifera: A tool for the reconstruction of surface water stratification. In *Use of proxies in paleoceanography,* Fischer G, Wefer G, (Eds.). Springer-Verlag: Germany; 165–189.

O'Neil JR. 1986. Theoretical and experimental aspects of isotopic fractionation. In Stable Isotopes in High Temperature Geological Processes, Valley JW, Taylor HP, O'Neil JR. (Eds.). *Reviews in Mineralogy* **16**: 1–40.

Orme AR. 2007. The tectonic framework of South America. In *The physical geography of South America*, Veblen TT, Young KR, Orme AR. (Eds.). Oxford University Press: Oxford; 3–22.

Owen RB, Crossley R. 1992. Spatial and temporal distribution of diatoms in sediments of Lake Malawi, Central Africa and ecological implications. *Journal of Paleolimnology* **7**: 55–71.

Pace ML, Cole JJ, Carpenter SR, Kitchell JF, Hodgson JR, Van de Bogert MC, Bade DL, Kritzberg ES, Bastviken D. 2004. Whole-lake carbon-13 additions reveal terrestrial support of aquatic food webs. *Nature* **427**: 240–243.

Paduano GM, Bush MB, Baker PA, Fritz SC, Seltzer GO. 2003. A vegetation and fire history of Lake Titicaca since the Last Glacial Maximum. *Palaeogeography, Palaeoclimatology, Palaeoecology* **194**: 259–279.

Park J. 1992. Envelope estimation for quasi-periodic geophysical signals in noise: a multitaper approach. In *Statistics in the Environmental and Earth Sciences*, Walden AT, Guttorp P. (Eds.). Edward Arnold: London; 189–219.

Pfitzer E. 1869. Über den Bau und die Zellteilung der Diatomeen. *Botanische Zeitung* **27**: 774–776.

Pilskaln CH, Johnson TJ. 1991. Seasonal signals in Lake Malawi sediments. *Limnology and Oceanography* **36**: 544–557.

Placzek C, Quade J, Patchett PJ. 2006. Geochronology and stratigraphy of late Pleistocene lake cycles on the southern Bolivian Altiplano: implications for causes of tropical climate change. *GSA Bulletin* **118**: 515–532.

Polissar PJ, Abbott MB, Shemesh A, Wolfe AP, Bradley RS. 2006. Holocene hydrologic balance of tropical South America from oxygen isotopes of lake sediment opal, Venezuelan Andes. *Earth and Planetary Science Letters* **242**: 375–389.

Popp BN, Laws EA, Bidigare RR, Dore JE, Hanson KL, Wakeham SG. 1998. Effect of phytoplankton cell geometry on carbon isotopic fractionation. *Geochimica et Cosmochimica Acta* **62**: 69–77.

Prasad S, Brauer A, Rein B, Negendank JFW. 2006. Rapid climate change during the early Holocene in western Europe and Greenland. *The Holocene* **16**: 153–158.

Ragotzkie RA. 1978. Heat budgets of lakes. *Lakes, Chemistry, Geology and Physics*, Lerman A. (Ed.). Springer Verlag: 1–19.

Ramos VA. 1999. Los depósitos sinorogénicos terciarios de la región andina. *Geología Argentina, Anales* **29**: 651–682.

Ramos VA. 2009. Anatomy and global context of the Andes: Main geologic features and the Andean orogenic cycle. In Backbone of the Americas: Shallow Subduction, Plateau Uplift, and Ridge and Terrane Collision, Kay SM, Ramos VA, Dickinson W. (Eds.). *Geological Society of America, Memoir* **204**: 31–65.

Rasband WS. 1997-2009. ImageJ. U. S. National Institutes of Health: Bethesda, Maryland, USA; http://rsb.info.nih.gov/ij/

Ravelo C, Hillaire-Marcel C. 2007. The use of oxygen and carbon isotopes of foraminifera in paleoceanography. In *Late Cenozoic Paleoceanography*, Hillaire-Marcel C, de Vernal A. (Eds.). Elsevier: Amsterdam; 735–764.

R Development Core Team. 2008. R: a Language and Environment for Statistical Computing. R Foundation for Statistical Computing: Vienna, Austria; http://www.R-project.org

Reimer PJ, Baillie MGL, Bard E, Bayliss A, Beck JW, Bertrand CJH, Blackwell PG, Buck CE, Burr GS, Cutler KB, Damon PE, Edwards RL, Fairbanks RG, Friedrich M, Guilderson TP, Hogg AG, Hughen KA, Kromer B, McCormac G, Manning S, Ramsey CB, Reimer RW, Remmele S, Southon JR, Stuiver M, Talamo S, Taylor FW, van der Plicht J, Weyhenmeyer CE. 2004a. IntCal04 terrestrial radiocarbon age calibration, 0–26 Cal Kyr BP. *Radiocarbon* **46**: 1029–1058.

Reimer P, Brown T, Reimer R. 2004b. Discussion: reporting and calibration of post-bomb ^{14}C data. *Radiocarbon* **46**: 1299–1304.

Renberg I. 1981. Formation, structure and visual appearance of iron-rich varved lake sediments. *Verhandlungen Internationale Vereinigung für Limnologie* **21**: 94–101.

Reynolds CS. 2006. *The Ecology of Phytoplankton*. Cambridge University Press: Cambridge, UK.

Richardson CA. 2001. Molluscs as archives of environmental change. *Oceanography and Marine Biology: an Annual Review* **39**: 103–164.

Ricketts RD, Anderson RF. 1998. A direct comparison between the historical record of lake level and $\delta^{18}O$ signal in carbonate sediments from Lake Turkana, Kenya. *Limnology and Oceanography* **43**: 811–822.

Riebesell U, Wolf-Gladrow D, Smetacek V. 1993. Carbon dioxide limitation of marine phytoplankton growth rates. *Nature* **361**: 249 –251.

Rietti-Shati M, Shemesh A, Karlen W. 1998. A 300-year climate record from biogenic silica oxygen isotopes in an equatorial highaltitude lake. *Science* **281**: 980–982.

Rigsby CA, Bradbury JP, Baker PA, Rollins SM, Warren MR. 2005. Late Quaternary palaeolakes, rivers, and wetlands on the Bolivian Altiplano and their palaeoclimatic implications. *Journal of Quaternary Science* **20**: 671–691.

Rings A, Lucke A, Schleser GH. 2004. A new method for the quantitative separation of diatom frustules from lake sediments. *Limnology and Oceanography: Methods* **2**: 25–34.

Rioual P, Andrieu-Ponel V, Rietti-Shati M, Battarbee RW, de Beaulieu JL, Cheddadi R, Reille M, Svobodova H, Shemesh A. 2001. High-resolution record of climate stability in France during the last interglacial period. Nature 413: 293–296.

Rittenour TR, Brigham-Grette J, Mann ME. 2000. El Niño-like climate teleconnections in New England during the Late Pleistocene. *Science* **288**: 1039–1042.

Robbins EI. 1983. Accumulation of fossil fuels and metallic minerals in active and ancient rift lakes. *Tectonophysics* **94**: 633–658.

Robinson RS, Brunelle BG, Sigman DM. 2004. Revisiting nutrient utilization in the glacial Antarctic: Evidence from a new method for diatom-bound N isotopic analysis. *Paleoceanography* **19**: PA3001.
Rodbell DT, Seltzer GO. 2000. Rapid ice margin fluctuations during the Younger Dryas in the tropical Andes. *Quaternary Research* **54**: 328–338.
Rodbell DT, Seltzer GO, Anderson DM, Abbott MB, Enfield DB, Newman JH. 1999. An 15, 000-year record of El Niño-driven alluviation in southwestern Ecuador. *Science* **283**: 516–520.
Rodó X, Rodríguez-Arias MA. 2004. El Niño–Southern oscillation: absent in the early holocene? *Journal of Climate* **17**: 423–426.
Romero-Viana L, Julià R, Camacho A, Vicente E, Miracle MR. 2008. Climate signal in varve thickness: Lake La Cruz (Spain), a case study. *Journal of Paleolimnology* **40**: 703–714.
Rosenthal Y, Dahan M, Shemesh A. 2000 Southern Ocean contributions to glacial-interglacial changes of atmospheric pCO_{2}: An assessment of carbon isotope records in diatoms. *Paleoceanography* **15**: 65–75.
Rosqvist GC, Rietti-Shati M, Shemesh A. 1999. Late glacial to middle Holocene climatic record of lacustrine biogenic silica oxygen isotopes from a Southern Ocean island. *Geology* **27**: 967–970.
Rosqvist GC, Jonsson C, Yam R, Karlen W, Shemesh A. 2004. Diatom oxygen isotopes in pro-glacial lake sediments from northern Sweden: a 5000 year record of atmospheric circulation. *Quaternary Science Reviews* **23**: 851– 859.
Round FE, Crawford RM, Mann DG. 1990. *The Diatoms, Biology & Morphology of the Genera*. Cambridge University Press: Cambridge; 747.
Rowe HD, Dunbar RB, Mucciarone DA, Seltzer GO, Baker PA, Fritz S. 2002. Insolation, moisture balance and climate change on the South American Altiplano since the Last Glacial Maximum. *Climate Change* **52**: 175–199.
Rowe HD, Guilderson TP, Dunbar RB, Southon JR, Seltzer GO, Mucciarone DA, Fritz SC, Baker PA. 2003. Late Quaternary lakelevel changes constrained by radiocarbon and stable isotope studies on sediment cores from Lake Titicaca, South America. *Global and Planetary Change* **38**: 273–290.
Ruhlemann C, Mulitza S, Muller PJ, Wefer G, Zahn R. 1999. Warming of the tropical Atlantic Ocean and slowdown of thermohaline circulation during the last deglaciation. *Nature* **402**: 511–514.
Saade A, Bowler C. 2009. Molecular tools for discovering the secrets of diatoms. Bioscience 59: 757–765.
Sáez A, Cabrera L. 2002. Sedimentological and palaeohydrological responses to tectonics and climate in a small, closed, lacustrine system: Oligocene As Pontes Basin (Spain). *Sedimentology* **49**: 1073–1094.
Sáez A, Valero-Garcés BL, Moreno A, Bao R, Pueyo JJ, González-Sampériz P, Giralt S, Taberner C, Herrera C, Gibert RO. 2007. Volcanic controls on lacustrine sedimentation: the late Quaternary depositional evolution of lake Chungará (northern Chile). *Sedimentology* **54**: 1191–1222.
Sarnthein M, Winn K, Jung SJA, Duplessy JA, Labeyrie L, Erlenkeuser H, Ganssen G. 1994. Changes in east Atlantic deepwater circulation over the last 30,000 years: Eight time slice reconstructions. *Paleoceanography* **9**: 209–267.
Saulo AC, Nicolini M, Chou SC. 2000. Model characterization of the South American low-level flow during the 1997–98 spring–summer season. *Climate Dynamics* **16**: 867–881.
Schauble EA. 2004. Applying stable isotope fractionation theory to new systems. In Geochemistry of Non-Traditional Stable Isotopes, Johnson CM, Beard BL, Albarède F. (Eds.). *Mineralogical Society of America Reviews in Mineralogy & Geochemistry* **55**: 65–111.
Schelske CL, Hodell DA. 1991. Recent changes in productivity and climate of Lake Ontario detected by isotopic analysis of sediments. *Limnology and Oceanography* **36**: 961–975.
Schleser GH, Lücke A, Moschen R, Rings A. 2001. Separation of diatoms from sediment and oxygen isotope extraction from their siliceous valves — a new approach. Terra Nostra: Schriften der Alfred-Wegener-Stiftung, 6th Workshop of the European Lake Drilling Programme; 187–191.
Schmidt M, Botz R, Rickert D, Bohrmann G, Hall SR, Mann S. 2001. Oxygen isotopes of marine diatoms and relations to opal-A maturation. *Geochimica et Cosmochimica Acta* **65**: 201–211.
Schneider N, Cornuelle BD. 2005. The forcing of the Pacific Decadal Oscillation. *Journal of Climate* **18**: 4355–4373.
Schneider-Mor A, Yam R, Bianchi C, Kunz-Pirrung M, Gersonde R, Shemesh A. 2005. Diatom stable isotopes, sea ice presence and sea surface temperature records of the past 640 ka in the Atlantic sector of the Southern Ocean. *Geophysical Research Letters* **32**: L10704.
Scholz CA, Johnson TC, McGill JW. 1993. Deltaic sedimentation in a rift valley lake: new seismic reflection data from Lake Malawi (Nyasa), East Africa. *Geology* **21**: 395–398.
Schwalb A. 2003. Lacustrine ostracods as stable isotope recorders of late-glacial and Holocene environmental dynamics and climate. *Journal of Paleolimnology* **29**: 265–351.
Schwalb A, Dean WE. 2002. Reconstruction of hydrological changes and response to effective moisture variations from north-central USA lake sediments. *Quaternary Science Reviews* **21**: 1541–1554.
Schwalb A, Burns SJ, Kelts K. 1999. Holocene environments from stable isotope stratigraphy of ostracods and authigenic carbonate in Chilean Altiplano lakes. *Palaeogeography, Palaeoclimatology, Palaeoecology* **148**: 153–168.
Seltzer G, Rodbell D, Burns S. 2000. Isotopic evidence for late Quaternary climatic change in tropical South America. *Geology* **28**: 35–38.
Servant M, Servant-Vildary S. 2003. Holocene precipitation and atmospheric changes inferred from river paleowetlands in the Bolivian Andes. *Palaeogeography, Palaeoclimatology, Palaeoecology* **194**: 187–206.
Shackleton NJ, Opdyke ND. 1973. Oxygen isotope and palaeomagnetic stratigraphy of equatorial Pacific core V28-238: oxygen isotope temperatures and ice volumes on a 10^5 and 10^6 year scale. *Quaternary Research* **3**: 39–55.
Shackleton NJ, Hall MA, Pate D. 1995. Pliocene stable isotope stratigraphy of ODP Site 846. In *Proceedings ODP*, Pisias NG, Mayer LA, Janecek TR, Palmer-Julson A, van Andel TH. (Eds.). Scientific Results 138: College Station, TX.
Shemesh A, Charles CD, Fairbanks RG. 1992. Oxygen isotopes in biogenic silica: global changes in ocean temperature and isotopic composition. *Science* **256**: 1434–1436.

Shemesh A, Macko SA, Charles CD, Rau GH. 1993. Isotopic evidence for reduced productivity in the glacial Southern-Ocean. *Science* **262**: 407–410.
Shemesh A, Burckle LH, Hays JD. 1995. Late Pleistocene oxygen-isotope records of biogenic silica from the Atlantic Sector of the Southern-Ocean. *Paleoceanography* **10**: 179–196.
Shemesh A, Rosqvist G, Rietti-Shati M, Rubensdotter L, Bigler C, Yam R, Karlen W. 2001. Holocene climatic change in Swedish Lapland inferred from an oxygen-isotope record of lacustrine biogenic silica. *Holocene* **11**: 447–454.
Shemesh A, Hodell D, Crosta X, Kanfoush S, Charles C, Guilderson T. 2002. Sequence of events during the last deglaciation in Southern Ocean sediments and Antarctic ice cores. *Paleoceanography* **17**: 1056–1062.
Shunk AJ, Driese SG, Dunbar JA. (2009). Late Tertiary paleoclimatic interpretation from lacustrine rhythmites in the Gray Fossil Site, northeastern Tennessee, USA. *Journal of Paleolimnology* **42**: 11–24.
Sicko-Goad LM, Schelske CL, Stoermer EF. 1984. Estimation of intracellular carbon and silica content of diatoms from natural assemblages using morphometric techniques. *Limnology and Oceanography* **29**: 1170–1178.
Sicko-Goad L, Stoermer EF, Kociolek JP. 1989. Diatom resting cell rejuvenation and formation: time course, species records and distribution. *Journal of Plankton Research* **11**: 375–389.
Simola H. 1992. Structural elements in varved lake sediments. *Geological survey of Finland, special paper* **14**: 5–9.
Simola H. 2007. Diatom records. Freshwater laminated sediments. In *Encyclopedia of Quaternary Science*, Elias SA. (Ed.).Elsevier: Amsterdam; 541–548.
Singer AJ, Shemesh A. 1995. Climatically linked carbon-isotope variation during the past 430,000 years in Southern-Ocean sediments. *Paleoceanography* **10**: 171–177.
Skinner LC, Shackleton NJ, Elderfield H. 2003. Millennial-scale variability of deep-water temperature and $\delta^{18}O_{dw}$ indicating deepwater source variations in the Northeast Atlantic, 0–34 cal. ka BP. *Geochemistry, Geophysics, Geosystems—G3*: 4.
Smetacek VS. 1985. Role of sinking in diatom life-history cycles: ecological, evolutionary and geological significance. *Marine Biology* **84**: 239–251.
Smith ND, Ashley GM. 1985. Proglacial lacustrine environment. In *Glacial Sedimentary Enuironments*, Ashley GM, Shaw J, Smith ND. (Eds.). Society of Economic Palaeontologists and Mineralogists Short Course Notes: Tulsa.
Smol JP. 2008. *Pollution of Lakes an Rivers. A Palaeoenvironmental Perspective*. Blackwell Publishing: Malden.
Solíz C, Villalba R, Argollo J, Morales MS, Christie DA, Moya J, Pacajes J. 2009. Spatio-temporal variations in Polylepis tarapacana radial growth across the Bolivian Altiplano during the 20th Century. *Palaeogeography, Palaeoclimatology, Palaeoecology* **281**: 296–308
Sorhannus U. 2007. A nuclear-encoded small-subunit ribosomal RNA timescale for diatom evolution. *Marine Micropaleontology* **65**: 1–12.
Sterken M, Verleyen E, Sabbe K, Terryn G, Charlet F, Bertrand S, Boës X, Fagel N, De Batist M, Vyverman W. 2008. Late Quaternary climatic changes in southern Chile, as recorded in a diatom sequence of Lago Puyehue (40°402 S). *Journal of Paleolimnology* **39**: 219–235.
Stockwell RG, Mansinha L, Lowe RP. 1996. Localization of the complex spectrum: the S transform. *IEEE Transactions on Signal Processing* **44**: 998–1001.
Stoermer EF, Julius ML. 2003. Centric diatoms. In *Freshwater Algae of North America*, Wehr JD, Sheath RG. (eds.). San Diego: Elsevier Science (USA); 559-594.
Stoermer EF, Smol JP. 1999. *The Diatoms: Applications for the Environmental and Earth Sciences*. Cambridge: Cambridge University Press.
Strecker MR, Alonso RN, Bookhagen B, Carrapa B, Hilley GE, Sobel ER, Trauth MH. 2007. Tectonics and climate of the southern central Andes. *Annual Review of Earth and Planetary Sciences* **35**: 747–787.
Street-Perrott FA, Harrison SP. 1985. Lake levels and climate reconstruction. In *Paleoclimate analysis and modeling*, Hecht AD (Ed.). Wiley: New York; 291–340.
Stuiver M. 1968. Oxygen-18 content of atmospheric precipitation during the last 11,000 Years in Great Lakes region. *Science* **162**: 994–997.
Sumper M, Kröger N. 2004. Silica formation in Diatoms: the function of long-chain polyamines and silaffins. *Journal of Materials Chemistry* **14**: 2059–2065.
Swann GEA, Leng MJ. 2009. A review of diatom $\delta^{18}O$ in palaeoceanography. *Quaternary Science Reviews* **28**: 384–398.
Swann GEA, Leng MJ, Sloane HJ, Maslin MA. 2008. Isotope offsets in marine diatom $\delta^{18}O$ over the last 200 ka. *Journal of Quaternary Science* **23**: 389–400.
Swann G, Leng MJ, Juschus O, Melles M, Brigham-Grette J, Sloane HJ. 2010. A combined oxygen and silicon diatom isotope record of Late Quaternary change in Lake El'gygytgyn, North East Siberia. *Quaternary Science Reviews* **29**: 774–786.
Swihart GH, McBay EH, Smith DH, Siefke JW. 1996. A boron isotopic study of a mineralogically zoned lacustrine borate deposit: the Kramer deposit, California, U.S.A. *Chemical Geology* **127**: 241–250.
Sylvestre F. 2009. Moisture Pattern During the Last Glacial Maximum in South America. In *Past Climate Variability in South America and Surrounding Regions*, Vimeux F, Sylvestre F, Khodri M. (eds.). Springer: Dordrecht, Netherlands; 3–27.
Sylvestre F, Servant M, Servant-Vildary S, Causse C, Fournier M, Ybert JP. 1999. Lake-level chronology on the southern Bolivian Altiplano (18°–23°S) during late-glacial time and the early Holocene. *Quaternary Research* **51**: 54–66.
Talbot MR. 1988. The origins of the lacustrine oil source rocks: Evidence from the lakes of tropical Africa. In *Lacustrine Petroleum Source Rocks*, Fleet AJ, Kelts K, Talbot MR. (Eds.). Oxford/Boston: Blackwell Scientific Publications 40; 29–43.
Talbot MR. 2001. Nitrogen isotopes in palaeolimnology. In *Tracking Environmental Change Using Lake Sediments*, *Physical and Geochemical Techniques*, vol.2. Last WM, Smol JP. (Eds.). Kluwer Academic Publishers: Dordrecht, The Netherlands; 401–439
Talbot MR, Allen PA. 1996. Lakes. In *Sedimentary Environments*, Reading HG (Ed.). Blackwell: Oxford; 83–124.
Talbot MR, Lærdal T. 2000. The late Pleistocene-Holocene palaeolimnology of Lake Victoria, East Africa, based upon elemental and isotopic analyses of sedimentary organic matter. *Journal of Paleolimnology* 23: 141–164.

Talbot MR, Kelts K. 1990. Paleolimnological signatures from carbon and oxygen isotopic ratios in carbonates from organic carbon-rich lacustrine sediments. In Lacustrine Basin Exploration: Case Studies and Modern Analogs, Katz BJ. (Ed.). *AAPG Memoir* **50**: 88–112.

Talling JF. 1976. Depletion of carbon-dioxide from lake water by phytoplankton. *Journal of Ecology* **64**: 79–121.

Tapia PM, Fritz SC, Baker PA, Seltzer GO, Dunbar RB. 2003. A late Quaternary diatom record of tropical climatic history from Lake Titicaca (Bolivia/Peru). *Palaeogeography, Palaeoclimatology, Palaeoecology* **194**: 139–164.

Tassara A, Yañez G. 2003. Relación entre el espesor elástico de la litosfera y la segmentación tectónica del margen andino (15-47°S). *Revista Geológica de Chile* **30**: 159–186.

Teranes JN, McKenzie JA, Bernasconi SM, Lotter AF, Sturm M. 1999. A study of oxygen isotopic fractionation during bio-induced calcite precipitation in eutrophic Baldeggersee, Switzerland. *Geochimica et Cosmochimica Acta* **63**: 1981–1999.

Teranes JL, Bernasconi SM. 2000. The record of nitrate utilization and productivity limitation provided by ^{15}N values in lake organic matter – A study of sediment trap and core sediments from Baldeggersee, Switzerland. *Limnology and Oceanography* **45**: 801–813.

Theissen KM, Dunbar RB, Rowe HD, Mucciarone DA. 2008. Multidecadal- to century-scale arid episodes on the Northern Altiplano during the middle Holocene. *Palaeogeography, Palaeoclimatology, Palaeoecology* **257**: 361–376.

Theriot E. 2001. Diatoms. In *Encyclopedia of Life Sciences*. John Wiey and Sons: Chichester.

Thompson DJ. 1982. Spectrum estimation and harmonic analysis. *Proceedings of the Institute of Electrical and Electronics Engineers* **70**: 1055–1096.

Thompson L, Mosley-Thompson E, Davis ME, Lin PN, Henderson KA, Cole-Dai J, Bolzan JF, Liu KB. 1995. Late glacial stage and Holocene tropical ice core records from Huascaran, Peru. *Science* **269**: 46–50.

Thompson LG, Davis ME, Mosley-Thompson E, Sowers TA, Henderson KA, Zagorodnov VS, Lin PN, Mikhalenko VN, Campen RK, Bolzan JF, Cole-Dai J, Francou B. 1998. A 25,000-year tropical climate history from Bolivian ice cores. *Science* **282**: 1858–1864.

Thompson LG, Davis ME, Mosley-Thompson E, Lin PN, Henderson KA, Mashiotta TA. 2005. Tropical ice core records: evidence for asynchronous glaciation on Milankovitch timescales. *Journal of Quaternary Science* **20**: 723–734.

Thompson JB, Schultze-Lam S, Berveridge TJ, Des Marais DJ. 1997. Whiting events: biogenic origin due to the photosynthetic activity of cyanobacterial picoplankton. *Limnology and Oceanography* **42**: 133–141.

Thornton DCO. 2002. Diatom aggregation in the sea: mechanisms and ecological implications. *European Journal of Phycology* **37**: 149–161.

Tiedemann R, Sarnthein M, Shackleton NJ. 1994. Astronomic timescale for the Pliocene Atlantic and ^{18}O and dust flux records of Ocean Drilling Program site 659. *Paleoceanography* **9**: 619–638.

Tiercelin JJ. 1991. Natural resources in the lacustrine facies of the Cenozoic rift basins of east Africa. In *Lacustrine facies analysis*, Anadón P, Cabrera L, Kelts K (Ed.). Special Publication Number 13 of the International Association of Sedimentologists. Blackwell: Oxford; 1–37.

Tilman D, Kilham SS, Kilham P. 1982. Phytoplankton community ecology: the role of limiting nutrients. *Annual Review of Ecology and Systematics* **13**: 349–372.

Timmermann A, Okumura Y, An SI, Clement A, Dong B, Guilyardi E, Hu A, Jungclaus JH, Renold M, Stocker TF, Stouffer RJ, Sutton R, Xie SP, Yin J. 2007. The influence of a weakening of the Atlantic meridional overturning circulation on ENSO. *Journal of Climate* **20**: 4899–4919.

Torrence C, Compo GP. 1998. A practical guide to wavelet analysis. Bulletin of the American Meteorological Society 79: 61–78.

Tranvik LJ. 1988. Availability of dissolved organic carbon for planktonic bacteria in oligotrophic lakes of differing humic content. *Microbial Ecology* **16**: 311–322.

Tranvik L, Downing JA, Cotner JB, Loiselle SA, Striegl RG, Ballatore TJ, Dillon P, Finlay K, Fortino K, Knoll LB, Kortelainen PL, Kutser T, Larsen S, Laurion I, Leech DM, McCallister SL, McKnight DM, Melack JM, Overholt E, Porter JA, Prairie Y, Renwick WH, Roland F, Sherman BS, Schindler DW, Sobek S, Tremblay A, Vanni MJ, Verschoor AM, von Wachenfeldt E, Weyhenmeyer GA. 2009. Lakes and reservoirs as regulators of carbon cycling and climate. *Limnology and Oceanography* **54**: 2298–2314.

Tyler JJ, Leng MJ, Sloane HJ, Sachse D, Gleixner G. 2008. Oxygen isotope ratios of sedimentary biogenic silica reflect the European transcontinental climate gradient. *Journal of Quaternary Science* **23**: 341–350.

Urey HC. 1947. The thermodynamic properties of isotopic substances. *Journal of the Chemical Society* **1947**: 562–581.

Urey HC, Lowenstam HA, Epstein S, McKinney CR. 1951. Measurement of palaeotemperatures and temperatures of the upper cretaceous of England, Denmark and southeastern United States. *Geological Society of America Bulletin* **62**: 399–416.

Valero-Garcés BL, Grosjean M, Schwalb A, Geyn M, Messerli B, Kelts K. 1996. Limnogeology of Laguna Miscanti: evidence for mid to late Holocene moisture changes in the Atacama altiplano. *Journal of Paleolimnology* **16**: 1–21.

Valero-Garcés BL, Grosjean M, Kelts K, Schreir H, Messerli B. 1999. Holocene lacustrine deposition in the Atacama Altiplano: facies models, climate and tectonic forcing. *Palaeogeography, Palaeoclimatology, Palaeoecology* **151**: 101–125.

Valero-Garces BL, Grosjean M, Schwalb A, Schreir H, Kelts K, Messerli B. 2000. Late Quaternary lacustrine deposition in the Chilean Altiplano (18°–28°S). In *Lake Basins through Space and Time*, Gierlowski-Kordesch E, Kelts K (eds). American Association of Petroleum Geologists Studies in Geology 46: 625–636.

Valero-Garcés BL, Delgado-Huertas A, Navas A, Edwards L, Schwalb A, Ratto N. 2003. Patterns of regional hydrological variability in central-southern Altiplano (18°-26°S) lakes during the last 500 years. *Palaeogeography, Palaeoclimatology, Palaeoecology* **194**: 319– 338.

Vanormelingen P, Verleyen E, Vyverman W. 2008. The diversity and distribution of diatoms: from cosmopolitanism to narrow endemism. *Biodiversity and Conservation* **17**: 393-405.

Vaulot D. 2006. Phytoplankton. *Encyclopedia of Life Sciences*. Chichester: John Wiley & Sons.

Velasco VM, Mendoza B. 2008. Assessing the relationship between solar activity and some large scale climatic phenomena. *Advances in Space Research* **42**: 866–878.

Vera C, Higgins W, Amador J, Ambrizzi T, Garreaud R, Gochis D, Gutzler D, Lettenmaier D, Marengo J, Mechoso CR, Nogues-Paegle J, Silva Diaz PL, Zhang C. 2006. Towards a unified view of the American Monsoon System. *Journal of Climate* **19**: 4977–5000.

Villalba R, D'Arrigo RD, Cook ER, Wiles G, Jacoby GC. 2001. Decadal-scale climatic variability along the extra-tropical western coast of the Americas over past centuries inferred from tree-ring records. In *Interhemispheric Climate Linkages*, Markgraf V. (Ed.). Cambridge University Press: Cambridge, UK.

Villalba R, Grosjean M, Kiefer T. 2009. Long-term multi-proxy climate reconstructions and dynamics in South America (LOTRED-SA): State of the art and perspectives. *Palaeogeography, Palaeoclimatology, Palaeoecology* **281**: 175–179.

Villwock W, Kies L, Thiedig F, Thomann R. 1985. *Geologish-ökologishe Untersuchungen am Lago Chungará/ Nord Chile*. Zielsetzungen und erste Ergebnisse 9: IDESIA, Chile; 21–34.

Volcani BE. 1981. Cell wall formation in diatoms: morphology and biochemistry. In *Silicon and Siliceous Structures in Biological Systems*, Simpson X, Volcani BE. (Eds.). Springer Verlag: New York; 157–200.

Vuille M. 1999. Atmospheric circulation over the Bolivian altiplano during dry and wet periods and extreme phases of the Southern Oscillation. *International Journal of Climatology* **19**: 1579–1600.

Vuille M, Keimig F. 2004. Interannual variability of summertime convective cloudiness and precipitation in the central Andes derived from ISCCP-B3 data. *Journal of Climate* **17**: 3334–3348.

Vuille M, Werner M. 2005. Stable isotopes in precipitation recording South American summer monsoon and ENSO variability: Observations and model results. *Climate Dynamics* **25**: 401–413.

Vuille M, Bradley RS, Keimig F. 2000. Interannual climate variability in the Central Andes and its relation to tropical Pacific and Atlantic forcing. *Journal of Geophysical Research-Atmospheres* **105**: 12447–12460.

Wanner H, Beer J, Bütikofer J, Crowley TJ, Cubasch U, Flückiger J, Goosse H, Grosjean M, Joos F, Kaplan JO, Küttel M, Müller SA, Prentice C, Solomina O, Stocker TF, Tarasov P, Wagner M, Widmann M. 200.: Mid- to Late Holocene climate change: an overview. *Quaternary Science Reviews* **27**: 1791–1828.

Weng C, Bush MB, Curtis JH, Kolata AL, Dillehay TD, Binford MW. 2006. Deglaciation and Holocene climate change in the western Peruvian Andes. *Quaternary Research* **66**: 87–96.

Werner D. 1977. *The Biology of Diatoms*. University California Press: Berkeley.

Wetzel RG. 2001. *Limnology. Lake and rivers ecosystems.* 3rd ed. Academic Press: San Diego, USA.

Willén E. 1991. *Planktonic diatoms - an ecological review*. Archiv für Hydrobiologie: 69–106.

Whitman D, Isacks BL, Kay SM. 1996. Lithospheric structure and along-strike segmentation of the central Andean Plateau: Seismic Q, magmatism, flexture, topography and tectonics. *Tectonophysics* **259**: 29-40.

Wolfe BB, Aravena R, Abbott MB, Seltzer GO, Gibson JJ. 2001. Reconstruction of paleohydrology and paleohumidity from oxygen isotope records in the Bolivian Andes. *Palaeogeography, Palaeoclimatology, Palaeoecology* **176**: 177–192.

Wörner G, Harmon RS, Davidson J, Moorbath S, Turner DL, McMillan N, Nye C, López-Escobar L, Moreno H. 1988. The Nevados de Payachata volcanic region (18°S/69°W, N. Chile): I. Geological, geochemical, and isotopic observations. *Bulletin of Volcanology* **50**: 287–303.

Wörner G, Hammerschmidt K, Henjes-Kunst F, Wilke H. 2000. Geochronology ($^{40}Ar/^{39}Ar$, K-Ar and He-exposure ages) of Cenozoic magmatic rocks from northern Chile (18–22°S): implications for magmatism and tectonic evolution of the central Andes. *Revista Geológica de Chile* **27**: 205–240.

Yansa CH, Dean WE, Murphy EC. 2007. Late Quaternary paleoenvironments of an ephemeral wetland in North Dakota, USA: relative interactions of groundwater hydrology and climate change. *Journal of Paleolimnology* **38**: 441–457.

Zachos J, Pagani M, Sloan L, Thomas E, Billups K. 2001. Trends, rhythms, and aberrations in global climate 65 Ma to present. *Science* **292**: 686–693.

Zech R, Smith J, Kaplan MR. 2009 Chronologies of the Last Glacial Maximum and its Termination in the Andes (~10–55°S) Based on Surface Exposure Dating. In *Past Climate Variability in South America and Surrounding Regions*, Vimeux F, Sylvestre F, Khodri M. (eds.). Springer: Dordrecht, Netherlands; 61–88.

Zhou J, Lau KM. 1998. Does a Monsoon Climate Exist over South America?. *Journal of Climate* **11**: 1020–1040.

Zolitschka B. 1992. Climatic change evidence and lacustrine varves from maar lakes, Germany. Climate Dynamics 6: 229–232.

Zolitschka B, Negendank JFW. 1996. Sedimentology, dating and palaeoclimatic interpretation of a 76.3 ka record from Lago Grande di Monticchio, southern Italy. *Quaternary Science Reviews* **15**: 101–112.

Zolitschka B, Brauer A, Negendank JFW, Stockhausen H, Lang A. 2000. Annually dated late Weichselian continental palaeoclimate record from the Eifel, Germany. *Geology* **28**: 783–786.

Appendices

Appendix A

Glossary

Symbols

α	Fractionation factor
δ	Isotope composition
δD	Stable hydrogen isotopes; the ratio of ^{2}H to ^{1}H in a sample relative to a standard
$\delta^{13}C$	Stable carbon isotopes; the ratio of ^{13}C to ^{12}C in a sample relative to a standard
$\delta^{13}C_{carbonate}$	Carbon isotope composition of carbonates
$\delta^{13}C_{diatom}$	Carbon isotope composition of diatom organic cell wall inclusions
$\delta^{13}C_{DIC}$	Carbon isotope composition of dissolved inorganic carbon
$\delta^{13}C_{DOC}$	Carbon isotope composition of dissolved organic carbon
$\delta^{13}C_{bulk}$	Carbon isotope composition of bulk organic matter
$\delta^{15}N$	Stable nitrogen isotopes; the ratio of ^{15}N to ^{14}N in a sample relative to a standard
$\delta^{15}N_{bulk}$	Nitrogen isotope composition of bulk organic matter
$\delta^{15}N_{diatom}$	Nitrogen isotope composition of diatom organic cell wall inclusions
$\delta^{18}O$	Stable oxygen isotopes; the ratio of ^{18}O to ^{16}O in a sample relative to a standard
$\delta^{18}O_{carbonate}$	Oxygen isotope composition of carbonates
$\delta^{18}O_{diatom}$	Oxygen isotope composition of diatom silica
$\delta^{18}O_{lakewater}$	Oxygen isotope composition of water of the lake
$\delta^{18}O_{precipitation}$	Oxygen isotope composition of rainfall
$\delta^{30}Si$	Stable silicon isotopes; the ratio of ^{30}Si to ^{28}Si in a sample relative to a standard
$\delta^{30}Si_{diatom}$	Silicon isotope composition of diatom silica
ε	Isotope enrichment factors
σ	Probability distribution

Elements

H	Hydrogen
C	Carbon
N	Nitrogen
O	Oxygen
F	Fluorine
Na	Sodium
Mg	Magnesium
Si	Silicon
P	Phosphorus
S	Sulphur
Cl	Chlorine
K	Potassium
Ca	Calcium
Fe	Iron
Br	Bromine
Pt	Platinum

Chemical Formulas

CO_2	Carbon dioxide
$CO_{2(aq)}$	CO_2 dissolved in water
CH_4	Methane
O_2	Oxygen in its molecular form
OH^-	Hydroxide ion
H_2O	Distilled water
H_2O_2	Hydrogen peroxide
HCO_3^-	Bicarbonate ion
HCl	Hydrochloric acid
HNO_3	Nitric acid
N_2	Nitrogen gas
NO_2^-	Nitrite ion

NO_3^-	Nitrate ion
NH_4^+	Ammonium cation
PO_4^{3-}	Ortophosphate ion
SiO_2	Silicon dioxide or silica
$Si(OH)_4$	Silicic acid
SO_4^-	Sulfate ion
$CaCO_3$	Calcium carbonate
ClF_3	Chlorine trifluoride
BrF_5	Bromine pentafluoride

Acronyms and abrevations

AAO	Antarctic Oscillation
AMS	Accelerator Mass Spectrometry
B-A	Bølling-Allerød chronozone
BFC	Diatomite Control Sample
BP	Before Present
BSi	Biogenic Silica
CSIC	Consejo Superior de Investigaciones Científicas
DIC	Dissolved Inorganic Carbon
DOC	Dissolved Organic Carbon
EL	Evaporation Line
ENSO	El Niño-Southern Oscillation
GISP	Greenland Ice Sheet Precipitation
GMWL	Globale Meteroric Water Line
IAEA	International Atomic Energy Agency
IBiS	Isotopes in Biogenic Silica
ICP	Inductively Coupled Plasma
ICTJA	Institut de Ciències de la Terra-'Jaume Almera'
IPE	Instituto Pirenaico de Ecología
IRMS	Isotope ratio mass spectrometry
ITCZ	InterTropical Convergence Zone
LEC	Lancaster Environmental Center
LGM	Last Glacial Maximun
LML	Local Meteoric Line
LRC	Limnological Research Center
MSCL	Multi-Sensor Core Logger
MTM	Multi-Taper Method
NAO	North Atlantic Oscillation
NBS	National Bureau of Standards; National Institute of Standards and Technology
NERC	Natural Environment Research Council
NIGL	NERC Isotope Geosciences Laboratory
OM	Organic Matter
OES	Optical Emission Spectroscopy
PCA	Principal Component Analysis
PDO	Pacific Decadal Oscillation
P/E	Precipitation/Evaporation ratio
PhD	Doctor of Philosophy
RDA	Redundancy Analysis
RML	Regional Meteoric Line
SASM	South American Summer Monsoon
SDV	Silica Deposition Vesicle
SEM	Scanning Electron Microscopes
SLAP	Standard Light Antarctic Precipitation
SPCZ	South Pacific Convergence Zone
SPLITT	Gravitational split-flow lateral-transport thin
SST	Sea Surface Temperature

SWF	Stepwise Fluorination
TC	Total Carbon
TDS	Total Dissolved Solids
TF	Time-Frequency
TOC	Total Organic Carbon
UB	Universitat de Barcelona
UCN	Universidad Católica del Norte
UDC	Universidade da Coruña
UK	United Kingdom
USA	United States of America
VPDB	Vienna Peedee Belemnite
VSMOW	Vienna Standard Mean Ocean Water
XRD	X-Ray Diffraction
XRF	X-Ray Fluorescence
YD	Younger Dryas chronozone
3D	Three Dimensions

aff	affinis
asl	above sea level
ca	circa
cal	calibrated
m/e	mass-to-charge ratio
n	number of samples
na	not available
sd	standard deviation
spp	species

Units

ppm	parts per million
‰	per mil; one part per thousand
%	percentage
wt%	weight percentage
cps	counts per second
µm	micrometre
mm	millimetre
cm	centimetre
m	metre
km	kilometre
km^2	square kilometre
ml	millilitre
Hm^3	cubic hectometre
mm yr^{-1}	millimetre per year
l s^{-1}	litre per second
m^3yr^{-1}	cubic metre per year
l s^{-1}	litre per second
g l^{-1}	grams per litre
mg cm^{-2} yr^{-1}	milligrams per square metres and year
million valves g^{-1}	million valves per gram
º	degree
ºC	degree Celsius
h	hour
Myrs	million years
µS cm^{-1}	microsiemens per centimetre
Wm^{-2}	Watts per square metres
Hz	hertz

Appendix B

Final isotope data

Sample Identifier	Extraction Number (FF____)	Yield %	del 18 O V-SMOW Raw	Run Correction	**del 18 O V-SMOW Run Corrected**	**Within Run Reproducibility (1 sigma)**	**Between Run Reproducibility (1 sigma)**	Comments
TA-02	FF24958	71	+41,56	-1,27	**40,3**			
TA-04	FF24957	71,5	+41,34	-1,27	**40,1**			
TA-05	FF24960	71	+42,21	-1,27	**40,9**			
TA-08	FF24961	62,9	+42,41	-1,27	**41,1**			
TA-09	FF24962	72,1	+42,62	-1,27	**41,3**			
TA-12	FF24963	55,9	+49,64	-1,27	**48,4**			SAMPLE WET- REPEATED
TA-12/X	FF24968	68	+43,50	-1,56	**41,9**			
TA-13	FF24966	71,6	+41,12	-1,27	**39,8**			
TA-15	FF24969	69,4	+42,35	-1,56	**40,8**			
TA-18	FF24970	70	+43,17	-1,56	**41,6**			
TA-20	FF24972	62	+41,64	-1,56	**40,1**			
TA-22	FF24944	65,7	+40,25	-1,47	**38,8**			DROPPED - AIR IN VESSEL ANALYSIS POOR
TA-22/X	FF24964	71,5	+41,38	-1,27	**40,1**			
TA-23	FF24946	66,1	+41,91	-1,47	**40,4**			
TA-25	FF24947	67,8	+42,24	-1,47	**40,8**			
TA-27	FF24948	66,2	+41,67	-1,47	**40,2**			
TA-31	FF24949	69,2	+41,08	-1,47	**39,6**			
TA-34	FF24951	68,8	+41,49	-1,47	**40,0**			
TA-36	FF24952	64,7	+41,06	-1,47	**39,6**			
TA-37	FF24954	68,5	+40,56	-1,47	**39,1**			
TA-40	FF24973	67,0	+42,12	-1,56	**40,6**			
TA-41	FF24974	74,4	+40,82	-1,56	39,3			
TA-41/B	FF24978	59,7	+40,94	-1,56	39,4			
				MEAN	**39,3**	**0,1**		
TB-02	FF25072	64,7	+40,93	-1,31	**39,6**			
TB-04	FF25073	69,0	+41,00	-1,31	**39,7**			
TB-06	FF25074	69,1	+40,26	-1,31	**38,9**			
TB-07	FF25080	68,3	+40,86	-1,72	**39,1**			
TB-09	FF25081	67,0	+39,70	-1,72	38,0			
TB-09/B	FF25086	69,4	+39,65	-1,72	37,9			
				MEAN	**38,0**	**0,03**		
TB-12	FF25083	73,6	+40,73	-1,72	**39,0**			
TB-14	FF25084	64,7	+41,06	-1,72	**39,3**			
TB-16	FF25085		+40,73	-1,72	**39,0**			
TB-20	FF25088	66,7	+39,19	-1,43	**37,8**			
TB-21	FF25089	71,8	+40,37	-1,43	**38,9**			
TB-24	FF25090	72,2	+40,46	-1,43	**39,0**			
TB-25	FF25092	70,3	+40,11	-1,43	38,7			
TB-25/B	FF25096	72,6	+39,93	-1,43	38,5			
				MEAN	**38,6**	**0,13**		
TB-27	FF25093	70,6	+40,12	-1,43	**38,7**			
TB-29	FF25106	71,0	+37,50	-1,52	**36,0**			
TB-32	FF25097	73,7	+38,10	-1,43	**36,7**			
TB-33	FF25098	73,9	+39,11	-1,43	**37,7**			
TB-36	FF25094	69,0	+40,91	-1,43	**39,5**			
TC-001	FF24975	71,7	+40,26	-1,56	**38,70**			
TC-004	FF24976	69,7	+38,32	-1,56	**36,76**			
TC-005	FF24985	73,6	+38,69	-1,61	**37,08**			
TC-005/X	FF24993	72,7	+38,30	-1,21	**37,09**			
				MEAN	**37,08**		**0,01**	
TC-007	FF24981	65,8	+39,62	-1,61	**38,01**			
TC-009	FF24982	73,1	+38,55	-1,61	**36,94**			

TC-010	FF24983	72,7	+39,58	-1,61	**37,97**			
TC-011	FF25828	72,7	+37,94	-1,07	**36,87**			
TC-012	FF24986	60,2	+37,24	-1,61	**35,63**			
TC-013	FF24987	71,6	+39,96	-1,61	**38,35**			
TC-014	FF25829	73,0	+37,34	-1,07	**36,27**			
TC-015	FF25830	67,2	+38,93	-1,07	**37,86**			
TC-015/B	FF25835	72,0	+39,22	-1,07	**38,15**			
				MEAN	**38,01**	**0,21**		
TC-016	FF24988	63,6	+39,46	-1,61	**37,85**			
TC-017	FF24989	68,9	+39,54	-1,61	**37,93**			
TC-018	FF25832	67,6	+40,74	-1,07	**39,67**			
TC-019	FF24994	73,5	+39,56	-1,21	**38,35**			
TC-020	FF25833	71,7	+38,44	-1,07	**37,37**			
TC-021	FF24995	73,2	+40,00	-1,21	**38,79**			
TC-021/X	FF25834	71,5	+38,59	-1,07	37,52			
TC-021/X	FF26278	61,8	+38,62	-1,09	**37,53**			
				MEAN	**37,53**		**0,00**	
TC-022	FF25836	69,6	+39,14	-1,07	**38,07**			
TC-023	FF25838	71,7	+38,36	-1,07	**37,29**			
TC-024	FF24996	75,8	+39,86	-1,21	**38,65**			
TC-025	FF25840	71,7	+38,38	-1,02	**37,36**			
TC-026	FF24998	77,2	+38,12	-1,21	**36,91**			
TC-027	FF24999	71,7	+39,00	-1,21	**37,79**			
TC-028	FF25841	70,2	+37,88	-1,02	**36,86**			
TC-029	FF25000	77,3	+39,56	-1,21	**38,35**			
TC-030	FF25842	74,4	+39,75	-1,02	**38,73**			
TC-031	FF25843	74,9	+39,51	-1,02	**38,49**			
TC-032	FF25001	72,0	+39,56	-1,21	**38,35**			
TC-032	FF25845	70,5	+38,92	-1,02	**37,90**			
TC-032/B	FF25849	74,6	+39,08	-1,02	**38,06**			
				MEAN	**38,10**		**0,23**	
TC-033	FF25002	77,5	+38,15	-1,21	**36,94**			
TC-034	FF25846	77,3	+38,60	-1,02	**37,58**			
TC-035	FF25004	75,0	+37,85	-1,33	**36,52**			
TC-036	FF25847	75,2	+38,64	-1,02	**37,62**			
TC-037	FF25006	68,7	+37,29	-1,33	**35,96**			
TC-038	FF25848	77,4	+38,69	-1,02	**37,67**			
TC-039	FF25007	69,1	+39,65	-1,33	**38,32**			
TC-039/X	FF25101	69,7	+39,52	-1,52	**38,00**			
				MEAN	**38,16**		**0,22**	
TC-040	FF25853	72,7	+37,28	-0,77	**36,51**			
TC-041	FF25854	64,7	+38,69	-0,77	**37,92**			
TC-042	FF25008	71,5	+38,88	-1,33	**37,55**			
TC-042/B	FF25011	72,9	+38,14	-1,33	**36,81**			
				MEAN	**37,18**	**0,53**		
TC-042/X	FF26277	70,4	+36,87	-1,09	**35,78**			
TC-042/XX	FF26298	68,8	+36,42	-0,88	**35,54**			
				MEAN	**35,66**		**0,17**	
TC-043	FF25009	70,6	+38,82	-1,33	**37,49**			
TC-044	FF25855	65,6	+36,95	-0,77	**36,18**			
TC-044/B	FF25858	65,1	+37,27	-0,77	**36,50**			
				MEAN	**36,34**	**0,11**		
TC-046	FF25012	71,4	+36,86	-1,33	**35,53**			
TC-046	FF258566	64,2	+36,17	-0,77	**35,40**			
				MEAN	**35,46**		**0,09**	
TC-047/X	FF26008	74,7	+37,54	-0,6	**36,94**			
TC-047	FF25859	67,0	+37,94	-0,77	**37,17**			
				MEAN	**37,05**		**0,16**	
TC-049	FF25014	74,6	+38,90	-1,33	**37,57**			
TC-050	FF25860	?	+38,12	-0,77	**37,35**			
TC-051	FF25861	71,0	+38,97	-0,77	**38,20**			
TC-052	FF25016	70,6	+38,12	-1,5	**36,62**			
TC-053	FF25862	69,4	+38,68	-0,77	**37,91**			
TC-054	FF25017	70,1	+39,20	-1,5	**37,70**			
TC-055	FF25864	77,9	+37,66	-0,36	**37,30**			
TC-056	FF25019	68,8	+39,34	-1,5	**37,84**			
TC-057	FF25020	68,4	+39,22	-1,5	**37,72**			

TC-058	FF25021	68,8	+39,21	-1,5	**37,71**			
TC-059	FF25022	67,1	+38,13	-1,5	**36,63**			
TC-059/B	FF25026	68,7	+38,70	-1,5	**37,20**			
				MEAN	**36,92**	**0,40**		
TC-059/X	FF26279	71,7	+38,71	-1,09	**37,61**			
				MEAN	**37,15**	**0,49**		
TC-060	FF25024	72,5	+38,80	-1,5	**37,30**			
TC-061	FF25025	68,5	+38,66	-1,5	**37,16**			
TC-062	FF25866	74,3	+36,89	-0,36	**36,53**			
TC-063	FF25028	76,7	+37,78	-1,28	**36,50**			
TC-064	FF25867	71,9	+37,54	-0,36	**37,18**			
TC-065	FF25868	75,3	+37,75	-0,36	**37,39**			
TC-066	FF25029	73,0	+39,69	-1,28	**38,41**			
TC-066/B	FF25034	73,8	+40,18	-1,28	**38,90**			
				MEAN	**38,65**	**0,35**		
TC-066	FF25869	79,0	+38,19	-0,36	**37,83**			
				MEAN	**38,38**		**0,53**	
TC-067	FF25030	71,2	+39,44	-1,28	**38,16**			
TC-068	FF25871	75,1	+38,25	-0,36	**37,89**			
TC-068/B	FF25874	74,0	+38,44	-0,36	**38,08**			
				MEAN	**37,99**	**0,13**		
TC-069	FF25872	79,6	+36,27	-0,36	**35,91**			
TC-069/X	FF26009	?	+36,42	-0,6	**35,82**			
				MEAN	**35,86**		**0,06**	
TC-070	FF25032	73,9	+38,26	-1,28	**36,98**			
TC-071	FF25033	73,8	+39,98	-1,28	**38,70**			
TC-072	FF26010	77,3	+35,66	-0,6	**35,06**			
TC-073	FF25888	68,2	+38,21	-1,02	**37,19**			
TC-074	FF25035	70,8	+39,77	-1,28	**38,49**			
TC-075	FF25037	79,0	+39,28	-1,28	**38,00**			
TC-076	FF25038	74,4	+39,29	-1,28	**38,01**			
TC-076	FF25889	69,0	+39,56	-1,02	**38,54**			
				MEAN	**38,28**		**0,38**	
TC-077	FF26046	75,9	+38,61	-0,8	**37,81**			
TC-077/B	FF26050	78,5	+38,48	-0,8	**37,68**			
				MEAN	**37,75**	**0,09**		
TC-078	FF25040	74,2	+38,69	-1,39	**37,30**			
TC-079	FF25892	69,8	+38,60	-1,02	**37,58**			
TC-079/B	FF25897	66,0	+38,85	-1,02	**37,83**			
				MEAN	**37,70**	**0,17**		
TC-080	FF25041	73,7	+40,05	-1,39	**38,66**			
TC-081	FF25053	68,8	+38,98	-1,39	**37,59**			
TC-082	FF25893	67,1	+38,83	-1,02	**37,81**			
TC-083	FF25043	70,6	+40,31	-1,39	**38,92**			
TC-084	FF25894	72,3	+41,15	-1,02	**40,13**			
TC-085	FF25695	68,9	+39,36	-1,02	**38,34**			
TC-086	FF25045	74,0	+40,02	-1,39	**38,63**			BATCH#10 BFC DATA POOR USE AVERAGE RUN CORRECTION
TC-086/B	FF25050	67,2	+39,63	-1,39	**38,24**			
				MEAN	**38,44**	**0,28**		
TC-087	FF24046	77,5	+40,30	-1,39	**38,91**			
TC-088	FF25047	73,3	+39,41	-1,39	**38,02**			
TC-089	FF25048	75,6	+39,29	-1,39	**37,90**			
TC-090	FF25054	69,3	+40,58	-1,34	**39,24**			
TC-091	FF25055	70,0	+40,14	-1,34	**38,80**			AVERAGE RUN CORRECTION = 28.88 - 30.22 = -1.34
TC-091/X	FF25102	69,9	+40,03	-1,52	**38,51**			
				MEAN	**38,66**		**0,20**	
TC-092	FF25056	64,5	+39,01	-1,34	**37,67**			
TC-093	FF25057	69,1	+40,58	-1,34	**39,24**			
TC-094	FF25898	68,4	+39,01	-1,02	**37,99**			
TC-095	FF25900	67,0	+38,82	-0,82	**38,00**			
TC-096	FF25058	66,4	+39,96	-1,34	**38,62**			
TC-097	FF25076	67,8	+38,76	-1,72	**37,04**			
TC-098	FF25901	71,7	+37,78	-0,82	**36,96**			
TC-099	FF25903	69,2	+38,40	-0,82	**37,58**			
TC-100	FF25077	67,1	+40,03	-1,72	**38,31**			
TC-101	FF25079	68,2	+39,15	-1,72	**37,43**			
TC-102	FF25905	70,1	+39,36	-0,82	**38,54**			

TC-103	FF25906	72,1	+39,26	-0,82	**38,44**			
				MEAN	**38,03**		**0,58**	
TC-103/X	FF26274	67	+38,49	-1,09	**37,39**			
				MEAN	**37,51**	**0,16**		
TC-104	FF25909	59,8	+38,83	-1,13	**37,70**			
TC-104/X	FF26012	74,2	+38,04	-0,6	**37,44**			
				MEAN	**37,57**		**0,18**	
TC-105	FF25066	69,2	+39,81	-1,31	**38,50**			
TC-106	FF26013	73,7	+37,99	-0,6	**37,39**			
TC-107	FF25067	71,0	+39,02	-1,31	**37,71**			
TC-107/B	FF25070	67,1	+38,81	-1,31	**37,50**			
				MEAN	**37,60**	**0,15**		
TC-108	FF25068	69,8	+32,38	-1,31	**31,07**			
TC-108/X	FF25103	71,5	+32,73	-1,52	**31,21**			
				MEAN	**31,14**		**0,10**	
TC-109	FF25911	72,1	+36,47	-1,13	**35,34**			
TC-110	FF25071	67,4	+37,57	-1,31	**36,26**			
TC-110/X	FF25105	67,5	+36,92	-1,52	**35,40**			
				MEAN	**35,83**		**0,60**	
TC-110/X	FF26276	68,8	+36,58	-1,09	**35,49**			
				MEAN	**35,45**	**0,06**		
TC-111	FF26048	77,8	+37,85	-0,8	**37,05**			
3-060	FF25993	76,8	+41,51	-0,77	**40,7**			
3-070	FF25995	69,1	+40,87	-0,77	**40,1**			
3-080	FF25996	74,7	+40,10	-0,77	**39,3**			
3-090	FF25997	74,6	+40,28	-0,77	**39,5**			
3-095	FF25944	69,0	+37,77	-1,42	**36,3**			
3-100	FF25845	71,4	+38,08	-1,42	**36,7**			
3-110	FF25946	74,7	+39,92	-1,42	38,5			
3-110/B	FF25949	66,6	+40,30	-1,42	38,9			
				MEAN	**38,7**			
3-115	FF25848	76,3	+38,95	-1,42	**37,5**			
3-120	FF25951	69,6	+40,24	-1,42	**38,8**			
3-130	FF25952	71,7	+39,98	-1,42	**38,6**			
3-135	FF25953	69,3	+40,82	-1,42	**39,4**			
3-140	FF25954	68,5	+40,46	-1,42	**39,0**			
3-145	FF25956	73,4	+40,46	-0,99	**39,5**			
3-149	FF25957	74,1	+40,25	-0,99	**39,3**			
4-001	FF25958	76,8	+40,59	-0,99	**39,6**			
4-005	FF25959	74,2	+40,23	-0,99	**39,2**			
4-010	FF25961	66,3	+40,70	-0,99	**39,7**			
4-015	FF25962	69,6	+40,82	-0,99	**39,8**			
4-020	FF25964	76,8	+41,25	-0,99	**40,3**			
4-025	FF25971	77,2	+41,11	-0,99	40,1			
4-025/B	FF25976	76,8	+40,85	-0,99	39,9			
				MEAN	**40,0**	**0,2**		
4-030	FF25972	78,4	+41,10	-0,99	**40,1**			
4-040	FF25973	73,0	+41,07	-0,99	**40,1**			
4-045	FF25974	74,1	+40,71	-0,99	**39,7**			
4-050	FF25977	71,8	+39,30	-0,99	**38,3**			
4-060	FF25978	74,0	+40,06	-0,99	**39,1**			
4-070	FF25980	69,1	+38,86	-1,24	**37,6**			
4-080	FF25982	74,0	+39,44	-1,24	**38,2**			
4-085	FF25983	73,4	+39,83	-1,24	**38,6**			
4-090	FF25984	71,8	+39,28	-1,24	38,0			
4-090/B	FF25987	72,6	+40,12	-1,24	38,9			
				MEAN	**38,5**	**0,6**		
4-100	FF25985	69,0	+37,06	-1,24	**35,8**			
4-110	FF25986	69,0	+38,92	-1,24	**37,7**			
4-120	FF26052	74,8	+36,27	-0,8	**35,5**			
4-130	FF25989	70,2	+35,94	-1,24	**34,7**			
4-140	FF25990	72,8	+39,01	-1,24	**37,8**			
4-147	FF25992	72,7	+38,73	-0,77	**38,0**			
5-001	FF25913	65,2	+39,16	-1,13	**38,0**			
5-010	FF25914	75,0	+40,38	-1,13	**39,3**			
5-015	FF25915	71,2	+40,08	-1,13	**39,0**			
5-020	FF25918	74,0	+39,17	-1,13	**38,0**			

5-020	FF25918	74,0	+39,17	-1,13	**38,0**			
5-030	FF25920	67,3	+38,19	-1,23	**37,0**			
5-040	FF25922	76,5	+38,13	-1,23	**36,9**			
5-050	FF25923	73,4	+39,29	-1,23	**38,1**			
5-060	FF25924	67,2	+38,89	-1,23	37,7			
5-060/X	FF26049	77,0	+38,57	-0,8	37,8			
				MEAN	**37,7**		**0,1**	
5-070	FF25925	70,6	+38,79	-1,23	**37,6**			
5-080	FF25927	69,1	+39,18	-1,23	**37,9**			
6-001	FF25928	74,0	+36,46	-1,23	**35,2**			
6-002	FF25929	67,8	+38,81	-1,23	**37,6**			
6-010	FF25932	71,8	+37,44	-0,52	**36,9**			
6-020	FF25933	69,5	+39,13	-0,52	**38,6**			
6-030	FF25935	70,8	+39,09	-0,52	**38,6**			
6-050	FF25936	70,8	+38,51	-0,52	38,0			
6-050/B	FF25842	69,8	+38,91	-0,52	38,4			
				MEAN	**38,2**	**0,3**		
6-060	FF25938	74,8	+38,53	-0,52	**38,0**			
6-062	FF25939	71,8	+38,50	-0,52	**38,0**			
6-070	FF25940	74,9	+37,44	-0,52	**36,9**			
6-076	FF25941	71,9	+37,75	-0,52	**37,2**			
TEPHRA								
2-007-T	FF25998	80,1	+8,31	-0,77	7,5			
2-007-T/B	FF26002	82,5	+8,14	-0,77	7,4			
				MEAN	**7,5**	**0,1**		
2-041-T	FF25999	73,2	+8,33	-0,77	**7,6**			
2-121-T	FF26000	79,7	+7,93	-0,77	**7,2**			
2-080-T	FF26004	81,2	+7,84	-0,6	**7,2**			
3-040-T	FF26005	80,5	+8,15	-0,6	**7,6**			
BFC	FF24945		+30,35					
BFC	FF24959		+30,49					
BFC	FF24962		+29,78					
BFC	FF24965		+30,17					
BFC	FF24977		+30,22					
BFC	FF24971		+30,65					
		MEAN	**30,28**					
		1s	**0,3**					
FF25065/BFC		76,1	+30,42					
FF25069/BFC		76,6	+29,95	-1,31				RUN CORRECTION IS OFFSET OFMEAN OF THE BFC STDS FROM THE PREFFERED VALUE
FF25078/BFC		75,8	+30,58					
FF25082/BFC		76,3	+30,61	-1,72				
FF25091/BFC		78,8	+30,39					
FF25095/BFC		78,9	+30,22	-1,43				
FF25104/BFC		78,2	+30,40	-1,52				PREFERED VALUE BFC = 28.88 WRT NBS 28
		MEAN	**+30,37**					
		1s	**0,2**					
BFC	FF24971	74,0	+30,65					
	FF24977	79,2	+30,22					
	FF24984	73,2	+30,72					
	FF24990	75,4	+30,26					
	FF24992	79,0	+29,50					
	FF24997	80,3	+30,11					
	FF25005	78,0	+30,21					
	FF25010	82,9	+28,85					
	FF25018	78,1	+30,41					
	FF25023	78,0	+30,35					
	FF25031	78,9	+30,27					
	FF25036	81,5	+30,05					
	FF25044	78,4	+30,32					
	FF25049	78,8	+30,22					
	FF25065	76,1	+30,42					
	FF25069	76,6	+29,95					
	FF25078	75,8	+30,58					

	FF25104	78,2	+30,40					
	FF25831	78,9	+29,81					
	FF25837	77,9	+30,09					
	FF25844	81,0	+29,68					
	FF25850	81,4	+30,12					
	FF25852	76,3	+29,38					
	FF25857	76,3	+29,91					
	FF25865	84,1	+28,75					
	FF25870	78,8	+29,72					
	FF25891	74,0	+29,72					
	FF25896	75,9	+30,07					
	FF25904	80,7	+29,70					
	FF25908	78,3	+29,60					
	FF25917	76,2	+30,41					
	FF26007	80,1	+29,15					
	FF26014	79,6	+29,81					
	FF26047	80,7	+29,64					
	FF26041	79,6	+29,71					
	FF26275	79,8	+30,11					
	FF26283	80,4	+29,83					
		MEAN	**+29,98**					
		1s	**0,5**					
BFC	FF25908	78,3	+29,60					
	FF25917	76,2	+30,41					
	FF25930	76,3	+30,11					
	FF25934	78,9	+28,86					
	FF25937	77,4	+29,93					
	FF25947	78,4	+30,12					
	FF25950	76,8	+30,47					
	FF25960	81,3	+29,84					
	FF25963	79,4	+30,09					
	FF25875	81,5	+30,13					
	FF25968	80,4	+29,60					
	FF25988	78,8	+30,16					
	FF25981	79,4	+30,08					
	FF25994	79,6	+29,69					
	FF26001	78,4	+29,60					
	FF26007	80,1	+29,15					
	FF26053	83,0	+30,02					
	FF26054	77,9	+29,68					
	FF26055	78,1	+29,90					
	FF26056	80,2	+29,11					
		MEAN	**29,83**					
		1s	**0,4**					
Carbon Samples								
Sample	depth	depth	Age	**d13C**	**%C**	**%N**	**C/N**	
11-3-060	351,3	-351,3	-7357	-25,0	0,09	0,13	0,67	
11-3-070	365,8	-365,8	-7493	-25,7	0,04	0,13	0,34	
11-3-080	421,7	-421,7	-8016	-25,0				
11-3-090	445,7	-445,7	-8265	-23,2	0,20	0,15	1,38	
11-3-095	453,2	-453,2	-8354	-24,6	0,54	0,18	3,06	
11-3-100	460,7	-460,7	-8444	-25,3	0,42	0,21	1,98	
11-3-110	473,5	-473,5	-8595	-26,5	0,17	0,16	1,10	
11-3-115	479,9	-479,9	-8671	-26,2	0,24	0,07	3,23	
11-3-120	486,3	-486,3	-8747	-25,5	0,29	0,07	3,85	
11-3-130	499,1	-499,1	-8913	-25,8	0,26	0,08	3,49	
11-3-135	506,0	-506,0	-9008	-26,4	0,07	0,10	0,74	
11-3-140	513,0	-513,0	-9103	-24,3	0,44	0,08	5,23	
11-3-145	521,0	-521,0	-9211	-29,8	0,08	0,11	0,72	
11-3-149	527,4	-527,4	-9298	-24,3	0,41	0,11	3,68	
11-4-001	531,0	-531,0	-9348	-24,5	0,22	0,07	3,33	
11-4-005	539,2	-539,2	-9459	-26,0	0,17	0,08	2,29	
11-4-010	549,5	-549,5	-9598	-26,7	0,26	0,11	2,47	
11-4-015	559,7	-559,7	-9720	-27,5	0,09	0,06	1,71	
11-4-020	569,9	-569,9	-9842	-25,7	0,17	0,07	2,38	

11-4-025	576,0	-576,0	-9915	-24,0	0,19	0,04	5,11	
11-4-030	582,1	-582,1	-9987	-23,6	0,27	0,04	6,83	
11-4-040	592,3	-592,3	-10108	-23,3	0,23	0,06	3,93	
11-4-040 (II)				-24,8	0,11	0,04		
11-4-045	597,4	-597,4	-10168	-22,6	0,29	0,04	6,77	
11-4-050	602,5	-602,5	-10228	-22,9	0,42	0,07	5,97	
11-4-060				-24,9				
11-4-060 (II)	612,6	-612,6	-10349	-25,7	0,24	0,05	4,49	
11-4-070	622,8	-622,8	-10432	-26,8	0,20	0,05	3,74	
11-4-080	633,0	-633,0	-10502	-27,1	0,20	0,05	3,74	
11-4-085	638,0	-638,0	-10538	-26,8	0,26	0,05	5,59	
11-4-090	643,1	-643,1	-10573	-25,9	0,16	0,05	3,35	
11-4-100	653,3	-653,3	-10643	-24,5	0,24	0,05	5,02	
11-4-110	663,5	-663,5	-10714	-27,7	0,21	0,04	5,12	
11-4-120	673,6	-673,6	-10784	-26,8	0,37	0,06	6,53	
11-4-130	683,8	-683,8	-10855	-27,3	0,37	0,06	6,22	
11-4-140	693,9	-693,9	-10925	-27,3	0,18	0,05	3,83	
11-4-147	701,1	-701,1	-10966	-28,0	0,10	0,03	3,85	
11-5-001	705,1	-705,1	-10988	-25,4	0,21	0,05	4,10	
11-5-010	714,3	-714,3	-11037	-27,0	0,08	0,09	0,95	
11-5-015	719,4	-719,4	-11064	-26,0	0,25	0,05	4,57	
11-5-020	724,4	-724,4	-11091	-26,5	0,24	0,11	2,15	
11-5-030	734,6	-734,6	-11145	-28,6	0,21	0,03	6,84	
11-5-030				-26,7				
11-5-040	744,8	-744,8	-11205	-27,9	0,06	0,10	0,54	
11-5-050	754,9	-754,9	-11279	-26,8	0,04	0,12	0,35	
11-5-060	765,1	-765,1	-11354	-27,7	0,02	0,11	0,16	
11-5-070	774,2	-774,2	-11422	-27,3	0,08	0,05	1,55	
11-5-080	775,3	-775,3	-11429	-26,7	0,08	0,06	1,44	
11-6-001	790,5	-790,5	-11558	-28,9	0,19	0,07	2,76	
11-6-002	791,7	-791,7	-11568	-26,6	0,09	0,06	1,53	
11-6-010	799,7	-799,7	-11654	-26,9	0,07	0,06	1,14	
11-6-020	809,8	-809,8	-11760	-27,1	0,08	0,05	1,46	
11-6-030	820,0	-820,0	-11867	-27,2	0,07	0,06	1,15	
11-6-040	830,2	-830,2	-11986					
11-6-050	840,3	-840,3	-12105	-27,5	0,02	0,06	0,33	
11-6-060	850,5	-850,5	-12232	-27,4	0,30	0,06	5,32	
11-6-060 (II)				-29,2				
11-6-062	852,5	-852,5	-12257	-28,6	0,01	0,06	0,11	
11-6-070	860,7	-860,7	-12359	-30,3	0,16	0,03	5,75	
11-6-076	863,7	-863,7	-12396	-29,6	0,04	0,06	0,65	
	%C	%N	C/N					
BROC1	41,4	4,5	9,2					
BROC1	38,9	4,2	9,3					
BROC1	39,6	4,4	9,0					
BROC1	40,5	4,0	10,1					
BROC1	40,4	4,2	9,7					
BROC1	39,1	4,1	9,5					
BROC1	40,4	3,9	10,3					
BROC1	41,7	4,3	9,6					
BROC1	41,7	4,8	8,7					
BROC1	41,0	5,1	8,1					

Appendix C

Original papers

JOURNAL OF QUATERNARY SCIENCE (2008) **23**(4) 351–363

Published online in Wiley InterScience
(www.interscience.wiley.com) DOI: 10.1002/jqs.1173

The palaeohydrological evolution of Lago Chungará (Andean Altiplano, northern Chile) during the Lateglacial and early Holocene using oxygen isotopes in diatom silica

ARMAND HERNÁNDEZ,[1]* ROBERTO BAO,[2] SANTIAGO GIRALT,[1] MELANIE J. LENG,[3,4] PHILIP A. BARKER,[5] ALBERTO SÁEZ,[6] JUAN J. PUEYO,[6] ANA MORENO,[7,8] BLAS L. VALERO-GARCÉS[7] and HILARY J. SLOANE[3]
[1] Institute of Earth Sciences 'Jaume Almera' (CSIC), Barcelona, Spain
[2] Faculty of Sciences, University of A Coruña, A Coruña, Spain
[3] NERC Isotope Geosciences Laboratory, British Geological Survey, Nottingham, UK
[4] School of Geography, University of Nottingham, Nottingham, UK
[5] Department of Geography, Lancaster Environment Centre, Lancaster University, Lancaster, UK
[6] Faculty of Geology, University of Barcelona, Barcelona, Spain
[7] Pyrenean Institute of Ecology (CSIC), Zaragoza, Spain
[8] Limnological Research Center, University of Minnesota, Minneapolis, Minnesota, USA

Hernández, A., Bao, R., Giralt, S., Leng, M. J., Barker, P. A., Sáez, A., Pueyo, J. J., Moreno, A., Valero-Garcés, B. L. and Sloane, H. J. 2008. The palaeohydrological evolution of Lago Chungará (Andean Altiplano, northern Chile) during the Lateglacial and early Holocene using oxygen isotopes in diatom silica. *J. Quaternary Sci.*, **Vol. 23** pp. 351–363. ISSN 0267-8179.

Received 30 July 2007; Revised 21 December 2007; Accepted 22 December 2007

ABSTRACT: Oxygen isotopes of diatom silica and petrographical characterisation of diatomaceous laminated sediments of Lago Chungará (northern Chilean Altiplano) have allowed us to establish its palaeohydrological evolution during the Lateglacial–early Holocene (ca. 12 000–9400 cal. yr BP). These laminated sediments are composed of light and dark pluriannual couplets of diatomaceous ooze formed by different processes. Light sediment laminae accumulated during short-term diatom blooms whereas dark sediment laminae represent the baseline limnological conditions during several years of deposition. Oxygen isotope analysis of the dark diatom laminae show a general $\delta^{18}O$ enrichment trend during the studied period. Comparison of these $\delta^{18}O_{diatom}$ values with the previously published lake-level evolution suggests a correlation between $\delta^{18}O_{diatom}$ and the precipitation:evaporation ratio, but also with the evolution of other local hydrological factors as changes in the groundwater outflow as well as shifts in the surface:volume ratio of Lago Chungará. The lake expanded (probably increasing this ratio) during the rising lake-level trend due to changes in its morphology, enhancing evaporation. Furthermore, the lake's hydrology was probably modified as the groundwater outflow became sealed by sediments, increasing lake water residence time and potential evaporation. Both factors could cause isotope enrichment. © Natural Environment Research Council (NERC) copyright 2008. Reproduced with the permission of NERC. Published by John Wiley & Sons, Ltd.

KEYWORDS: diatom ooze; laminated sediments; oxygen isotopes; rhythmites; Holocene; Andean Altiplano.

Introduction

Oxygen isotopes of diatom silica have been widely used in palaeoenvironmental reconstructions from lake sediments in the last decade (see Leng and Barker, 2006, for a comprehensive review). Using oxygen isotope ratios in palaeoenvironmental reconstruction is, however, not easy, because the sedimentary record can be influenced by a wide range of interlinked environmental processes ranging from regional climate change to local hydrology. The oxygen isotopic composition of diatom silica depends on the isotope composition of the water when the skeleton of the siliceous micro-organisms is secreted, and also on the ambient water temperature (Shemesh *et al.*, 1992). Therefore, knowledge of all the environmental factors that may have influenced the isotope composition of the lake water is vital for the interpretation of the

* Correspondence to: A. Hernández, Institute of Earth Sciences 'Jaume Almera' (CSIC), C/Lluís Solé i Sabarís s/n, E-08028 Barcelona, Spain.
E-mail: ahernandez@ija.csic.es

Contract/grant sponsor: Spanish Ministry of Science and Education; contract/grant numbers: BTE2001-3225, BTE2001-5257-E, CGL2004-00683/B, TECGL2007-60932/BTE.

$\delta^{18}O_{diatom}$ signal (Leng *et al.*, 2005a). One of these environmental factors is evaporation, which has a major influence on the isotope composition of any standing water body (Leng and Marshall, 2004). The $\delta^{18}O$ record can therefore be used, at least in closed lakes, as an indicator of changes in the precipitation to evaporation ratio (*P*/*E*) related to climatic changes (Leng and Marshall, 2004). Yet, before any palaeoclimatic interpretation of the isotope records from a lake is considered, other local palaeohydrological intervening factors from the basin need to be taken into account (Sáez and Cabrera, 2002; Leng *et al.*, 2005a).

The sedimentary records of high-altitude Andean Altiplano lakes are good candidates for carrying out oxygen isotope studies to reconstruct the late Quaternary palaeoclimatology of the region. They preserve an excellent centennial- to millennial-scale record of effective moisture fluctuations and source changes during the Lateglacial and Holocene, although the interpretation is not always straightforward (Abbot *et al.*, 1997; Argollo and Mourguiart, 2000; Valero-Garcés *et al.*, 2000, 2003; Grosjean *et al.*, 2001; Baker *et al.*, 2001a, 2001b; Tapia *et al.*, 2003; Fritz *et al.*, 2004, 2006; Placzek *et al.*, 2006). The $\delta^{18}O$ analyses of carbonates, cellulose and biogenic silica have successfully been used to reconstruct the hydrological responses to climate change in different Andean lacustrine systems (Schwalb *et al.*, 1999; Seltzer *et al.*, 2000; Abbott *et al.*, 2000, 2003; Wolfe *et al.*, 2001; Polissar *et al.*, 2006).

Up to now, only stable isotopes in carbonates have been examined in Lago Chungará (Valero-Garcés *et al.*, 2003), although its sedimentary record is made up of rich diatomaceous ooze ideal for diatom silica oxygen isotope studies. Lago Chungará currently behaves as a closed lake, without any surface outlet, and evaporation is the dominant water loss process (Herrera *et al.*, 2006); however, it has shown a complex depositional history since the Lateglacial (Sáez *et al.*, 2007) and the relative role of other factors (groundwater *versus* evaporation) should be evaluated.

Here we examine a high-resolution $\delta^{18}O$ diatom silica record of three selected sections belonging from the Lateglacial to early Holocene (ca. 12,000–9400 cal. yr BP) from Lago Chungará. We emphasise the role that some local factors such as sedimentary infill and palaeohydrology can play on the interpretation of the $\delta^{18}O$ diatom silica record and therefore the need to discriminate between the climatic and local environmental signals.

The Lago Chungará

Geology, climate and limnology

Lago Chungará (18°15′ S, 69°10′ W, 4520 m a.s.l.) is located at the NE edge of Lauca Basin, in the Chilean Altiplano. It lies in a highly active tectonic and volcanic context (Clavero *et al.*, 2002). The lake sits in the small hydrologically closed Chungará Sub-Basin, which was formed as a result of a debris avalanche during the partial collapse of the Parinacota Volcano, damming the former Lauca River (Fig. 1(A)). Lago Chungará and Lagunas Cotacotani were formed almost immediately. The collapse post-avalanche event has been dated and the ages range between 18 000 cal. yr BP, using He-exposure techniques (Wörner *et al.*, 2000; Hora *et al.*, 2007), and 11 155–13 500 ^{14}C yr BP, employing radiocarbon dating methods (Francis and Wells, 1988; Baied and Wheeler, 1993; Amman *et al.*, 2001). In these cases the authors dated lacustrine sediments from Lagunas Cotacotani. In addition, Clavero *et al.* (2002, 2004) dated palaeosol horizons by radiocarbon and proposed a maximum age of 8000 ^{14}C yr BP for the collapse.

Lago Chungará is situated in the arid Central Andes, in a region dominated by tropical summer moisture (Garreaud *et al.*, 2003). The isotope composition of rainfall (Aravena *et al.*, 1999; Herrera *et al.*, 2006) and the synoptic atmospheric precipitation patterns (Ruttlant and Fuenzalida, 1991) indicate that the main moisture source comes from the Atlantic Ocean via the Amazon Basin. During the summer months (DJFM) weak easterly flow prevails over the Altiplano as a consequence of the southward migration of the subtropical jet stream and the establishment of the Bolivian high-pressure system (Garreaud *et al.*, 2003). This narrow time window defines the wet season in the Altiplano (Valero-Garcés *et al.*, 2003). Mean annual rainfall in the Chungará region is about 350 mm · yr^{-1}, but the actual range is variable (100–750 mm · yr^{-1}). Mean temperature is 4.2°C and the potential evaporation was estimated at over 4750 mm · yr^{-1} (see references in Valero-Garcés *et al.*, 2000).

In this region, a significant fraction of the inter-annual variability of summer precipitation is currently related to the El Niño Southern Oscillation (ENSO) (Vuille, 1999). El Niño years seem to be recorded in the Sajama and Quelcaya ice cores by significant decreases in snow accumulation (Thompson *et al.*, 1986; Vuille, 1999). Instrumental data from the Chungará region show a reduction of the precipitation during moderate to intense El Niño years. However, there is no direct relationship between the relative El Niño strength and the amount of rainfall reduction (for further details see Valero-Garcés *et al.*, 2003).

Rainfall isotope composition in this region is characterised by a large variability in $\delta^{18}O$ (between +1.2 and −21.1‰ SMOW) and of δD (between +22.5 and −160.1‰ SMOW). The origin of the lightest isotope values are the strong kinetic fractionation in the air masses from the Amazon. The altitudinal isotopic gradient of $\delta^{18}O$ in the Chungará region is very high (between +0.76‰/100 m and +2.4‰/100 m) compared with other worldwide regions (Herrera *et al.*, 2006).

Lago Chungará has an irregular shape with a maximum length of 8.75 km, maximum water depth of 40 m, a surface area of 21.5 km^2 and a volume of 400×10^6 m^3 (Mühlhauser *et al.*, 1995; Herrera *et al.*, 2006) (Fig. 1(B)). The western and northern lake margins are steep, formed by the eastern slopes of Ajoya and Parinacota volcanoes. The eastern and southern margins are gentle, formed by the distal fringe of recent alluvial fans and the River Chungará valley (Sáez *et al.*, 2007). At present, the main inlet to the lake is the Chungará River (300–460 L · s^{-1}), although secondary streams enter the lake in the southwestern margin. The main water loss is by evaporation (3.10^7 m^3 · yr^{-1}) but it has been estimated that groundwater outflow from Lago Chungará to Lagunas Cotacotani is about 6–7.10^6 m^3 · yr^{-1} (Dorador *et al.*, 2003). The calculated residence time for the lake's water is approximately 15 yr (Herrera *et al.*, 2006). The lake is polymictic, oligomesotrophic to meso-eutrophic (Mühlhauser *et al.*, 1995), contains 1.2 g · L^{-1} of total dissolved solids, its conductivity ranges between 1500 and 3000 μS · cm^{-1} (Dorador *et al.*, 2003) and the water chemistry is of Na–Mg–HCO_3–SO_4 type. Temperature profiles measured in November 2002 showed a gradient from the lake surface (9.1–12.1°C) to the lake bottom (6.2–6.4°C at 35 m of water depth), with a thermocline (0.5–0.6°C) located at about 19 m of water depth. Oxygen ranged from 11.9–12.5 ppm (surface) to 7.6 ppm (bottom) and the pH oscillated between 8.99 (surface) and 9.30 (bottom). Lake water is enriched by evaporation with regard to rainfall and spring waters. The mean values of $\delta^{18}O$ and δD are −1.4‰ SMOW and −43.4‰ SMOW, respectively (Herrera *et al.*,

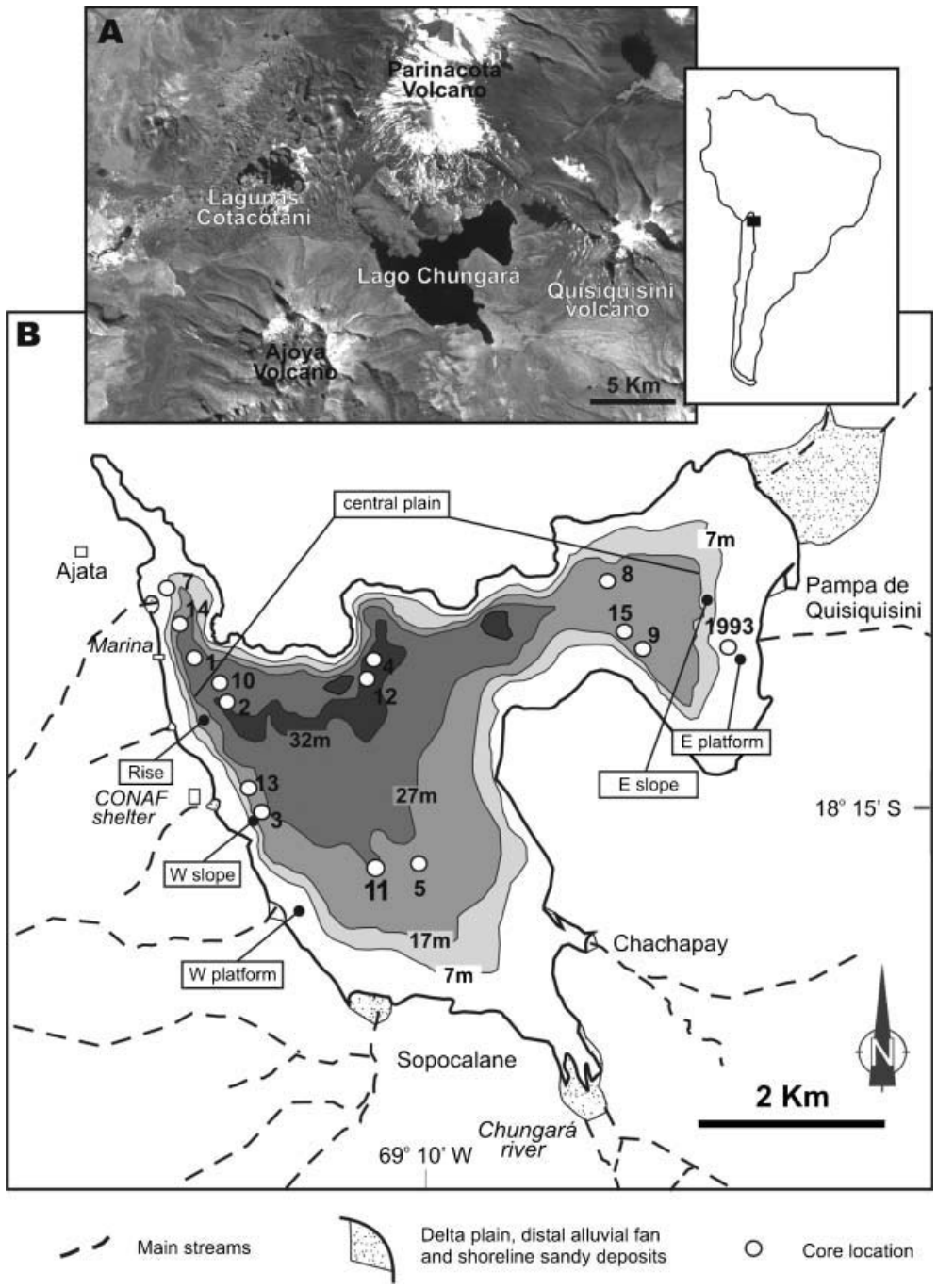

Figure 1 (A) Location of Lago Chungará on NE edge of Lauca Basin. (B) Bathymetric map of Lago Chungará showing the main morphological units of the lake floor and position of the sediment cores

2006). Primary productivity is mainly governed by diatoms and chlorophyceans (Dorador *et al.*, 2003). Macrophyte communities in the littoral zone form dense patches that contribute to primary productivity. Seasonal measurements of conductivity, nitrate, phosphate and chlorophyll reveal these changes in productivity and in the composition of algal communities are mainly due to changes in water temperature and salinity (Dorador *et al.*, 2003). The absence of raised lacustrine deposits around the lake margins suggests that the current level of the lake is at its highest since lake formation (Sáez *et al.*, 2007).

Previous work and sedimentary sequence

In November 2002 15 sediment cores (6.6 cm inner diameter and up to 8 m long) were recovered from Lago Chungará using a raft equipped with a Kullenberg system. All cores were cut in 1.5 m sections and physical properties (GRAPE density, p-wave velocity and magnetic susceptibility) were measured in the laboratory using a GEOTEK™ multi-sensor core logger (MSCL) at 1 cm intervals. Afterwards, the cores were split into two halves, scanned using a DMT colour scanner, and the textures, colours and sedimentary structures were described. Smear slides were prepared for the description of the sediment composition and to estimate the biogenic, clastic and endogenic mineral content.

After a detailed lithological correlation of the cores (Sáez *et al.*, 2007), cores 10 and 11 located offshore were selected for conducting the palaeoenvironmental reconstruction. A composite core recording the whole sedimentary infill (minimum thickness of 10 m) of the offshore zone was constructed from the detailed description and correlation of cores 10 and 11. From here on all core depths are referred to this composite core.

DOI: 10.1002/jqs

From the bottom to the top of the core, two sedimentary units (units 1 and 2) were identified and correlated mainly using tephra keybeds. These lithological units were subdivided into two subunits (subunits 1a, 1b, 2a and 2b). Basal unit 1a ranges between 0.58 m and 2.56 m of thickness and is made up of finely laminated green and whitish diatomaceous ooze. Unit 1b (from 0.62 m to 1.87 m thick) is composed of laminated and massive brown diatomaceous ooze with carbonate-rich intervals. Unit 2a (between 1.56 m and 3.44 m thick) is made up of a brown diatomaceous ooze with tephra layers and carbonate-rich intervals. The sediments of the uppermost unit 2b range from 0.86 m to 3 m in thickness and they are composed of dark grey to black diatomaceous ooze with abundant tephra layers (for further details see Moreno *et al.*, 2007, and Sáez *et al.*, 2007).

The cores have been analysed for a number of proxies including X-ray fluorescence (XRF), X-ray diffraction (XRD), total organic and inorganic carbon (TOC and TIC), pollen, diatoms and total biogenic silica (Moreno *et al.*, 2007; Sáez *et al.*, 2007).

The chronological model for the sedimentary sequence of Lago Chungará is based on 17 AMS ^{14}C dates of bulk organic matter and aquatic plant macrofossils, and one ^{238}U/^{230}Th date from carbonates. The radiocarbon dates were performed in the Poznan Radiocarbon Laboratory (Poland), whereas the ^{238}U/^{230}Th sample was analysed by high-resolution inductively coupled plasma–infrared mass spectrometry (ICP-IRMS) at the University of Minnesota (Edwards *et al.*, 1987; Cheng *et al.*, 2000; Shen *et al.*, 2002). The present-day reservoir effect was determined by dating the dissolved inorganic carbon (DIC) of the lake water at the Beta Analytics Inc. laboratory (USA). The real reservoir effect of the lake was calculated by correcting the DIC radiocarbon date for the effects of thermonuclear bomb tests (Hua and Barbetti, 2004). The calibration of radiocarbon dates was performed using CALIB 5.02 software and the INTCAL98 curve (Stuiver *et al.*, 1998; Reimer *et al.*, 2004). The software described in Heegaard *et al.* (2005) was used to construct the final age–depth model (see Moreno *et al.*, 2007, and Giralt *et al.*, 2007, for details).

Materials and methods

Three intervals from unit 1 were selected and sampled for thin-section study and δ^{18}O diatom silica analysis. Interval 1 (located at the subunit 1a, between 831 cm and 788 cm core depth) is made up of finely laminated green and whitish sediments. Interval 2 (between 605 cm and 622 cm core depth) is found in the transition between subunits 1a and 1b and is made up of laminated green and pale-brown diatomaceous ooze. Interval 3 (located at subunit 1b, between 537 cm and 574 cm core depth) is made up of laminated dark-brown and white diatomaceous ooze with carbonates. The selection criteria of these three intervals are discussed below.

The chronological model defines the corresponding age of the three intervals. Interval 1 was deposited between 11 990 and 11 530 cal. yr BP, interval 2 between 10 430 and 10 260 cal. yr BP and interval 3 between 9890 and 9430 cal. yr BP.

Each interval was continuously covered by thin sections. Thin sections of 120 mm × 35 mm (30 μm in thickness), with an overlap of 1 cm at each end, were obtained after freeze-drying and balsam-hardening. Detailed petrographical descriptions and lamina thickness measurements were performed using a Zeiss Axioplan 2 Imaging petrographic microscope. Several samples were also selected for observation with a Jeol JSM-840 electron microscope in order to complement the petrographical study.

Each lamina of the three intervals was sampled with a blade for isotope analysis. A total of 190 samples (111 samples from interval 1, 37 samples from interval 2 and 42 samples from interval 3) were obtained. However, a selection of 37 samples from dark laminae were selected for $\delta^{18}O_{diatom}$ analyses to investigate the baseline hydrological evolution of Lago Chungará. These dark laminae would represent a normal annual cycle of the lake with alternating phases of stratification and mixing. These conditions would lead to the development of a complex diatom community, among other algal groups (Hernández *et al.*, 2007). Analysis of the oxygen isotope composition of diatom silica from these 37 samples requires that the material is almost pure diatomite (Juillet-Leclerc, 1986), so a meticulous protocol involving chemical attack, sieving, settling and laminar flow separation was performed. Specifically, our samples were treated following the method proposed by Morley *et al.* (2004), with some variations (Fig. 2(A)). The first stage (chemical attack) followed the standard method in order to remove the carbonates (10% HCl) and organic matter (hydrogen peroxide) (Battarbee *et al.*, 2001), but also included a further step using concentrated HNO_3 in order to remove any remaining organic matter. The second stage (sieving at 125 μm) allowed us to eliminate resistant charcoal and terrigenous particles. The 63 μm and 38 μm sieves allowed us to obtain a fraction of quasi-monospecific diatoms (*Cyclostephanos andinus*) in most of the samples. The third stage was an alternative approach to heavy liquid separation. Gravitational split-flow thin fractionation (SPLITT) was employed at Lancaster University (UK) (Rings *et al.*, 2004; Leng and Barker, 2006). The SPLITT technique was only applied to the most problematic samples which contained remaining difficult-to-separate clay and fine tephra particles. In the final step, the purified diatom samples were dried at 40°C for 24–48 h. After the cleaning process six samples were checked with XRD, total carbon (TC) analysis and scanning electron microscopy (SEM) observations. This checking process revealed that the samples did not contain significant terrigenous matter. The TC values were below 0.5% wt and the terrigenous content (clays or tephra) was less than 1% wt (Fig. 2(B)). Although a large number of diatoms were broken during the cleaning process, this did not affect the final isotope data. We therefore assume that the δ^{18}O values of the purified samples retained climatic and hydrological information (Morley *et al.*, 2004; Leng and Barker, 2006).

Oxygen extraction for isotope analyses followed the classical step-wise fluorination method (Matheney and Knauth, 1989). The method involved three steps. First, the hydrous layer was stripped by outgassing in nickel reaction tubes at room temperature. Second, a pre-fluorination clean-up step involved a stoichiometric deficiency of reagent, bromine pentafluoride (BrF_5), heated at 25°C for several minutes. The final step was a full reaction at 450°C for 12 h with an excess of BrF_5. The oxygen liberated was converted to CO_2 by exposure to hot graphite (following Clayton and Mayeda, 1963). The oxygen yield was monitored, for every sample, by comparison with the calculated theoretical yield for SiO_2. The intervals examined here had mean yields of 69–70% of their theoretical yield based on silica. This fact suggests that around 30% of the material, including hydroxyl and loosely bonded water (both OH^- and H_2O), was removed during prefluorination. A random selection of five samples was analysed in duplicate, giving a reproducibility between 0.01‰ and 0.6‰ (1σ). The standard laboratory quartz and a diatomite control sample (BFC) had a mean reproducibility over the period of analysis of 0.2‰. The CO_2 was analysed for ^{18}O/^{16}O using a Finnigan™ Matt 253 mass spectrometer. The results were calibrated *versus*

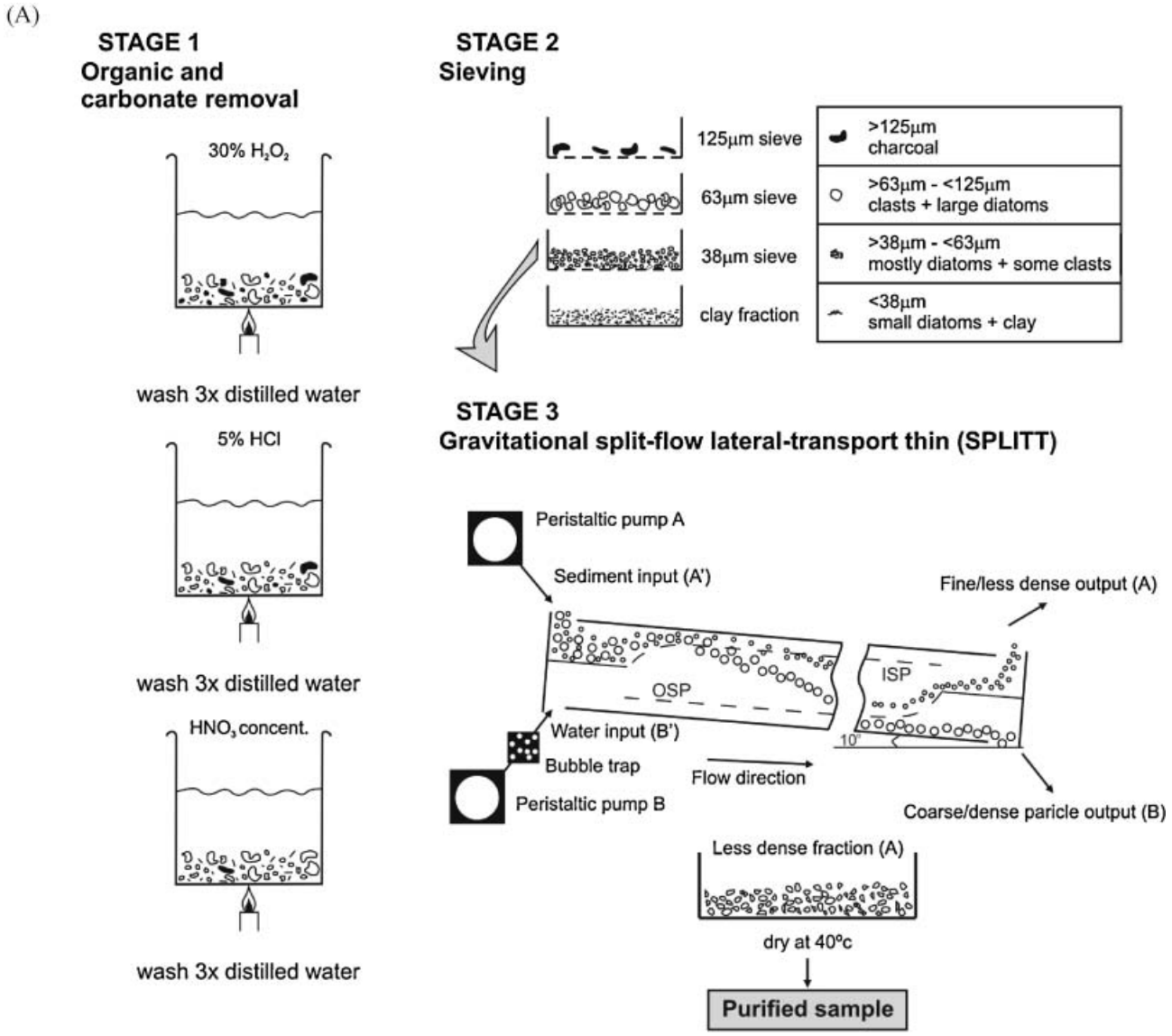

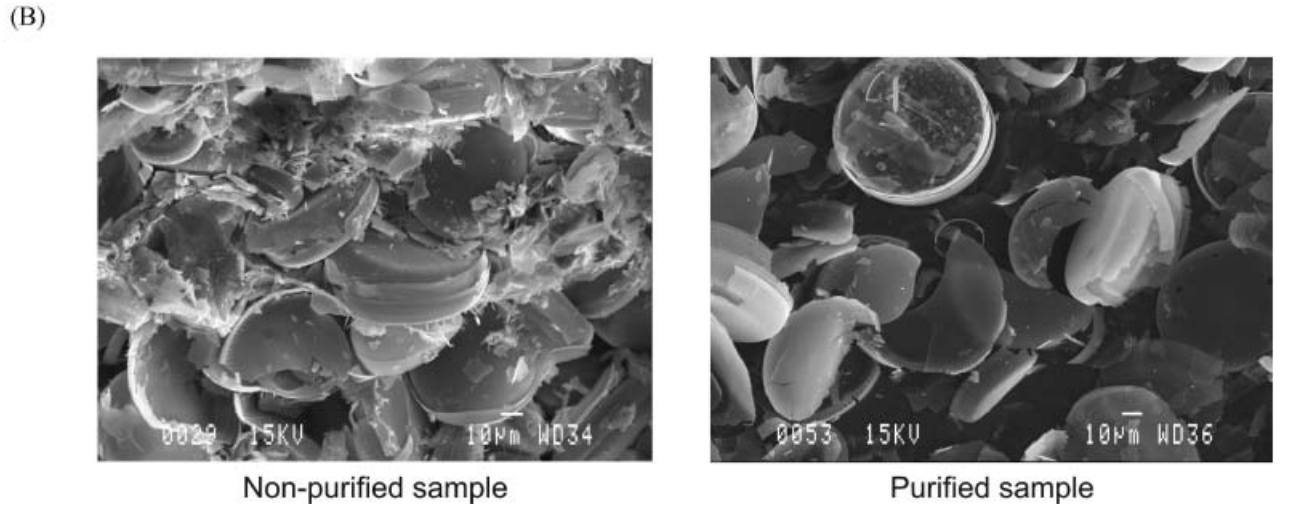

Figure 2 (A) Diagram showing the three-stage cleaning method for concentrating diatoms for oxygen isotope analysis (modified from Morley *et al.*, 2004). (B) SEM images of two samples before cleaning (left) and after cleaning (right)

NBS-28 quartz international standard. Data are reported in the usual delta form (δ) as per mil (‰) deviations from V-SMOW. The fluorination process and the $^{18}O/^{16}O$ ratios measured were carried out at the NERC Isotope Geosciences Laboratory, British Geological Survey (UK).

Results: petrography and isotope composition of diatoms

Smear slide, SEM and several analyses (XRD, TC, biogenic silica) of the lake sediments before they were prepared for isotope analysis showed that the samples were composed of both amorphous and crystalline material. The amorphous fraction comprises biogenic silica (between 47% and 58% weight), organic matter and volcanic glass. The crystalline fraction represented <10% of the sediments.

Interval 1 (11 990–11 530 cal. yr BP)

Diatom concentration ranges from 108.3 to 633.8 million valves g^{-1}. The interval is dominated by euplanktonic diatoms ranging from 79.1% to 93.9% of the diatom assemblage. The thicknesses of the laminae are between 0.9 and 10.3 mm (Fig. 3(A)). Smear slide, thin section and SEM observations showed that light laminae were quasi-monospecific layers of large *Cyclostephanos andinus* (diameter > 50 μm) (Fig. 4(D)). The upper contact of the light laminae with the dark laminae is transitional, showing an increase in diatom diversity with subdominant tychoplanktonic (*Fragilaria* spp.) and benthic diatoms (mainly *Cocconeis* spp., *Achnanthes* spp., *Navicula* spp. and *Nitzschia* spp.) (Fig. 4(C)), whereas the lower contact is abrupt (Fig. 4(A)). Diatom valves show good preservation with no preferred orientation in the lower part, but increasingly orientated upwards. The content of the organic matter also increases upwards. Dark laminae comprise a more diverse mixture of diatoms, including the euplanktonic (those having a strict planktonic character) smaller *Cyclostephanos andinus* (diameter < 50 μm) than those found in light laminae, and diatoms of the *Cyclotella stelligera* complex, as well as tychoplanktonic (those usually having a benthic life form but which can occasionally be facultatively planktonic) and benthic diatoms (bottom-dwelling forms) (Fig. 4(B)). These dark laminae are also enriched in organic matter, probably from diatoms and other algal groups. Up to 41 light and dark laminae couplets were defined. The thickness of these couplets ranges between 4.2 mm and 22.5 mm and, according to the chronological model, they are pluriannual (mean about 10 yr). The rhythmite starts with the dominance of light laminae, progressively changing to a dominance of dark laminae.

The $\delta^{18}O_{diatom}$ values of the purified diatoms in interval 1 range from +35.5‰ to +39.2‰ (Fig. 3(A)). Higher $\delta^{18}O_{diatom}$ occur in the lower part of the interval (around 822 cm of core depth). There is an upward decreasing trend (~1.9‰ 100 yr^{-1}) attaining a minimum of +35.5‰ around 803 cm depth. This stretch is followed by an increasing shift of ~2.9‰ 100 yr^{-1} towards the upper part of the interval, where a relative maximum of +38.8‰ is reached at 793 cm depth. The uppermost two samples show a light depletion. The mean $\delta^{18}O_{diatom}$ value of this interval is $+37.8 \pm 0.85$‰.

Interval 2 (10 430–10 260 cal. yr BP)

Diatom concentration ranged from 95.2 to 218 million valves g^{-1} in interval 2. Almost 94% of the diatom assemblages of this interval were made up of euplanktonic diatoms. Benthic taxa show the minimum values for the three analysed intervals. The thickness of diatomaceous ooze laminae ranged from 1.8 mm to 16 mm (Fig. 3(B)). Light laminae were dominated by large *Cyclostephanos andinus* (diameter > 50 μm), with some tychoplanktonic (*Fragilaria* spp.) and benthic diatoms, as well as minor amounts of siliciclasts and organic matter. Dark laminae are composed of a mixture of small and large *Cyclostephanos andinus* valves, with more abundant tychoplanktonic and benthic diatoms (as well as organic matter) compared to light laminae. Diatom valves are not so well preserved as in interval 1, sometimes showing a high degree of fragmentation and a preferred orientation. The contact between the laminae is similar to those found in interval 1. Clear couplets were only observed in the upper two-thirds of the interval and only 10 couplets could be identified (Fig. 3(B)). They are pluriannual (mean couplet represents about 10 yr of sedimentation) and their thicknesses range between 5.5 and 19 mm. Light laminae were more abundant in the upper part of interval 2, whereas dark laminae are more abundant in the lower part.

The $\delta^{18}O_{diatom}$ curve shows a clear increasing trend during this interval (Fig. 3(B)). The lowest $\delta^{18}O_{diatom}$ value (+36‰) was recorded at the bottom of the interval (617 cm depth) and the maximum at the two uppermost samples (+39.7‰ and +39.6‰; 606–605 cm of core depth). The magnitude of the increasing trend is much higher between the two lowermost samples (~18.5‰ 100 yr^{-1}) than for the rest of the interval (~0.6‰ 100 yr^{-1}). The mean $\delta^{18}O_{diatom}$ value of this interval is $+38.7 \pm 1.4$‰.

Interval 3 (9890–9430 cal. yr BP)

Diatom concentration ranges between 163.8 and 255.8 million valves g^{-1} for interval 3. Euplanktonic diatoms (68.6–98.1%) also dominate this interval, and have the minimum values for the three intervals. On the contrary, benthic diatoms show moderate values (up to 31.4%), being the highest for the three intervals.

Light diatomaceous ooze laminae ranged between 0.9 and 12.3 mm in thickness (Fig. 3(C)) and they comprise *Cyclostephanos andinus* (diameter > 50 μm), increasing upwards in both taxonomic diversity and organic matter content. The lower contact with dark laminae shows an abrupt change in diatom size, whereas the upper one is gradual. Diatom valves show good preservation with no orientation in the lower part but are preferentially oriented upwards. Dark laminae comprise a mixture of smaller *Cyclostephanos andinus* (diameter < 50 μm), with subdominant tychoplanktonic and benthic diatoms, as well as a high organic matter content. The lower contact is gradual whereas the upper one abrupt. Up to 18 light and dark pluriannual couplets were defined (mean couplet represent around 12 yr). These couplets are 3–18 mm thick. The rhythmite starts with light laminae, progressively changing to dark laminae.

The $\delta^{18}O_{diatom}$ curve for interval 3 (Fig. 3(C)) shows an overall continuous increasing trend of ~0.9‰ 100 yr^{-1} from +39.1‰ (570 cm of core depth) to +41.3‰ (548 cm of core depth). Superimposed over the general trend are short-term fluctuations. The mean $\delta^{18}O_{diatom}$ value of this interval is $+40.1 \pm 0.77$‰.

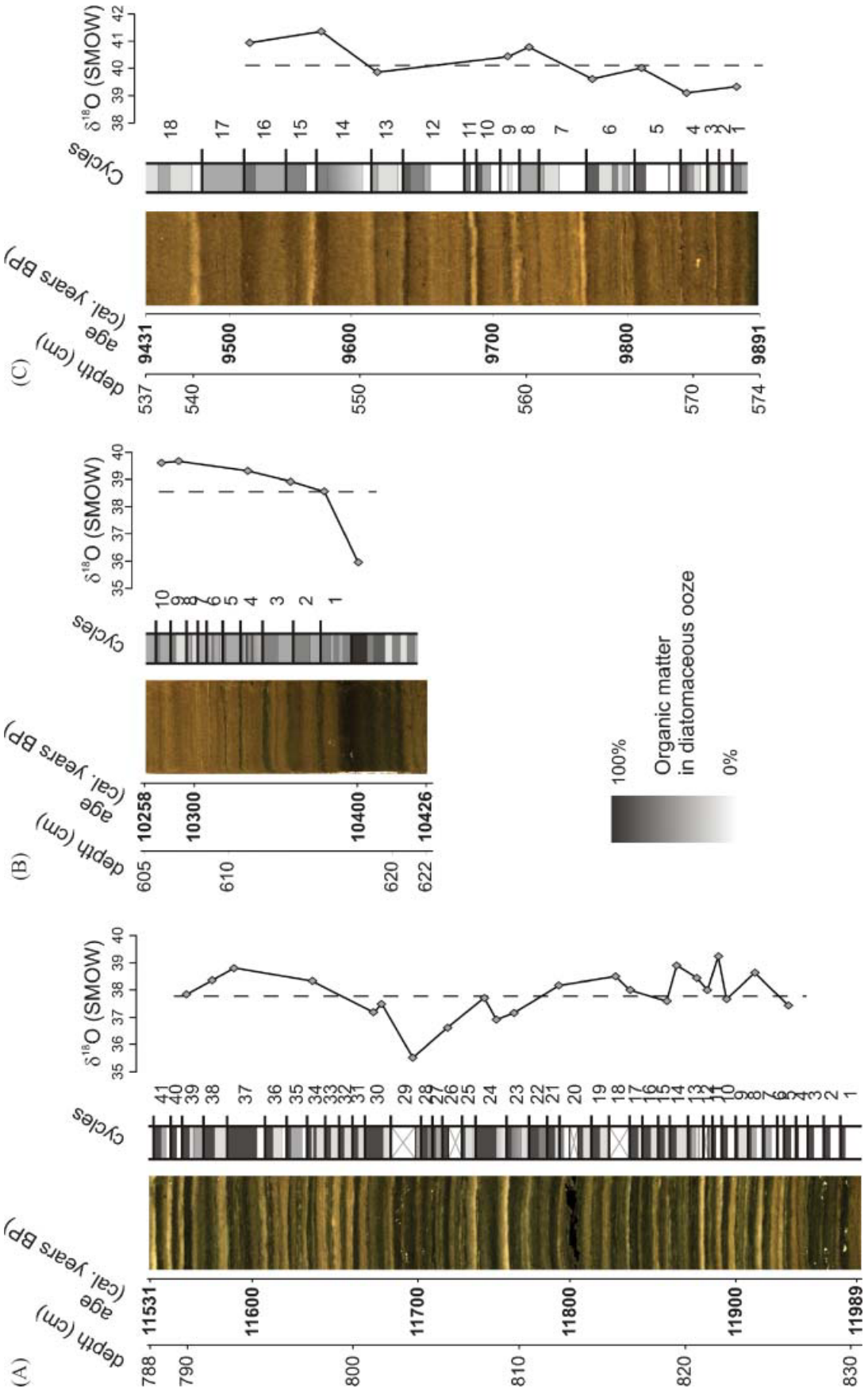

Figure 3 Digital images of the three intervals selected according to its depth and timescale. The identified couplets and the $\delta^{18}O$ values from diatom silica have been plotted for interval 1 (A), interval 2 (B) and interval 3 (C). Stippled line shows mean values

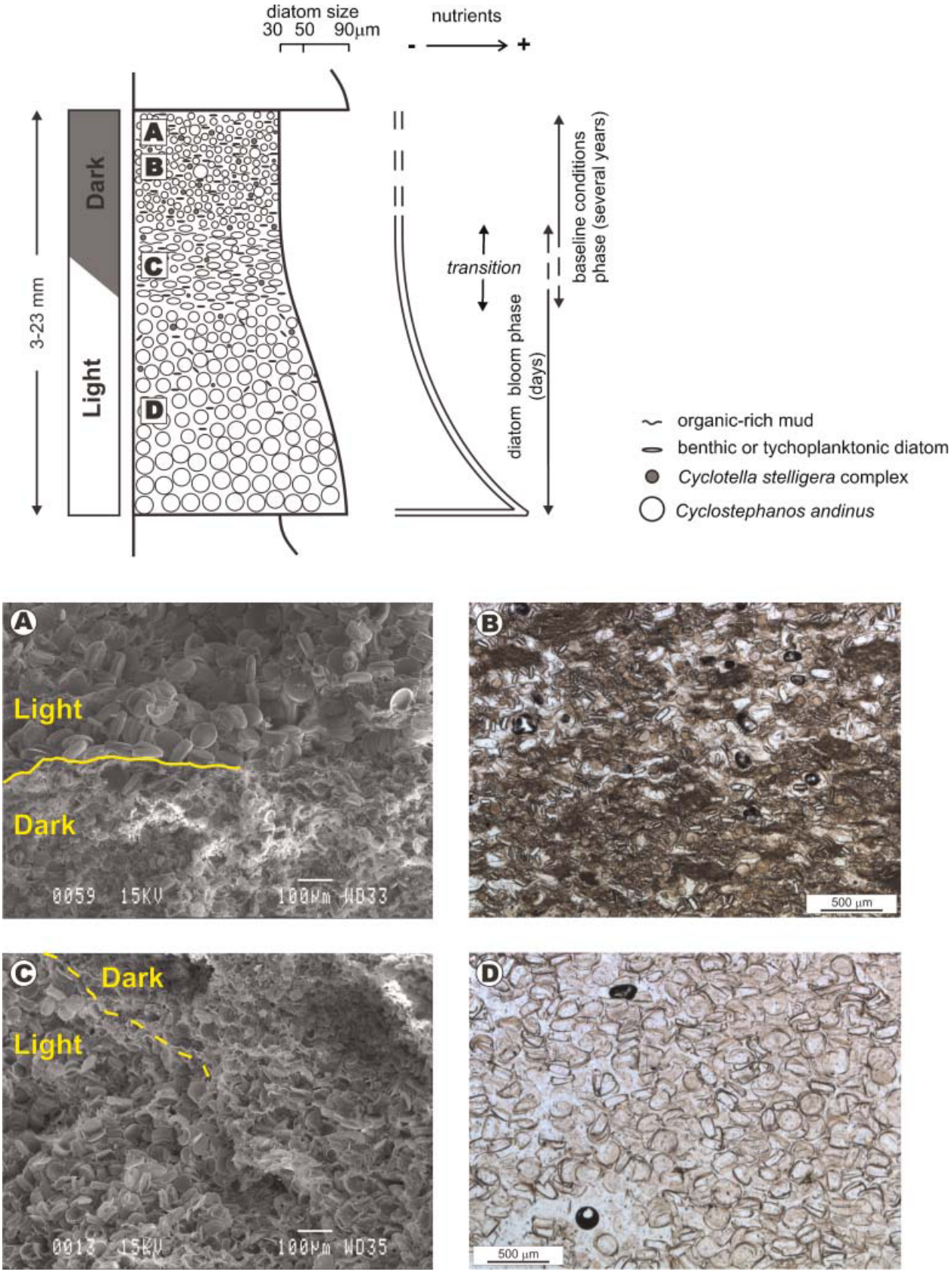

Figure 4 Rhythmite type showing thickness, colour, ecological succession and temporal scale. (A) SEM image showing the contact between dark (bottom) and light lamina (top). (B) Petrographical microscope image of the dark lamina. (C) SEM image showing the transitional contact between light (bottom) and dark lamina (top). (D) Petrographical microscope image of the light lamina. See text for details. This figure is available in colour online at www.interscience.wiley.com/journal/jqs

The three intervals have different $\delta^{18}O_{diatom}$ averages displaying a progressive low-frequency enrichment from interval 1 ($+37.8 \pm 0.85$‰) to interval 3 ($+40.1 \pm 0.77$‰). The overall isotopic enrichment is 2.1‰ throughout these intervals.

Discussion

The sedimentary model of diatom rhythmites

Laminated diatomaceous oozes in the sedimentary record of Lago Chungará comprise variable-thickness couplets of alternating light and dark laminae. These couplets display different features (colour and mean thickness) in the three intervals described here, although they exhibit similar diatom assemblages and textural characteristics, and therefore it is assumed that their formation is by similar environmental processes. Rhythmite types have been established (Fig. 4); light laminae are formed almost exclusively by diatom skeletons of a quasi-monospecific assemblage of *Cyclostephanos andinus*, while dark laminae, with a high organic matter content, comprise a mixture of a more diverse diatom assemblage, including the euplanktonic *Cyclostephanos andinus*, although diatoms of the *Cyclotella stelligera* complex are co-dominant taxa. Subdominant groups are some tychoplanktonic (*Fragilaria* spp.) and benthic taxa (*Cocconeis* spp., *Achnanthes* spp., *Navicula* spp., *Nitzschia* spp.).

Each couplet was deposited during time intervals ranging from 4 to 24 yr according to our chronological model. Couplets are therefore not a product of annual variations in sediment supply but due to some kind of pluriannual processes. The good preservation and size of diatom valves in the light laminae suggest accumulation during short-term extraordinary diatom blooms, perhaps of only days to weeks in duration. These diatom blooms could have been triggered by climatically driven strong nutrient inputs to the lake and/or to nutrient recycling under extreme turbulent conditions and mixing affecting the whole water column. On the contrary, the baseline conditions are represented by the dark laminae. Each of these laminae is made up of the remains (organic matter and diatom skeletons) of a diverse planktonic community deposited throughout several years under different water column mixing regimes. The preserved remains are therefore a reflection of different stages in the phytoplankton succession throughout several years (Reynolds, 2006).

Lake level and $\delta^{18}O_{diatom}$ changes

A preliminary lake-level reconstruction of Lago Chungará was undertaken employing the variations of euplanktonic diatoms, *Botryococcus* and macrophyte remains (see Sáez *et al.*, 2007). This reconstruction shows a general deepening trend during the Lateglacial and early Holocene. This overall increase in lake level is punctuated by one deepening (D1; Fig. 5) and by two shallowing episodes (S1 and S2; Fig. 5). According to Sáez *et al.* (2007) the three selected intervals described here represent two different lacustrine conditions. Intervals 1 and 3 are likely shallower episodes that occurred in different climatic periods, whereas interval 2 occurred during a period between two shallow intervals, and likely with higher lake-level conditions. However, the resolution of the lake-level reconstruction provided by Sáez *et al.* (2007) does not preclude the occurrence of shallowing episodes other than those previously detected. The isotope analyses presented here of these three intervals have allowed us to characterise the hydrological evolution of the lake for these different lacustrine conditions during the Lateglacial and early Holocene. Dark laminae were selected for $\delta^{18}O_{diatoms}$ analyses to investigate the baseline hydrological evolution of Lago Chungará. These dark laminae would represent a normal annual cycle of the lake with alternating phases of stratification and mixing. These conditions would lead to the development of a complex diatom community among other algal groups (Hernández *et al.*, 2007). The $\delta^{18}O_{diatom}$ variation can result from a variety of processes (Jones *et al.*, 2004; Leng *et al.*, 2005b) but for closed lakes, particularly in arid regions where water loss is mainly through evaporation, measured $\delta^{18}O_{water}$ values are always more enriched than those of ambient precipitation since the oxygen lighter isotope (^{16}O) is preferentially lost via evaporation. Under these circumstances, the $\delta^{18}O_{diatom}$ record can be used as an indicator of

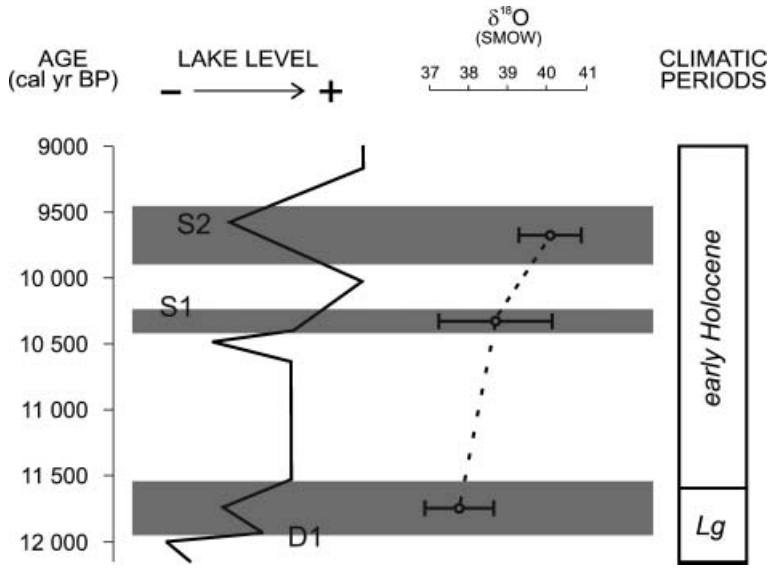

Figure 5 Lake-level evolution curve based on biological indicators (modified from Sáez *et al.*, 2007). Deepening–shallowing episode (D1) and shallowing–deepening episodes (S1 and S2) are indicated. The lake followed an overall deepening trend (see Sáez *et al.*, 2007, for further details). Shaded bands mark the three studied intervals. On the right corresponding mean values of $\delta^{18}O$ from diatom silica of the studied intervals are shown

DOI: 10.1002/jqs

changes in the precipitation:evaporation ratio (*P*/*E*) related to climatic changes (Leng and Marshall, 2004).

Lago Chungará is a hydrologically closed lake and its main water loss is currently via evaporation, meaning that changes in $\delta^{18}O$ values should be directly related to shifts in *P*/*E*. The lake-level change from the deeper-water conditions recorded during the sedimentation of interval 2 to the shallower conditions that occurred during the deposition of interval 3, according to the Sáez *et al*. (2007) reconstruction, is compatible with the observed increase in $\delta^{18}O$ values. However, the isotope values and the lake-level reconstruction do not agree over the transition from interval 1 to interval 2. The isotope values suggest a reduced *P*/*E* (shallower) stage, whereas several proxy indicators suggest deeper conditions (Fig. 5). A possible explanation for this could involve shifts in $\delta^{18}O$ related to other environmental circumstances, such as variations in the morphometrical parameters and changes in the groundwater outflow. Changes in the surface:volume ratio and in groundwater outflow of Lago Chungará from the Lateglacial to early Holocene are the factors likely to account for most of the shifts found in the $\delta^{18}O$ values.

Besides fluctuations in *P*/*E*, another factor to take into account is basin morphology. During the lake's evolution the lake's surface:volume ratio would have changed. A tentative palaeobathymetric reconstruction of Lago Chungará based on the lake-level curve from Sáez *et al*. (2007) (Fig. 6) shows that during the Lateglacial the lake only occupied the present central plain area. The rise in the lake level during the early Holocene, although punctuated by some oscillations, flooded the extensive eastern and southern margins of the basin. Under these circumstances, the lake underwent a significant increase in its surface area (Fig. 6). Because the eastern margin is much shallower than the central plain (Fig. 1), the whole lake's surface:volume ratio would have significantly increased, and also concurrently the relative importance of evaporation. Thus the observed $\delta^{18}O$ high values of interval 3 could be explained

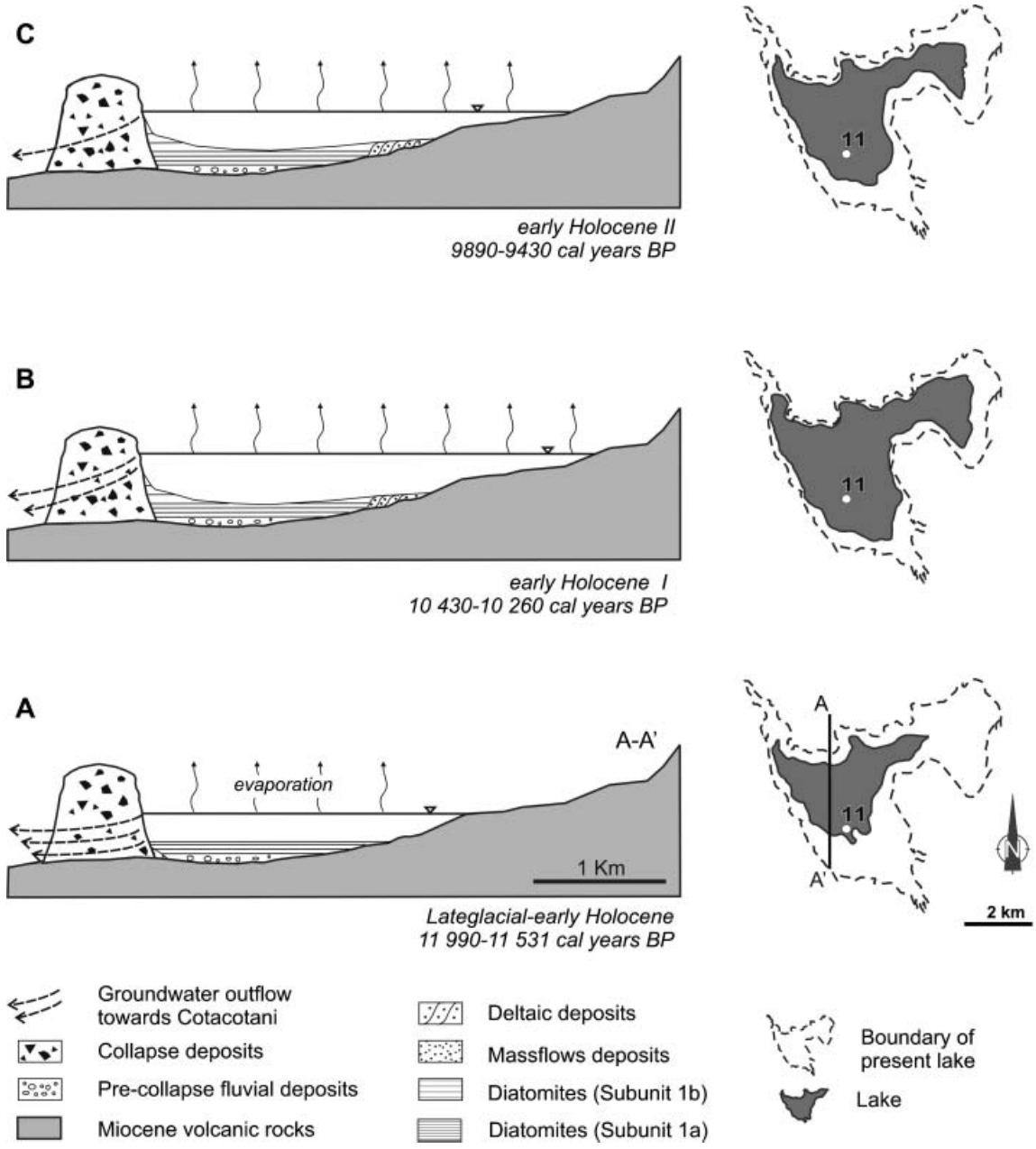

Figure 6 Hydrological evolution of the Lago Chungará in the Lateglacial–early Holocene. North–South cross-section of the lake (left) and water lake surface area (right) for the sedimentation of interval 1 (11 990–11 530 cal. yr BP (A)), interval 2 (10 430–10 260 cal. yr BP (B)) and interval 3 (9890–9431 cal. yr BP (C))

not only by the shallowing trend from interval 2 to interval 3, but also by the increase in the lake's surface:volume ratio between both intervals.

There are no signs of subaerial exposure in the recovered sediments of the eastern platform, which indicates that lake water level did not drop significantly afterwards. Although the lake was deeper during interval 3 than during interval 1, the mean isotope value is higher during interval 3. This fact could be explained by the increase in the surface:volume ratio and by the reduction of groundwater losses. Hence the morphology of the lake, and not only water depth, must be considered as a key factor in any interpretation of the $\delta^{18}O_{diatom}$ in terms of changes in *P*/*E*.

Furthermore, changes in the groundwater fluxes in Lago Chungará could have been a significant factor in the shifts found in the $\delta^{18}O$ values from the Lateglacial to early Holocene. The groundwater outflow from the lake during the Lateglacial was probably higher than during the Holocene. This condition would progressively change with the sedimentary infill of the basin. Drainage, through the breccia barrier, would progressively become less efficient as the groundwater outflows silted up (Leng *et al.*, 2005a). Thus, evaporative losses would have predominated over groundwater during the early Holocene. This highlights the fact that stable isotopes would not, in this case, have a direct correspondence with changes in the lake water level.

In summary, the relative increase in evaporation due to the increase in the lake's surface:volume ratio between the studied intervals could have played a significant role. Superimposed onto this situation, the increase in $\delta^{18}O$ values from the Lateglacial (when the lake was at its shallowest) to the early Holocene (when the overall deepening trend started) is also likely to have been related to a change to a predominantly evaporative lake as the lake's bottom became more impermeable due to sediment basin sealing.

Conclusions

The thin section study of diatomaceous laminated sediments shows that the rhythmites are made up of light quasi-monospecific lamina of the euplanktonic diatom *Cyclostephanos andinus* and a pluriannual dark lamina rich in organic matter and a mixture of a more diverse diatom assemblage. The formation of light laminae is apparently related to short-term (days to weeks) diatom blooms, whereas dark laminae represent baseline conditions lasting several years.

The oxygen isotope record of the dark laminae diatoms of Lago Chungará indicates a progressive $\delta^{18}O$ enrichment from the Lateglacial to early Holocene. Besides changes in the *P*/*E* ratio, two other factors could have governed shifts in the Lago Chungará $\delta^{18}O$ record. The basin's stepped morphology forced the expansion of the lake towards the eastern and southern shallow margins during the rising trend. These changes could have caused an increase in the lake's surface:volume ratio, thus enhancing the evaporation which caused isotope enrichment during the early Holocene. In addition, the hydrology of the lake was probably modified during the Lateglacial to early Holocene transition as the lake's groundwater outflow became progressively sealed by sediments, thereby increasing lake water residence time and potential evaporation. In summary, changes in the groundwater:evaporation loss ratio and changes in the lake's extent caused isotope enrichment during the Lateglacial and early Holocene.

Previous work has focused on issues of diagenesis, contamination and host–water interactions that can all influence $\delta^{18}O_{diatom}$, whereas local hydrological factors have been largely neglected. These results point to the complex interplay among the different factors which intervene in the diatom oxygen isotope record of closed lakes and how interpretation needs to be adapted to the different evolutionary stages of the lake's ontogeny. This study highlights the importance of reconstructing local palaeohydrology as this may be only indirectly related to palaeoclimate.

Acknowledgements The Spanish Ministry of Science and Education funded the research at Lago Chungará through the projects ANDESTER (BTE2001-3225), BTE2001-5257-E, LAVOLTER (CGL2004-00683/BTE) and GEOBILA (CGL2007-60932/BTE). The Limnological Research Center (University of Minnesota, USA) provided the technology and expertise to retrieve the cores. NERC (UK) funded the isotope analysis. We are grateful to CONAF (Chile) for the facilities provided in Chungará. We thank Michael Köhler (GFZ-Potsdam) for the thin sections preparation. Sarah Metcalfe and Antje Schwalb are thanked for their reviews.

References

Abbott MB, Seltzer GO, Kelts K, Southon J. 1997. Holocene paleohydrology of the tropical Andes from Lake Records. *Quaternary Research* **47**: 70–80.

Abbott MB, Wolfe PW, Aravena R, Wolfe AP, Seltzer GO. 2000. Holocene hydrological reconstructions from stable isotopes and paleolimnology, Cordillera Real, Bolivia. *Quaternary Science Reviews* **19**: 1801–1820.

Abbott MB, Wolfe BB, Wolfe AP, Seltzer GO, Aravena R, Mark BG, Polissar PJ, Rodwell DT, Rowe HD, Vuille M. 2003. Holocene paleohydrology and glacial history of the central Andes using multiproxy lake sediment studies. *Palaeogeography, Palaeoclimatology, Palaeoecology* **194**: 123–138.

Amman C, Jenny B, Kammer K, Messerli B. 2001. Late Quaternary glacier response to humidity changes in the arid Andes of Chile (18-29° S). *Palaeogeography, Palaeoclimatology, Palaeoecology* **172**: 313–326.

Aravena R, Suzuki O, Peña H, Pollastri A, Fuenzalida H, Grilli A. 1999. Isotopic composition and origin of the precipitation in northern Chile. *Applied Geochemistry* **14**: 411–422.

Argollo J, Mourguiart P. 2000. Late Quaternary climate history of the Bolivian Altiplano. *Quaternary International* **72**: 37–51.

Baied CA, Wheeler JC. 1993. Evolution of High Andean Puna ecosystem environment, climate and culture change over the last 12 000 years in the Central Andes. *Mountain Research and Development* **13**: 145–156.

Baker PA, Seltzer GO, Fritz SC, Dunbar RB, Grove MJ, Tapia PM, Cross SL, Rowe HD, Broda JP. 2001a. The history of South American tropical precipitation for the past 25 000 years. *Science* **291**: 640–643.

Baker PA, Rigsby CA, Seltzer GO, Fritz SC, Lowenstein TK, Bacher NP, Veliz C. 2001b. Tropical climate changes at millennial and orbital timescales on the Bolivian Altiplano. *Nature* **409**: 698–701.

Battarbee RW, Jones VJ, Flower RJ, Cameron NG, Bennion H, Carvalho L, Juggins S. 2001. Diatoms. In *Tracking Environmental Change Using Lake Sediments*, Smol JP, Birks HJB, Last WM (eds). Kluwer Academic: Dordrecht, Netherlands; 155–202.

Cheng H, Edwards RL, Hoff J, Gallup CD, Richards DA, Asmeron Y. 2000. The half-lives of uranium-234 and thorium-230. *Chemical Geology* **169**: 17–33.

Clavero JE, Sparks SJ, Huppert HE. 2002. Geological constraints on the emplacement mechanism of the Parinacota debris avalanche, northern Chile. *Bulletin of Volcanology* **64**: 40–54.

Clavero JE, Sparks SJ, Polanco E, Pringle M. 2004. Evolution of Parinacota volcano, Central Andes, northern Chile. *Revista Geológica Chile* **31**: 317–347.

Clayton RN, Mayeda TK. 1963. The use of bromine pentafluoride in the extraction of oxygen from oxide and silicates for isotope analysis. *Geochimica et Cosmochimica Acta* **27**: 43–52.

Dorador C, Pardo R, Vila I. 2003. Variaciones temporales de parámetros físicos, químicos y biológicos de un lago de altura: el caso del Lago Chungará. *Revista Chilena de Historia Natural* **76**: 15–22.

Edwards RL, Chen JH, Wasserburg GJ. 1987. ^{238}U-^{234}U-^{230}Th–^{232}Th systematics and the precise measurement of time over the past 500 000 years. *Earth and Planetary Science Letters* **81**: 175–192.

Francis PW, Wells G. 1988. Landsat thematic mapper observations of debris avalanche deposits in the Central Andes. *Bulletin of Volcanology* **50**: 258–278.

Fritz SC, Baker PA, Lowenstein TK, Seltzer GO, Rigsby CA, Dwyer GS, Tapia PM, Arnold KK, Ku TL, Luo S. 2004. Hydrologic variation during the last 170 000 years in the southern hemisphere tropics of South America. *Quaternary Research* **61**: 95–104.

Fritz SC, Baker PA, Tapia P, Garland J. 2006. Spatial and temporal variation in cores from Lake Titicaca, Bolivia/Peru during the last 13 000 years. *Quaternary International* **158**: 23–29.

Garreaud RD, Vuille M, Clement AC. 2003. The climate of the Altiplano: observed current conditions and mechanisms of past changes. *Palaeogeography, Palaeoclimatology, Palaeoecology* **194**: 5–22.

Giralt S, Moreno A, Bao R, Sáez A, Prego R, Valero BL, Pueyo JJ, González-Sampériz P, Taberner C. 2007. Statistical approach to disentangle environmental forcings in a lacustrine record: the Lago Chungará case (Chilean Altiplano). *Journal of Palaeolimnology* (in press). DOI: 10.1007/s10933-007-9151-9.

Grosjean M, van Leeuwen JFN, van der Knaap WO, Geyh MA, Ammann B, Tanner W, Messerli B, Núñez L, Valero-Garcés BL, Veit H. 2001. A 22 000 ^{14}C year BP sediment and pollen record of climate change from Laguna Miscanti (231S), northern Chile. *Global and Planetary Change* **28**: 35–51.

Heegaard E, Birks HJB, Telford RJ. 2005. Relationships between calibrated ages and depth in stratigraphical sequences: an estimation procedure by mixed-effect regression. *The Holocene* **15**: 612–618.

Hernández A, Bao R, Giralt S, Leng MJ, Barker PA, Pueyo JJ, Sáez A, Moreno A, Valero-Garcés B, Sloane HJ. 2007. A high-resolution study of diatom oxygen isotopes in a Late Pleistocene to early Holocene laminated record from Lake Chungará (Andean Altiplano, Northern Chile). *Geochimica et Cosmochimica Acta* **71**: A398.

Herrera C, Pueyo JJ, Sáez A, Valero-Garcés BL. 2006. Relación de aguas superficiales y subterráneas en el área del lago Chungará y lagunas de Cotacotani, norte de Chile: un estudio isotópico. *Revista Geológica de Chile* **33**: 299–325.

Hora J, Singer B, Wörner G. 2007. Volcan eruption and evaporative flux on the thick curst of the Andean Central Volcanic Zone: $^{40}Ar/^{39}Ar$ constrains from Volcán Parinacota, Chile. *Geological Survey of America Bulletin* **119**: 343–362.

Hua Q, Barbetti M. 2004. Review of tropospheric bomb C-14 data for carbon cycle modeling and age calibration purposes. *Radiocarbon* **46**: 1273–1298.

Jones V, Leng MJ, Solovieva N, Sloane H, Tarasov P. 2004. Holocene climate on the Kola Peninsula: evidence from the oxygen isotope record of diatom silica. *Quaternary Science Reviews* **23**: 833–839.

Juillet-Leclerc A. 1986. *Cleaning process for diatomaceous samples*. In *8th Diatom Symposium*, Ricard M (ed.). Koeltz Scientific: Koenigstein, Germany; 733–736.

Leng MJ, Barker PA. 2006. A review of the oxygen isotope composition of lacustrine diatom silica for palaeoclimate reconstruction. *Earth-Science Reviews* **75**: 5–27.

Leng MJ, Marshall JD. 2004. Palaeoclimate interpretation of stable isotope data from lake sediment archives. *Quaternary Science Reviews* **23**: 811–831.

Leng MJ, Lamb AL, Heaton THE, Marshall JD, Wolfe BB, Jones MD, Holmes JA, Arrowsmith C. 2005a. Isotopes in lake sediments. In *Isotopes in Palaeoenvironmental Research*, Leng MJ (ed.). Springer: Dordrecht, Netherlands; 147–184.

Leng MJ, Metcalfe SE, Davies SJ. 2005b. Investigating late Holocene climate variability in Central Mexico using carbon isotope ratios in organic materials and oxygen isotope ratios from diatom silica within lacustrine sediments. *Journal of Palaeolimnology* **34**: 413–431.

Matheney RK, Knauth LP. 1989. Oxygen-isotope fractionation between marine biogenic silica and seawater. *Geochimica et Cosmochimica Acta* **53**: 3207–3214.

Moreno A, Giralt S, Valero-Garcés BL, Sáez A, Bao R, Prego R, Pueyo JJ, González-Sampériz P, Taberner C. 2007. A 13 kyr high-resolution record from the tropical Andes: the Chungará Lake sequence (18° S, northern Chilean Altiplano). *Quaternary International* **161**: 4–21.

Morley DW, Leng MJ, Mackay AW, Sloane HJ, Rioual P, Battarbee RW. 2004. Cleaning of lake sediment samples for diatom oxygen isotope analysis. *Journal of Paleolimnology* **31**: 391–401.

Mühlhauser H, Hrepic N, Mladinic P, Montecino V, Cabrera S. 1995. Water-quality and limnological features of a high-altitude Andean lake, Chungará in northern Chile. *Revista Chilena de Historia Natural* **68**: 341–349.

Placzek C, Quade J, Patchett PJ. 2006. Geochronology and stratigraphy of late Pleistocene lake cycles on the southern Bolivian Altiplano: implications for causes of tropical climate change. *GSA Bulletin* **118**: 515–532.

Polissar PJ, Abbott MB, Shemesh A, Wolfe AP, Bradley RS. 2006. Holocene hydrologic balance of tropical South America from oxygen isotopes of lake sediment opal, Venezuelan Andes. *Earth and Planetary Science Letters* **242**: 375–389.

Reimer PJ, Baillie MGL, Bard E, Bayliss A, Beck JW, Bertrand CJH, Blackwell PG, Buck CE, Burr GS, Cutler KB, Damon PE, Edwards RL, Fairbanks RG, Friedrich M, Guilderson TP, Hogg AG, Hughen KA, Kromer B, McCormac G, Manning S, Ramsey CB, Reimer RW, Remmele S, Southon JR, Stuiver M, Talamo S, Taylor FW, van der Plicht J, Weyhenmeyer CE. 2004. IntCal04 terrestrial radiocarbon age calibration, 0-26cal kyr BP. *Radiocarbon* **46**: 1029–1058.

Reynolds CS. 2006. *The Ecology of Phytoplankton*. Cambridge University Press: Cambridge, UK.

Rings A, Lucke A, Schleser GH. 2004. A new method for the quantitative separation of diatom frustules from lake sediments. *Limnology and Oceanography: Methods* **2**: 25–34.

Ruttlant J, Fuenzalida H. 1991. Synoptic aspects of the central Chile rainfall variability associated with the Southern Oscillation. *International Journal of Climatology* **111**: 63–76.

Sáez A, Cabrera L. 2002. Sedimentological and palaeohydrological responses to tectonics and climate in a small, closed, lacustrine system: Oligocene As Pontes Basin (Spain). *Sedimentology* **49**: 1073–1094.

Sáez A, Valero-Garcés BL, Moreno A, Bao R, Pueyo JJ, González-Sampériz P, Giralt S, Taberner C, Herrera C, Gibert RO. 2007. Volcanic controls on lacustrine sedimentation: the late Quaternary depositional evolution of lake Chungará (northern Chile). *Sedimentology* **54**: 1191–1222.

Schwalb A, Burns SJ, Kelts K. 1999. Holocene environments from stable isotope stratigraphy of ostracods and authigenic carbonate in Chilean Altiplano lakes. *Palaeogeography, Palaeoclimatology, Palaeoecology* **148**: 153–168.

Seltzer GO, Rodbell DT, Burns S. 2000. Isotopic evidence for late Quaternary climatic change in tropical South America. *Geology* **28**: 35–38.

Shemesh A, Charles CD, Fairbanks RG. 1992. Oxygen isotopes in biogenic silica: global changes in ocean temperature and isotopic composition. *Science* **256**: 1434–1436.

Shen CC, Edwards RL, Cheng H, Dorale JA, Thomas RB, Moran SB, Edmonds HN. 2002. Uranium and thorium isotopic and concentration measurements by magnetic sector inductively coupled plasma mass spectrometry. *Chemical Geology* **185**: 165–178.

Stuiver M, Reimer PJ, Bard E, Beck JW, Burr GS, Hughen KA, Kromer B, McCormac G, van der Plicht J, Spurk M. 1998. INTCAL98 radiocarbon age calibration, 24000-0 cal BP. *Radiocarbon* **40**: 1041–1083.

Tapia PM, Fritz SC, Baker PA, Seltzer GO, Dunbar RB. 2003. A late Quaternary diatom record of tropical climatic history from Lake Titicaca (Bolivia/Peru). *Palaeogeography, Palaeoclimatology, Palaeoecology* **194**: 139–164.

Thompson LG, Mosley-Thompson E, Dansgaard W, Grootes PM. 1986. The Little Ice Age as recorded in the stratigraphy of the tropical Quelccaya Ice Cap. *Science* **234**: 361–364.

Valero-Garces BL, Grosjean M, Schwalb A, Schreir H, Kelts K, Messerli B. 2000. Late Quaternary lacustrine deposition in the Chilean Alti-

plano (18°–28° S). In *Lake Basins through Space and Time*, Gierlowski-Kordesch E, Kelts K (eds). American Association of Petroleum Geologists Studies in Geology, no. 46; 625–636.

Valero-Garcés BL, Delgado-Huertas A, Navas A, Edwards L, Schwalb A, Ratto N. 2003. Patterns of regional hydrological variability in central-southern Altiplano (18°–26° S) lakes during the last 500 years. *Palaeogeography, Palaeoclimatology, Palaeoecology* **194**: 319–338.

Vuille M. 1999. Atmospheric circulation over the Bolivian altiplano during dry and wet periods and extreme phases of the Southern Oscillation. *International Journal of Climatology* **19**: 1579–1600.

Wolfe BB, Aravena R, Abbott MB, Seltzer GO, Gibson JJ. 2001. Reconstruction of paleohydrology and paleohumidity from oxygen isotope records in the Bolivian Andes. *Palaeogeography, Palaeoclimatology, Palaeoecology* **176**: 177–192.

Wörner G, Hammerschmidt K, Henjes-Kunst F, Wilke H. 2000. Geochronology ($^{40}Ar/^{39}Ar$, K-Ar and He-exposure ages) of Cenozoic magmatic rocks from northern Chile (18–22° S): implications for magmatism and tectonic evolution of the central Andes. *Revista Geológica de Chile* **27**: 205–240.

J Paleolimnol
DOI 10.1007/s10933-010-9412-x

ORIGINAL PAPER

ENSO and solar activity signals from oxygen isotopes in diatom silica during late glacial-Holocene transition in Central Andes (18°S)

Armand Hernández · Santiago Giralt · Roberto Bao · Alberto Sáez · Melanie J. Leng · Philip A. Barker

Received: 8 April 2009 / Accepted: 1 February 2010

Abstract The late glacial-Holocene transition from the Lago Chungará sedimentary record in northern Chilean Altiplano (18°S) is made up of laminated sediments composed of light-white and dark-green pluriannual couplets of diatomaceous ooze. Light-white sediment laminae accumulated during short-term extraordinary diatom blooms whereas dark-green sediment laminae represent the baseline limnological conditions during several years of deposition. Diatom oxygen isotope ratios ($\delta^{18}O_{diatom}$) from 40 consecutive dark-green laminae, ranging from 11,990 to 11,450 cal year BP, show that a series of decadal-to-centennial dry–wet oscillations occurred. Dry periods are marked by relatively high isotope values whereas wet episodes are indicated by lower values. This interpretation agrees with the reconstructions of terrigenous inputs and regional effective moisture availability carried out in the lake but there is a systematic temporal disagreement between them owing to the non-linear response of the lacustrine ecosystem to environmental forcings. Furthermore, the $\delta^{18}O_{diatom}$ record tracks effective moisture changes at a centennial scale. Three major phases have been established (11,990–11,800, 11,800–11,550, and 11,550–11,450 cal year BP). Each phase is defined by an increasing isotope trend followed by a sudden depletion. In addition, several wet and dry events at a decadal scale are superimposed onto these major trends. Spectral analyses of the $\delta^{18}O_{diatom}$ values suggest that cycles and events could have been triggered by both El Niño-Southern Oscillation (ENSO) and solar activity. Significant ENSO frequencies of 7–9 years and 15–17 years, and periodicities of the solar activity cycles such as 11 years (Schwabe), 23 years (Hale) and 35 years (Brückner) have been recognised in the oxygen isotope time series. Time–frequency analysis shows that although solar and ENSO forcing were present at the onset of the Holocene, they were more intense during the late glacial period. The early Holocene might have been mainly governed by La Niña-like

A. Hernández (✉) · S. Giralt
Institute of Earth Sciences Jaume Almera-CSIC, C/Lluís Solé i Sabarís s/n, 08028 Barcelona, Spain
e-mail: ahernandez@ija.csic.es

R. Bao
Faculty of Sciences, University of A Coruña, Campus da Zapateira s/n, 15701 A Coruña, Spain

A. Sáez
Faculty of Geology, University of Barcelona, C/Martí Franquès s/n, 08028 Barcelona, Spain

M. J. Leng
NERC Isotope Geosciences Laboratory, British Geological Survey, Nottingham NG12 5GG, UK

M. J. Leng
School of Geography, University of Nottingham, Nottingham NG7 2RD, UK

P. A. Barker
Lancaster Environment Centre, Lancaster University, Lancaster LA1 4YQ, UK

Published online: 21 February 2010

conditions that correspond to wet conditions over the Andean Altiplano.

Keywords Lake · Oxygen isotopes · Late glacial · Holocene · Andean altiplano · ENSO · Solar activity · Diatoms

Introduction

The study of Andean Altiplano lacustrine records plays a prominent role for interpreting the Quaternary palaeoclimatic history of the South American tropics and therefore for understanding the function of the tropics in the Earth's climate system (Grosjean et al. 2001; Valero-Garcés et al. 2003; Placzek et al. 2006) (Fig. 1). For this reason, studies on the sedimentary records from this area have increased in the last few decades. Most of these studies have focussed on the reconstruction of climatic events at millennial time scales, especially since the Last Glacial Maximum (Baker et al. 2001a). There is a general consensus that orbital forces are the main factor triggering the climatic conditions at a millennial-scale (Rowe et al. 2002; Placzek et al. 2006), and are therefore responsible for those climatic events. Superimposed onto this long term variability, changes in the hydrologic balance at a sub-millennial scale in the Andean Altiplano, have been attributed to the variability of the Pacific Sea Surface Temperatures (SSTs) and the strength of the zonal winds (Rowe et al. 2002; Garreaud et al. 2003). Both factors are controlled by El Niño-Southern Oscillation (ENSO) and changes in the solar activity (Theissen et al. 2008). A number of studies have detected multidecadal- to centennial-scale hydrological balance shifts, suggesting that these relationships have been active since, at least, the mid-Holocene (Valero-Garcés et al. 2003; Theissen et al. 2008).

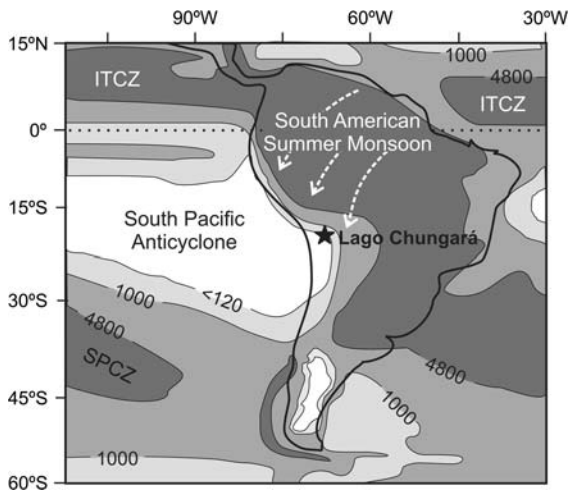

Fig. 1 Location of Lago Chungará on a South America rainfall rate map (mm/year) simplified from Negri et al. (2004). Main atmospheric systems are indicated. ICTZ: Intertropical Convergence Zone, SPCZ: South Pacific Convergence Zone

Diatom oxygen isotopes ($\delta^{18}O_{diatom}$) are increasingly being used for palaeoenvironmental reconstructions in lacustrine sedimentary records (Rietti-Shati et al. 1998; Barker et al. 2001). However, application of this proxy to high-resolution centennial to millennial lacustrine records is still in its infancy (Barker et al. 2007). $\delta^{18}O_{diatom}$ in decadal-to-centennial resolution palaeoclimatic reconstructions has not been utilised, mainly due to the difficulty in obtaining high resolution samples from sites with sufficient variation in $\delta^{18}O_{diatom}$ (outside of analytical error) that can be characterised at this fine temporal scale. Additional difficulties in using $\delta^{18}O_{diatom}$ are related to the difficulty in obtaining monospecific diatom samples in order to eliminate any species-specific effect variability, to acquire the necessary amount of sample from these short periods of time, and to have pure diatom samples, since significant contaminants can produce excursions in $\delta^{18}O_{diatom}$ that are similar to those produced by climate variations (Brewer et al. 2008).

The diatomaceous ooze from Lago Chungará has previously been the subject of a preliminary diatom oxygen isotope study at low resolution. This earlier study was aimed at three non-consecutive stretches of the sedimentary record, and did not include all the dark-green laminae (Hernández et al. 2008). For the present study we have analysed 40 consecutive dark-green laminae, corresponding to the late glacial and early Holocene, which represent a continuous record of the background limnological conditions (Hernández et al. 2008) (see the sedimentary model in the sedimentary sequence and rhythmite type section below). The excellent preservation and high diatom content of the record of Lago Chungará allow a detailed study of the regional moisture balance at decadal and centennial timescales.

Here, we present the decadal-to-centennial time scale moisture balance reconstruction for the Andean Altiplano during the late glacial-Holocene transition (11,990–11,450 cal year BP) based on high-resolution analysis of $\delta^{18}O_{diatom}$. This analysis was performed on successive and continuous 40 dark-green laminae of lacustrine sediments present in a core located in the offshore zone of Lago Chungará. In order to support the interpretation, isotope data are compared with the reconstructions of the terrigenous inputs and inferred regional effective moisture in the Lago Chungará performed in the same core by Giralt et al. (2008).

Lago Chungará setting

Geology and hydrology

Lago Chungará (18°15′S, 69°10′W, 4,520 m a.s.l.) is located in the Chilean Altiplano (Central Andes) lying in a highly active tectonic and volcanic context (Hora et al. 2007). The lake sits in the small hydrologically closed Chungará sub-Basin which was formed as a result of a debris avalanche during the partial collapse of the Parinacota Volcano, damming the former Lauca River (Fig. 2). Lago Chungará and Lagunas Cotacotani were formed almost immediately. However, the age of this collapse is not well constrained, with estimates ranging from 13,000 to 20,000 year BP (Hora et al. 2007).

The lake has an irregular shape with a maximum length of 8.75 km, maximum water depth of 40 m, a surface area of 21.5 km^2 and a volume of 400 $\times$ 10^6 m^3 (Mühlhauser et al. 1995; Herrera et al. 2006) (Fig. 2a). At present, the main inlet to the lake is the Chungará River (300–460 l s^{-1}) although secondary streams enter to the lake in the south-western margin. Evaporation is the main water loss (3 $\times$ 10^7 m^3 $year^{-1}$), and groundwater outflow from Lago Chungará to Lagunas Cotacotani (6–7 $\times$ 10^6 m^3 $year^{-1}$, Dorador et al. 2003) represents about 20% of the total outflow. The calculated residence time for the lakewater is approximately 15 years (Herrera et al. 2006). Water inputs to the lake have, on average, the following composition: 42 ppm HCO_3^-, 3 ppm Cl^-, 17 ppm SO_4^{2-}, 7 ppm Na^+, 4 ppm Mg^{2+}, 8 ppm Ca^{2+}, 3 ppm K^+ and 22 ppm Si. The Mg/Ca ratio of water inputs ranges from 0.22 to 0.71, depending on the local lithology of the catchment (Herrera et al. 2006; Sáez et al. 2007). Isotope data, temperature, pH, O_2 and conductivity profiles of the lake water and the water inputs to the lake are shown in Table 1. The lake can be considered as polymictic and oligo- to meso-eutrophic (Mühlhauser et al. 1995). The $\delta^{18}O$ and δD composition of the lake water reveal that it diverges from the Global Meteoric Water Line

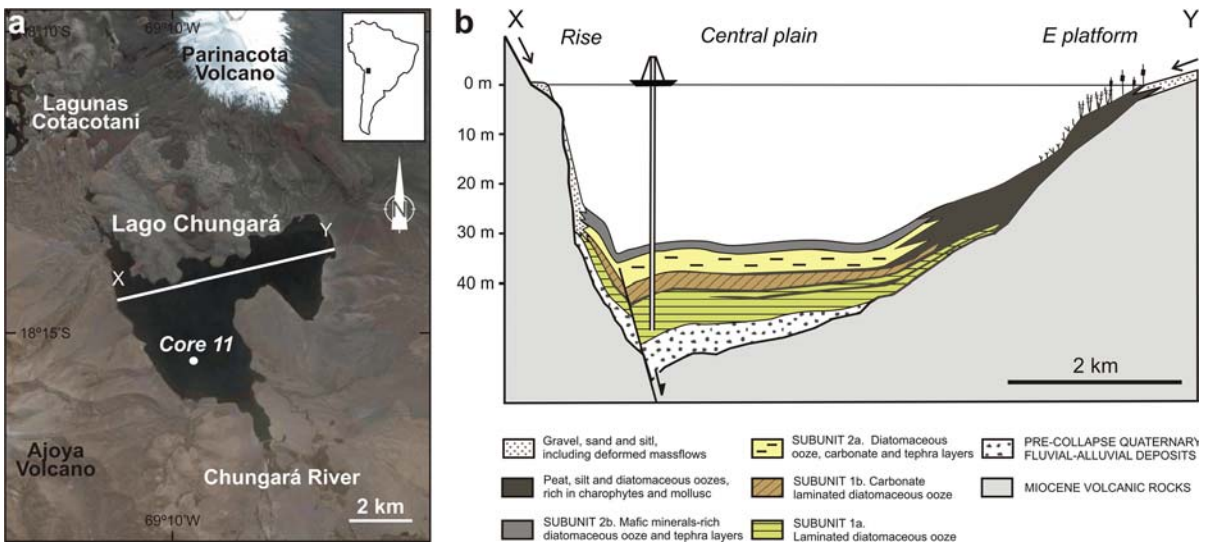

Fig. 2 **a** Location of the Chungará-Cotacotani lake district (modified from Google Earth). **b** Cross section of sediments infilling Lago Chungará. Position of core 11 is shown; note that the position of the core is projected in its equivalent position at the lake central plain. *Arrows* indicate major hydrological inputs and sedimentary contributions to the lake. Simplified from Sáez et al. (2007)

Table 1 Isotopic and other chemical and physical data analysed from water samples collected in the Lago Chungará (Modified from Herrera et al. 2006)

Site	Depth (m)	Date	$\delta^{18}O$	δD	$\delta^{13}C$	Conductivity ($\mu S\ cm^{-1}$)	pH	Temp (°C)	O_2
Lake									
Chungará	0	Nov-02	−1.52	−42.0	4.96	1,444	9.30	9.1	12.10
Chungará	20	Nov-02	−1.62	−42.6	4.26	1,433	9.17	7.2	7.80
Chungará	0	Jan-02	−3.85	−48.8	NA	1,262	9.63	17	NA
Chungará	2	Nov-02	−1.54	−44	NA	1,423	9.23	10.2	9.10
Chungará	2	Nov-02	−1.58	−44.7	4.62	1,451	9.23	9.9	9.30
Chungará	5	Nov-02	−1.53	−43.2	5.52	1,462	9.17	9.5	8.90
Chungará	20	Nov-02	−1.59	−44.4	5.34	1,455	9.05	7.1	7.60
Chungará	0	Nov-02	−1.49	−44,2	5.43	1,473	9.20	12.1	11.90
Chungará	5	Nov-02	NA	NA	NA	1,461	NA	9.5	NA
Chungará	10	Nov-02	NA	NA	NA	1,459	NA	9	NA
Chungará	15	Nov-02	NA	NA	NA	1,458	NA	8.1	NA
Chungará	20	Nov-02	NA	NA	NA	1,457	NA	7.6	NA
Chungará	25	Nov-02	NA	NA	NA	1,457	NA	7	NA
Chungará	31	Nov-02	−1.61	−45.8	−3.55	NA	9.02	NA	NA
Chungará	2	Nov-02	−1.50	−44.3	5.97	1,464	9.20	9.9	NA
Chungará	21	Nov-02	−1.76	−41.7	3.68	1,473	9.08	7.6	NA
Chungará	0	Nov-02	NA	NA	NA	1,464	NA	10.4	NA
Chungará	5	Nov-02	NA	NA	NA	1,461	NA	9.6	NA
Chungará	10	Nov-02	NA	NA	NA	1,461	NA	9.3	NA
Chungará	15	Nov-02	NA	NA	NA	1,461	NA	9.1	NA
Chungará	20	Nov-02	NA	NA	NA	1,456	9.15	7.2	NA
Chungará	25	Nov-02	NA	NA	NA	1,456	NA	7	NA
Chungará	30	Nov-02	NA	NA	NA	1,455	NA	6.8	NA
Chungará	35	Nov-02	NA	NA	NA	1,454	NA	6.4	NA
Chungará	0	Nov-02	−1.56	−39.9	3.21	1,439	9.08	9	11.20
Chungará	15	Nov-02	−1.54	−43.4	5.17	1,438	8.99	8.3	8.30
Chungará	33	Nov-02	−1.58	−43.4	4.56	1,435	9.10	6.2	6.20
Chungará	0	Nov-02	−2.05	−44.4	7.03	1,388	9.22	10.7	NA
Chungará	0	Jan-02	−3.39	−46.8	6.40	1,400	9.19	11.4	NA
Chungará	0	Jun-06	NA	NA	NA	1,463	9.42	5	10.50
Chungará	12	Jan-02	NA	NA	8.10	NA	NA	NA	NA
Chungará	0	Jun-06	NA	NA	NA	1,493	9.70	2	9.30
Chungará	0	Jun-06	NA	NA	NA	1,418	9.48	9	13.00
Chungará	0	Jun-06	NA	NA	NA	220	9.70	5	25.00
Springs									
Bofedal	0	Jan-02	−14.98	−116	−2.20	52	7.15	7.9	NA
Bofedal	0	Nov-02	−16.49	−116.6	−7.04	48.7	7.07	7.8	NA
Mal paso	0	Jan-02	−15.58	−120.5	NA	46.8	7.31	9.7	NA
Mal paso	0	Nov-02	−17.04	−121.9	−8.97	51.2	6.97	10/11.6	NA
Mal paso	0	Jan-04	−17.3	−121.3	NA	122	7.71	10.8	NA
Ajata	0	Jan-02	−14.07	−106.2	NA	59.8	7.80	7.6	NA

Table 1 continued

Site	Depth (m)	Date	$\delta^{18}O$	δD	$\delta^{13}C$	Conductivity ($\mu S\ cm^{-1}$)	pH	Temp (°C)	O_2
Ajata	0	Nov-02	−15.28	−205.9	−6.86	50	7.46	5.3	NA
Canal	0	Nov-02	−17.12	−121.7	−10.14	66.7	8.09	10	NA
Canal	0	Jan-04	−17.26	−119.3	NA	380	7.62	9.4	NA
Colada Ajata	0	Jan-02	−14.88	−111	−2.80	155.1	5.82	4.9	NA
Colada Ajata	0	Nov-02	−16.23	−112.1	−2.69	136.1	5.94	4.5	NA
River									
Chungará	0	Jan-02	−14.82	−111.8	NA	241	9.28	16	NA
Chungará	0	Nov-02	−16.09	−113.1	−1.15	223	8.99	17	NA
Chungará	0	Jan-04	−16.27	−114.1	NA	316	8.02	14.2	NA

NA not available data

(GMWL) and the Regional Meteoric Line (RML). This divergence can be attributed to the enrichment of the lake water by evaporation with regard to rainfall and springwater (Fig. 3a; Herrera et al. 2006). The mean lake water values of $\delta^{18}O$ and δD (January 2002 to January 2004) are −1.4‰ SMOW and −43.4‰ SMOW, respectively (Table 1).

Climate

Climate in the Chungará-Cotacotani lake district is dominated by arid conditions due to the influence of the South Pacific Anticyclone (Fig. 1). Modern mean annual temperature at Lago Chungará is +4.2°C. Annual rainfall ranges from 100 to 750 mm $year^{-1}$ (mean 411 mm $year^{-1}$), losing 1,200 mm $year^{-1}$ via evaporation, which exceeds precipitation (Fig. 3b; Valero-Garcés et al. 2000). The lake region shows pronounced seasonal contrasts due to the dominance of the tropical summer moisture (Garreaud et al. 2003), known as the South American Summer Monsoon (SASM) (Vuille and Werner 2005). Regional moisture originates from the tropical Atlantic Ocean and is transported to the Altiplano throughout Amazonia during the summer months (DJFM). During these months weak easterly flow prevails over the Altiplano as a consequence of the southward migration of the subtropical jet stream and the establishment of the Bolivian high-pressure system (Garreaud et al. 2003). This climatic situation defines this time window as the wet season in the Altiplano accounting for more than 70% of the annual precipitation (Fig. 3b). The SASM is a major component of the climate system over tropical and subtropical South America during the austral summer and is remotely forced by tropical Pacific SSTs (Vuille and Werner 2005). Thus, the inter-annual to decadal climate variability is currently related to ENSO-like variations over the Pacific basin (Valero-Garcés et al. 2003). Instrumental data from the Chungará area show a reduction of the precipitation during moderate to intense El Niño years (Fig. 3c). However, there is no direct relationship between the relative El Niño strength and the amount of rainfall reduction (Valero-Garcés et al. 2003). Furthermore, on longer timescales, it is speculated that changes in tropical-Atlantic meridional SST gradients also force precipitation variability on the Altiplano (Baker et al. 2001b).

Rainfall isotope composition in Central Andes (Fig. 3d) is characterised by a large variability in $\delta^{18}O$ (between +1.2 and −21.1‰) and of δD (between +22.5 and −160.1‰). The origin of the lightest oxygen isotope values is the strong fractionation in the air masses from the Amazon and is directly related to higher rainfall intensity ('amount effect') (Herrera et al. 2006). However, the rainfall oxygen isotope composition in the Chungará-Cotacotani lake district only oscillates by 6‰, between −14 and −20‰, with a mean value of −14.3‰ (Fig. 3a, d).

Sedimentary sequence and rhythmite type

The sedimentary infill of Lago Chungará was characterised by the lithological description of fifteen lake cores obtained in 2002 (Sáez et al. 2007) and by seismic imagery obtained in 1993 (Valero-Garcés et al. 2000; Sáez et al. 2007). From the bottom to the top of core 11,

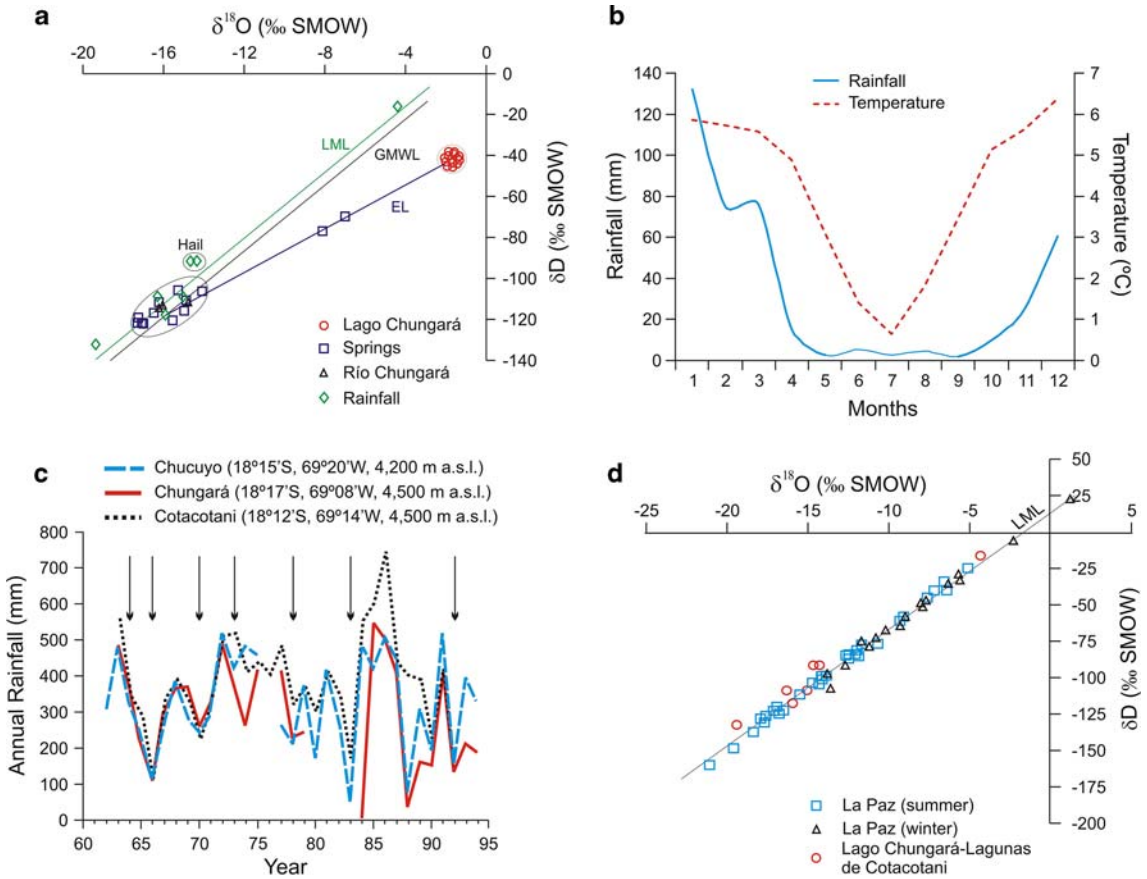

Fig. 3 **a** Isotope values ($\delta^{18}O/\delta D$) from rainfall, Lago Chungará, Río Chungará and studied area springs. GMWL: Global Meteoric Water Line; LML: Local Meteoric Line; EL: Evaporation Line. Note the isotopic enrichment of the lake water by evaporation with regard to rainfall and springwater. **b** Mean monthly rainfall (mm) and temperature (°C) at Chungará meteorological station (18.17S, 69.08W, 4,500 m a.s.l.). Note the seasonality of both parameters. **c** Annual rainfall in the Chungará region from 1962 to 1994. The arrows indicate strong El Niño years. Modified from Valero-Garcés et al. (2003). **d** Isotope composition ($\delta^{18}O/\delta D$) of rainfall samples from La Paz (Bolivia) obtained by the International Atomic Energy Agency (IAEA) since 1995 until 1998 (*blue squares* and *black triangles*), and the samples of Lago Chungará and the very close Lagunas de Cotacotani obtained from Herrera et al. (2006) (*red circles*). LML: Local Meteoric Line ($\delta D = 7.9\delta^{18}O + 14$). Note the variability in $\delta^{18}O$ and of δD values

two sedimentary units (units 1 and 2) were identified and correlated over the offshore zone of the lake mainly using tephra keybeds (Figs. 2a, 2b). Unit 1 is made up of diatomaceous ooze with variable types and quantities of carbonates (calcite, aragonite) and amorphous organic matter. It is continuous across the lake, although thickest in the NW sector of the central plain and thins towards the south and west, probably overlapping the Miocene substrate. Unit 1 occurs in the central plain and the sharply rising flank of the lake (Fig. 2b) and is divided in two subunits. Subunit 1a is composed by light-white and dark-green diatomaceous ooze couplets and a rhythmite type was defined (Hernández et al. 2008). Light-white laminae are formed by the skeletons of the diatom *Cyclostephanos andinus* (Theriot, Carney, and Richerson) Tapia, Theriot, Fritz, Cruces and Riv. Dark-green laminae, with higher organic matter content, are made up by a mixture of diatoms, including the euplanktonic *Cyclostephanos andinus*, although diatoms of the *Cyclotella stelligera* complex are co-dominant taxa. Subdominant groups are some tychoplanktonic (*Fragilaria* spp.) and benthic taxa (*Cocconeis* spp., *Achnanthes* spp., *Navicula* spp., *Nitzschia* spp.). Subunit 1b is composed of centimetre- to decimetre-thick laminated brown diatomaceous ooze and endogenic carbonates that occur in low concentrations. Unit 2 is about 6 m-thick and grades laterally to the west and south into alluvial and

deltaic deposits, and towards the east into macrophyte, organic-rich facies (Fig. 2b). It is mainly composed of massive to slightly banded diatomaceous ooze interbedding with 13 tephra layers. Unit 2 is also divided in two subunits. Subunit 2a is composed of brownish-red massive to slightly banded sapropelic diatomaceous ooze with common calcitic crystals (silt grain-sized) and carbonate-rich layers. Subunit 2b consists of dark-grey diatomaceous ooze with frequent macrophyte remains alternating with massive black tephra layers, mainly composed of plagioclase, glass and mafic minerals (Sáez et al. 2007; Moreno et al. 2007).

The chronological model for the sedimentary sequence of Lago Chungará is based on 17 ^{14}C AMS dates obtained from bulk organic matter from the central plain cores and aquatic organic macrofossils picked from littoral cores, and one $^{238}U/^{230}Th$ date from carbonate. Details on the construction of the chronological framework are discussed elsewhere (Giralt et al. 2008). According to the chronological model, the studied interval records the late glacial-Holocene transition (11,990–11,450 cal year BP) and each couplet was deposited during time intervals ranging from 4 to 24 years. Light-white sediment laminae accumulated during short term diatom blooms (occurring from days to weeks) whereas dark-green sediment laminae represent the baseline limnological conditions during several years of deposition (Hernández et al. 2008).

Previous work has characterised the surface and underground waters from the Chungará and Cotacotani lake district (Herrera et al. 2006), as well as the sediments of Lago Chungará. X-Ray Fluorescence (XRF), X-Ray Diffraction (XRD), Total Carbon and Total Organic Carbon (TC and TOC), Total Biogenic Silica (TBSi), pollen and diatom analyses were performed. These multiproxy studies have allowed us to establish the sedimentary, hydrological and environmental evolution of the Lago Chungará at different time scales (Sáez et al. 2007; Moreno et al. 2007; Giralt et al. 2008).

Methods

An interval of 46.5 cm from the laminated dark-green and light-white sediments of Subunit 1a (deposited between 11,990 and 11,450 cal year BP) was selected and sampled, lamina by lamina, from core 11 (Fig. 2). All the dark-green laminae (40 samples) of this interval were selected for $\delta^{18}O_{diatom}$ analyses to carry out a very high-resolution study of the baseline environmental evolution of Lago Chungará (sampling ranging from 4.1 to 24.4 years; average temporal resolution is ca. 12 years) during the late glacial and early Holocene transition period. Of these, 22 samples were also previously used in a lower resolution study (Hernández et al. 2008). The thickness of the dark-green laminae sampled ranges between 2 and 9 mm.

Analysis of the oxygen isotope composition of diatom silica requires the material to be almost pure diatomite (Juillet-Leclerc 1986). Our samples were treated following the method proposed by Morley et al. (2004) with some variations (Hernández et al. 2008). The samples were treated to remove organics and carbonate, then sieved at 125 μm to eliminate resistant charcoal and terrigenous particles. The 63- and 38-μm sieves were used to obtain a diatom concentrate made up almost exclusively by large valves of the centric diatom *Cyclostephanos andinus,* eliminating in the samples any species-specific effect variability (Fig. 4). Gravity settling in a water column during the sieving process also helped to remove any remaining tephra and clay particles. The Gravitational Split-flow Thin Fractionation (SPLITT) was then applied to the most problematic samples, at Lancaster University (UK), as an alternative approach to heavy liquid separation (Rings et al. 2004; Leng and Barker

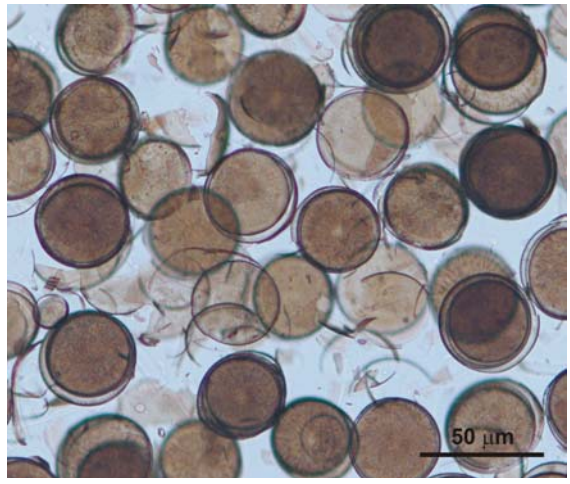

Fig. 4 Diatom-rich sediment from Lago Chungará after the cleaning process. Large *Cyclostephanos andinus* valves are the unique component

2006). Finally, the purified diatom samples were dried at 40°C between 24 h and 48 h. After the cleaning process, all the samples were checked under the light microscope and some of them also with XRD and scanning electron microscope (SEM), as well as analysed for TC to verify that they did not contain any significant amount of terrigenous matter (Fig. 4).

For oxygen isotope analysis, a stepwise fluorination method was applied to 5–10 mg of the purified diatoms in order to strip the frustule hydrous layer before a full reaction with BrF_5 (Leng and Barker 2006). The oxygen liberated was then converted to CO_2 using the method of Clayton and Mayeda (1963), measured by IRMS and normalised against NBS standards. A random selection of 7 samples were analysed in duplicate or triplicate giving a mean reproducibility value of <0.2‰ (1σ), only one sample gave a reproducibility value of 0.4‰ (1σ). The fluorination process and the $^{18}O/^{16}O$ ratios measured were carried out at the NERC Isotope Geosciences Laboratory, British Geological Survey (UK).

We employed two methods of spectral analyses to examine any periodic components in the $\delta^{18}O_{diatom}$ values: Multi-Taper Method (MTM) and Time–Frequency analysis. These two spectral analyses allowed us to examine statistically significant signals in the time series in both the frequency and time domains. MTM provided both a means of spectral estimation and signal reconstruction for time series with spectra that contain both singular and continuous components (Theissen et al. 2008). Time–Frequency (TF) analysis is a hybrid tool between the Fourier Transform and wavelets that intends to use a localised spectrum. For that, this analysis does not use a fixed-size Gaussian window but a Gaussian window that adapts to the spectrum (Stockwell et al. 1996).

All the statistical treatments of the datasets were performed using the R software package (R Development Core Team 2008).

Results

Oxygen isotopes

The $\delta^{18}O_{diatom}$ record (Fig. 5d) shows both short-term (decadal) and long-term oscillations (centennial time scales) ranging from +35‰ to +39.2‰ (mean = +37.4 ± 0.8‰). From the bottom to the top, the studied record can be subdivided into three phases. These intervals correspond to three enrichment/depletion phases (Fig. 5c). Each phase starts with a continuous centennial isotope enrichment which abruptly ends with a sharp depletion:

Phase 1. Lower interval (11,990–11,800 cal year BP). It shows the maximum and minimum $\delta^{18}O_{diatom}$ values (+39.2‰ and +35.1‰ respectively, with a mean value of +37.7 ± 1‰) throughout the whole record. It starts with an increasing trend of ~3.3‰/100 year which finishes at 11,860 cal year BP. This trend is followed by a shift to lighter values of ~8.1‰/100 year with a sharp final decrease in the $\delta^{18}O_{diatom}$ values of 3.5‰ in less than 10 years, acquiring the minimum value for the whole record at ca. 11,800 cal year BP. Both trends are interrupted by ca. 5–20 years depletion/enrichment excursions ranging between ± 0.9 and ± 1.7‰.

Phase 2. Middle interval (11,800–11,550 cal year BP). This section (mean value +37.3 ± 0.7‰) starts with an enrichment trend showing an upwards gradient of ~1.3‰/100 year which finishes at 11,570 cal year BP with a +38.3‰ $\delta^{18}O_{diatom}$ value. This trend is however punctuated by one sudden rise (+2.3‰) and up to four minor depletions (ranging from −0.6 to −1.3‰) of the $\delta^{18}O_{diatom}$ values on a 40–55 years basis. The enrichment trend is followed by a shift of ~9.1‰/100 year to lighter values reaching a minimum value of +36.2‰.

Phase 3. Upper interval (11,550–11,450 cal year BP). This interval (mean value +37.2 ± 0.7‰) also starts with an enrichment trend but, because the section only comprises three samples, this enrichment has not been estimated. This trend is also followed by depletion of 1.3‰ in 10 years.

Spectral analyses of the diatom oxygen isotope record

Multi-taper analysis (MTM) performed on the $\delta^{18}O_{diatom}$ values shows a number of clear periodicities (Fig. 6a). Almost all identified periodicities (7.2, 8.9, 11.1, 13, 18.6, 22.3 and 39.4 years) exceed the 99% confidence interval whereas only two (3.7 and

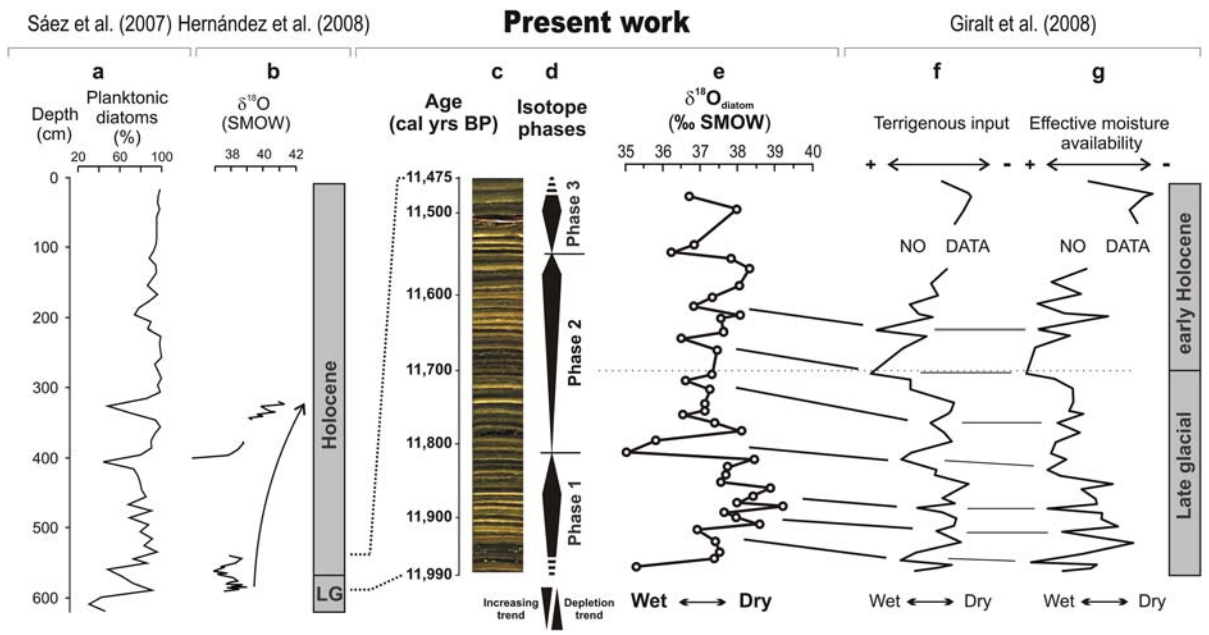

Fig. 5 $\delta^{18}O_{diatom}$ data for the period 11,990–10,475 cal year BP from Lago Chungará, compared with other paleoenvironmental records of the lake. **a** Planktonic diatoms percent abundance curve for the whole Lago Chungará sequence (Sáez et al. 2007). **b** $\delta^{18}O_{diatom}$ data of non-consecutive dark-green laminae from three intervals of the record (Hernández et al. 2008). **c** Photography of laminated sediments corresponding to the sampled interval of subunit 1a in core 11. **d** Oxygen isotope enrichment/depletion phases, in the studied interval, interpreted from the data. **e** $\delta^{18}O_{diatom}$ data from the present study and interpretation in terms of wet and dry conditions. The values correspond to 40 consecutive dark-green laminae throughout the whole selected interval. **f** Terrigenous input variations derived from the first eigenvector of Principal Component Analysis (PCA) on magnetic susceptibility, X-Ray Fluorescence (XRF), X-Ray Diffraction (XRD), Total Carbon and Total Organic Carbon (TC and TOC), Total Biogenic Silica (TBSi) (Giralt et al. 2008). **g** Effective moisture availability variations from the second eigenvector of the mentioned PCA (Giralt et al. 2008). Correlation lines correspond to the main oxygen isotope depletion peaks. Note that the main trends of the three curves are similar but there is a systematic temporal disagreement between them

8 years) lie between 95 and 99% confidence interval (Fig. 6a). Most of the sub-decadal identified frequencies are close to the minimum temporal resolution of the sampling (4.1 years), which explains in great part the weaker intensity of the short periodicities between 3 and 8 years. Therefore, only the most significant frequencies and above the minimum temporal sampling resolution have been taken into account in the discussion.

Time–Frequency (TF) analysis reveals the strongest energy for the lower values of frequency, mainly focussed on the 35-years cycles, whereas it decreases towards higher frequency values, i. e., the higher periodicities (Fig. 6b). This fact can mostly be explained by the decadal sampling resolution, making periodicities lower than 10 years less significant. Additionally, TF analysis indicates that the highest energies of the significant frequencies are located in the late glacial period between ca. 11,950 and 11,700 cal year BP, decreasing just from the onset of the Holocene until, at least, approximately 11,550 cal year BP (Fig. 6b). TF diagram also highlights that the identified frequencies did not have the same intensity (energy) during all the studied period. For instance, the shortest significant periodicity observed in the MTM (7.2 years) was mainly active during the first 150 years of the record, whereas it was only active during three short time windows in the following 500 years. A similar pattern is also observed for the rest of the significant periodicities (8.9, 11.1, 13, 18.6, 22.3 and 39.4 years). The maximum energy areas correspond to depletions in the $\delta^{18}O_{diatom}$ values, i.e. 11,800 and 11,550 cal year BP (Fig. 6b).

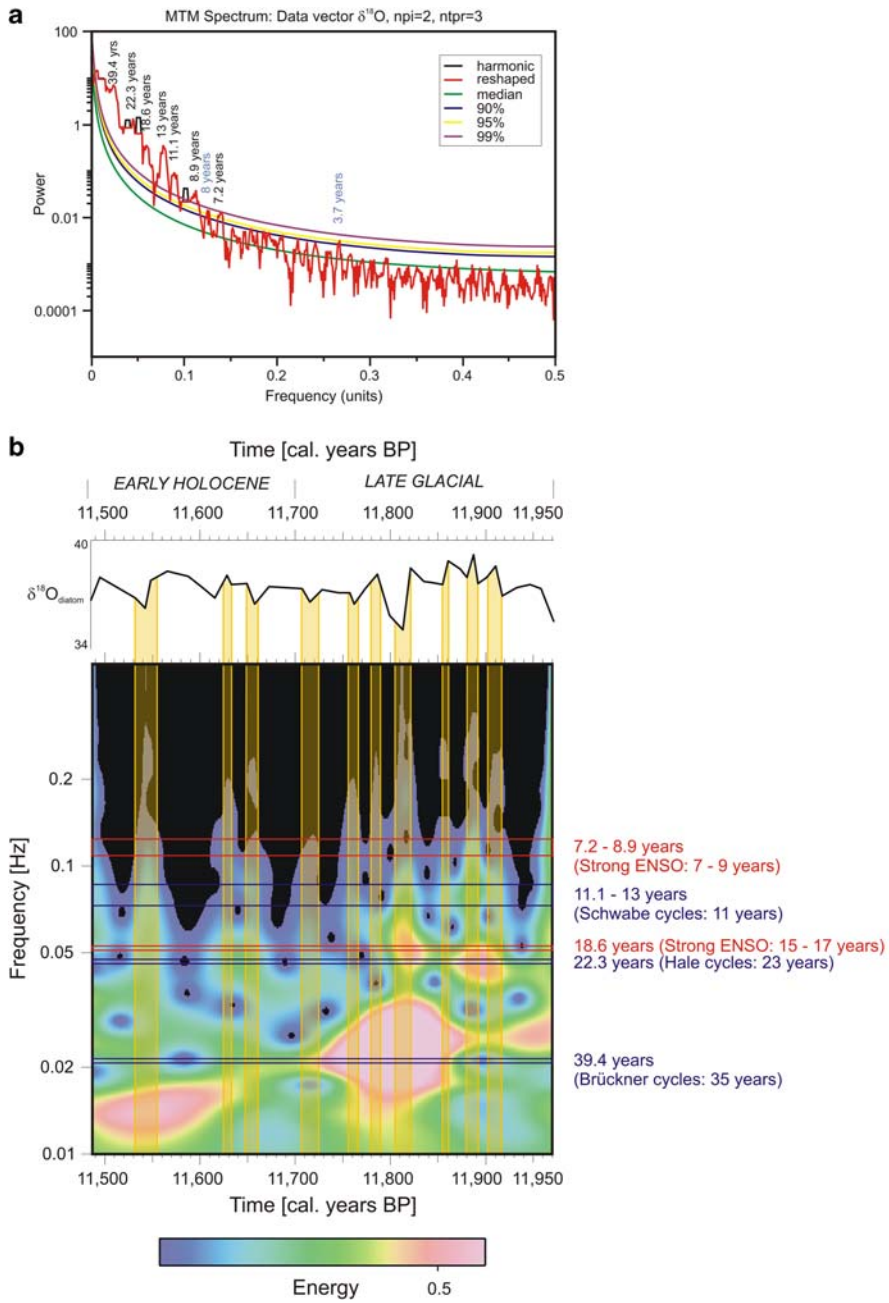

Fig. 6 **a** Multi-taper analysis of the $\delta^{18}O_{diatom}$ values. The 90, 95 and 99% confidence levels are indicated and significant periodicities are shown. Note that periodicities with more than 99% of significance are shown in *black* and those with more than 95% significance in *blue*. **b** Time–Frequency analysis of the $\delta^{18}O_{diatom}$ values. *Pink* indicates high energy whereas *blue* displays low energy areas. Energies below 0.03 were clipped in order to facilitate understanding of the graph. *Red* and *blue horizontal bands* mark different frequency bands of the ENSO and solar activity forcings. *Yellow vertical bands* show zones with $\delta^{18}O_{diatom}$ shifts and their corresponding power values for each frequency. A weakening pattern in ENSO and solar activity energies can be observed through the late glacial-early Holocene transition

Discussion

Controlling factors of $\delta^{18}O_{diatom}$ in Lago Chungará

$\delta^{18}O_{diatom}$ in lake sediments is controlled by the oxygen isotope composition of the lake water ($\delta^{18}O_{lakewater}$), temperature, and the possible disequilibrium by vital effects or diagenesis (Leng and Barker 2006). We discount vital effects and diagenesis as analyses were made on near-monospecific diatom samples and preservation of the diatom frustules is excellent (Fig. 4).

$\delta^{18}O_{lakewater}$ depends on the balance between the isotope composition of water inputs (including the

source and amount of precipitation, surface runoff and groundwater inflow) and outputs (evaporation and groundwater loss) in the lake. The measured $\delta^{18}O$ of the inputs (springs, Río Chungará and rainfall) in the Lago Chungará is homogeneous, giving values close to the isotope composition of precipitation ($\delta^{18}O_{precipitation}$) (Fig. 3a). $\delta^{18}O_{precipitation}$ is a function of the isotope composition of the moisture source and air-mass trajectory, but in the Lago Chungará there are no changes in the moisture source composition since the air masses always come from the Atlantic Ocean throughout the Amazon basin (Grosjean et al. 1997). During moisture transport from the Atlantic to the lake area, three processes are directly responsible for the low and variable values of the present $\delta^{18}O_{precipitation}$ throughout the Andean Altiplano (Aravena et al. 1999). These processes include interaction of the air masses within the Amazon basin, an altitude effect due to the ascent of the air masses along the eastern slope of the Andes, and the convective nature of the storms in the Altiplano region. Nevertheless, in the Lago Chungará region the values obtained for the measured $\delta^{18}O_{precipitation}$ are relatively stable with almost all values around −14 and −20‰ (Figs. 3a, 3d; Herrera et al. 2006), whereas $\delta^{18}O_{lakewater}$ is much higher (Fig. 3a). This result is in accordance with a $\delta^{18}O_{lakewater}$ enrichment via evaporation. Thus, any isotopic variation of $\delta^{18}O_{lakewater}$ will be more related to changes in the amount of precipitation ("amount effect") and evaporation rather than to the variability of $\delta^{18}O_{precipitation}$. Evaporation enriches $\delta^{18}O$ of lake water by 14‰ relative to the inlets (precipitation, springs and river) in the present day (Figs. 3a, 3b; Table 1). During the late glacial and early Holocene the water residence time of the lake was shorter than present because of the different palaeohydrological context, but even so it can be considered closed for that period (Hernández et al. 2008).

Accordingly, the variations in the $\delta^{18}O_{diatom}$ must be mainly derived from changes in the $\delta^{18}O_{lakewater}$ resulted from shifts in the balance between the precipitation and the evaporation (P-E), rather than dominated by temperature. However, two factors should be considered in the interpretation of the $\delta^{18}O_{diatom}$ values in terms of temperature oscillations. The first factor is related to $\delta^{18}O_{precipitation}$ that correlates directly with changes in the air temperature. The global relationship between changes in $\delta^{18}O_{precipitation}$ with air temperature is commonly referred to as the 'Dansgaard relationship', and it implies changes between +0.2 and +0.7‰/°C (Dansgaard 1964). The second is the lakewater temperature dependence of oxygen isotope fractionation between diatom silica and the lake water (Brandriss et al. 1998). Nevertheless, the fractionation factor value of this temperature dependence is still controversial. Published fractionation factors range from −0.2‰ and −0.5‰/°C (Brandriss et al. 1998; Moschen et al. 2005).

The two temperature factors have opposing effects on $\delta^{18}O_{diatom}$ but, owing to its larger variability, the effects of the first factor (air temperature) usually dominate over the second. However, even in the case of the largest change due to the Dansgaard relationship, its magnitude will be greatly damped by the effect of the isotope fractionation between diatom silica and lake water. Moreover, it is known that most of the tropical rainfall isotope datasets exhibit a far stronger correlation with total precipitation than with air temperature (Leng et al. 2005), indicating in the Lago Chungará case a magnification of the P-E balance in wetter periods.

Hence, we can assume that in the Lago Chungará the effects of precipitation variability and temperature oscillations in the $\delta^{18}O_{diatom}$ values will be small in comparison to evaporative concentration, as pointed by other authors for closed lakes in general (Gat 1980; Gasse and Fontes 1992).

Variations of the precipitation-evaporation balance in the lake

Oxygen isotopes have widely been used to carry out lake level reconstructions and to establish consequent palaeoclimatic interpretations (Barker et al. 2001; Valero-Garcés et al. 2003).

There is a relationship between lake level change and the P-E balance for Lago Chungará during the late glacial and early Holocene, but this dependency is hampered by local palaeohydrological factors such as changes in the groundwater outflow and shifts in the lake surface/volume ratio which produce a background long term enrichment trend (Hernández et al. 2008). This effect is however negligible when considering isotopic changes at a decadal to centennial time scale. Both present (Fig. 3) and past (Thompson et al. 1998) rainfall isotope values in

the Lago Chungará region are much lighter than those measured for the lakewater, and the magnitude of the long-term enrichment trend is very small compared to them. Therefore, depletions of $\delta^{18}O_{diatom}$ would directly be related to wet episodes in the Andean Altiplano, whereas exceptionally high values, which stand out over the general enrichment trend, would indicate arid episodes.

The observed $\delta^{18}O_{diatom}$ enrichment trends agree with periods where light-white laminae are more common, whereas depletion episodes coincide with poorly developed and less abundant light-white laminae (Figs. 5c, 5d). These light-white laminae are most likely the result of exceptional periods of mixing of the shallow water column during low-stands, which recycle nutrients from the hypolimnion and therefore trigger extraordinary diatom blooms (Hernández et al. 2007). This interpretation is also supported by terrigenous input and regional effective moisture reconstructions previously performed on the Lago Chungará sedimentary record (Giralt et al. 2008) (Figs. 5f, 5g). These reconstructions were carried out by applying multivariate statistical analyses (Cluster, Redundancy Analysis (RDA) and Principal Component Analysis (PCA)) to magnetic susceptibility, XRF, XRD, TC, TOC, TBSi and grey-colour curve data. The terrigenous inputs curve was derived from the first eigenvector of the PCA, whereas the regional effective moisture reconstruction was obtained from the second eigenvector. For the lower part of Chungara sequence (Unit 1), the more positive values of the terrigenous inputs were interpreted, as increasing erosion rate of catchment volcanic sediments, suggesting humid conditions. Similarly, the effective moisture availability proxy depends on the P-E balance, with positive values corresponding to drier conditions (Giralt et al. 2008). The comparison of the three proxies (Figs. 5e, 5f, 5g) shows that the hydrological response of the diatom silica oxygen isotopes (a biological proxy) and of the other two reconstructions to the environmental variations is not the same.

The main trends in the three curves (Figs. 5e, 5f, 5g) are similar but there is a systematic temporal disagreement (ranging between ca. 5 and 50 cal year BP) between the terrigenous inputs and the regional effective moisture availability (which both react first) and the $\delta^{18}O_{diatom}$ (reacting afterwards). This time lag between the two proxies highlights the complex and non-linear response of the lacustrine ecosystem to environmental forcings (Fritz 2008). After rainfall the increased runoff and input of terrigenous material is almost immediate. On the contrary, the oxygen isotope homogenisation of the lakewater which later will be incorporated on the diatom frustule, has a delayed time of response. This depends on the epilimnion water residence time and, furthermore, whether the lake is hydrologically closed or not. Hence, the observed time lag can be showing these different responses of the system to the same forcing. However, we cannot discount the poorly understood concept of silica maturation, where pores in the silica matrix close through early diagenesis creating differences in the $\delta^{18}O$ between living diatoms and sediment assemblages (Schmidt 2001) and therefore a lag in the $\delta^{18}O_{diatom}$ record.

At centennial scale, the Lago Chungará isotopic values show a general pattern of increasing $\delta^{18}O_{diatom}$ (Fig. 5b), with an enhanced enrichment period at the bottom, but interrupted by three major depletion events. The depletion events, accentuated by the "amount effect", correspond to heavy rainfall conditions, whereas enriched values would indicate exceptionally dry conditions favouring the evaporation. This interpretation is reinforced by the terrigenous input and effective regional moisture availability independent reconstructions.

Three wet/dry phases have been identified in the $\delta^{18}O_{diatom}$ record (Fig. 5d). Phase 1 (11,990–11,800 cal year BP) shows a significantly increased gradient in $\delta^{18}O_{diatom}$ suggesting that dominantly dry climate conditions played a key role triggering this isotope enrichment. Because of this drier situation the lake level would be lower, as also indicated by the important development and major presence of light-white laminae in this part of the interval. Three low-intensity and short-term wet episodes punctuate the established late glacial arid period (Fig. 5e). These episodes can also be recognised and correlated with events of increased terrigenous inputs and effective moisture availability (Figs. 5e, 5f, 5g).

The much weaker isotope enrichment for phase 2 (11,800 and 11,550 cal year BP) can be mainly ascribed to the general low magnitude palaeohydrological background trend towards heavier isotope conditions of the late glacial-early Holocene transition (Hernández et al. 2008). This fact, together with the poorer development and minor presence of the

light-white laminae with respect to the previous interval, suggests that the enrichment via evaporation was much less important than during the sedimentation of phase 1, corresponding to a more humid period. Furthermore, the terrigenous inputs and effective regional moisture availability curves show relatively wetter conditions for this period (Figs. 5f, 5g). This trend is also punctuated by a sudden rise in the lowest part of the interval indicating a short dry event and slight depletions in $\delta^{18}O_{diatom}$ indicating wet decadal-scale events (Fig. 5e).

In phase 3 any clear trend is difficult to identify (Fig. 5e). Although the $\delta^{18}O_{diatom}$ record seems to show a new trend towards drier conditions after the sudden wet event dated at 11,550 cal year BP, the lack of suitable samples has hampered any firm conclusions.

Long-term, centennial- to millennial-scale palaeoclimatic implications

There are many Late Quaternary palaeoclimatic reconstructions from the Andean Altiplano region (Sylvestre et al. 1999; Rigsby et al. 2005) but the climatic context for the late glacial-Holocene transition still remains unclear. Some authors have defined a cold period (12,600–11,500 cal year BP) coincident with the Northern hemisphere's Younger Dryas event (Baker et al. 2001b). The wet ("Coipasa phase", Thompson et al. 1998; Placzek et al. 2006) or dry (Maslin and Burns 2000; Weng et al. 2006) character of this event remains controversial. On the contrary, other authors consider this period just the final part of the deglaciation towards the present interglacial ("Ticaña phase", Sylvestre et al. 1999), as part of a long-term dry pattern (Rowe et al. 2002; Abbott et al. 2003).

The previous lake level reconstruction, mainly based on the abundance of planktonic diatoms, shows a shallowing followed by a long term rising trend for the interval presented here (Sáez et al. 2007). Additionally, recent data on the Lago Chungará record, mainly based on XRF core scanner analysis, has established the late glacial to Holocene transition as a relatively wet period (Giralt et al. 2008). The centennial scale $\delta^{18}O_{diatom}$ record is congruent with the lake level reconstruction performed by Sáez et al. (2007) which represents the palaeoclimatic evolution related to the major lake level variations (Fig. 5a). The non-continuous isotopic data (Fig. 5b) also displays a persistent, but minor, background isotope enrichment trend. This enrichment is related to changes in the lake morphology due to shifts in its surface/volume ratio, as well as changes in the groundwater outflow during the lake ontogeny (Hernández et al. 2008). In any case, the new $\delta^{18}O_{diatom}$ data presented here highlights that the glacial-interglacial transition in the central Andean Altiplano was punctuated by abrupt and high-frequency centennial climatic variability.

Short-term, decadal- to centennial-scale palaeoclimatic implications

Millennial-scale shifts in the Atlantic-Amazon-Altiplano hydrologic system have been attributed to orbitally induced changes in solar insolation, coupled with long-term changes in the ENSO variability (Rowe et al. 2002; Abbott et al. 2003; Servant and Servant-Vildary 2003). However, higher-resolution changes are not directly related to orbitally induced insolation forcing (Abbott et al. 2003). The interannual climate variability in the Andean Altiplano is most likely related to changes in the Pacific Tropical SSTs, and the sign and strength of the zonal winds above the Altiplano (Garreaud et al. 2003). Both factors would affect the strength and position of the Bolivian high and, hence, the moisture distribution over the region. The main force controlling the SSTs is the ENSO variability, involving dry or wet situations in the Altiplano during El Niño- or La Niña-like conditions respectively (Garreaud et al. 2003; Vuille and Werner 2005). This is consistent with instrumental data from the Chungará area where precipitation is reduced during moderate to intense El Niño years (1965, 1972, 1983, and 1992) (Fig. 3c). Additionally, the sign and strength of the zonal winds above the Altiplano would be modulated by decadal and multidecadal variations in solar activity, possibly related to the mode of the ENSO system (Theissen et al. 2008). Although ENSO modulation by solar activity has been suggested (Velasco and Mendoza 2008), no clear relationship has been demonstrated between both forcings. Nevertheless, there is broad agreement that ENSO events are the main control governing the moisture distribution in the Altiplano (Servant and Servant-Vildary 2003), and that decadal-scale changes in the effective moisture could be

related to the solar activity during the mid-Holocene (Theissen et al. 2008).

The results presented here would suggest a similar pattern during the late glacial-Holocene transition over the Andean Altiplano (Fig. 6b). The identified frequencies can be attributed to different periodicities of the solar activity cycles such as Schwabe 11 years (identified as 11.1 and 13 years), Hale 23 years (22.3 years) and Brückner 35 years (39.4 years), and of the ENSO frequency (main frequency at 7–9 years (7.2 and 8.9 years) and its decadal frequency 15–17 years (18.6 years)). The influence of solar activity and ENSO variability on the isotope record is supported by the fact that several periodicities concordant with both forces were identified. The time–frequency analysis suggests that the driest period (11,950–11,800 cal year BP) was ruled by high solar activity, mainly represented by a Brückner cycle, and strong ENSO-like conditions.

The ENSO and solar activity signals remain present for the early Holocene period (between 11,750 until 11,500 cal year BP), although they show a weakening pattern through this period (Fig. 5b). This fact is congruent with the progressive weakening of the ENSO suggested by other authors for the late glacial-Holocene transition (Rodbell et al. 1999; Moy et al. 2002; Rodó and Rodríguez-Arias 2004). In Lago Chungará, the onset of the Holocene was characterised by minor $\delta^{18}O_{diatom}$ enrichment by evaporation and by the occurrence of multi-decadal weak depletions that would be governed by the more humid La Niña-like conditions. This would agree with previous observations that suggest a reduction in the El Niño intensity within the region during the early-Holocene in favour of long-term La Niña-like conditions in the tropical Pacific (Betancourt et al. 2000; Koutavas et al. 2002).

Conclusions

The late glacial to Holocene transition from the Lago Chungará record is made up of laminated diatom-rich sediments which provide excellent material for the application of oxygen isotope analysis in biogenic silica. $\delta^{18}O_{diatom}$ data have for the first time provided palaeoclimatic reconstruction at decadal-to-centennial resolution. The well-laminated nature of these sediments allowed a lamina by lamina continuous sampling, giving one of the highest resolution records available for $\delta^{18}O_{diatom}$. It has also revealed important insights into the usefulness of this method, as well as provided decisive palaeoenvironmental information for this critical period.

$\delta^{18}O_{diatom}$ from dark-green diatom laminae represent the baseline in the environmental evolution of Lago Chungará, and show decadal to centennial variability in the moisture conditions of the Andean Altiplano. The isotopic record displays a persistent background isotope enrichment trend related to changes in the lake morphology and groundwater outflow during the late glacial and early Holocene. Overprinted onto this long-term (centennial to millennial) trend there are cyclically short-term (decadal to centennial) shifts which are not related to changes in temperature or isotopic composition of the source of precipitation, but to the P-E balance variability in the Altiplano.

The record shows two major isotope depletions, occurring at a centennial time scale (11,800 and 11,550 cal year BP) indicating a long-term increase in moisture conditions, and one major isotope enrichment above the background levels that occurred between 11,990 and 11,800 cal year BP indicating a short dry phase during the late glacial. Minor depletions at a decadal time scale are associated with weaker rainfall short-term events. The comparison with terrigenous input and effective moisture availability reconstructions previously performed for Lago Chungará shows agreement, but includes a systematic time lag (up to 50 years) among these proxies and $\delta^{18}O_{diatom}$. This is mainly due to the time necessary to change the $\delta^{18}O_{lakewater}$ values and its subsequent incorporation into the diatom frustules, but other factors should not be completely disregarded. The time lag highlights the fact that not all the proxies react at the same time to environmental forcing and this needs to be more often recognised in high resolution palaeolimnological reconstructions.

Sub-millennial shifts in the hydrological balance of Lago Chungará are hypothesised to be the result of changes in the strength and position of the Bolivian High. Spectral analyses of $\delta^{18}O_{diatom}$ suggest that these changes in the atmospheric conditions over the Altiplano during the wet events were triggered by both ENSO and solar activity. The change from the late glacial dry period to a wetter early Holocene period confirms a weakening of El Niño intensity in

the Andean Altiplano region in favour of La Niña-like conditions found elsewhere. Nested upon the underlying climate dynamics are the different cyclicities of solar activity (Schwabe, Hale and Brückner) that were active during different time windows. There is undoubtedly an interaction between these and ENSO at the decadal and greater scales and it is likely that apparent solar forcing of the Lago Chungará record is transmitted via ENSO modulation of the South American monsoon. The complexity of Andean Altiplano palaeoenvironmental conditions, and the absence of other high resolution studies for this time interval, does not allow us to establish any clear conclusion on the existence of significant climatic events synchronous to the Younger Dryas in the northern hemisphere. While many studies have demonstrated ENSO-like forcing during the glacial-interglacial transition, this highly resolved record is one of the few that preserves key ENSO frequencies, therefore further implicating this major climatic process with events governing the transition to the Holocene.

Acknowledgments The Spanish Ministry of Science and Innovation funded the research at Lago Chungará through the projects ANDESTER (BTE2001-3225), Complementary Action (BTE2001-5257-E), LAVOLTER (CGL2004-00683/BTE), GEOBILA (CGL2007-60932/BTE) and CONSOLIDER-Ingenio 2010 GRACCIE (CSD2007-00067). A. Hernández have benefited from a FPI grant from The Spanish Ministry of Science and Innovation. The Limological Research Center (USA) provided the technology and expertise to retrieve the cores. We are grateful to CONAF (Chile) for the facilities provided in Chungará. The NIGL (UK) funded the isotope analysis, and Hilary Sloane is specially thanked for assistance with the diatom oxygen isotope measurements.

References

Abbott MB, Wolfe BB, Wolfe AP, Seltzer GO, Aravena R, Mark BG, Polissar PJ, Rodwell DT, Rowe HD, Vuille M (2003) Holocene paleohydrology and glacial history of the central Andes using multiproxy lake sediment studies. Palaeogeogr Palaeoclimatol Palaeoecol 194:123–138. doi:10.1016/s0031-0182(03)00274-8

Aravena R, Suzuki O, Peña H, Pollastri A, Fuenzalida H, Grilli A (1999) Isotopic composition and origin of the precipitation in northern Chile. Appl Geochem 14:411–422

Baker PA, Seltzer GO, Fritz SC, Dunbar RB, Grove MJ, Tapia PM, Cross SL, Rowe HD, Broda JP (2001a) The history of South American tropical precipitation for the past 25, 000 years. Science 291:640–643

Baker PA, Rigsby CA, Seltzer GO, Fritz SC, Lowenstein TK, Bacher NP, Veliz C (2001b) Tropical climate changes at millennial and orbital timescales on the Bolivian Altiplano. Nature 409:698–701

Barker PA, Street-Perrott FA, Leng MJ, Greenwood PB, Swain DL, Perrott RA, Telford RJ, Ficken KJ (2001) A 14 ka oxygen isotope record from diatom silica in two alpine tarns on Mt Kenya. Science 292:2307–2310

Barker PA, Leng MJ, Gasse F, Huang Y (2007) Century-to-millennial scale climatic variability in Lake Malawi revealed by isotope records. Earth Planet Sci Lett 261:93–103. doi:10.1016/j.epsl.2007.06.010

Betancourt JL, Latorre C, Rech JA, Quade J, Rylander KA (2000) A 22,000-year record of monsoonal precipitation from Northern Chile's Atacama Desert. Science 289: 1542–1546

Brandriss ME, O'Neil JR, Edlund MB, Stoermer EF (1998) Oxygen isotope fractionation between diatomaceous silica and water. Geochim Cosmochimi Acta 62:1119–1125

Brewer TS, Leng MJ, Mackay AW, Lamb AL, Tyler JJ, Marsh NG (2008) Unravelling contamination signals in biogenic silica oxygen isotope composition: the role of major and trace element geochemistry. J Quat Sci 23:321–330. doi: 10.1002/jqs.1171

Clayton RN, Mayeda TK (1963) The use of bromine pentafluoride in the extraction of oxygen from oxide and silicates for isotope analysis. Geochim Cosmochim Acta 27:43–52

Dansgaard W (1964) Stable isotopes in precipitation. Tellus 16:436–468

Dorador C, Pardo R, Vila I (2003) Variaciones temporales de parámetros físicos, químicos y biológicos de un lago de altura: el caso del Lago Chungará. Rev Chil Hist Nat 76:15–22

Fritz SC (2008) Deciphering climatic history from lake sediments. J Paleolimnol 39:5–16. doi:10.1007/s10933-007-9134-x

Garreaud RD, Vuille M, Clement AC (2003) The climate of the Altiplano: observed current conditions and mechanisms of past changes. Palaeogeogr Palaeoclimatol Palaeoecol 194:5–22. doi:10.1016/S0031-0182(03)00269-4

Gasse F, Fontes JC (1992) Climatic changes in northwest Africa during the last deglaciation (16–7 ka BP). NATO ASI Series 12. Kluwer, Dordrecht, pp 295–325

Gat JR (1980) Isotope hydrology of very saline lakes. In: Nissenbaum A (ed) Hypersaline brines and evaporitic environments. Elsevier, Amsterdam, pp 1–8

Giralt S, Moreno A, Bao R, Sáez A, Prego R, Valero BL, Pueyo JJ, González-Sampériz P, Taberner C (2008) Statistical approach to distangle environmental forcings in a lacustrine record: the Lago Chungará case (Chilean Altiplano). J Palaeolimnol 40:195–215. doi:10.1007/s10933-007-9151-9

Grosjean M, Valero-Garcés B, Geyh MA, Messerli B, Schreier H, Kelts K (1997) Mid and late holocene limnogeology of laguna del negro francisco, northern chile, and its paleoclimatic implications. The Holocene 7:151–159

Grosjean M, van Leeuwen JFN, van der Knaap WO, Geyh MA, Ammann B, Tanner W, Messerli B, Núñez L, Valero-Garcés BL, Veit H (2001) A 22,000 14C year BP sediment and pollen record of climate change from Laguna Miscanti (23°S), Northern Chile. Glob Planet Change 28:35–51

Hernández A, Bao R, Giralt S, Leng MJ, Barker PA, Pueyo JJ, Sáez A, Moreno A, Valero-Garcés B, Sloane HJ (2007) A high-resolution study of diatom oxygen isotopes in a Late Pleistocene to Early Holocene laminated record from Lake Chungará (Andean Altiplano, Northern Chile). Geochim Cosmochim Acta 71:A398

Hernández A, Bao R, Giralt S, Leng MJ, Barker PA, Sáez A, Pueyo JJ, Moreno A, Valero-Garcés BL, Sloane HJ (2008) The palaeohydrological evolution of Lago Chungará (Andean Altiplano, northern Chile) during the Lateglacial and early Holocene using oxygen isotopes in diatom silica. J Quat Sci 23:351–363. doi:10.1002/jqs.1173

Herrera C, Pueyo JJ, Sáez A, Valero-Garcés BL (2006) Relación de aguas superficiales y subterráneas en el área del lago Chungará y lagunas de Cotacotani, norte de Chile: un estudio isotópico. Rev Geol Chile 33:299–325

Hora J, Singer B, Wörner G (2007) Volcano eruption and evaporative flux on the thick curst of the Andean Central Volcanic Zone: $40^{Ar}/39^{Ar}$ constrains from Volcán Parinacota, Chile. Geol Surv Am Bull 119:343–362. doi:10.1130/B25954.1

Juillet-Leclerc A (1986) Cleaning process for diatomaceous samples. In: Ricard M (ed) 8th diatom symposium. Koeltz Scientific Books, Koenigstein, pp 733–736

Koutavas A, Lynch-Stieglitz J, Marchitto T, Sachs J (2002) El Niño-like pattern in ice age tropical Pacific sea surface temperature. Science 297:226–230

Leng MJ, Barker PA (2006) A review of the oxygen isotope composition of lacustrine diatom silica for palaeoclimate reconstruction. Earth Sci Rev 75:5–27. doi:10.1016/j.earscirev.2005.10.001

Leng MJ, Lamb AL, Heaton THE, Marshall JD, Wolfe BB, Jones MD, Holmes JA, Arrowsmith C (2005) Isotopes in lake sediments. In: Leng MJ (ed) Isotopes in palaeoenvironmental research. Springer, Dordrecht, pp 147–184

Maslin MA, Burns SJ (2000) Reconstruction of the Amazon Basin effective moisture availability over the past 14,000 years. Science 290:2285–2287

Moreno A, Giralt S, Valero-Garcés BL, Sáez A, Bao R, Prego R, Pueyo JJ, González-Sampériz P, Taberner C (2007) A 13 kyr high-resolution record from the tropical Andes: The Chungará Lake sequence (18°S, northern Chilean Altiplano). Quat Int 161:4–21. doi:10.1016/j.quaint.2006.10.020

Morley DW, Leng MJ, Mackay AW, Sloane HJ, Rioual P, Battarbee RW (2004) Cleaning of lake sediment samples for diatom oxygen isotope analysis. J Paleolimnol 31:391–401

Moschen R, Lücke A, Schleser G (2005) Sensitivity of biogenic silica oxygen isotopes to changes in surface water temperature and palaeoclimatology. Geophys Res Lett 32:L07708. doi:10.1029/2004GL022167

Moy CM, Seltzer GO, Rodbell DT, Anderson DM (2002) Variability of El Niño/Southern Oscillation activity at millenial timescales during the Holocene epoch. Nature 420:162–165

Mühlhauser H, Hrepic N, Mladinic P, Montecino V, Cabrera S (1995) Water-quality and limnological features of a high-altitude andean lake, Chungará in northern chile. Rev Chil Hist Nat 68:341–349

Negri AJ, Adler RF, Shepherd JM, Huffman G, Manyin M, Neklin EJ (2004) A 16-year climatology of global rainfall from SSM/I highlighting morning versus evening differences. 13th Conference on Satellite Meteorology and Oceanography. American Meteorological Society, Norfolk, VA P6. 16

Placzek C, Quade J, Patchett PJ (2006) Geochronology and stratigraphy of late Pleistocene lake cycles on the southern Bolivian Altiplano: Implications for causes of tropical climate change. Geol Soc Am Bull 118:515–532. doi:10.1130/B25770.1

Rietti-Shati M, Shemesh A, Karlen W (1998) A 3000-year climatic record from biogenic silica oxygen isotopes in an equatorial high-altitude lake. Science 281:980–982

Rigsby CA, Bradbury JP, Baker PA, Rollins SM, Warren MR (2005) Late Quaternary palaeolakes, rivers, and wetlands on the Bolivian Altiplano and their palaeoclimatic implications. J Quat Sci 20:671–691. doi:10.1002/jqs.986

Rings A, Lucke A, Schleser GH (2004) A new method for the quantitative separation of diatom frustules from lake sediments. Limnol Oceanogr Methods 2:25–34

Rodbell DT, Seltzer GO, Anderson DM, Abbott MB, Enfield DB, Newman JH (1999) An 15, 000-year record of El Niño-driven alluviation in southwestern Ecuador. Science 283:516–520

Rodó X, Rodríguez-Arias MA (2004) El Niño–Southern oscillation: absent in the early holocene? J Clim 17:423–426

Rowe HD, Dunbar RB, Mucciarone DA, Seltzer GO, Baker PA, Fritz S (2002) Insolation, moisture balance and climate change on the South American Altiplano since the Last Glacial Maximum. Clim Change 52:175–199

Sáez A, Valero-Garcés BL, Moreno A, Bao R, Pueyo JJ, González-Sampériz P, Giralt S, Taberner C, Herrera C, Gibert RO (2007) Volcanic controls on lacustrine sedimentation: The late Quaternary depositional evolution of lake Chungará (Northern Chile). Sedimentology 54:1191–1222. doi:10.1111/j.1365-3091.2007.00878.x

Servant M, Servant-Vildary S (2003) Holocene precipitation and atmospheric changes inferred from river paleowetlands in the Bolivian Andes. Palaeogeogr Palaeoclimatol Palaeoecol 194:187–206

Stockwell RG, Mansinha L, Lowe RP (1996) Localization of the complex spectrum: the S transform. IEEE TSP 44:998–1001

Sylvestre F, Servant M, Servant-Vildary S, Causse C, Fournier M, Ybert J-P (1999) Lake-level chronology on the southern Bolivian Altiplano (18°–23°S) during late-glacial time and the early Holocene. Quat Res 51:54–66

R Development Core Team (2008) R: a language and environment for statistical computing. R Foundation for statistical computing, Vienna, Austria ISBN 3-900051-07-0. http://www.R-project.org

Theissen KM, Dunbar RB, Rowe HD, Mucciarone DA (2008) Multidecadal- to century-scale arid episodes on the Northern Altiplano during the middle Holocene. Palaeogeogr Palaeoclimatol Palaeoecol 257:361–376. doi:10.1016/j.palaeo.2007.09.011

Thompson LG, Davis ME, Mosley-Thompson E, Sowers TA, Henderson KA, Zagorodnov VS, Lin PN, Mikhalenko VN, Campen RK, Bolzan JF, Cole-Dai J, Francou B

(1998) A 25, 000-year tropical climate history from Bolivian ice cores. Science 282:1858–1864

Valero-Garcés BL, Grosjean M, Schwalb A, Schreir H, Kelts K, Messerli B (2000) Late Quaternary lacustrine deposition in the Chilean Altiplano (18°–28°S). In: Gierlowski-Kordech E, Kelts K (eds) Lake basins through space and time. Studies in Geology 46. Am Assoc Petr Geol, pp 625–636

Valero-Garcés BL, Delgado-Huertas A, Navas A, Edwards L, Schwalb A, Ratto N (2003) Patterns of regional hydrological variability in central-southern Altiplano (18°-26°S) lakes during the last 500 years. Palaeogeogr Palaeoclimatol Palaeoecol 194:319–338

Velasco VM, Mendoza B (2008) Assessing the relationship between solar activity and some large scale climatic phenomena. Adv Space Res 42:866–878. doi:10.1016/j.asr.2007.05.050

Vuille M, Werner M (2005) Stable isotopes in precipitation recording South American summer monsoon and ENSO variability: observations and model results. Clim Dyn 25:401–413. doi:10.1007/s00382-005-0049-9

Weng C, Bush MB, Curtis JH, Kolata AL, Dillehay TD, Binford MW (2006) Deglaciation and Holocene climate change in the western Peruvian Andes. Quat Res 66:87–96. doi:10.1016/j.yqres.2006.01.004

Biogeochemical processes controlling oxygen and carbon isotopes of diatom silica in lacustrine rhythmites

Armand Hernández[1,2*], Roberto Bao[3], Santiago Giralt[1], Philip A. Barker[4], Melanie J. Leng[5], Hilary J. Sloane[5], Alberto Sáez[2]

[1]*Institute of Earth Sciences 'Jaume Almera'-CSIC, C/Lluís Solé i Sabarís s/n, 08028 Barcelona, Spain*
[2]*Faculty of Geology, University of Barcelona, C/ Martí Franquès s/n, 08028 Barcelona, Spain*
[3]*Faculty of Sciences, University of A Coruña, Campus da Zapateira s/n, 15701 A Coruña, Spain*
[4]*Lancaster Environment Centre, Lancaster University, Lancaster LA1 4YQ, UK*
[5]*NERC Isotope Geosciences Laboratory, British Geological Survey, Nottingham NG12 5GG, UK*

Abstract

Biogeochemical cycles and sedimentary records in lakes are related to climate controls on hydrology and catchment processes. Changes in the isotopic composition of the diatom frustules ($\delta^{18}O_{diatom}$ and $\delta^{13}C_{diatom}$) in lacustrine sediments can be used to reconstruct palaeoclimatic and palaeoenvironmental changes. The Lago Chungará diatomaceous laminated record is made up of white and green multiannual rhythmites. White laminae were formed during short-term super-blooms, and are composed almost exclusively of large-size *Cyclostephanos andinus* which bloom during mixing events when recycled nutrients from the bottom waters are brought to the surface and/or when nutrients are introduced from the catchment during periods of strong runoff. Conversely, the green laminae, are thought to have been deposited over several years and are composed of a mixture of diatoms (mainly smaller valves of *Cyclostephanos andinus* and *Discostella stelligera*) and organic matter. These green laminae reflect the lake's hydrological recovery from the conditions favouring the diatom super-blooms (white laminae) towards baseline conditions. Analyses of both $\delta^{18}O_{diatom}$ and $\delta^{13}C_{diatom}$ in these rhythmites are interpreted in terms of shifts in the precipitation/evaporation ratio and changes in the lake water dissolved carbon concentration, respectively. $\delta^{18}O_{diatom}$ composition shows that white laminae formation occurred mainly during low lake level stages, whereas green laminae formation generally occurred during high lake level stages. The isotope and chronostratigraphical data together suggest that white laminae deposition is caused by extraordinary environmental events. El Niño-Southern Oscillation and solar activity are the most likely main climate forcing mechanisms that could trigger such events, favouring hydrological changes at interannual-to-decadal scale. This study demonstrates the potential for laminated lake sediments to document extreme events.

Keywords: Oxygen isotopes, carbon isotopes, diatoms, Lago Chungará, ENSO

Corresponding author:
Institute of Earth Sciences 'Jaume Almera' (CSIC). C/Lluis Solé i Sabarís s/n. E-08028 Barcelona (Spain).
Phone: +34.934.095.410
Fax: +34.934.110.012
E-mail: ahernandez@ija.csic.es

1.Introduction

Rhythmites are finely laminated sequences (millimetre- to submillimetre thick) made up of regular alternations of two or three contrasting sediment types called couplets or triplets (Talbot and Allen, 1996). Rhythmite formation is generally associated with seasonally heterogeneous sediment supply and a lack of physical or biological reworking processes (Grimm et al. 1996). Thus, laminated sediments indicate high-frequency environmental change through time. A number of studies have described laminated lacustrine sediments, but they have mainly dealt with annual-rhythmites (varves) with different clastic grain-size and/or biogenic content deposited over different seasons (e.g. Bird et al. 2009). At mid- to high latitudes the processes that lead to rhythmite formation are often well constrained (e.g. Chang et al. 2003), whereas the biogeochemical processes and climate events which prompt laminated sediments in tropical lacustrine sediments are often less understood. In these cases, tropical rainfall regimes associated with intense storms and wind may be responsible for extraordinary external nutrient loading or upwelling of nutrient rich-waters which trigger phytoplankton blooms (Talbot and Allen, 1996). These tropical climate regimes follow a seasonal behaviour (e.g. monsoons), but they can also be highly influenced by climatic multiannual phenomena (e.g. ENSO).

Changes in the oxygen isotopic composition of the diatom frustules ($\delta^{18}O_{diatom}$) in lacustrine sediments are used to infer hydrological variations. For closed lakes in the tropics, these variations are mostly related to the precipitation-evaporation ratio (P/E), which is generally directly linked to lake level change (Leng and Barker, 2008). The isotope-inferred reconstructions can thus be used to unreveal the climate history of the region (e.g. Barker et al. 2007) although this may be mitigated by biological and sedimentary processes. Besides $d^{18}O_{diatom}$, the isotopic signature of carbon occluded within the diatom silica ($\delta^{13}C_{diatom}$), can give other relevant palaeoenvironmental information, including insights on the lakes' carbon cycle. There are few studies of carbon isotopes from organic inclusions within diatom frustules, and of those published, most have dealt with marine sedimentary records (e.g. Crosta and Shemesh, 2002). Studies on $\delta^{13}C_{diatom}$ in lake sediments are now emerging and providing valuable insights into the complex carbon cycle of lakes (Hurrell et al., submitted).

The aim of this paper is to understand high frequency biological, chemical and sedimentary processes which cause the laminae formation in the sedimentary record of Lago Chungará, a high altitude tropical lake located in the Central Andes. $\delta^{18}O_{diatom}$ and $\delta^{13}C_{diatom}$ data from individual lamina are presented for a period between 11,990 and 11,530 cal yr BP. High frequency environmental perturbations brought about by interannual-decadal climatic events are rarely recorded in lake sediments, and therefore, the laminated sediments here are a good record of their intensity and their effect on lacustrine hydrological and carbon cycles.

2. Lago Chungará setting

2.1. Climate, geology and limnology

A variable precipitation pattern dominates the Lago Chungará region, where the annual rainfall ranges from 100 to 750 mm yr^{-1} (mean 411 mm yr^{-1}), and more than the 70% of it falls during the austral summer (December–February). At this time, a strong low pressure region, known as the South American Summer Monsoon (SASM), is formed over Central South America driving convection and pulling moisture from the equatorial Atlantic to the Andean Altiplano (Zhou and Lau, 1998; Vuille and Werner, 2005). The SASM is a major component of the climate system over tropical and subtropical South America during the austral summer and is remotely forced by tropical Pacific SSTs (Vuille and Werner 2005). At interannual timescales, El Niño-Southern Oscillation (ENSO) is the most important forcing causing climatic fluctuations over the tropical Americas owing it controls changes in the Pacific Tropical Sea Surface Temperatures (SSTs) (Dettinger et al. 2001; Vuille et al. 2003). Moreover, decadal variations in solar activity are currently modulating the sign and strength of the zonal winds above the Altiplano (Theissen et al. 2008). There is an interaction between the solar activity and ENSO at the decadal and greater scales and it is likely that solar forcing is

transmitted to the Lago Chungará record via ENSO modulation of the South American monsoon (Hernández et al. in press).

Lago Chungará (18º15'S, 69º10'W, 4520 m a.s.l.) is a cold-polymictic and oligo- to meso-eutrophic lake located in the Andean Altiplano (Central Andes). The lake sits on the Cenozoic Lauca Basin sedimentary deposits surrounded by volcanoes. The Chungará infill mostly comprises organic diatomaceous sediments with abundant tephra from the Parinacota Volcano which was active during most of the Late Glacial and Holocene (Sáez et al. 2007) (Fig. 1A). The lake occupies 21.5 km^2 and has a maximum water depth of 40 m (Fig. 1B). It is moderately alkaline (pH between 8.99 and 9.30), well mixed (7.6 ppm O_2 at 34 m deep), salinity is around 1.2 $g \cdot l^{-1}$, conductivity values range between 1500 and 3000 mS cm^{-1} and waters are of the Na^+-Mg^{2+}-HCO_3^--SO_4^{2-} type (Sáez et al., 2007). The phytoplankton community is made up of a few major species; diatoms dominant the cold season, whereas Chlorophyceae dominate during the austral summer (Dorador et al. 2003). Macrophyte communities form dense patches and microbial colonies in the littoral zone contribute to primary productivity. The local vegetation in the catchment is characterised by low cover values (<30%), being dominated by grasses, shrubs, soligenous peatlands, and Quenoa dwarf forests (Baied and Wheeler, 1993; Moreno et al. 2007).

The lake is considered hydrologically closed as there is no surface outlet and the residence time of the lake water is approximately 15 years (Herrera et al. 2006). The main inlet to the lake is the Chungará River (300-460 l s^{-1}), whereas evaporation causes the main water loss (3.10^7 $m^3 \cdot yr^{-1}$), and represents about 80% of the total outflow. The $d^{18}O$ and dD composition of the lake water in 2002 and 2004 (–1.4‰ SMOW and –43.4‰ SMOW, respectively) diverge significantly from the Global Meteoric Water Line (GMWL), the Regional Meteoric Water Line (RMWL, where $d^{18}O$ presents a mean value of - –14.3‰ and dD shows a mean value of -–95‰) and isotope composition of the inflowing water (–12.6‰ SMOW and –108.5‰ SMOW, respectively) (Herrera et al. 2006). The lake water is enriched compared to the

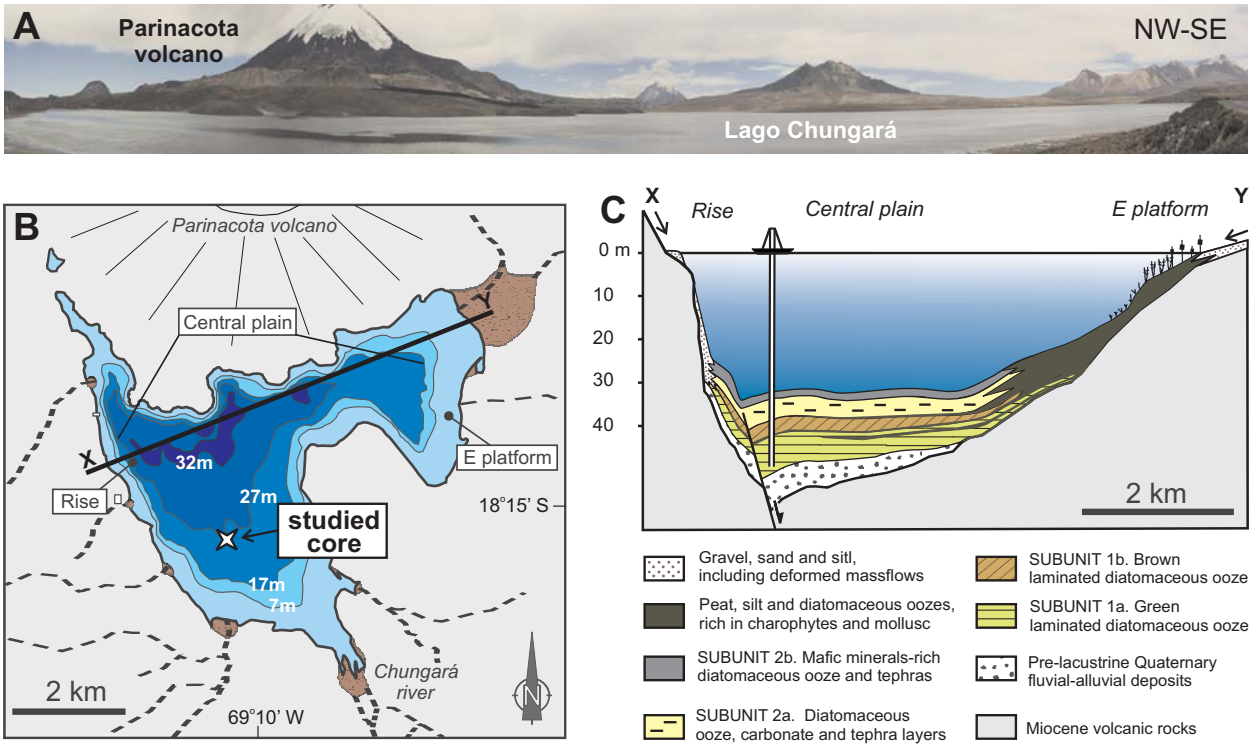

Fig. 1. A. Panoramic view of Lago Chungará. B. Bathymetric map of Lago Chungará showing the main morphological units of the lake floor cited in the text, and position of the studied core. Black line indicates the cross section *(C)* throughout the lake. C. Cross section of sediment infilling of Lago Chungará. Position of the studied core is shown; note that the position of the core is projected in its equivalent position at the lake central plain. Arrows indicate major hydrological inputs and sedimentary contributions to the lake. Simplified from Sáez et al. (2007).

inflowing water ($\delta^{18}O$ by +11.2‰ and δD by +65‰) due to evaporation.

2.2. Rhythmite type sedimentary model

Stratigraphy and facies association for the uppermost part of the sedimentary sequence infill of Lago Chungará was established by fifteen Kullenberg cores and seismic imagery (Valero-Garcés et al. 2000; Sáez et al. 2007). Laminated sediments present in the lower sedimentary unit 1 defined in Sáez et al. (2007) were divided in the subunits 1a and 1b according to its green or brown dominating colour and were correlated over the lake offshore zone (central basin) (Fig. 1C).

A petrographical study established a preliminary depositional rhythmite type for those sediments where rhythmites are composed by variable-thickness couplets of light-white and dark-green laminae (Hernandez et al. 2008). According to the chronological model, based on 17 ^{14}C AMS and one $^{238}U/^{230}Th$ dates (Giralt et al. 2008), each couplet was deposited during time intervals ranging from 4 to 24 yr (Hernandez et al. 2008). The oxygen isotope composition of diatoms from selected samples taken from subunits 1a and 1b have been previously published (Hernández et al. 2008, in press).

3. Methods

A 43 cm-thick section of the finely laminated greenish sediments from subunit 1a (831 cm to 788 cm core depth) was selected as this had well resolved laminae and abundant diatom frustules, and sampled for $\delta^{18}O_{diatom}$, $\delta^{13}C_{diatom}$ and %C on diatom-bound organic matter ($\%C_{diatom}$) analyses. These sediments were continuously sampled for thin sections in order to carry out a detailed petrographical study. Thin sections of 120 mm x 35 mm (30 mm in thickness), with an overlap of 1 cm at each end, were obtained after freeze-drying and balsam-hardening. Detailed petrographical descriptions and lamina thickness measurements were performed with a Zeiss Axioplan 2 Imaging petrographic microscope. A number of samples were also selected for observation with a Jeol JSM-840 electron microscope in order to complement the petrographical study. Moreover, a grey-colour curve was calculated using the ImageJ software package (Rasband 1997–2009). The results are presented in a 21 running mean smoothed curve.

A total of 102 samples were obtained and 100 were successfully analysed for $\delta^{18}O_{diatom}$. Additionally, 11 of these samples, due to the difficulty to get enough amount of sample and obtain reliable results, were also analysed for $\delta^{13}C_{diatom}$ and $\%C_{diatom}$. Two previous studies described $\delta^{18}O_{diatom}$ data from 22 (Hernández et al. 2008) and 40 (Hernández et al. In press) dark-green sample levels to establish the baseline environmental evolution of Lago Chungará.

$\delta^{18}O_{diatom}$, $\delta^{13}C_{diatom}$ and $\%C_{diatom}$ samples were treated following the method proposed by Morley et al. (2004) with some modifications (Hernández et al., 2008; Hurrell et al; submitted). For $\delta^{18}O_{diatom}$ analyses the classical stepwise fluorination method was applied to strip hydrous components from diatom silica before a full reaction with BrF_5 (Leng and Barker, 2006; Leng and Sloane, 2008). The oxygen liberated was then converted to CO_2 and normalised through the laboratory standard (BFC) and the NBS-28 quartz standard, referenced to VSMOW. A random selection of more than 30 samples were analysed in duplicate or even in triplicate giving a reproducibility between 0.0‰ and 0.3‰ with a mean value of 0.15‰. Three samples with a reproducibility >0.3‰ were rejected. Isotope variations of consecutive samples are between 0‰ and 6.5‰, with a mean value of 1.0‰. Samples with differences <0.15‰ have not been used because they were considered essentially the same. As a result, until 81 inter-samples relationships between samples have been included in the analysis.

The $\delta^{13}C_{diatom}$ content on diatom-bound organic matter analyses were performed by combustion in an elemental analyser (Costech ECS4010) interfaced with a VG dual inlet isotope ratio mass spectrometer. The $\delta^{13}C_{diatom}$ values were calculated to the VPDB scale using a within-run laboratory standards calibrated against NBS 18 and 19, and additionally cross checked with NBS 22. %C analyses were performed by combustion separately in the elemental analyser calibrated against an Acetanilide standard. Replicate $ä^{13}C_{diatom}$ and %C analysis of well-mixed samples indicated a precision of ± <0.1. All the analyses were carried out at the NERC Isotope Geosciences Laboratory, British Geological Survey (UK).

4. Results

4.1 Laminae biogenic composition

The present study extends the petrographical examination of the diatomaceous laminated sediments of Lago Chungará for the Late Glacial to early Holocene transition (11,990 - 11,530 cal yr BP) described in Hernández et al. (2008). A hundred laminae have been differentiated and grouped under the white, light-green and dark-green laminae categories according to their diatom composition, organic matter content and colour. Additionally, nine laminae were undifferentiated due to their mixed features between the three groups (Fig. 2).

White laminae are formed almost exclusively by diatom frustules of the large (diameter > 50 µm) euplanktonic diatom *Cyclostephanos andinus* (Fig. 3G). Dark-green laminae, which contain a higher organic matter content, probably derived from diatoms and other algal groups, are made up of a mixture of different diatom species. This mixture is mainly composed of smaller (diameter < 50 µm) *Cyclostephanos andinus* valves, with diatoms of the *Discostella stelligera* species complex as co-dominant taxa. Subdominant diatom taxa comprise a number of tychoplanktonic (mainly *Staurosira construens* aff. *venter* and *Fragilaria* spp.) and benthic life forms (including *Cocconeis placentula*, *Gomphonema minutum*, *Nitzschia tropica* and *Opephora* sp. aff. *mutabilis*) (Fig. 3C). The light-green laminae are made up of components from the white laminae progressively grading upwards to the typical constituents of the dark-green laminae. Diatoms of the light-green laminae are

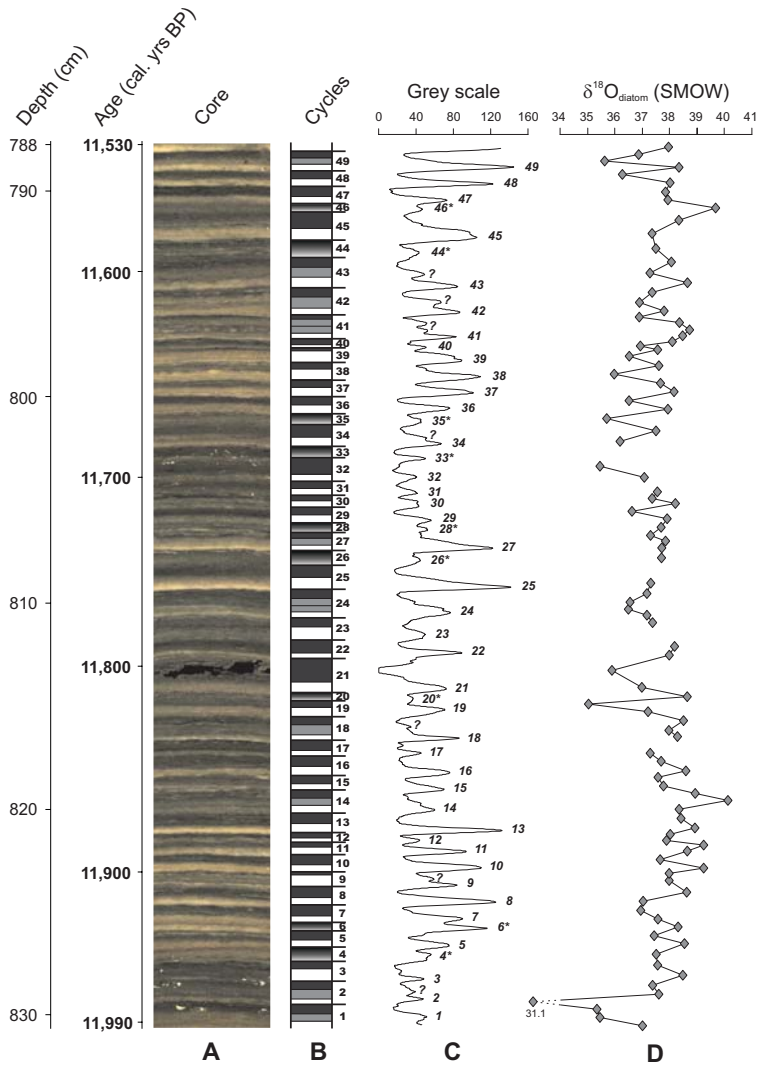

Fig. 2. A. Digital XRF ITRAX core scanner image from the selected and sampled interval indicating the age and its correspondent core depth. B. The 49 defined cycles composed by couplet/triplets from 102 sampled laminae. C. The smoothed grey-colour curve D. $\delta^{18}O_{diatom}$ values associated to each lamina. Note the diatom super-blooms are indicated by thicker white laminae and the higher values of the curve..

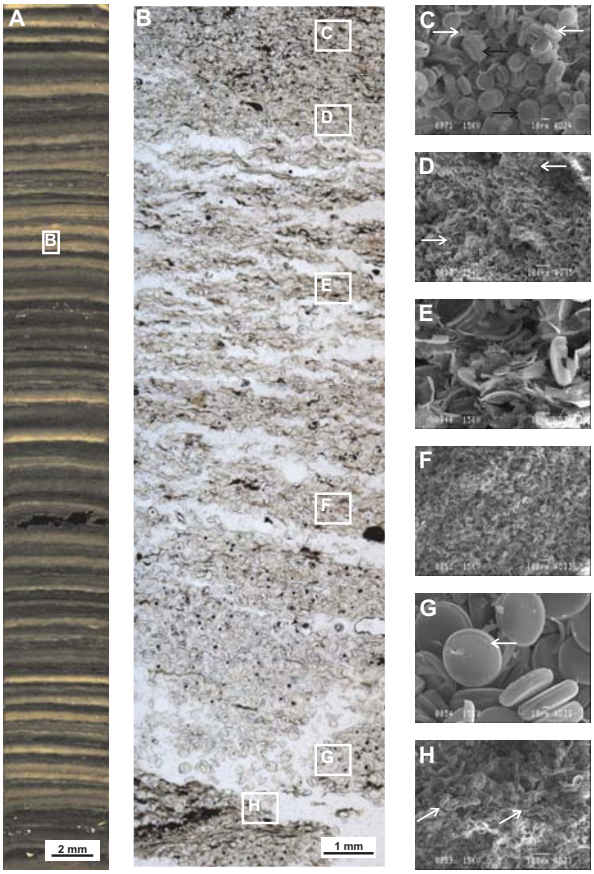

Fig. 3. A. Digital XRF ITRAX core scanner image of laminated sediments of core 11 corresponding to the sampled interval of Subunit 1a. Note that the lamination is composed by millimetre thick white lamina and green lamina forming rhythmites.

B. Photomosaic from a thin-section showing an ideal triplet rhythmite sequence made up of (from base to top): *(H)* Abrupt contact between dark-green and white laminae; *(G)* A white lamina formed by skeletons of the large diatom *Cyclostephanos andinus* (> 50 µm); *(F)* Gradual contact between white and light-green laminae; *(E)* A light-green lenticular and discontinous lamina which is made up of a mixture of white and dark-green lamina; *(D)* Gradual contact between light- and dark- green laminae; *(C)* A dark-green lamina made up of diatoms embedded in an organic matter matrix.

C. SEM image of dark-green lamina mainly made up by *Cyclostephanos andinus* (black arrows) and diatoms of the *Discostella stelligera* species complex (white arrows). Note the smaller *Cyclostephanos andinus* size (diameter < 50µm)

D. SEM image showing the decreasing upwards size of the diatoms throughout an intra-cycle contact between a light-green lamina and a dark-green lamina. Arrows indicate the different size of the diatoms.

E. SEM image of a light-green lamina. The lamina is made up of complete valves and fragments of *Cyclostephanos andinus* valves, both showing a preferential orientation.

F. SEM image showing an intracycle contact between the white and light-green laminae. Note the preferential orientation of de diatoms placed at the top of the image (light-green lamina).

G. SEM image of a white lamina. The lamina is exclusively composed by large *Cyclostephanos andinus* (diameter > 50µm). The excellent preservation of the diatom frustules can be observed in the image (white arrow). There are no signs of dissolution.

H. SEM image showing an intercycle contact between a dark-green and a white lamina. The arrows indicate the exact position of the contact which can be perfectly followed. Note the different size of the diatoms.

usually embedded in an organic matrix creating a preferential orientation of the valves (Fig. 3B and E). Thus, a lower white lamina, an intermediate light-green lamina and an upper dark-green lamina form a typical sedimentary triplet. These light-green laminae may be variable in thickness or even absent. The transition between well-defined laminae within the triplets (from here on called *intra*-cycle relationships) is gradual, whereas the transition between different triplets is abrupt (from here on called *inter*-cycle relationships) (Fig. 3 B, D, F and H).

4.2. Laminae isotope composition

In spite of the very high sampling resolution (mean=4 yr, sd=1.5, n=101) $\delta^{18}O_{diatom}$ values display a large variability, ranging between +40.1‰ and +31.1‰ with a mean value of +37.5‰ for the whole record (sd=1.1, n=97) (Fig. 2). The studied interval shows three $\delta^{18}O_{diatom}$ major enrichment trends which coincide with similar trends in the grey-colour curve (Fig. 4). The $\%C_{diatom}$ values range from 0.63% in the uppermost sample (rhythmite 48) to 0.32% in the lowermost sample (rhythmite 8) (mean=0.42%, sd=0.10, n=11) whereas $\delta^{13}C_{diatom}$ values oscillate between –26.1‰ and –29.5‰ (mean=–28.1‰, sd=0.95, n=11). The white laminae generally display lower $\%C_{diatom}$ and $\delta^{13}C_{diatom}$ values than the dark laminae from the same rhythmite, in addition there is an increase in C/Si ratios and $\delta^{13}C_{diatom}$ values throughout the 5 studied intra-cycle relationships (Table 1).

$\delta^{18}O_{diatom}$ inter-cycle relationships have been studied in 49 cases. From these, 12 cases could not be taken into account due to the absence of $\delta^{18}O_{diatom}$ data or because the difference between the two consecutive isotopic values was below the mean analytical error. Valid $\delta^{18}O_{diatom}$ inter-cycle relationships (n=37) are characterised by higher oxygen isotope values. The most common inter-cycle relationship is the dark-green to white laminae (n = 25), and it shows isotope enrichment (i.e. values increase) in 60% of the cases. Likewise, the difference between dark-green laminae to undifferentiated laminae shows similar levels of increasing $\delta^{18}O_{diatom}$, whereas relationships between undifferentiated and white laminae show both increases and decreases in $\delta^{18}O_{diatom}$ (Table 2A).

There are 51 valid (out of 62) relationships between

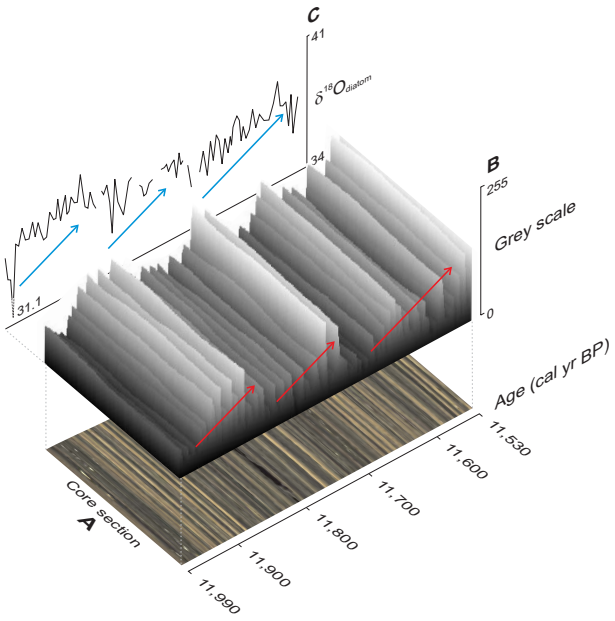

Fig. 4. A. Digital XRF ITRAX core scanner image from the selected interval. B Grey-colour surface plot elaborated from the digital image. Decadal-scale main grey-colour trends to whiter values are indicated by means of red arrows. C. $d^{18}O_{diatom}$ record. Decadal-scale main $d^{18}O_{diatom}$ trends to higher values are indicated by means of blue arrows. Note the good agreement between both proxies.

laminae that take place within a rhythmite (intra-cycle relationships). These intra-cycle relationships are dominated by isotope depletion (values decrease). The most usual case shows changes from white to dark-green laminae (n=23) where isotope decreases occur in 67% of the cases (Table 2B).

5. Discussion

5.1. Biological and sedimentary processes forming rhythmites

White laminae features (relatively thick, good diatom preservation and monospecific diatom composition) suggest accumulation during short-term massive diatom blooms, perhaps of only days to weeks in duration. According to the chronological model rhythmites are not a product of annual variations in sediment supply, but due to some kind of multiannual processes (Hernández et al., 2008). Causes of super-blooms can be different to regular seasonal blooms which occur as part of the normal phytoplankton succession (Reynolds, 2006). We suggest that our diatom super-blooms may have been triggered by abnormally high nutrient concentrations coupled with hydrological conditions prompting diatom population growth. Low lake level stages and/or strong wind episodes would favour upwelling of nutrient-rich hypolimnion waters (Talbot and Allen, 1978). Strong mixing would also select diatoms over other types of phytoplankton due to their relative buoyancy. Alternatively, the increase in nutrient external loading due to exceptional catchment erosion during wet events could also have had the same effect (Bradbury et al. 2002). ENSO cyclicity signals recorded at this time in the Lago Chungará record (Hernández et al., in press) provide

Table 1
List of samples where both $\delta^{18}O_{diatom}$ and $\delta^{13}C_{diatom}$ analyses were carried out, including main sample features.

Sample	Cycle	Colour	Depth (cm)	Age (cal yr BP)	$\delta^{18}O_{diatom}$ (SMOW)	$\delta^{13}C_{diatom}$ (PDB)	$\%C_{diatom}$
5	48	Dark-green	789.1	11,543	36.27	-28,99	0,63
6	48	White	789.5	11,547	38.01	-28,51	0,47
13	43	Dark-green	793.4	11,588	38.07	-26,05	0,57
14	43	Light-green	794.1	11,595	37.29	-28,30	0,38
15	43	White	794.5	11,599	38.65	-28,46	0,39
29	37	Dark-green	799.3	11,650	37.67	-27,87	0,40
30	37	White	799.6	11,653	38.16	-29,01	0,33
77	13	Dark-green	820.5	11,872	38.44	-27,21	0,44
78	13	White	820.9	11,876	38.91	-29,53	0,32
87	8	Dark-green	824	11,909	38.62	-27,69	0,38
88	8	White	824.3	11,912	37.03	-28,89	0,32

Table 2
A. Intercycle isotope relationships between the defined rhythmites. B. Intracycle isotope relationships between the defined rhythmites. Relationship types are established according to the colour of the laminae that are in contact.

Intercycle relationship types	Enrichments (%)	Depletions (%)	*n*
Dark-green to white laminae	60	40	25
Dark-green to undifferentiated laminae	67	33	6
Undifferentiated to white laminae	50	50	6
Total			37

Intracycle relationship types	Enrichments (%)	Depletions (%)	*n*
White laminae to light-green laminae	33	67	9
Light-green to light-green laminae	0	100	1
Light-green to dark-green laminae	56	44	9
White laminae to dark-green laminae	35	65	23
White laminae to dark-green laminae *(non-consecutive laminae, base to top of the rhythmite)*	33	67	9
Total			51

support to the existence of those two contrasting dry (El Niño) and wet (La Niña) conditions (Vuille et al., 2000; Valero-Garcés et al., 2003).

Dark-green laminae (made up of a mixture of diatom valves belonging to several planktonic and benthic taxa, all embedded in an organic matter matrix) represent the baseline lake conditions where the complete phytoplankton successions over several years are preserved. These laminae therefore record the 'normal' intra- and inter-annual changes in the water column mixing regime characterised by the shifting species composition throughout general annual phythoplankton cycles. Preservation occurs as skeletons belonging to several diatom taxa, or simply as the organic matter mainly belonging to other algal groups (likely Chlorophycean, Cyanobacteria, etc.) that embed the valves in the dark-green laminae. Regular seasonal diatom blooms, are likely manifested in the dark-green laminae by the abundance of the small *Cyclostephanos andinus* (< 50 μm), a large centric diatom whose buoyancy depends on the existence of a turbulent regime. Seasonal *Cyclostephanos andinus* (< 50 μm) blooms reflected in the dark-green laminae would therefore be triggered by the same process during the super-blooms of the larger *Cyclostephanos andinus* (> 50 μm) that make up the white laminae (i.e. water stratification breakdown). The dark-green laminae are sometimes preceded by light-green laminae. This observation indicates that recovery of the baseline conditions from the super-blooms can be more or less gradual (forming couplets or triplets, respectively).

Flocculation of diatoms by extracellular polymeric substances is a common feature in the marine realm (Thornton, 2002). This phenomenon occurs towards the end of a diatom bloom, due to the onset of nutrient limitation. Diatom aggregation and subsequent rapid sedimentation of species having any kind of resting cell stages would favour future recruitment once nutrient resources were again available (Smetacek, 1985). Biosiliceous laminae in marine sediments have been interpreted as the product of changes in the mass sedimentation of diatoms by means of the formation of aggregates (Grimm et al., 1996, 1997). At Lago Chungará a similar phenomenon could have taken place in the formation of the light-green laminae once the super-blooms of the large (> 50 μm) *Cyclostephanos andinus* come to an end. Aggregation of cells enclosed in a gelatinous

matrix could therefore have taken place, being rapidly deposited in the form of the transitional light-green laminae. Although the life cycle details of *Cyclostephanos* are far from fully known, the closely related genera *Stephanodiscus*, to which *Cyclostephanos* once belonged (Round et al., 1990), is known to produce resting cells (Sicko-Goad et al., 1989), whose aggregation and rapid sedimentation represents a transition to a resting phase (Smetacek, 1985; Alldredge et al., 1995). It is therefore likely that the mechanism of formation of triplets is mediated by processes of self-sedimentation triggered by *Cyclostephanos andinus* (Grimm et al., 1997).

5.2. $\delta^{18}O_{diatom}$ and $\delta^{13}C_{diatom}$ interpretation

Variation in $\delta^{18}O_{diatom}$ can result from a variety of processes, such as oxygen isotope composition of the lake water ($\delta^{18}O_{lakewater}$), temperature, vital effects and post depositional diagenesis (Leng and Barker, 2006). In hydrologically closed lakes under arid climate conditions evaporative concentration processes have a much larger effect on $\delta^{18}O_{lakewater}$ than any other process (Gasse and Fontes, 1992; Leng and Marshall, 2004; Hernández et al, in press). In these circumstances, the $\delta^{18}O_{diatom}$ record can be used as an indicator of changes in the P/E related to climatic change (Leng and Barker, 2006).

At present, Lago Chungará can be considered a closed lake due to its water residence time (ca. 15 years), and the fact that $\delta^{18}O_{lakewater}$ is enriched by 14‰ relative to $\delta^{18}O$ of the inputs (precipitation, springs and river) (Herrera et al. 2006). This was probably also the case in the Late Glacial-early Holocene described here because $d^{18}O_{diatom}$ values are similar (around +37.5‰) to other diatom-isotope sequences in tropical sites (e.g. Lakes from Mount Kenya (Kenya), Barker et al. 2001; Lake Malawi (Malawi, Mozambique, Tanzania), Barker et al. 2007; Lake Tilo (Ethiopia); Lamb et al. 2005). Thereby the variations in the $\delta^{18}O_{diatom}$ from Lago Chungará sediments must be mainly derived from changes in the $\delta^{18}O_{lakewater}$ resulting from shifts in the balance between P/E, rather than other factors.

The organic matter enclosed within diatom frustules contains polysaccharides, proteins and long-chain polyamines (Kröger and Poulsen, 2008). These substances host carbon which is protected from post-depositional diagenetic alteration (Des Combes et al. 2008). As these carbon compounds will be synthesised from the surrounding waters, isotope analysis of the carbon contained in the diatom frustules can be used as a proxy for reconstructing the lake's carbon cycle. Previously published studies suggest primary productivity and $CO_{2(aq)}$ concentration as the main factors which determine $\delta^{13}C_{diatom}$ in marine environments (Schneider-Mor et al. 2005), although lake $\delta^{13}C_{diatom}$ is likely controlled by more complex environmental conditions (Hurrell et al. submitted). $\delta^{13}C_{diatom}$ variations due to the species effect, cell size, growth rate or/and metabolic pathway are neglected here since in our case the $\delta^{13}C_{diatom}$ analysis was always carried out on similar sized-cells (38-62 µm) and on the same diatom species (*Cyclostephanos andinus*).

In lakes, it is usually assumed that the carbon pool in the water becomes enriched in ^{13}C during the periods of enhanced productivity (Leng et al. 2005; Singer and Shemesh, 1995) since phytoplankton preferentially use the lighter isotope. However, the maximum productivity events found here, associated with the white laminae (short-term diatom super-blooms), show the lowest $\delta^{13}C_{diatom}$ values. Therefore, although the diatom blooms will have preferentially incorporated ^{12}C, this cannot have been sufficient to positively shift the isotope value of the dissolved carbon. Instead, the supply of carbon available to the diatoms must have been sufficient not to lead to limiting conditions.

The carbon isotope values from bulk sediment ($\delta^{13}C_{bulk}$) in the Lago Chungará laminated unit range from −21‰ to −19‰ (J.J. Pueyo, unpublished data), yielding a difference of more than 5‰ when compared to the measured $\delta^{13}C_{diatom}$ values. Nevertheless, the C/N ratio from bulk sediments of the laminated unit have values ranging between 7 and 11 (J.J. Pueyo, unpublished data), indicating that the $\delta^{13}C_{bulk}$ signal would have a mainly algal origin (Meyers and Terranes, 2001). For this reason, it seems that the $\delta^{13}C_{diatom}$, rather than being mainly affected by changes in the source of organic matter, is mostly conditioned by changes in dissolved carbon concentration. Mineralisation of terrestrial or previously deposited carbon through microbial decomposition could create a pool of isotopically lighter carbon available to the diatoms. Release of this through respiration

($CO_{2(aq)}$ and possible also CH_4) would be partly controlled by lake dynamics under the control of external forcing factors. Lake water dynamics are mainly governed by two contrasting situations (Hernández et al. 2008): (1) a water column subjected to episodes of very strong mixing, which is represented by the white laminae, and (2) a more stable condition, including periods of lake water stratification, and represented by the dark-green laminae. During the stratified periods, concentrations of oxygen and other electron acceptors typically decrease in the hypolimnion, while $CO_{2(aq)}$, CH_4, and nutrients accumulate (Bedard and Knowles 1991). These dissolved nutrients, as well as the accumulated $CO_{2(aq)}$ and CH_4, are released into the entire lake during mixis (Houser et al., 2003), when the diatom blooms occur, being the carbon incorporated into the diatom frustules.

5.3. $\delta^{18}O_{diatom}$ inter-cycle relationships (white laminae formation)

The characterisation of $\delta^{18}O_{diatom}$ values through the inter-cycle relationships gives clues to understand the underlying processes involved in the formation of the white laminae. The massive diatom blooms that produce the white laminae have to be triggered by an exceptional injection of nutrients into the water column which may or may not be associated with a water mass change. The start of the rhythmite is usually accompanied by $\delta^{18}O_{diatom}$ enrichment (Table 2A), indicating a decrease in the P/E ratio, a drop in the lake water level and a remobilization of nutrients from the hypolimnion as the more likely scenario during the white laminae formation (Fig. 5A and B, transition 1).

Episodes of diatom super-blooms occur throughout the whole studied section, but their formation is a time scale-dependent process. At decadal-centennial scales white laminae are more marked (higher values in the grey colour curve) and thicker (around 6 mm) with higher isotope oxygen values (up to 39.2‰) than during other laminae deposition periods (Hernandez et al. in press). Deposition of these white laminae stretches are related to low-stand conditions, as shown in the uppermost part of the three shallowing upwards trends observed in the $d^{18}O_{diatom}$ record (Fig. 4). However, at interannual scales the inter-cycle isotope relationships reveal that both changes to drier or wetter conditions may trigger the formation of the white laminae, but falls in lake level were more likely responsible for the development of the massive diatom blooms (Table 2A).

5.4. $\delta^{18}O_{diatom}$ and $\delta^{13}C_{diatom}$ intra-cycle relationships (green laminae formation)

The intra-cycle relationship between $d^{18}O_{diatom}$ and $\delta^{13}C_{diatom}$ provides a means of better understanding of the environmental processes involved in the origin of the green laminae. The $\delta^{18}O_{diatom}$ intra-cycle relationships show that transitions from white to dark-green laminae are mainly governed by $\delta^{18}O_{diatom}$ depletions by up to -2.7‰ (65%; n = 23), although there are also a significant percentage of enrichments (Table 2B). As in the case of the white laminae formation, green laminae can be formed under both lake-water level drops and rises, but their formation is clearly favoured by increasing P/E ratios with subsequent lake-water level rises (Fig. 5A and C, transitions 2 and 3).

Green laminae record the baseline conditions in the water column mixing regime including water table stratification periods. The intra-cycle relationships which show $\delta^{18}O_{diatom}$ depletions indicate that the lake tended to progressively recover the previous environmental conditions by means of a gradual increase in water availability (Fig. 5A and C, transition 2 and 3). Conversely, the intra-cycle relationships which show $\delta^{18}O_{diatom}$ enrichments would indicate the recovery to a lower lake level after a super-bloom caused by a massive allochthonous nutrient input associated to enhanced rainfall. This is suggested by the prevalence of $\delta^{18}O_{diatom}$ depletions that precede those super-blooms (90%; n= 10) (Table Additional Material). This model suggests that the green laminae occurred most of the time as a result of the recovery phase favoured by lake water rises. Finally, when the lake is already in the recovery phase (transitional and baseline conditions) it may evolve, indistinctly, towards rise or fall lake water level stands, as indicated by the light- to dark-green isotope transitions (enrichments= 56%; n= 9) (Fig. 5A and C, transition 4).

Comparison between $\delta^{13}C_{diatom}$ and $\delta^{18}O_{diatom}$ in the intra-cycle relationships show that the former can be associated to either $\delta^{18}O_{diatom}$ enrichments or depletions.

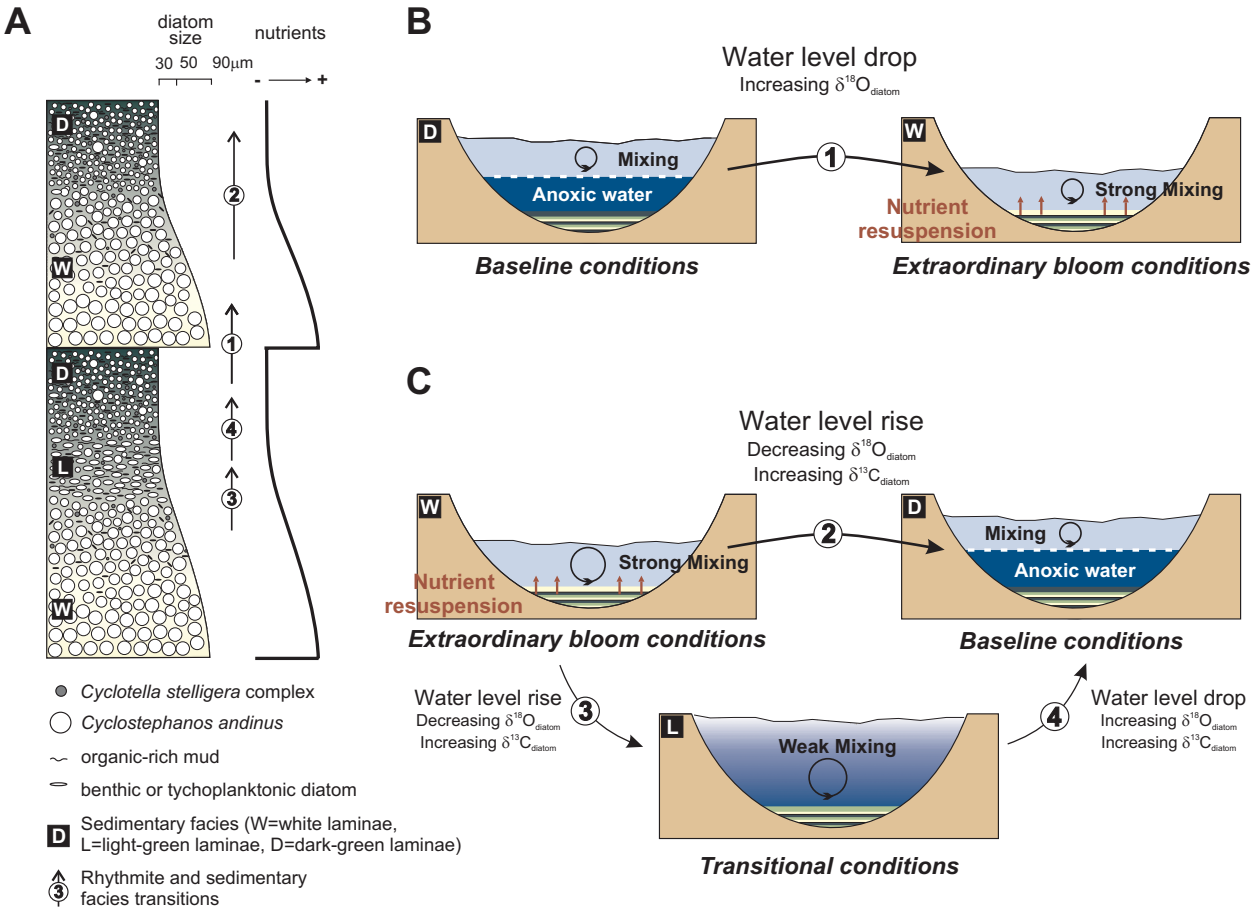

Fig. 5. A. Rhythmite log succession showing facies and transitions (indicated by letters and numbers, respectively). B. The most frequent intercycle relationship scenarios. Transition case 1: From dark-green to white laminae, the white laminae formation (diatom super-blooms) is more often favoured by drops of the lake water level (increases in $\delta^{18}O_{diatom}$ values) and therefore related to recycled nutrients from the hypolimnion. C. The most common intracycle relationship scenarios. Transition case 2: From white to dark-green laminae, the dark-green lamina formation is usually favoured by rises of the lake level water (decreases in $\delta^{18}O_{diatom}$ values). Transition case 3: From white to light-green laminae, the light-green laminae formation is usually favoured by rises of the lake water level (lower $\delta^{18}O_{diatom}$ values). Transition case 4: From light-green to dark green laminae, the dark-green laminae formation is almost indistinctly favoured by drops or rises of the lake water level, with a slight predominance of the former as the $\delta^{18}O_{diatom}$ show.

However, $\delta^{13}C_{diatom}$ values show that all intra-cycle relationships yield carbon isotope enrichment during the formation of the organic-rich green laminae (Table 1). This occurs because during the white laminae formation, the strong mixing necessary for the formation of the massive diatom blooms break the lake water stratification. Transport of $CO_{2(aq)}$ and CH_4 from an hypolimnion enriched in these compounds is then allowed, depleting the $\delta^{13}C$ of the total carbon pool.

5.5. Climatic forcing of the laminae formation

The biogeochemical reconstruction presented above suggests that laminae are formed by the occurrence of diatom super-blooms. These are directly affected by nutrient availability which, in turn, is mainly controlled by the lake level fluctuations and mixing as stable isotopes ($\delta^{13}C_{diatom}$ and $\delta^{18}O_{diatom}$) demonstrate. Hence, the laminae formation in Lago Chungará seems to be mainly induced by environmental forcing such as short-term climate variability.

ENSO and solar activity, as well as interactions between both phenomena, have been key factors prompting changes in the atmospheric conditions over the Altiplano region during the Late Glacial-early Holocene at decadal and longer term time scales (Hernandez et al. in press). ENSO and solar activity, as responsible for the more accentuated sub-millennial wet or dry conditions over the Andean Altiplano (Theissen et al. 2008), are very likely the main environmental factors in the frequency and production of the white laminae. In the Central Andes, there is a weak trend towards wet conditions

during La Niña phase and to dry conditions during El Niño phase (Valero-Garcés et al., 2003). According to our depositional model, white laminae formation could be triggered by both phases. However, El Niño events seem most likely to be responsible, since the white laminae formation is usually favoured by changes from wet-to-dry conditions, which is seen in the isotope enrichments. It is important to point out that white laminae are more intense (higher intensity grey colour values) and better developed (thicker) during periods showing higher isotope values which point to their formation during drier conditions (Hernández et al. in press). Thus, the diatom super-blooms likely occurred during El Niño-like periods. The presence of exceptionally intense and thick white laminae could, on the other hand, be indicative of the overlapping of both ENSO and solar activity phenomena during such periods. Isotope data show that high intensity of ENSO and solar activities can be recorded beyond the white laminae deposition. The short duration (days) of extreme blooms in relation to lake water residence time gives an isotope signature that will remain for longer periods (years) being recorded in the dark laminae (Hernández et al. in press).

6. Conclusions

Lago Chungará rhythmites record multiannual diatom super-blooms lasting from days to weeks (white laminae) and the lake hydrology recovery towards the baseline conditions throughout several years (dark-green laminae). Self-sedimentation phenomena taking place immediately after the diatom super-blooms cannot be discarded as a sign of the end of the super-bloom (light-green laminae). The diatom super-blooms are favoured episodes of extreme turbulent conditions affecting the whole water column, and/or by strong runoff during wet episodes. In the first case upwelling from nutrient-rich hypolimnion waters allowed an extraordinary nutrient availability, whereas in the second case allochthonous nutrient enrichment would be implicated.

In Lago Chungará, the $\delta^{18}O_{diatom}$ record can be used as an indicator of changes in the precipitation to P/E related to climatic changes, whereas the $\delta^{13}C_{diatom}$ variability would be mainly influenced by changes in $CO_{2(aq)}$ concentration. $\delta^{18}O_{diatom}$ values show that both white and green laminae formation may occur in either dry or wet conditions, but the diatom super-blooms were more intense (thicker white laminae) during decadal-centennial lowstands. $\delta^{18}O_{diatom}$ composition shows that the white laminae formation was mainly favoured by low lake levels, whereas the green laminae formation was especially prompted by lake level rises.

ENSO and solar activity are the most likely main climate forcing mechanisms triggering the white laminae formation. Both El Niño and La Niña phases could be responsible for this, but geochemical data indicate that dry conditions associated to El Niño could have the primary role since the white laminae formation was usually favoured by changes from wet-to-dry conditions in the Altiplano region. Moreover, the periods where the white laminae present major thickness and whiter colours might be indicative of phases with overlapping El Niño and solar activity. On the contrary, green-laminae were deposited during the baseline climate phases, when the normal plankton succession throughout several years and associated regular diatom blooms occur.

High resolution isotope analysis of the oxygen and carbon isotopes in diatom silica in this uniquely laminated sequence has displayed links between limnology, catchment runoff variations, hydrology and climate forcing at different time scales. Strong El Niño phases have triggered nutrient and carbon release from the hypolimnion and sediments that has led to diatom super-blooms. Such phenomena may be found in many lakes but few preserve evidence in their sedimentary architecture. Further work on other parts of this record and in similarly laminated sites may reveal the full impact of these multi-annual events on lake ecosystems and biogeochemical cycles.

Acknowledgments

The Spanish Ministry of Science and Innovation funded the research at Lago Chungará through the projects ANDESTER (BTE2001-3225), Complementary Action (BTE2001-5257-E), LAVOLTER (CGL2004-00683/BTE), GEOBILA (CGL2007-60932/BTE) and CONSOLIDER-Ingenio 2010 GRACCIE (CSD2007-00067). A. Hernández have benefited from a FPI grant from The Spanish Ministry of Science and Innovation. The Limological Re-

search Center (USA) provided the technology and expertise to retrieve the cores. We are grateful to CONAF (Chile) for the facilities provided in Parque Nacional Lauca. The NIGL (UK) funded the isotope analyses, Chris P. Kendrick is thanked for conducting the carbon isotope measurements. We also wish to thank Alice Chang and Juan J. Pueyo for valuable discussions on the self-sedimentation process and on the manuscript, respectively.

References

Alldredge AL, Gotschalk C, Passow U, Riebesell U. 1995. Mass aggregation of diatom blooms: Insights from a mesocosm study. Deep Sea Research Part II: Topical Studies in Oceanography 42: 9-27.

Baied CA, Wheeler JC. 1993. Evolution of high Andean puna ecosystems: environment, climate, and culture change over the last 12 000 years in the central Andes. Mountain Research & Development 13: 145-156.

Barker PA, Leng MJ, Gasse F, Huang Y. 2007. Century-to-millennial scale climatic variability in Lake Malawi revealed by isotope records. Earth and Planetary Science Letters 261: 93–103. doi:10.1016/j.epsl.2007.06.010

Bedard C, Knowles R. 1991. Hypolimnetic O_{2} consumption, denitrification, and methanogenesis in a thermally stratified lake. Canadian Journal of Fisheries and Aquatic Sciences 48: 1048–1054.

Bird BW, Abbott MB, Kutchko B, Finney BP. 2009. A 2000-year Varve-Based Climate Record from the Central Brooks Range, Alaska. Journal of Paleolimnology 41: 25-41.

Bradbury P, Cumming B, Laird K. 2002. A 1500-year record of climatic and environmental change in Elk Lake, Minnesota III: measures of past primary productivity. Journal of Paleolimnology 27: 321–40.

Chang AS, Patterson RT, McNeely R. 2003. Seasonal sediment and diatom record from late Holocene laminated sediments, Effingham Inlet, British Columbia, Canada. Palaios 18: 477–494.

Crosta X, Shemesh A. 2002. Reconciling down core anticorrelation of diatom carbon and nitrogen isotopic ratios from the Southern Ocean. Paleoceanography 17: 1010. doi:10 1029/2000PA000565.

Des Combes HJ, Esper O, De la Rocha CL, Abelmann A, Gersonde R, Yam R, Shemesh A. 2008. Diatom δ13C, δ15N, and C/N since the Last Glacial Maximum in the Southern Ocean: Potential impact of species composition. Paleoceanography 23: PA4209. doi:10.1029/2008PA0001589.

Dettinger MD, Battisti DS, Garreaud RD, McCabe GJ, Bitz CM. 2001. Interhemispheric effects of interannual and decadal ENSO-like climate variations on the Americas. In Interhemispheric climate linkages: Present and Past climates in the Americas and their Societal Effects. Markgraf V. (ed.). Academic Press: 1-16.

Dorador C, Pardo R, Vila I. 2003. Variaciones temporales de parámetros físicos, químicos y biológicos de un lago de altura: el caso del Lago Chungará. Revista Chilena de Historia Natural 76: 15–22.

Gasse F, Fontes JC. 1992. Climatic changes in northwest Africa during the last deglaciation (16–7 ka BP). NATO ASI Series 12: Kluwer, Dordrecht; 295–325.

Giralt S, Burjachs F, Roca JR, Julià R. 1999. Late glacial to early Holocene environmental adjustment in the Mediterranean semi-arid zone of the Salines playa-lake (Alicante, Spain). Journal of Paleolimnology 21: 449–460.

Grimm KA, Lange CB, Gill AS. 1996. Biological forcing of hemipelagic sedimentary laminae: evidence from ODP site 893, Santa Barbara Basin, California. Journal of Sedimentary Research 66: 613–624.

Grimm KA, Lange CB, Gill AS. 1997. Self-sedimentation of phytoplankton blooms in the geologic record. Sedimentary Geology 110: 151–161.

Hernández A, Bao R, Giralt S, Leng MJ, Barker PA, Sáez A, Pueyo JJ, Moreno A, Valero-Garcés BL, Sloane HJ. 2008. The palaeohydrological evolution of Lago Chungará (Andean Altiplano, northern Chile) during the Lateglacial and early Holocene using oxygen isotopes in diatom silica. Journal of Quaternary Science 23: 351–363.doi: 10.1002/jqs.1173

Hernández A, Giralt S, Bao R, Leng MJ, Barker PA. In press. ENSO and solar activity signals from oxygen isotopes in diatom silica during late glacial-Holocene transition in Central Andes (18ºS). Journal of Paleolimnogeology.

Herrera C, Pueyo JJ, Sáez A, Valero-Garcés BL. 2006. Relación de aguas superficiales y subterráneas en el área del lago Chungará y lagunas de Cotacotani, norte de Chile: un estudio isotópico. Revista Geológica de Chile 33: 299–32.

Houser JN, Bade DL, Cole JJ, Pace ML. 2003. The dual influences of dissolved organic carbon on hypolimnetic metabolism: organic substrate and photosynthetic reduction. Biogeochemistry 64: 247–269.

Hurrell ER. 2009. Climate change and biogeochemical cycles on East African mountains by stable isotopes of diatom frustules. PhD Thesis. Lancaster Environment Center, Lancaster University: Lancaster.

Hurrell ER, Barker PA, Leng MJ, Vane CH, Wynn P, Kendrick CP, Verschuren D, Street-Perrott FA. Developing a methodology for carbon isotope analysis of lacustrine diatoms. Journal of Palaeolimnology: Submitted.

Jones V, Leng MJ, Solovieva N, Sloane H, Tarasov P. 2004. Holocene climate on the Kola Peninsula; evidence from the oxygen isotope record of diatom silica. *Quaternary Science Reviews* 23: 833–839. DOI:10.1016/j.quascirev.2003.06.014

Kröger N, Poulsen N. 2008. Diatoms: from Cell Wall Biogenesis to Nanotechnology. Annual Review of Genetics 42: 83–107.

Leng MJ, Barker PA. 2006. A review of the oxygen isotope composition of lacustrine diatom silica for palaeoclimate reconstruction. Earth-Science Reviews 75: 5–27. doi: 10.1016/j.earscirev.2005.10.001

Leng MJ, Marshall JD. 2004. Palaeoclimate interpretation of stable isotope data from lake sediment archives. Quaternary Science Reviews 23: 811– 831. doi: 10.1016/j.quascirev.2003.06.012

Leng MJ, Sloane HJ. 2008. Combined oxygen and silicon isotope analysis of biogenic silica. Journal of Quaternary Science 23: 313–319.

Leng MJ, Lamb AL, Heaton THE, Marshall JD, Wolfe BB, Jones MD, Holmes JA, Arrowsmith C. 2005a. Isotopes in lake sediments. In Isotopes in Palaeoenvironmental Research, Leng MJ (ed.). Springer: Dordrecht, Netherlands; 147–184.

Meyers PA, Teranes JL. 2001. Sediment organic matter. In Tracking Environmental Change Using Lake Sediments, Physical and

Geochemical Techniques, vol. 2. Last WM, Smol JP. (Eds.). Kluwer Academic Publishers: Dordrecht, The Netherlands; 239–270.

Moreno A, Giralt S, Valero-Garcés BL, Sáez A, Bao R, Prego R, Pueyo JJ, González-Sampériz P, Taberner C. 2007. A 13 kyr high-resolution record from the tropical Andes: the Chungará Lake sequence (18º S, northern Chilean Altiplano). Quaternary International 161: 4–21. doi: 10.1016/j.quaint.2006.10.020

Morley DW, Leng MJ, Mackay AW, Sloane HJ, Rioual P, Battarbee RW. 2004. Cleaning of lake sediment samples for diatom oxygen isotope analysis. Journal of Paleolimnology 31: 391–401.

Rasband WS. 1997-2009. ImageJ. U. S. National Institutes of Health: Bethesda, Maryland, USA; http://rsb.info.nih.gov/ij/

Reynolds CS. 2006. The Ecology of Phytoplankton. Cambridge University Press: Cambridge, UK.

Rosqvist GC, Jonsson C, Yam R, Karlen W, Shemesh A. 2004. Diatom oxygen isotopes in pro-glacial lake sediments from northern Sweden: a 5000 year record of atmospheric circulation. Quaternary Science Reviews 23: 851– 859.

Round FE, Crawford RM, Mann DG. 1990. The Diatoms, Biology & Morphology of the Genera. Cambridge University Press: Cambridge; 747.

Rundel PW, Palma B. 2000. Preserving the unique puna ecosystems of the Andean Altiplano: A descriptive account of Lauca National Park, Chile. Mountain Research and Development 20: 262-271.

Sáez A, Valero-Garcés BL, Moreno A, Bao R, Pueyo JJ, González-Sampériz P, Giralt S, Taberner C, Herrera C, Gibert RO. 2007. Volcanic controls on lacustrine sedimentation: the late Quaternary depositional evolution of lake Chungará (northern Chile). Sedimentology 54: 1191–1222. doi: 10.1111/j.1365-3091.2007.00878.x

Schneider-Mor A, Yam R, Bianchi C, Kunz-Pirrung M, Gersonde R, Shemesh A. 2005. Diatom stable isotopes, sea ice presence and sea surface temperature records of the past 640 ka in the Atlantic sector of the Southern Ocean. Geophysical Research Letters 32: L10704.

Sicko-Goad L, Stoermer EF, Kociolek JP. 1989. Diatom resting cell rejuvenation and formation: time course, species records and distribution. Journal of Plankton Research 11: 375–389.

Singer AJ, Shemesh A. 1995. Climatically linked carbon-isotope variation during the past 430,000 years in Southern-Ocean sediments. Paleoceanography 10: 171–177.

Smetacek VS. 1985. Role of sinking in diatom life-history cycles: ecological, evolutionary and geological significance. Marine Biology 84: 239–251.

Talbot MR, Allen PA. 1996. Lakes. In Sedimentary Environments, Reading HG (Ed.). Blackwell: Oxford; 83–124.

Theissen KM, Dunbar RB, Rowe HD, Mucciarone DA. 2008. Multidecadal- to century-scale arid episodes on the Northern Altiplano during the middle Holocene. Palaeogeography, Palaeoclimatology, Palaeoecology 257: 361–376.

Thornton DCO. 2002. Diatom aggregation in the sea: mechanisms and ecological implications. European Journal of Phycology 37: 149–161.

Valero-Garcés BL, Delgado-Huertas A, Navas A, Edwards L, Schwalb A, Ratto N. 2003. Patterns of regional hydrological variability in central-southern Altiplano (18º-26ºS) lakes during the last 500 years. Palaeogeography, Palaeoclimatology, Palaeoecology 194: 319– 338.

Valero-Garces BL, Grosjean M, Schwalb A, Schreir H, Kelts K, Messerli B. 2000. Late Quaternary lacustrine deposition in the Chilean Altiplano (18º–28ºS). In Lake Basins through Space and Time, Gierlowski-Kordesch E, Kelts K (eds). American Association of Petroleum Geologists Studies in Geology 46: 625–636.

Vuille M, Werner M. 2005. Stable isotopes in precipitation recording South American summer monsoon and ENSO variability: Observations and model results. Climate Dynamics 25: 401–413.

Vuille M, Bradley RS, Werner M, Keimig F. 2003. 20th century climate change in the tropical Andes: observations nd model results. Climatic Change 59: 75-99.

Zhou J, Lau KM. 1998. Does a Monsoon Climate Exist over South America?. Journal of Climate 11: 1020–1040.